Synthesis, characterization and evaluation of biological activity of some modified lead molecules

THESIS

SUBMITTED TO

BABASAHEB BHIMRAO AMBEDKAR UNIVERSITY
(A CENTRAL UNIVERSITY)
LUCKNOW

BABASAHEB
BHIMRAO
AMBEDKAR
UNIVERSITY
LUCKNOW
प्रज्ञा शील करुणा
ESTABLISHED 1996

FOR THE DEGREE OF

Doctor of Philosophy

IN

APPLIED CHEMISTRY

Submitted by

Manoj Kumar Shrivash

Enrollment Number. 989/14

Co-Supervisor

Prof. Krishna Misra

Honorary Professor
Centre of Bio-Medical Research
SGPGIMS, Campus
Lucknow, 226014, India

Supervisor

Dr. Jyoti Pandey

Assistant Professor
Department of Applied Chemistry
School for Physical Sciences
Babasaheb Bhimrao Ambedkar University
Lucknow-226 025, India

2019

CERTIFICATE

This is to certify that the thesis entitled "**Synthesis, characterization and evaluation of biological activity of some modified lead molecules**" submitted by Mr. Manoj Kumar Shrivash is an original research work and has not been previously submitted in part or full for the award of any other degree or diploma to this or any other university.

The thesis submitted to Babasaheb Bhimrao Ambedkar University Lucknow satisfies all the requirements as stipulated in the Doctor of Philosophy (Ph.D.) regulation-1999 as amended in 2008/2010/2013 and it is fit for submission and evaluation for the award of the degree of Doctor of Philosophy of the University.

Krishna Misra
Co- Supervisor

Supervisor

K Amara Rao
Head of the Department
01.05.18

DECLARATION

I hereby declare that the thesis entitled "**Synthesis, characterization and evaluation of biological activity of some modified lead molecules**" submitted for the degree of Doctor of Philosophy (Ph.D), is the record of work carried out by me under the supervision of **Dr. Jyoti Pandey, Assistant Professor, Department of Applied Chemistry, School for Physical Sciences, Babasaheb Bhimrao Ambedkar University (A Central University), Lucknow, U.P., India** and co-supervision of **Prof. Krishna Misra, Hon. Professor, Centre of Biomedical Research, SGPGIMS Campus, Lucknow, U.P., India** and I further confirm that the work has not been published anywhere else for the award of any degree, diploma, fellowship etc. either in this or any other University or other institution of higher learning. I further declare that the material obtained from other sources has been duly acknowledged in the thesis. I also undertakes that the thesis is essentially free from all kinds of plagiarism.

Date: 29/4/19

Place: Lucknow

(Manoj Kumar Shrivash)
Research Scholar
Department of Applied Chemistry
Babasaheb Bhimrao Ambedkar University
Lucknow-226025, India

Acknowledgement

I owe the fulfilment of this endeavor to my esteemed supervisors ***Dr. Jyoti Pandey*** *and* ***Prof. Krishna Misra*** *for both their erudite and meticulous supervision and never failing patience, which gave me constant encouragement and guidance. Both their painstaking efforts, immense insight, inspiring attitude, evolutionary ideas and enthusiasm enabled me to complete this research work.* ***Prof. Krishna Misra's*** *thought provoking critical comments and keen insight in identifying various facets of problems have been a source of enduring patience to me without which this work could neither gather substance nor assume the present form. Her scholarship, humanity made my task a joy. Her efficacy led to broadcasting and deepening of my understanding of research problem. It is a great pleasure and privilege for me for being associated with her. I shall always remain beholden to her. Whatever that I have earned and will be earning in the future endeavor all owes to* ***Prof. Krishna Misra****. Her passion and dedication makes her what she is today, and I am proud to be part of her student family.*

Once again I would like to express my immense gratefulness to my supervisor ***Dr. Jyoti Pandey, Department of Chemistry, BBAU****, for her encouragement and support. I acknowledge her sincere efforts for continuous support from the time of registration at BBAU till the end of the thesis submission.*

I acknowledge the sincere efforts of Mr. Sarvesh, Anuj and Pankaj for their continuous support from the time of PhD registration at BBAU till the end of the thesis submission.

My heartfelt gratitude to my senior ***Dr. K. Adeppa and Dr. Soumen Sarkar*** *for their immense support and encouragement for my PhD admission and research career.*

My heartful thanks to my seniors and lab mates Dr. Ashok Kumar Yadav, Dr. Manoj Kumar Gupta and Dr. Atish Chandra for their immense support and encouragement to me for this research work. The thesis would not have gained this shape without their unique vision, deep thinking, better understanding and great

enthusiasm for the accomplishment of this research work. A thanks just won't be enough for his never ending ideas and efforts. I gratefully acknowledge the support, motivation affection showered by ***Prachi, Sahani and PJ*** *in the course of my Ph.D. Prachi has been an excellent support, a best friend and a source of encouragement in the hard times. I would also like to thank my dearest friend* ***Deepak,*** *and other Ph.D. mates for being my best friends Sonali, Anushree and also for their cheerful company, never ending laughter. My special thanks to my junior Akhilesh and my senior colleagues Abhishek, Dr. Ajay Kumar, and Dr. Azad Kumar. I would also like to thank my current lab mates Dr. Monika Mishra, Ram, Anil, Vikram, and Tazeen for maintaining a friendly and cheerful research atmosphere. They made my working in the lab very enjoyable. I want to thank my friends Roshni, Balwant, Puneet, Mister Singh and Govind, for their help whenever it was required. Special acknowledgments to my post graduate friends Devendra Pandey, Veena, Vinay, Kapil (CDRI) for all kind of help that all have provided. I am also thankful to my teacher Prof. Sudha Jain, and Dr. Monika Mishra, who has taught me the basic chemistry and inspired me to become a Chemist by profession.*

It is equally difficult to put into words my gratitude and love to my Parents, younger brothers, sisters, and all the family members for their blessings, love, care and continuous encouragements throughout my education. Sincere thanks to my elder sister Santoshi and Jiju for the love, care and encouragement. Thanks to Drs. of PGI and Dr. Alka for the best possible treatment to cope up with my bad health conditions and providing a constant enthusiasm to deal with the situations. A special thanks to my friend Prashant for HRMS, Ajay sir for the NMR spectra, research, technical, helping and administrative staff at CBMR is greatly acknowledged. Finally, I thank ***Prof. Ganesh Pandey,*** *Director, CBMR, Lucknow, for providing the infrastructural failities to complete my work successfully. I am also thankful to UGC, NASI, Allahabad, DBT, and ICMR, Delhi for the financial assistance.*

M. Srivas

.....Manoj Kumar Shrivash

Abstract

The very objective of the present work was to design novel molecules based on reported lead structures for different ailments by docking against important molecular targets using computational methods. The selected molecules were synthesized and characterized using unambiguous protocols with necessary modifications wherever required. These compounds involve mainly polyphenols including curcumin analogues, flavonoids and stereoselective oximes which were subjected to *in vivo* testing. Some of these are being reported as potent anti-bacterials, antifungals, anticancer and anti-Parkinson's disease. This study is likely to be useful in developing these selected molecules as future drugs.

Whole research work is divided in to five chapters. The first chapter starts with the history of drugs describing human struggle to find alternative cures for different diseases since his existence on this planet. The earlier remedies were accidental discoveries. Human experiences transferred through generations have resulted in certain stabilized potent molecules for cure of different diseases. The three phases in Medicinal Chemistry for drug development have been described. The transformation of some lead molecules to effective drugs has been discussed. Lead molecule is a chemical compound that has pharmacological or biological activity likely to be therapeutically useful, but may nevertheless have suboptimal structure that requires modification to fit better to the target; lead drugs offer the prospect of being followed by back-up compounds. Some examples of lead molecules are given in chapter one. We have discussed about the role of polyphenols in human and plants, their origin and biological importance. We have also discussed about curcumin, the yellow pigment of turmeric as a lead molecule used in traditional medicine. Extraction of curcumin from turmeric rhizome, molecular targets of curcumin in human, therapeutic properties of curcumin and limitations of curcumin as a drug have been discussed. A concise account has been given about the tools of bioinformatics used for drug discovery. Computational methods and software's used for drug development are described. Sequential process of *in silico* drug design has been illustrated. A brief account of the work done has been given in chapters two to five.

In chapter two the introduction of Parkinson's disease (PD), its molecular targets including reported literature for its cure have been given. The marketed drugs for the treatment of Parkinson's disease are L-Dopa, Carbidopa and Dopamine. Curcumin is a wonder molecule but has certain limitations to be used as a drug due to its speedy metabolism, biotransformation, quick elimination, inefficient cellular uptake and transport across the blood brain barrier (BBB) resulting in low bioavailability. The literature reports indicate that deficiency of glucose in the brain causes neurogenetic diseases like PD and Alzheimer (AD). Our concept was that glucose moiety covalently bonded with curcumin can serve dual purpose i.e. enhance the uptake of curcumin via BBB barrier and also increase the concentration of glucose in the brain. Therefore, mono and di-glucosides of curcumin were prepared. However the *in silico* study with PD target (α-Synuclein) indicated that curcumin-di-glucoside is more effective as compared to the mono glucoside or curcumin. We synthesized curcumin via aldol condensation of vanillin and acetyl acetone using boric acid, m-xylene and catalytic amount of n-butyl amine. Curcumin was prepared, purified and characterized with ^{1}H NMR, ^{13}C NMR spectrum. The synthesis of mono and di-glucosides of curcumin was carried out by reacting acetobromoglucose, with vanillin followed by nucleophilic substitution reaction with base and phase transfer catalyst, benzyl tri butyl ammonium chloride (BTBAC) in aqueous NaOH and DCM to yield tetra-*O*-acetyl-β-D-glucopyranosyl vanillin. Tetra-*O*-acetyl-β-D-glucopyranosyl vanillin underwent aldol condensation with acetyl acetone in presence of tributyl borate to give B_2O_3 complex .The acetylated mono and di glucosides of curcumin were separated using column chromatography. The deacetylation of the tetra acetates of mono and di glucosides of curcumin was carried out with sodium methoxide in dry methanol at 0 °C, followed by neutralization of the reaction mixture with acidic Dowex resin. Pure mono and di-glucosides were characterized with ^{1}H NMR spectrum. Both glucosides were tested on neuro cell line which indicated that monoglucoside was more effective.

The *in vitro* and *in vivo* bioassay studies of curcumin versus it's mono and di-glucosides against Rotenone (ROT) induced toxicity in N27 cells demonstrated that Curcumin-4-*O*-β-D- monoglucoside has better bioavailability and protective effect than curcumin - diglucoside. Although *in silico* studies indicated that di glucoside has stronger binding with the target but in wet experiment the monoglucoside proved better. The probable reason may be that the free phenolic group of curcumin monoglucoside contributes to its antioxidant activity, the glucoside moiety attached to

the other phenolic helps in enhancing solubility, cellular uptake and bioavailability. According to our knowledge, this is the first report to show that curcumin monoglucoside has a protective effect in ROT-based PD models, suggesting that it could offer better pharmacokinetics and pharmacodynamics compared to curcumin in Parkinsons's disease (PD).

In third chapter, after successful preparation of curcumin as described in previous chapter we synthesized 10 other curcumin derivatives and nano curcumin. Literature reports suggest that active methylene group and the ketone moiety of curcumin are responsible for its initial metabolism. In order to overcome this problem and to improve its pharmacokinetics properties, we studied several synthetic modifications on the carbonyl, active methylene group and side functionalities on aromatic rings. Nitrogen and sulfur containing heterocyclic moieties such as pyrazoles, pyrimidines and thiazoles are well known for their broad-spectrum of pharmacological properties such as antimicrobial, anti-inflammatory, analgesic, enzyme inhibition, antioxidant, and anticancer. These scaffolds have important role in drug designing as important pharmacophores. Therefore towards the synthetic goal, we focused on incorporating heterocyclic moieties i.e. isoxazole, N-substituted pyrazoles, pyrimidine-2(1H)-thione and pyrimidine ring in the molecular scaffold of curcumin. In addition we focused on free phenolic group of curcumin and synthesized sulphate, phosphate and phthalimide glycine and tetra acetyl mono glucoside derivatives. Unambiguous methods were used for synthesis. Based on the *in silico* analysis we executed the chemical synthesis, *in vitro* analysis and validation of the obtained results.

The MIC / IC_{50} values and binding energies of curcumin and its analogues with MipZ and Pyruvate kinase proteins of *Pseudomonas aeruginosa* (Gram negative) and *Staphylococcus aureus* (Gram positive) bacteria respectively have been given in chapter third. We could arrange these compounds in the following order with respect to relative activities towards both Gram positive *(Staphylococcus aureus)* and Gram negative *(Pseudomonas aeruginosa)* bacteria. The IC_{50} of chloramphenicol against both bacteria was considerably less in comparison to the synthesized compounds. From the results obtained it can be concluded that curcumin analogues with the linker between two aromatic rings substituted with nitrogen containing heterocyclic rings e.g. isoxazole, pyrazole, thiazole, thione can prove to be much better drugs for antibacterial activity. Such molecules along with substituents like phosphate or

sulphate substituted at one of the two phenolic hydroxyls of curcumin can prove to be potent anti-inflammatory agents due to their multi-targeted effects. These compounds appear to act by some alternate mechanism too e.g. inhibiting cell division in addition to degradation of bacterial cell wall. These compounds can serve as better antibacterial alternatives, as now a days the microbes become resistant to antibiotics due to their unselective use.

In chapter fourth we have described the design and discovery of new plant based herbal antifungal compounds specifically for inhibiting filamentation in *Candida albicans* and thus attenuate its pathogenicity. These compounds are non-toxic and better solve the problem of drug resistance as well. *Candida albicans* is present in human biome in yeast shape and for most part found in skin and gastrointestinal cavity. It is generally sedate safe in nature, however polymorphic change causes flagellation leading to pathogenicity. The progress of yeast to hyphal shape is called dimorphism. The two structures are critical, however hyphal frame is one more obtrusive for human species.

Our study has revealed four foremost pathways occurring in various cell organelles of *C. albicans*, i.e., glyoxalate pathway, Ras1-pka pathway, Ergosterol pathway and flagging pathways. Further the key components which can possibly influence most extreme pathways have been recorded as Efg1 protein, 2QZX i.e. secreted aspartic proteinase (Sap5), Erg11 and Glyoxalate pathway. We docked *in-silico* all the above mentioned targets with a class of polyphenols such as flavonoids, coumarins, chalcones and curcumin analogs and the best compounds were sorted. The compounds chalcone **(54),** coumarin **(50),** quercetin tetraacetate **(56),** quercetin penta acetate **(55)** and (1E,6E)-1,7-di(1H-indol-3-yl) hepta-1,6-dience-3,5-dione) **(58)** were synthesised using unambiguous methods and further tested *in-vivo* for their sensitivity on the *Candidanian* strain SC5314. We synthesized coumarin **(50)** by Pechmann condensation reaction, chalcone **(54)** via claisen schmidt condensation, quercetin tetra and penta acetates by selective acetylation of quercetin. The synthesis of 1,7-di(1H-indol-3-yl)hepta-1,6-diene-3,5-dione **(58)** was done according to the synthesis of curcumin **(3)**. All these compounds were purified and characterized with ^{1}H NMR, ^{13}C NMR spectra. These were tested for their sensitivity on the *Candidanian* strain SC5314. Quercetin pentacetate **(55),** quercetin tetracetate **(56)** and coumarin **(50)** have been found active in all four targets illustrating their high affinity. The marketed antifungal drugs are mainly azoles e.g Fluconazole has been reported

with many side effects. Including fluconazole most azoles are very toxic for human biome. In such scenario the non-toxic polyphenols seem to show promising results as inhibitors of flagellation, the main cause of pathogenicity in *Candida* species.

In fifth chapter we have prepared stereoselective *Z* isomer of oximes by a novel method. Many methods for synthesis of oximes are reported in literature. Generally a mixture of *E* and *Z* isomers is obtained. Oximes are biologically important. Many oximes are known for their anticancer activity.

We have developed a novel method of synthesis of stereoselective oximes (mainly Z isomer) through direct conversion of substituted aryl/alkyl cyano esters to aryl/alkyl oximes. The alkene-bridged ethyl cyano arylacrylate compounds undergo unexpected C-C bond cleavage with the associated loss of the ethyl cyanoacetate group by Michael addition of hydroxylamine to a benzylidene cyanoacetate followed by a retro Knoevenagel reaction (1, 3 proton shift) without transition-metal catalysis. The significant advantage of the present method is the formation of stereoselective oximes (Mainly *Z* form) since this form is known to be more biologically active. Substituted benzylidene cyano acetates were synthesized via aldol condensation followed by substituted aldehydes with ethyl cyanoacetate using sodium ethoxide as catalyst. Different bases were used as standard, however, sodium ethoxide was found to give maximum yields under optimal conditions. The yields of oximes were in the order heterocyclic>aryl>alkyl. Our new strategy presents one step, time and cost effective cleaner preparation of predominantly *Z* -oximes. These oximes were tested against cancer cell lines MCF-7, A431, A549, PC-3, HepG2, MDAMB-231, L-132, NCIH-520, NCIH-460 .The MTT assay and IC_{50} values indicated that (*Z*)-2,3,4-tri methoxy benzaldehyde oxime **(114)** had maximum antiproliferative activity.

Overall objective of the present work was to develop novel potent molecules from known lead structures by appropriate chemical modification.The molecules were designed by computational methods i.e. docking against selected molecular targets. This was followed by their synthesis using unambiguous methods with necessary modifications wherever required, these compounds were then tested for their activity as compared with standard drugs. We have suggested new future drug like molecules for cure of Parkinson's disease, anti-bacterial, antifungals and anticancer pro-drugs. These molecules can be tested further on animal models for validation. These drugs are likely to prove safe answer to multiple resistance.

Table of Content

Chapter 1: Biological potential of polyphenols **1-21**

1.1. History of drugs 1

1.2. Bioinformatics and drug discovery 4

1.3. Present work 12

1.4. References 19

Chapter 2: Gram-scale synthesis of curcumin monoglucoside (CMG) and their inhibitory effect towards neurotoxicity in Parkinson's disease **22-54**

2.1. Introduction. 22

2.2. Earlier Methods of Synthesis of curcumin (3) and its mono and di-glucosides (24, 27) 23

2.3. Basis of present work. 24

2.4. Objective of the present work 30

2.5. Materials and methods 30

2.6. Experimental 30

2.7. Bioassay 34

2.8. Results & Discussion 35

2.9. Conclusion 40

2.10. Spectral Data (^{1}H and ^{13}C) 41

2.11. References 44

Chapter 3: Designing, synthesis, characterization and antibacterial properties of some curcumin analogues **55-88**

3.1. Introduction 55

3.2. Earlier methods of preparation of curcumin analogues 59

3.3. Basis of the present work. 62

3.4. Objectives of the research work 62

3.5. Material and Methods 63

3.6. Experimental 63

3.7. Bioassay 69

3.8. Results and discussion 72

3.9. Conclusion 78

3.10. Spectral Data (^{1}H and ^{13}C) 79
3.11 References 86
Chapter 4: Designing and synthesis of flavonoid derivatives for modulatory effect on flagellation of *Candida albicans* **89-124**
4.1. Introduction 89
4.2. Earlier methods of preparation of polyphenols 93
4.3. Basis of the present work 98
4.4. Object of the present work 99
4.5. Material and Methods 99
4.6. Experimental 100
4.7. Bioassay 106
4.8. Results and Discussion 106
4.9. Conclusion 115
4.10. Spectral Data (^{1}H and ^{13}C) 116
4.11. References 121
Chapter 5: Synthesis of stereospecific substituted aryl/alkyl oximes and studies of their inhibitory effect on different cancer cell lines **125-179**
5.1. Introduction 125
5.2. Earlier methods for synthesis of oximes 129
5.3. Basis of present work 133
5.4. Objective of present work 133
5.5. Materials and Methods 134
5.6. Experimental 134
5.6. (c) Bioassay 144
5.7. Result and discussion 146
5.8. Conclusion 154
5.9. Spectral Data (^{1}H and ^{13}C) 159
5.10. References 179
List of Publication **180-181**

List of Figures

Figure No.	Title	Page No.
1.1.	Some examples of lead molecules	3
1.2.	Therapeutic importance of polyphenols	5
1.3.	Structure of curcuminoids	7
1.4.	Therapeutic properties of curcumin	8
1.5.	Molecular targets of curcumin	8
1.6.	The sequential process of *in silico* drug design	12
2.1.	Anti-Parkinson's drugs	23
2.2	Mechanism of the synthesis of curcumin from vanillin	26
2.3.	Neuronal death of N27 cells with rotenone and neuroprotective effect of curcumin and curcumin monoglucoside	37
2.4.	Bioavailability of curcumin and curcumin monoglucoside in N27 dopaminergic neuronal cells	38
2.5.	Docked conformation of 4,4'-*O*-di-(β-D-glucosyl) curcumin **(27)** and 4-*O*-(β-D-glucosyl) curcumin **(24)** against α-Synuclein (G-Score- -9.2)/ (G-Score -9.5)	39
3.1.	Cell wall structure of gram positive and gram negative bacteria	56
3.2.	Mechanism of antibiotic resistance in bacteria	58
3.3.	Graphs showing absorbance against molar concentration of compounds (32-42) against *Styphylococcus aureus* and *Pseudomonas arigunosa*	71
3.4.	(A) and (C) show 3D interaction of (34) with 2XIT and 1A3W respectively while (B) and (D) represent (35) thione with 2XIT and 1A3W respectively	76
3.5.	(A) and (C) show 2D interaction diagram of (34) with 2XIT and 1A3W respectively while (B) and (D) represent interaction of (35) with 2XIT and 1A3W respectively	76
4.1.	Biological flow of *Candida albicans*	90

Figure No.	Title	Page No.
4.2.	Diagrammatic representation of steps in biofilm formation.	92
4.3.	Glyoxylate pathway in *candida albicans*	95
4.4	Flow chart of Methodology	100
4.5.	Showing 3D docking interaction of 1IYK with coumarin (50) and quercetin penta acetate (55)	111
4.6.	2D interaction diagrams of coumarin (50) and quercetin penta acetate (55) with N-myristoyl transferase.	111
4.7.	Showing 3D docking interaction Erg11 with chalcone (54) and quercetin tetra acetate (56)	111
4.8.	Showing 3D docking interaction Erg11 with coumarin (50)	112
4.9.	2D interaction diagrams of (a) chalcone (54) (b) coumarin (50) and (c) quercetin tetra acetate (56) with Erg11	112
4.10.	Showing 3D docking interaction of chalcone (54) and quercetin tetra acetate (56) with SAP5	112
4.11.	2D interaction diagrams of chalcone (54) and quercetin tetra acetate (56) with SAP5 respectively	112
4.12.	Showing 3D docking interaction of chalcone (54) and quercetin tetra acetate (56) with Efg1	113
4.13.	Showing 3D docking interaction chalcone (54) and quercetin tetra acetate (56) with Efg1 respective	113
4.14.	Showing the multiple filamentation growth of SC5315 candida albicans untreated strain against the same with our proposed lead molecule	114
4.15.	Showing the filament length growth of SC5315 *Candida albicans* untreated strain against the same with our proposed lead molecules	114
4.16.	Showing 3D docking interaction quercetin tetra acetate (56) with Efg1	115
5.1.	Structures of aldoxime and ketoxime	125
5.2.	Methyl glyoxime	125

Figure No.	Title	Page No.
5.3.	Cis-trans isomerism in oximes	125
5.4.	Steroid ring system (hydroximino group at position 6 of B-ring or in the side chain at position 17 have antiproliiferative properties against cancer)	127
5.5.	BRAFV600E, FAK and EGFR-TK kinases as inhibitors of tubulin polymerization	127
5.6.	Indirubin 3-oxime (Indox) [a] and 5-bromoindirubin 3'-(O-oxiran-2-ylmethyl) oxime [b]	128
5.7.	Percentage Cytotoxicity of synthetic oximes (109-126), flavanone and standard drug tamoxifen	146

List of Tables

Table No.	Title	Page No.
1.1.	Some examples of dietary flavonoids as food sources	4
1.2.	Computational method and software's for drug design	11
2.1.	The effect of solvent and pressure on preparation of curcumin	35
3.1.	Different modes of antibiotic drug resistance	58
3.2.	MIC/ IC_{50} values and binding energies of curcumin and its analogues with MipZ and Pyruvate kinase proteins of *Pseudomonas aeruginosa* and *Staphylococcus aureus* respectively	72
4.1.	Docking score, H-bonds of Ligands docked with protein targets showing amino acids in active sites	107
4.2.	Compound sensitivity and inhibition of Candida albicans filamentation with SC5314	110
5.1.	IC_{50} (μ mol) values of synthesized oximes for tested cell lines	145
5.2.	Optimization of reaction conditions for ethyl (*E*)-2-cyano-3-phenylacrylate	149
5.3.	Synthesized ethyl (*E*)-2-cyano-3-aryl/alkyl acrylate with yield	150
5.4.	Impact of solvent on yield of oximes	151
5.5.	Impact of base on yield of oximes	151
5.6.	Synthesized oximes with yield in percentage	152

List of Abbreviations

Ac	Acetyl	min	Minutes
Ar	Aryl	ml	Millilitre
aq	Aqueous	mmol	Millimole
BTBAC	Benzyl tributyl ammonium chloride	mp	Melting point
bp	boiling point	MeOH	Methanol
n-BuLi	*n*-Butyl lithium	Me	Methyl
BT	Boron trioxide	M	Molar
Boc	*t*-Butoxycarbonyl	mg	Miligram
DBU	1,8-diazabicyclo[5.4.0]undec-7-ene	NMR	Nuclear Magnetic Resonance
DCM	Dichloromethane	PTC	Phase transfer catalyst
DIBAL-H	Diisobutylaluminium hydride	rt	Room temperature
DNA	Deoxyribonucleic acid	RNA	Ribonucleic acid
DMAP	4-(dimethylamino)pyridine	TMS	Trimethyl silyl
DMF	Dimethyl formamide	TBAB	Tetrabutylammonium bromide
DMSO	Dimethyl sulfoxide	TLC	Thin Layer chromatography
Et_3N	Triethylamine	TFA	Trifluoroacetic acid
EDC.HCl	N-(3-Dimethylaminopropyl)-N′-ethylcarbodiimide hydrochloride	*p*-TSA	*para*-toluene sulphonic acid
ESI	Electron spray Ionization	TCCA	Trichloro isocyanuric acid
EtOAc	Ethyl Acetate	THF	Tetrahydrofuran
EtOH	Ethanol	Ts	Tosyl
g	gram	py	Pyridine
HRMS	High resolution mass spectra	PD	Parkinson disease
h	hour	µM	Micromolar
Hz	Hertz	Mol%	Mole percent
IBX	*o*-iodoxybenzoic acid	ppm	Parts per million
IC_{50}	Inhibitory Concentration	UV	Ultraviolet

Chapter 1

Biological potential of polyphenols

1.1. History of drugs:

Man has been struggling to find alternative cures for different diseases since his existence on this planet. The earlier remedies were accidental discoveries [1]. Experiences transferred through generations resulted in certain established molecules which now have come to be known as lead molecules. Through centuries scientists have been extracting these active molecules from animal plant or mineral sources and using as remedies for human and animal ailments [2]. This resulted in emergence of a branch of science now known as "Medicinal Chemistry" Medicinal chemistry is the study of drugs, their biological properties and their structure-activity relationships (SAR) [3]. It tends to be characterized as the disclosure, improvement, distinguishing proof and translation of the method of activity of organically dynamic mixes at the subatomic dimension [4].

Human has investigated nature to fulfill two noteworthy requirements sustenance and herbs for lightening torment and enduring. More than multi year back human had treatises where herbs or blends of them treat infection [5]. Egyptian culture effectively utilized a scope of herbs from therapeutic plants that were portrayed in the Ebers Papyrus that was dated around 1550 BC [6]. It fuses around 800 medicines composed as hieroglyphics for more than 700 cures [7]. The majority of the Egyptian names of medications and fixings, somewhere around a third, have been related to medications and dynamic rules that show up in current models and formula books [8]. Notwithstanding formulas for laxatives, it makes reference to some alkaloid plants just as basics oils, turpentine, cedar wood, relieving analgesics for skin issues, and numerous different medicines. Fragrant pitches of Boswelia trees developing on the southern shore of Arabia, for example, frankincense (otherwise called olibanum) and myrrh were prized by Egyptian embalmers. Afterward, they were refered to in the book of scriptures [9], and have been utilized alongside different resins and gums during the time as antiperspirants and clean medications [10].

From thousand of year Ayurveda has been used in India. Hallucinogenic plants, Cannabis, Datura metel, Serpaghanda, Rauwolfia serpentine, which has been used for treatment of hypertension and insanity [11]. CIBA chemist, isolated reserpine (amongst other alkaloids) from the roots of Rauwolfia, and proved its ability as an

antihypertensive and tranquilizer [12]. Chaulmoogra oil has antilepropy activity [13]. The folk medicine practiced by various North American, Indian from the Ayurveda [14]. There are similarities in the medicinal plants used by American Indians and the East Indian Ayurvedic medicines for the treatment of various disease [15]. The Chinese have consumed considerable quantities of herbal remedies, many of which have been in use for centuries [16]. In the book on materia medica, Shen Nong Ben Cao Jing (Shen Nong's Canon on Materia Medica), seemed around the first centuries before and after Jesus Christ, and labelled the characteristics, processing, and prescription of about 50 drugs from minerals origin, 250 drugs from plant and 60 from animal origin [17]. In 1930, Chinese-American pharmacologist K. K. Chen has identified of ephedrine and isolated from Ephedra sinensis [18]. Most of drug are chemicals which interact with macromolecular targets to produce a biological response [19]. The biological response can be therapeutically useful in the case of medicine, or harmful in the case of poisons. Most drugs used in medicine are potential poisons. Any drug development program in Medicinal chemistry includes the following three phases:

i. The first phase includes identification of new active compounds or drugs and their preparation from natural sources, by organic chemical reactions or through biotechnological processes. These molecules are known as lead molecules.
ii. The second phase is optimization of lead structure to increase potency, selectivity and to decrease toxicity.
iii. Third phase is developmental stage, which includes optimization of synthetic route for large scale production, purification and modification of pharmacokinetic and pharmaceutical properties of active substance to make it clinically useful [20]. Medicinal chemistry development, scientists were predominantly concerned with the isolation of medicinal compounds from the plants [21].

Now a days, scientists in the medicinal field are also equally concerned with the design of new synthetic compounds as drugs. Medicinal chemistry is useful to gear toward drug discovery and development [22]. Medicinal chemists apply their chemistry training to the process development of synthesizing new pharmaceuticals

ingredients. They also work on improving the process by which other pharmaceuticals are made. Most chemists work with a team of scientists from different disciplines, including pharmacologists, theoretical chemists, biologists, toxicologists, microbiologists, and biopharmacists [23]. Collaborated team uses sophisticated analytical techniques to synthesized and test new drug products and to develop the most cost effective and eco friendly means of drug production.

1.1. (a) Lead compounds:

The lead compound has the desired biological or pharmacological activity but may have many undesired characteristics like high toxicity other biological activity, insolubility, low bioavailability and metabolism problem [24].

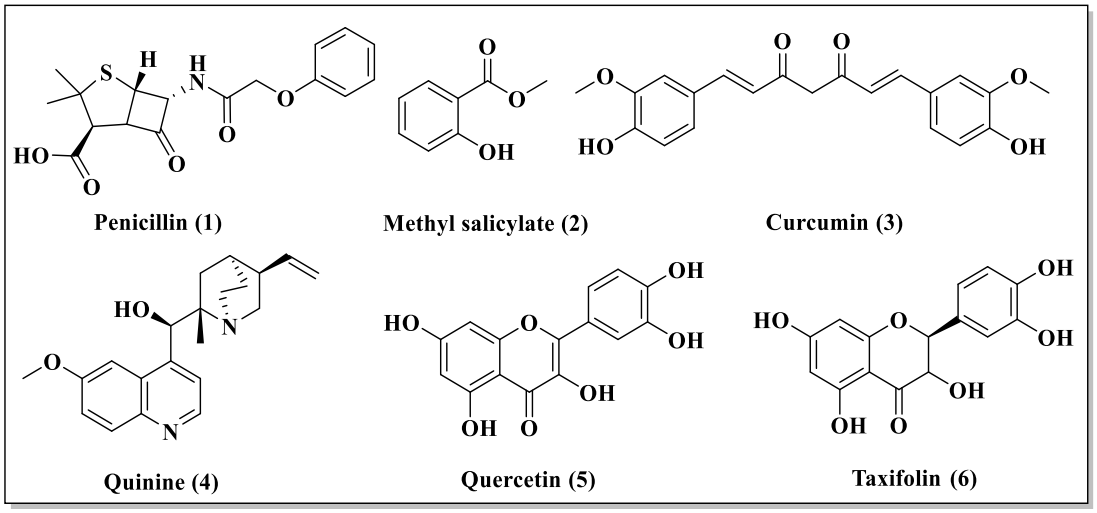

Figure 1.1. Some examples of lead molecules.

Lead compound may be a natural product, synthetic, or semi-synthetic compound which is biologically active [25]. Plants, minerals, and animals and microorganism are the common sources of natural products [26-30]. Quinine **(4)** is a lead molecule which was first isolated in 1820 from the bark of a Cinchona tree. The quinine **(4)** was the first successfully used chemical compound in the treatment of malaria [31-32]. A lot of examples of lead molecules have been reported in literature such as Paclitaxel, Methyl salicylate **(2)** [33], Curcumin **(3)**, Penicillin **(1)**, Flavanoids and other polyphenols (Fig.1.1).

1.1. (b) Importance of polyphenols:

Polyphenols are naturally occurring phytochemicals having antioxidant properties. There are over 8,000 well known polyphenols found in foods such as tea, wine, chocolates, fruits, vegetables, and olive oil. Polyphenols play a significant role in maintaining health and wellness. Antioxidants as a group help protect the cells in the body from free radical damage, thereby controlling the ageing process. If body does not get adequate protection, free radicals can become rampant, causing cells to perform disorderly. This can lead to tissue degradation and put at risk of diseases such as heart disease, cancer, and neuro diseases.

Table 1.1. Some examples of dietary flavonoids as food sources.

S. No.	**Subclass** (Name of flavonoid compound)	**Sources**	**Structure**
1	Flavanols (Quercetin)	Tomato, onion, beans, apple, berries, red wine, broccoli	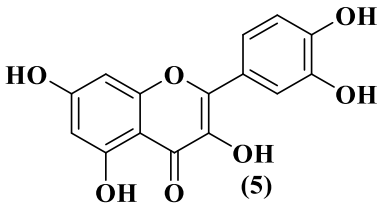 (5)
2	Flavones (Luteolin)	Parsley, celery	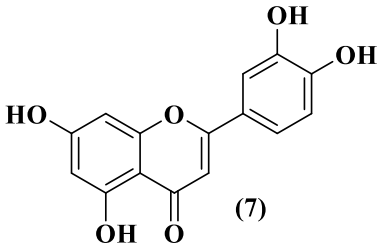 (7)
3	Flavanones (Butin)	citrus fruit	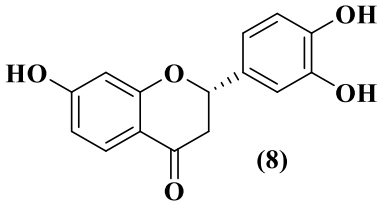 (8)
4	Flavanols Catechin	Dark chocolate, grape, apple, berries, tea, red wine	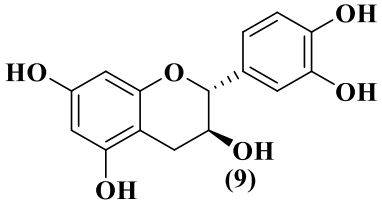 (9)

5	Proanthocyanidins	Dark chocolate, grape, apple, berries, red wine	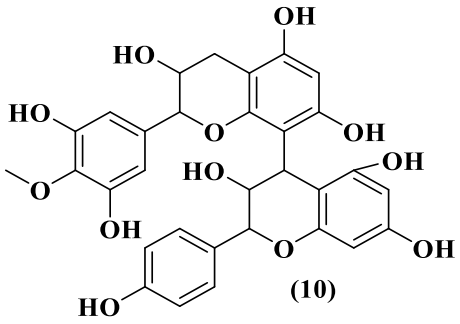 (10)
6	Anthocyanidins (Cyanidin)	Red cabbage, red onion, plum, cherry, berries, red grape, red wine	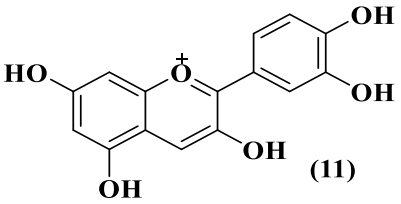 (11)
7	Isoflavones	Soyabean	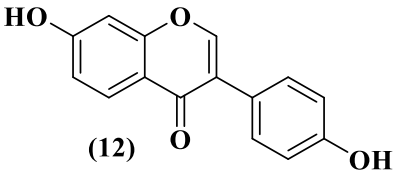 (12)
8	Chalcone	Rhus verniciflua	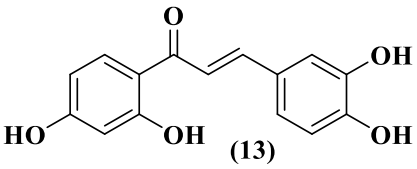 (13)

Polyphenols constitute are secondary metabolites synthesized by plants and which are ubiquitous throughout the plant kingdom. Multi thousand molecules having polyphenolic structure (i.e. several hydroxyl groups on aromatic rings) have been identified in higher plants, and several hundred are found in edible plants [34]. Polyphenols are divided into several classes and subclasses according to their chemical structure (Table 1.1). Proanthocyanidins (also called condensed tannins) are oligomers and polymers of flavonoids.

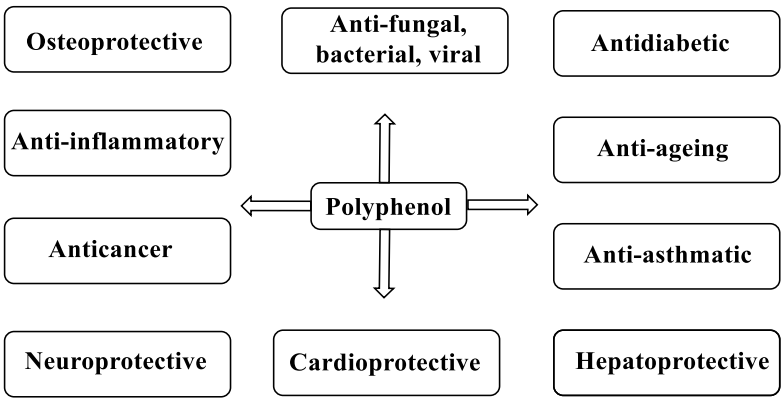

Figure 1.2. Therapeutic importance of polyphenols.

1.1 (c) Role of polyphenols in humans and plants:

Polyphenols protect plants from UV radiation, pathogens, oxidative stress, and harsh climatic conditions [35]. These polyphenols are consumed by humans as food sources .These act as antioxidants, and have diverse biological properties (Fig. 1.2) such as anti-diabetic [36-37], anticancer [38-39], anti-inflammatory [40-41], cardioprotective [42], osteoprotective [43-44], neuroprotective [45-46], antiasthmatic [47], antihypertensive [48], antiageing [49], antiseptic [50], cerebrovascular protection [51] cholesterol lowering [52], hepatoprotective [53], antifungal [54], antibacterial [55], and antiviral [56].

However, there is genetic difference between plants and humans, therefore appropriate modifications in the structure of these ligand molecules is necessary to make these potent drugs for animals and humans. It is being realized by scientists that excess of ROS formation in human body is the main cause of various disorders. Therefore, intake of these polyphenols can be helpful in preventing these disorders. In our present work we have used some of these polyphenols in order to prevent the early symptoms of pathogenic changes. Polyphenols are likely to act as lead compounds for future drugs.

1.1. (d) Curcumin as lead molecule, uses and limitations.

Curcumin **(3)** is a wonder molecule belonging to the class of polyphenols. It is the yellow pigment present in rhizome of *Curcuma longa* (turmeric spice). Turmeric is approved amply for ailments in both traditional Chinese and Indian medicine [57]. Turmeric paste is used to fresh wounds and bruises and as counterirritants for insect bites. Turmeric paste is used to facilitate scabbing in chicken pox and small pox, which is used in urologic diseases, hepatobiliary diseases and as an anthelminthic. Turmeric has also been labelled as a cancer remedy in Indian natural medical.

Diarylheptanoids are the major phytoconstituents of turmeric which occur in a mixture termed curcuminoids that is made up of approximately 1−5% of turmeric [58].The curcuminoids contain curcumin **(3)** (Fig.1.3. A) [(1E,6E)-1,7-bis(4-hydroxy-3-methoxyphenyl)- 1,6-heptadiene-3,5-dione, typically 60−70% of a crude extract],

demethoxycurcumin **(14)** (Fig. 1.3. B) (20−27%), and bisdemethoxycurcumin **(15)** (Fig 1.3 C) (10−15%), along with numerous and secondary metabolites.

Curcumin **(3)** has diverse therapeutic properties (Fig. 1.4). This molecule interacts with several biological targets linked to abundant diseases (Fig. 1.5). Unfortunately the clinical applications of curcumin **(3)** has been restricted by its poor bioavailability, solubility and high metabolic degradation rate. To overcome these limitations, curcumin **(3)** and its derivatives/analogues/conjugates have been prepared with different ligands such as amino acids, carbohydrate (mainly glucose), nanoparticles, liposome and metal complexes. Curcumin **(3)** alone and in association with other modified forms has been shown to have effective neuroprotective [59], anti-cytotoxicity, anti-angiogeneic [60], anti-diabetic [61], Antitumor, antioxidant, anticancer [62], anti-sexually transmitted infections [63], anti-inflammatory [64], anti-acidogenic, radioprotective, anti-esophageal, anti-nephrotoxicity, antimicrobial, anti-immune modulatory, antiviral, and anti-proliferative, hepatoprotective, antimalarial properties [65]. In short it is clear from the studies reported that curcumin **(3)** and its derivatives were highly bioactive and can be used as novel drugs in future. Curcumin **(3)** and its analogues as anti-cancer and anti-microbial agents has been summarized [66]. On the basis of literature, synthetic pure curcumin has used *in vitro* studies, while most *in vivo* studies and clinical trials use curcuminoid mixture.

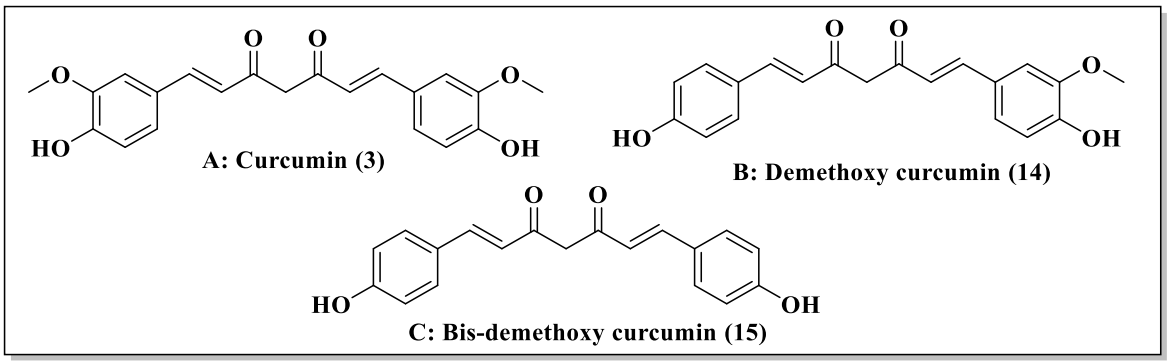

Figure 1.3. Structure of curcuminoids.

The dynamic nature of solubilized curcumin **(3)** makes it challenging to consider it a single compound *in vitro* or *in vivo*. From a drug discovery viewpoint, curcumin **(3)** appears to have numerous attractive qualities. There are many publications reporting a wide variety of biological activities for the compounds, which is "generally recognized as safe" by the FDA approved as a food additive at levels up to 20 mg per

allocation [67]. This designation, along with the long historical and cultural use of turmeric as a medication, has contributed to its popularity as a dietary supplement marketed for many common ailments.

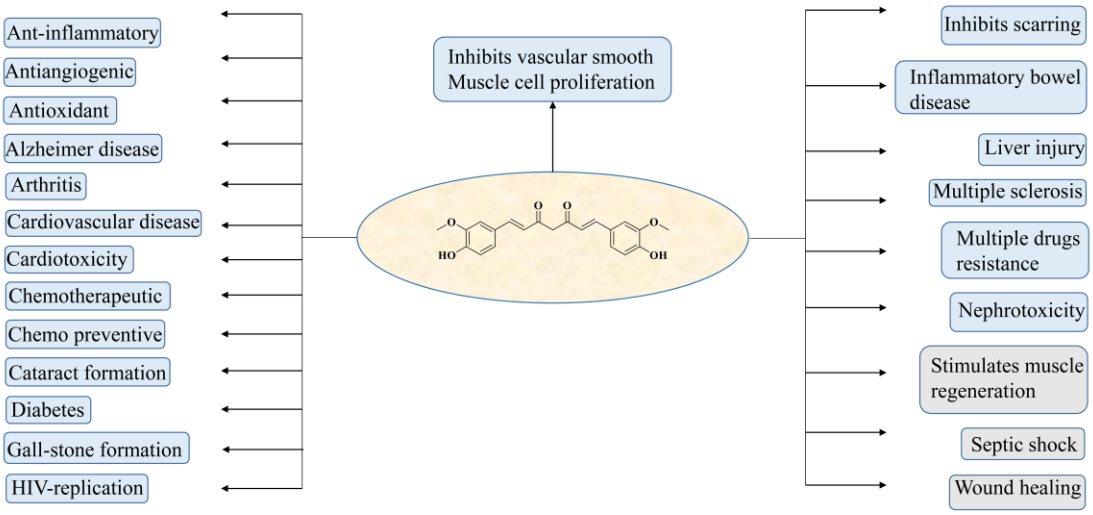

Figure 1.4. Therapeutic properties of curcumin **(3)**.

Sales of curcumin **(3)** supplements in the United States were reported to exceed $20 million in 2014, though a precise number is difficult to estimate [68].

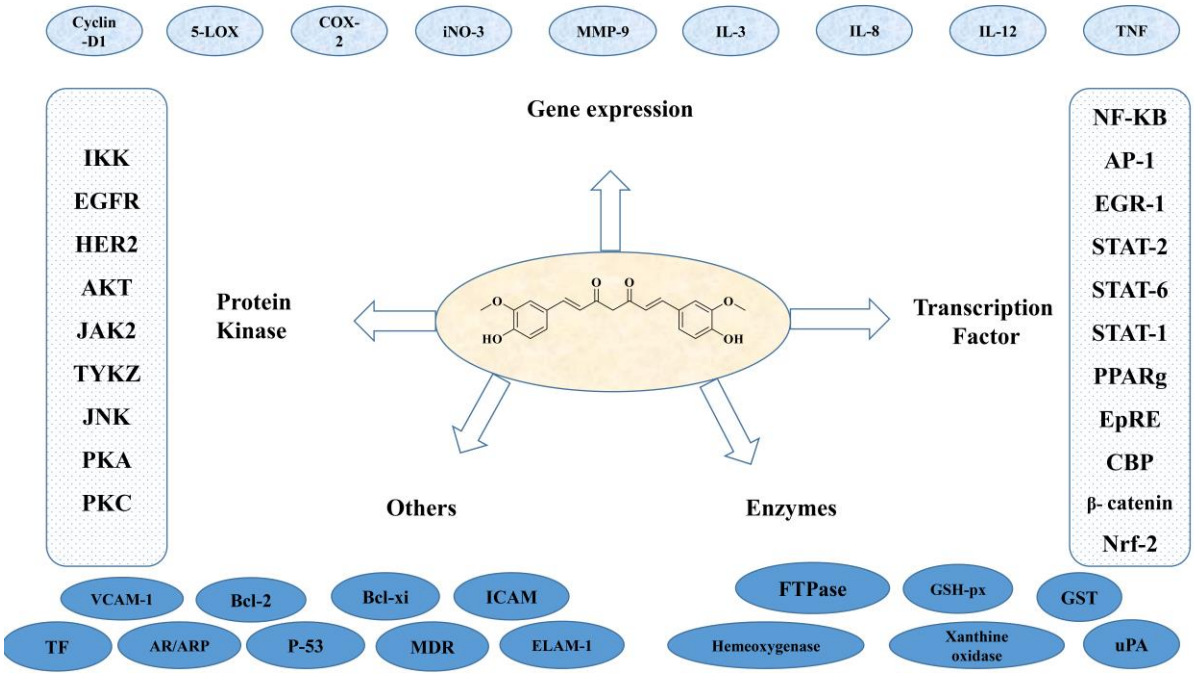

Figure 1.5. Molecular targets of curcumin **(3)**.

1.2. Bioinformatics and drug discovery:

Greatest achievement of Bioinformatics methods is the Human Genome Project (HGP) [69]. In post genomic area Bioinformatics is effected in several ways, genes from multiple species can be compared and conclusions drawn about evolution (comparative genomics). Computational genomics has been classified in three successive levels for management and analysis of genetic data in scientific data bases, **1.** Genomics **2.** Gene expression and **3.** Proteomics Functional genomics, functional proteomics & structural genomics are gaining importance in the form of Systems Biology. There is general shift in emphasis on medical informatics i.e. management of all biomedical experimental data associated with specific patients or molecules from NMR, Mass spectroscopy to in vitro assays to clinical side effects.

Chemoinformatics is the application of informatics methods to solve chemical problems. Chemoinformatics & Bioinformatics have become integral parts of Drug Discovery Process [70]. Genes, DNA, RNA and proteins are all chemical compounds. Real progress in understanding structure, properties and functions of proteins, DNA, RNA is possible only if Chemoinformatics and Bioinformatics work together [71]. Genomic methods identify protein targets for novel drug development Chemoinformatics methods find new lead structures and optimize them into drug candidates. Cheminformatic methods are extensively utilized in *in silico* ADME (Absorption, Distribution, Metabolism and Elimination) prediction and related issues that help in the reduction of the late stage failure of compounds [72].

1.2. (a) The following are the main drug targets,

1. Proteins
2. Nucleic acids (DNA, RNA)
3. Lipids
4. Carbohydrates

Four types of regulatory proteins are primary drug targets,

a. Enzymes
b. Receptors
c. Carrier proteins
d. Ion channels

Drugs may be agonists or antagonists, agonists activate the receptors and antagonists may combine at the same site without causing activation [73]. Binding and activation are two distinct steps in generation of receptor-mediated response binding is governed by affinity of drug, activation of receptor is denoted by efficacy.

In silico drug design represents computational methods and resources that are used to facilitate the opportunities for future drug discovery [74]. *In silico* is a term involving Latin phrases *in vivo, in vitro,* and *in situ* [75]. Therefore, *in silico* drug design means rational design by which drugs are designed/discovered by using computational methods. Databases of chemical compounds are either publically accessible or proprietary. It is now possible to search for structures and properties of compounds in these databases containing millions of compounds within seconds. A recent development is creation of databases of billions of virtual molecules which do not exist, but can be synthesized. Zinc and bingo are two important data bases publically available which contain compounds of medicinal importance. ChemDraw, cosmos and ISIS/Draw are easy to use programs for drawing 2D structures. The following are some software programs used for drug designing (Table 1.2).

1.2. (b) Structure based drug design (SBDD):

Structure based drug design is involved between drug target and ligand structure [76]. Drug targets are a specific metabolic or cell signaling pathway that is known, to be related to a particular disease state. Drug targets are most often proteins and enzymes in these pathways [77]. Drug molecules are designed to inhibit, restore or otherwise modify the structure and behavior of disease related proteins and enzymes better known as biomarkers [78].

Table. 1.2. Computational method and softwares for drug design.

S. No.	Computational methods	Softwares
1.	Molecular modeling	Charmm, gromacs
2.	Homology modeling	Modeler, lomets
3.	Binding site prediction	sc-pdb, pocketome, pockdrug..
4.	Docking	Autodoc, dock, gold, PyRx
5.	Screening	Pharmer, catalyst, blaster
6.	Target prediction	Patchsearch, sea..
7.	Ligand design	Gandi, ludi, breed…
8.	Binding free energy estimation	Hyde, X-score..
9.	QSAR	cQsar, Seesar..
10.	ADMET	Volsurf, Alogps
11.	Schrodinger software has many modules …	

SBDD uses the known 3D geometrical shape or structure of proteins to assist in the development of new drug molecules. The 3D structure of protein targets is most often derived from X-ray crystallography or NMR techniques. X-ray and NMR methods can resolve the structure of proteins to a resolution of a few angstroms [79]. In case the structure of any protein is not known homology modeling is done with a known structure and similarity upto 85-90% is usually taken as feasible. The ligand structure is extracted from database and docked to the target protein using Autodock, PyRx, gold or Schrodinger or other relevant softwares. The following non-covalent interactions are studied.

Non-covalent Interactions:

1. Electrostatic (ionic)
2. Hydrogen bonding
3. Van der Waals
4. Hydrophobic

Molecular mechanics (dynamics) is the prediction of binding free energies for molecules. Based on these results of docking the lead molecules can be modified to

enhance their potency leading to discovery of new drugs. From active molecules pharmacophore can be designed, which can help in extracting not only molecules with known structures but also virtual molecules which can be synthesized and tested in vivo.

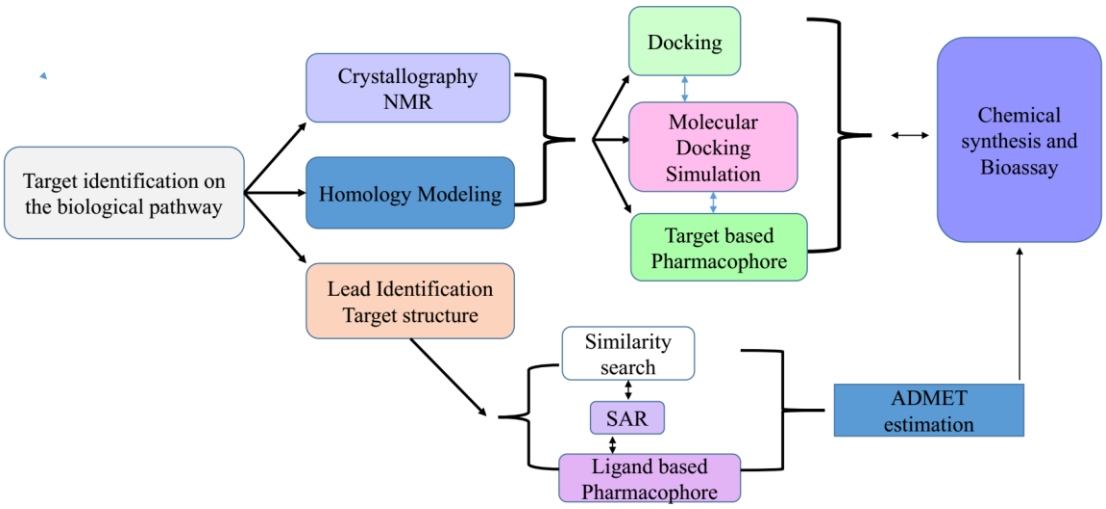

Figure 1.6. The sequential process of *in silico* drug design.

1.3. Present work:

Chapter 1 is introductory, gives history of drugs and therapeutic importance of Polyphenols. In chapter 2, Curcumin-4-*O*-β-monoglucoside **(24)** (CMG), and its 4,4'-di-*O*-glucoside **(27)** (CDG) have been prepared and tested against Rotenone (ROT) induced Parkinson's disease (PD) models *in vitro* and *in vivo*. These glucosides act via decreasing ROS level, improving intracellular Glutathione level, preventing dopamine depletion and inhibiting JNK mediated-caspase 3 dependent apoptosis. The advantage of CMG **(24)** is that while one free phenolic group of curcumin **(3)** contributes to its antioxidant activity, the glucoside moiety attached to the other phenolic helps in enhancing solubility, cellular uptake and bioavailability. The increase in glucose concentration in brain may also be proving helpful. According to our knowledge, this is the first report to show that CMG **(24)** has a protective effect in ROT-based PD models, suggesting that CMG **(24)** could offer better pharmacokinetics and pharmacodynamics compared to curcumin **(3)** in Parkinson's disease (PD).

Chapter 3 describes the synthesis of fourteen analogues of curcumin **(3)** designed for antibacterial activity against Gram positive and Gram negative bacteria. These analogues contain isoxazole, pyrazole, thiazole, thione, attached to the carbonyl functionality and phthalimide along with phosphate, sulphate and glucoside fragment attached to the hydroxyl group in the aromatic part of curcumin **(3)**. We planned synthetic route for these curcumin **(3)** based analogues in a way that would render an opportunity to access these natural products analogues in adequate amount enabling to explore their antibacterial properties and their mode of action on experimental level. All fourteen compounds were tested against *S. aureus and P. aeruginosa* for sensitivity, their MIC values and IC_{50} values were calculated. The results obtained have indicated that besides glycolysis i.e. cell wall damaging effect, other antibacterial mechanisms also appear to be operational.

From the results obtained it can be concluded that curcumin **(3)** analogues with the linker between two aromatic rings substituted with nitrogen containing heterocyclic rings e.g. isoxazole, pyrazole, thiazole, thione can prove to be much better drugs for antibacterial activity. Such molecules along with substituents like phosphate or sulphate substituted at one of the two phenolic hydroxyls of curcumin **(3)** can prove to be potent anti-inflammatory agents due to their multi-targeted effects. These compounds appear to act by some alternate mechanism too e.g. inhibiting cell division in addition to degradation of bacterial cell wall.

Chapter 4 contains the study of the effect of some polyphenols (flavonoids) on the hyphael growth in fungus *Candida albicans* leading to its pathogenicity. *C. albicans* is a friendly fungus residing in our body mainly gut, oral cavity and vagina. Under epigenetic conditions the gene modification in *C. albicans* leads to imbalance in human biome. In addition, the drug resistance and biofilm formation makes it a big concern to human health. In the present study the experiments have been conducted on four targets in major pathways leading to emergence of pathogenicity in *C. albicans*. The compounds that were found to have better affinity with all four targets viz. Efg1, Sap5, Erg11 and N-myristoyltransferase were 7-hydroxy-2H-chromen-2-one **(45)**, (*E*)-1,3-diphenylprop-2-en-1-one **(49)**, 2-(3,4-diacetoxyphenyl)-4-oxo-4H-chromene-3,5,7-triyltriacetate **(50)**, 4-(3,7-diacetoxy-5-hydroxy-4-oxo-4H-chromen-2-yl)-1,2-phenylene diacetate **(51)**, (1*E*,6*E*)-1,7-di(1H-indol-3yl) hepta-1,6-diene-3,5-

dione **(53)**, 2-(2,4-Difluorophenyl)-1,3-bis(1H-1,2,4-triazol-1-yl) propan-2-ol (Fluconazole). These polyphenols are safe alternative for toxic azoles. The polyphenols are naturally occurring antioxidants and can also be synthesized in laboratory. It has relevance in both ways as a drug or a supplement to help body in making a balance of biome. These will prove as better and safe alternative medicines in case of drug resistance of commercial azoles.

In chapter 5, we provide the details of α, β-unsaturated compounds synthesis by aldehyde and cyano ethyl acetate in the presence of 20 mol % sodium ethoxide in ethanol at rt. as well as 80-84 ^{0}C. And also stereoselective *Z*-isomers of oximes have been synthesized and evaluated for biological activity in cancer cell lines.

1.4. References:

1. J. Achan, A.O. Talisuna, A. Erhart, A. Yeka, J.K. Tibenderana, F.N. Baliraine, P.J. Rosenthal, U.D. Alessandro, Quinine, an old Anti-malarial Drug in a Modern World: Role in the Treatment of Malaria, Malaria Journal 10 (2011) 144–156.
2. C.J. Dillard, J. B. German, Review Phytochemicals: Nutraceuticals and Human Health, J. Sci. Food. Agric. 80 (2000) 1744–1756.
3. M. Wawer, L. Peltason, N. Weskamp, A. Teckentrup, J. Bajorath, Structure-Activity Relationship Anatomy by Network-like Similarity Graphs and Local Structure-Activity Relationship Indices, J. Med. Chem. 51 (2008) 6075–6084.
4. M.O.F. Khan, M.J. Deimling, A. Philip, Reviews: Medicinal Chemistry and the Pharmacy Curriculum, American Journal of Pharmaceutical Education 75 (2011) 161–171.
5. P.K. Mukherjee, A. Wahile, Integrated Approaches towards Drug Development from Ayurveda and other Indian System of Medicines, Journal of Ethnopharmacology 103 (2006) 25–35.
6. B.B. Petrovska, Historical Review of Medicinal Plants' Usage, Pharmacognosy Reviews 6 (2012) 1–6.
7. J.E. Buikstra, B.J. Baker, D.C. Cook, What disease plagues the ancient Egyptians? A century of controversy considered. In W. V. Davies and R. Walker, eds., Biological Anthropology and the Study of Ancient Egypt. London: British Museum (1993) Press. ISBN 0714109673.
8. Allen, Loyd, H.C. Ansel, Ansel's Pharmaceutical Dosage forms and Drug Delivery Systems, Lippincott Williams & Wilkins, 2013.
9. S.B. Yehoshua, C. Borowitz, L.O. Hanus, Frankincense, Myrrh, and Balm of Gilead: Ancient Spices of Southern Arabia and Judea, Horticultural Reviews 39 (2012) 1–76.
10. Saganuwan, A. Saganuwan, Some Medicinal Plants of Arabian Pennisula, Journal of Medicinal Plants Research 4 (2010) 766–788.
11. B. Patwardhan, R.A. Mashelkar, Traditional Medicine-inspired Approaches to Drug Discovery: can Ayurveda show the way forward?, Drug Discovery Today 14 (2009), 804–811.
12. F.R. Frankenburg, History of the Development of Antipsychotic Medication 17 (1994) 531–540.

13. M.R. Sahoo, S.P. Dhanabal, A.N. Jadhav, V. Reddy, G. Muguli, U.V. Babu, P. Rangesh, Hydnocarpus: Anethnopharmacological, Phytochemical and Pharmacological Review, Journal ofEthnopharmacology 154 (2014) 17–25.
14. K. Choudhary, M. Singh, U. Pillai, Ethnobotanical Survey of Rajasthan - An Update,
15. American-Eurasian Journal of Botany 1 (2008) 38–45.
16. A. Kaur, P. Nain, J. Nain, Herbal Plants Used in Treatment of Rheumatoid arthritis: A Review, Int. J. Pharm. Pharm. Sci. 4 (2012) 44–57.
17. N. H. Graham, Green Tea Composition, Consumption and Polyphenol Chemistry, Preventive Medicine 21(1992) 334–350.
18. Mishima, Saiichi, ed. The History of Ophthalmology in Japan. Vol. 10. Wayenborgh Publishing, 2018.
19. D.B. Kitchen, H. Decornez, J.R. Furr, J. Bajorath, Docking and Scoring in Virtual Screening for Drug Discovery: Methods and Applications, Nature Reviews Drug Discovery 4 (2004) 935–950.
20. Korolkovas, Andrejus, Essentials of medicinal chemistry, John Wiley & Sons, 2008.
21. Y. Caia, Q. Luob, M. Sunc, H. Corke, Antioxidant Activity and Phenolic Compounds of 112 Traditional Chinese Medicinal Plants associated with Anticancer, Life Sciences 74 (2004) 2157–2184.
22. A.R. Meuss, Herbal Medicine, 2000.
23. G.P. Asuncion, M.R. Marcos, R.G. Alejandro, V. Guillermo, V.N. Jose M, Ontologies in Medicinal Chemistry: Current Status and Future Challenges, Current Topics in Medicinal Chemistry 13 (2013) 576–590.
24. C. Lipinski, A. Hopkins, Navigating Chemical Space for Biology and Medicine, Nature 432 (2004) 855–862.
25. S.Z. Tasker, P.J. Hergenrother, Natural products: Taming Reactive Benzynes, Nat. Chem. 9 (2017) 504–506.
26. M. Lahlou, Screening of natural products for drug discovery, Expert Opin. Drug Discov. 2 (2007) 697–705.
27. T. Ashok Kumar, B. Rajagopal, PDTDB – An Integrative Structural Database and Prediction Server for Plant Metabolites and Therapeutic Drug Targets, Int. J. Curr. Res. 9 (2017) 46537–46541.
28. M. Lahlou, The Success of Natural Products in Drug Discovery, Pharmacol. Pharm. 04 (2013) 17–31.

29. T. Ashok Kumar, B. Rajagopal, Prediction of Potential Lead Molecules through Systematic Integration of Multi-omics Datasets - A Mini-Review, Int J Cur Res Rev 9 (2017) 26–31.
30. H. Yuan, Q. Ma, L. Ye, G. Piao, The Traditional Medicine and Modern Medicine from Natural Products, Molecules 21 (2016) 559–577.
31. J. Achan, A.O. Talisuna, A. Erhart, A. Yeka, J.K. Tibenderana, F.N. Baliraine, P.J. Rosenthal, U.D. Alessandro, Quinine, An Old Anti-malarial Drug in a Modern World: Role in the Treatment of Malaria, Malar. J. 10 (2011) 144–156.
32. M. Rottmann, C. Mcnamara, B.K.S. Yeung, Spiroindolones, A Potent Compound Class for the Treatment of Malaria, Science 329 (2010) 1175–1180.
33. C.R. Ganellin; Analogue-based Drug Discovery, John Wiley & Sons. p. 512. ISBN 9783527607495, from the original on (2016) 12–21.
34. C. Manach, A. Scalbert, C. Morand, C. Rémésy, L. Jime, Polyphenols: Food Sources and Bioavailability, Am. J. Clin. Nutr. 79 (2004) 727–747.
35. K.B. Pandey, S.I. Rizvi, Plant Polyphenols as Dietary Antioxidants in Human Health and Disease, Oxid. Med.Cell. Longev. 2 (2009) 270–278.
36. E.I. Omodanisi, Y.G. Aboua, O.O. Oguntibeju, Assessment of the Anti-hyperglycaemic, Anti-inflammatory and Antioxidant Activities of the Methanol Extract of Moringa oleifera in Diabetes-induced Nephrotoxic Male wistar rats, Molecules 22 (2017) 439.
37. K.C. Venkata, D. Bagchi, A.A. Bishayee, Small Plant with Big Benefits: Fenugreek (Trigonella foenum-graecum Linn.) for Disease Prevention and Health Promotion, Mol. Nutr. Food Res. 61 (2017) 1600950.
38. G.A. Odongo, N. Schlotz, C. Herz, F.S. Hanschen, S. Baldermann, S. Neugart, B. Trierweiler, L. Frommherz, C.M. Franz, B. Ngwene, The Role of Plant Processing for the Cancer Preventive Potential of Ethiopian kale (Brassica carinata), Food Nutr. Res. 61 (2017) 1271527.
39. J. Luo, Z. Wei, S. Zhang, X. Peng, Y. Huang, Y. Zhang, J. Lu, Phenolic Fractions from Muscadine Grape “Noble” Pomace can Inhibit Breast Cancer Cell MDA-MB-231 Better than those from European Grape “Cabernet Sauvignon” and Induces-phase Arrest and Apoptosis, Food Sci. 82 (2017) 1254–1263.

40. S. Franceschelli, M. Pesce, A. Ferrone, D. Maria, P. Gatta, A. Patruno, M.A. De Lutiis, L. Quiles, A. Grilli, M. Felaco, L. Speranza, Biological Effect of Licochalcone C on the Regulation of PI3K/Akt/eNOS and NF-B/iNOS/NO Signaling Pathways in H9c2 Cells in Response to LPS Stimulation, Int. J. Mol. Sci. 18 (2017) 690.
41. M. Sajid, M. Rashid, S. Afzal, M. Majid, H. Ismail, S. Maryam, T. Younis, Investigations on Anti-inflammatory and Analgesic Activities of Alnus nitida Spach (Endl). Stem Bark in Sprague Dawley rats, J. Ethnopharmacol. 198 (2017) 407–416.
42. P.R. Rodríguez, M. Figueiredo-González, C. González-Barreiro, J. Simal-Gándara, M. D. Salvador, B. Cancho-Grande, G. Fregapane, State of the Art on Functional Virgin Olive Oils Enriched with Bioactive Compounds and their Properties, Int. J. Mol. Sci. 18 (2017) 668.
43. L. Léotoing, F. Wauquier, M.J. Davicco, P. Lebecque, D. Gaudout, S. Rey, X. Vitrac, L. Massenat, S. Rashidi, Y. Wittrant, The Phenolic Acids of Agen prunes (dried plums) or Agen prune Juice Concentrates do not Account for the Protective Action on Bone in a Rat Model of Postmenopausal Osteoporosis, Nutr. Res. 36 (2016) 161–173.
44. J. An, D. Hao, Q. Zhang, B. Chen, R. Zhang, Y. Wang, H. Yang, Natural Products for Treatment of Bone-Erosive Diseases: The Effects and Mechanisms on Inhibiting Osteoclastogenesis and Bone Resorption, Int. Immunopharmacol. 36 (2016) 118–131.
45. R. Ben Mansour, M.K. Wided, S. Cluzet, S. Krisa, T. Richard, R. Ksouri, LC-MS Identification and Preparative HPLC Isolation of Frankenia Pulverulenta Phenolics with Antioxidant and Neuroprotective Capacities in PC12 Cell Line, Pharm. Biol. 55 (2017) 880–887.
46. A.G. Sarrías, M.Á. Núñez-Sánchez, F.A. Tomás-Barberán, J.C. Espín, Neuroprotective Effects of Bioavailable Polyphenol-Derived Metabolites Against Oxidative Stress-Induced Cytotoxicity in Human Neuroblastoma SH-SY5Y Cells, J. Agric. Food Chem. 65 (2017) 752–758.
47. O.M. Shaw, R.D. Hurst, J. L. Harper, Boysenberry Ingestion Supports Fibrolytic Macrophages with the Capacity to Ameliorate Chronic Lung Remodeling, Am. J. Physiol. Lung Cell. Mol. Physiol. 311 (2016) 628–638.
48. C.I.G. Gómez, R.F. González-Laredo, J.A. Gallegos-Infante, M.D. Pérez, M.R. Moreno-Jiménez, A.G. Flores-Rueda, N.E. Rocha-Guzmán, Antioxidant

and Angiotensin-converting Enzyme Inhibitory Activity of Eucalyptus camaldulensis and Litsea glaucescens Infusions Fermented with Kombucha consortium, Food Technol. Biotechnol. 54 (2016) 367–374.

49. V. Nobile, A. Michelotti, E. Cestone, N. Caturla, J. Castillo, O. Benavente-García, A. Pérez-Sánchez, V. Micol, Skin Photoprotective and Antiageing Effects of a Combination of Rosemary (Rosmarinus officinalis) and Grapefruit (Citrus paradisi) Polyphenols, Food Nutr. Res. 60 (2016) 31871.
50. F. Le Sage, O. Meilhac, M.P. Gonthier, Anti-inflammatory and Antioxidant Effects of Polyphenols Extracted from Antirhea borbonica Medicinal Plant on Adipocytes Exposed to Porphyromonas gingivalis and Escherichia coli lipopolysaccharides, Pharmacol. Res. 119 (2017) 303–312.
51. M. Forte, V. Conti, A. Damato, M. Ambrosio, A.A. Puca, S. Sciarretta, G. Frati, C. Vecchione, C. Carrizzo, Targeting Nitric Oxide with Natural Derived Compounds as a Therapeutic Strategy in Vascular Diseases. Oxid. Med. Cell. Longev. 2016 (2016) 7364138.
52. G.C. Tenore, D. Caruso, G. Buonomo, M. D'Avino, P. Campiglia, L. Marinelli, E. Novellino, A Healthy Balance of Plasma Cholesterol by a Novel Annurca apple-based Nutraceutical formulation: Results of a Randomized Trial, J. Med. Food 20 (2017) 288–300.
53. M. Jia, D. Ren, Y. Nie, X. Yang, Beneficial Effects of Apple Peel Polyphenols on Vascular Endothelial Dysfunction and Liver Injury in High Choline-fed Mice, Food Funct. 8 (2017) 1282–1292.
54. M.A. Ayub, A.I. Hussain, M.A. Hanif, S.A. Chatha, G.M. Kamal, M. Shahid, O. Janneh, Variation in Phenolic Profile-Carotene and Flavonoid contents, Biological Activities of two Tagetes Species from Pakistani flora, Chem. Biodivers. 14 (2017) 1600463.
55. T. Miyamoto, X. Zhang, Y. Ueyama, K. Apisada, M. Nakayama, Y. Suzuki, T. Ozawa, A. Mitani, N. Shigemune, K. Shimatani, Development of Novel Monoclonal Antibodies Directed Against Catechins for Investigation of Antibacterial Mechanism of Catechins, J. Microbiol. Methods 137 (2017) 6–13.
56. P. Alam, M.K. Parvez, A.H. Arbab, M.S. Al-Dosari, Quantitative Analysis of Rutin, Quercetin, Naringenin, and Gallic acid by Validated RP- and NP-HPTLC Methods for Quality Control of Anti-HBV Active Extract of Guiera senegalensis, Pharm Biol. 55 (2017) 1317–1323.

57. R. Kuttan, P. Bhanumathy, K. Nirmala, M.C. George, Potential Anticancer Activity of Turmeric (Curcuma longa), Cancer Lett. (N. Y., U. S.) 29 (1985) 197−202.
58. A. Niranjan, S. Singh, M. Dhiman, S.K. Tewari, Biochemical composition of Curcuma longa l. Accessions, Anal. Lett. 46 (2013) 1069–1083.
59. Y. Liu, R. Dargusch, P. Maher, D. Schubert, A Broadly Neuroprotective Derivative of Curcumin, Journal of Neurochemistry 105 (2008) 1336–1345.
60. B.K. Adams, E.M. Ferstl, M.C. Davis, M. Herold, S. Kurtkaya, R.F. Camalier, M.G. Hollingshead, G. Kaur, E.A. Sausville, F.R. Rickles, J.P. Snyder, D.C. Liotta, M. Shojia, Synthesis and Biological Evaluation of Novel Curcumin Analogs as Anti-cancer and Anti-angiogenesis Agents, Bioorganic& Medicinal Chemistry 12 (2004) 3871–3883.
61. M.T.A. Aziz, M.F E. Asmar, I.N. E. Ibrashy, A.M. Rezq, A.L.A. Malki, M.A. Wassef, H.H. Fouad, H.H. Ahmed, F.M. Taha, A.A. Hassouna, H.M. Morsi, Effect of Novel Water Soluble Curcumin Derivative on Experimental Type- 1 Diabetes mellitus (short term study), Diabetology & Metabolic Syndrome 4 (2012) 30–40.
62. V. Basile, E. Ferrari, S. Lazzari, S. Belluti, F. Pignedoli, C. Imbriano, Curcumin Derivatives: Molecular Basis of their Anti-cancer Activity, Biochemical Pharmacology 78 (2009) 1305–1315.
63. C. Bablon, Florence, L. Zaneveld, D. Waller, Microbicidal Compositions and Methods and Use, (2005) U.S. Patent Application No. 10/850,456.
64. N. Chainani-Wu, Safety and Anti-Inflammatory Activity of Curcumin: A Component of Tumeric (Curcuma longa), The Journal of Alternative and Complementary Medicine 9 (2003) 161–168.
65. A. Amalraj, A. Pius, S. Gopi, Biological Activities of Curcuminoids, other Biomolecules from Turmeric and their Derivatives: A review, Journal of Traditional and Complementary Medicine 7 (2017) 205–233.
66. A. Singha, N. Kaurb, S. Sharma, P.M. SinghBedi, Recent Progress in Biologically Active Xanthones , J. Chem. Pharm. Res., 8 (2016) 75–131.
67. K.M. Nelson, J.L. Dahlin, J. Bisson, J. Graham, G.F. Pauli, M.A. Walters, The Essential Medicinal Chemistry of Curcumin, Miniperspective, J. Med. Chem. 60 (2017) 1620–1637.

68. A. Niranjan, D. Prakash, Chemical Constituents and Biological Activities of Turmeric (Curcuma longa l.) - a review, J. Food Sci. Technol. (New Delhi, India) 45 (2008) 109–116.
69. A. Bayat, Bioinformatics, BMJ 324 (2002) 1018–1023.
70. A. Varnek, I.I. Baskin, Chemoinformatics as a Theoretical Chemistry Discipline, Mol. Inf. 30 (2011) 20–32.
71. D.S. Wishart, C. Knox, A.C. Guo, S. Shrivastava, M. Hassanali, P. Stothard, Z. Chang, J. Woolsey, DrugBank: a Comprehensive Resource for in silico Drug Discovery and Exploration, Nucleic Acids Research 34 (2006) D668–D672.
72. H. Hoeltje, W. Sippl, D. Rognan, G. Folkers. Molecular Modeling, Basics Principles and Applications (John Wiley & Sons, Chichester, U.K, 2003).
73. R.R. Neubig, M. Spedding, T. Kenakin, A. Christopoulos, International Union of Pharmacology Committee on Receptor Nomenclature and Drug Classification. XXXVIII. Update on Terms and Symbols in Quantitative Pharmacology, Pharmacol Rev. 55 (2003) 597–606.
74. Saeidnia, Soodabeh, A. Manayi, M. Abdollahi. The pros and cons of the *in silico* Pharmaco-toxicology in Drug Discovery and Development, Int. J. Pharm. 9 (2013) 176–181.
75. A.L. Harvey, Natural Products in Drug Discovery, Drug Discovery Today 13 (2008) 894–901.
76. T.L. Blundell, Structure-Based Drug Design, Nature 384 (1996) 23-26.
77. E.C. Butcher, E.L. Berg, E.J. Kunkel, Systems Biology in Drug Discovery, Nature Biotechnology 22 (2004) 1253–1259.
78. S. Salomone, F. Caraci, G.M. Leggio, J. Fedotova, F. Drago, New Pharmacological Strategies for Treatment of Alzheimer's disease: Focus on Disease Modifying Drugs, Br. J. Clin. Pharmacol. 73 (2011) 504–517.
79. L.A. Vu, P.T.C. Quyen, N.T. Huong, *In silico* Drug Design: Prospective for Drug Lead Discovery, International Journal of Engineering Science Invention, 4 (2015) 60–70.

Chapter 2

Gram-scale synthesis of curcumin glucosides and their inhibitory effect towards neurotoxicity in Parkinson's disease

2.1. Introduction:

Parkinson's disease (PD), is a neurodegenerative chronic disease of the Central Nervous System (CNS), which is characterized by motor symptoms and non-motor symptoms. Most motor symptoms of PD has muscle tremor, rigidity, dyskinesias, and imbalances in body posture, slowness of voluntary movement and non-motor symptoms square measure deadpan face, soft voice, sensory system loss, mood disturbances, dementia, sleep disorders, and involuntary pathology, constipation, internal organ arrhythmias, and cardiovascular disease. The clinical symptoms of PD patients show degeneration of dopaminergic neurons of the substantia nigra and loss of transmitters in dopaminergic neurons within the striatum. The working of nigrostriatal dopaminergic neurons is low, whereas the operation of cholinergic neurons becomes dominant, that causes the event of movement disorders [1-3]. Recently investigators propose the hypotheses of the unhealthful mechanisms of PD as mitochondrial injury, inflammatory reactions, oxidative stress, excitant amino acid toxicity, stress, immune disorders, dopamine neurotransmitter transporter inactivation, abnormal deposition of α-synuclein, and cell programmed cell death. Most of the investigators urge that fibrillation and abnormal aggregation of α--synuclein is the key factor within the cascade of PD pathological actions. α-Synuclein is a soluble macromolecule pre synaptically expressed in CNS. In addition, a crucial pathological hallmark of PD is the presence of Lewy bodies (LBs) which are composed of α-synuclein. Ubiquitination of alpha-synuclein in Lewy bodies is a pathological event, thus α-synuclein might incorporate a shut relation with Parkinson's (PD) [4-6].

2.1. (a) Anti-PD medicines:

As the concern of ageing within the population becomes progressively outstanding, the incidence of PD can bit by bit increase, and it'll positively become one among the main diseases that threatens human health globally. Presently, anti-PD medicine square measure is classified into two major terms, in 1st cluster, the medicine have affected the dopaminergic neurons and in second cluster anticholinergic medicine. The representative drug that affects dopaminergic neurons is L-dopa **(16)**. It's still the clinically most popular drug for PD treatment (Figure 2.1).

This drug is primarily catalyzed by dopa decarboxylase within the brain, and is reborn as dopamine neurotransmitter, producing therapeutic effects. The representative anti-cholinergic drug, trihexyphenidyl, might block striatal cholinergic receptors and inhibit the excitability of cholinergic nerves. It may inhibit dopamine neurotransmitter uptake within the conjunction cleft to reinforce the operation of dopaminergic neurons that results in anti-paralysis agitans effects. The effect of the two commonest anti-PD medicine mentioned above involves severe adverse reactions like a rise in transaminases and extrapyramidal reactions. Therefore, these medicine cannot basically improve the degenerative method of dopaminergic neurons [35-37].

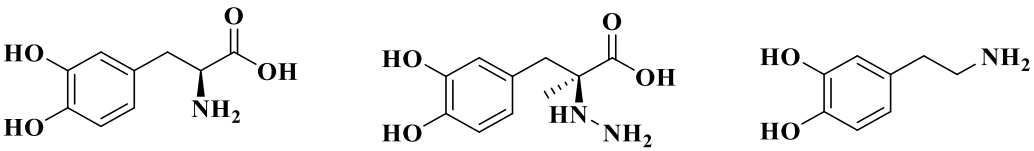

L-DOPA (16) **Carbidopa (17)** **Dopamine (18)**

Figure 2.1. Anti Parkinson's drugs.

In modern times, the pathological process of PD remains elusive. Genetic factors are confirmed for explanation of PD and, to some extent, participate in modifying the phenotypes of PD [38-40]. GBA gene, coding the lysosomal catalyst glucocerebrosidase (GCase), GBA cistron will raise the danger of PD [41-42]. PD is associated with age-related progressive neurodegenerative disorder characterized by the selective loss of neural structure (SN) dopamine neurotransmitterrgic neurons resulting in depletion of dopamine within the striate body [43].

2.1. (b) Neuroprotective effects of curcumin and analogues:

Recent research have highlighted the therapeutic potential of dietary polyphenols. Among these, curcumin (diferuloylmethane) **(3)**, obtained from the spice turmeric (*Curcuma longa*) has anti-oxidative, anti-inflammatory drug, anti-carcinogenic, hypocholesterolemic and wound healing properties [44-45]. Curcumin **(3)** displays neuroprotective effects in CNS diseases [46-48]. Curcumin **(3)** decreases neuro inflammation, astrocytic proliferation, oxidative stress and amyloid pathology in Alzheimer's disease (AD) [49-51]. Curcumin **(3)** scavenges reactive oxygen

species (ROS), inhibits supermolecule aggregation, induces neurogenesis [52-54] and exhibits neuroprotective properties in several experimental models of PD [55-56]. Curcumin **(3)** moderates varied therapeutic effects through suppression of NF-κB/IκB pathway, c-jun N-terminal kinase, cyclooxygenase2, Bcl-2 and Bcl-xL and is cellular inhibitor of necrobiosis protein-1 [57].

2.1. (c) Limitations of curcumin therapy:

Application of curcumin **(3)** is restricted because of its speedy metabolism and/ or biotransformation, general elimination, inefficient cellular uptake and transport across the blood brain barrier (BBB), low bioavailability and stability within the CNS [58-59]. To avoid this, liposomes, and micelles are used to extend the bioavailability of curcumin **(3)** [60-65]. Nanoparticle formulations have shown promising leads *in vitro*, however their efficaciousness *in vivo* is restricted [66-67]. Tiny molecular-weight surfactants, like cetyltrimethylammonium bromide (CTAB) [68-70], artificial amphiphilic polymers, like poly (ethylene glycol)-block-poly (caprolactone) [71] and methoxy poly (ethylene glycol)-palmitate [72], have additionally been used to encapsulate curcumin **(3)**. Curcumin **(3)** treatment as a lipid complex [73], and curcumin di piperoyl ester improved its bioavailability at intervals in the brain [74-75]. Earlier researchers tested the neuroprotective effects of bio conjugates of curcumin **(3)** against oxidative/nitrosative stress in cell models [76]. Our research group has shown that curcumin mono glucoside **(24)** inhibits agglomeration of α-Synuclein [77].

2.1. (d) Novel therapeutic molecules for PD:

The additionally used full robust exercise programs on PD, motor and non-motor symptom square measure controlled have been reported [78-84]. Foreseeable pharmacotherapies used to treat PD patients fill striatal dopamine neurotransmitter and delivered symptomatic relief. However, most of those medication don't have the capability to either halt or prevent the neurodegenerative method within the metallic element. Therefore, to explore anti-PD compounds that have a completely unique structure, high potency, and fewer facet effects has become a vital analysis direction within the field of neurodegenerative diseases. At present, exploration for leading

compounds in natural merchandise that have therapeutic functions has become important and therefore optimization of their structures became vital routes in fashionable medicinal chemistry analysis. So, with the steady improvement within the technologies employed for the isolation and purification of compounds, specific individual ingredients of natural merchandise are drawing attention as PD treatments. Hence, there's requisite for novel therapeutic molecules with neuroprotective ability that could be used as freelance or connected medical care beside dopamine neurotransmitter replacement as medical care in PD. The therapeutic molecules thus selected ought to be able to at the same time target multiple pathways and be non-toxic to humans at high concentrations.

2.2. Earlier methods of synthesis of curcumin (3) and its mono and di-glucosides (24, 27).

A large variety of synthetic approaches leading to the synthesis of curcumin **(3)** and its derivatives have been developed. For synthesis of curcumin **(3)** the general method involves use of vanillin **(21)** as a component along with acetyl acetone **(19)** and boron trioxide **(20)**. A boron complex is made in the first step by acetyl acetone **(19)** reacting with boron trioxide **(20)** the purpose of the complex is to reduce the reactivity of the methylene group between the carbonyls by making it less nucleofilic.

Due to the shielding, the terminal methyl groups will participate in the upcoming aldol reaction instead of the methylene by removing a hydrogen atom from one of the methyl groups, by using n-butyl amine, the carbon will act as a nucleophile on the carbonyl carbon in the vanillin **(21)** in an ordinary aldol condensation In this process a carbon- carbon bond is formed via aldol condensation involving n-butyl amine/tri-isopropyl borate [85] reaction mechanisms shown in (Figure 2.2) , 1,2,3,4-tetrahydroquinolin [86-88] , calcium hydroxide [89]. Another method to synthesize curcumin **(3)**, is by doing a microwave assisted reaction with the same components as mentioned above, by using a domestic microwave oven. The method is more rapid and environmental friendly than the conventional heating as less or no solvent is needed. The yields of the desired product in microwave-assisted reactions are many times excellent. [90-91]. However, the drawback in these type of reactions are the

possible overheating and problems in finding the optimal time for termination of the irradiation.

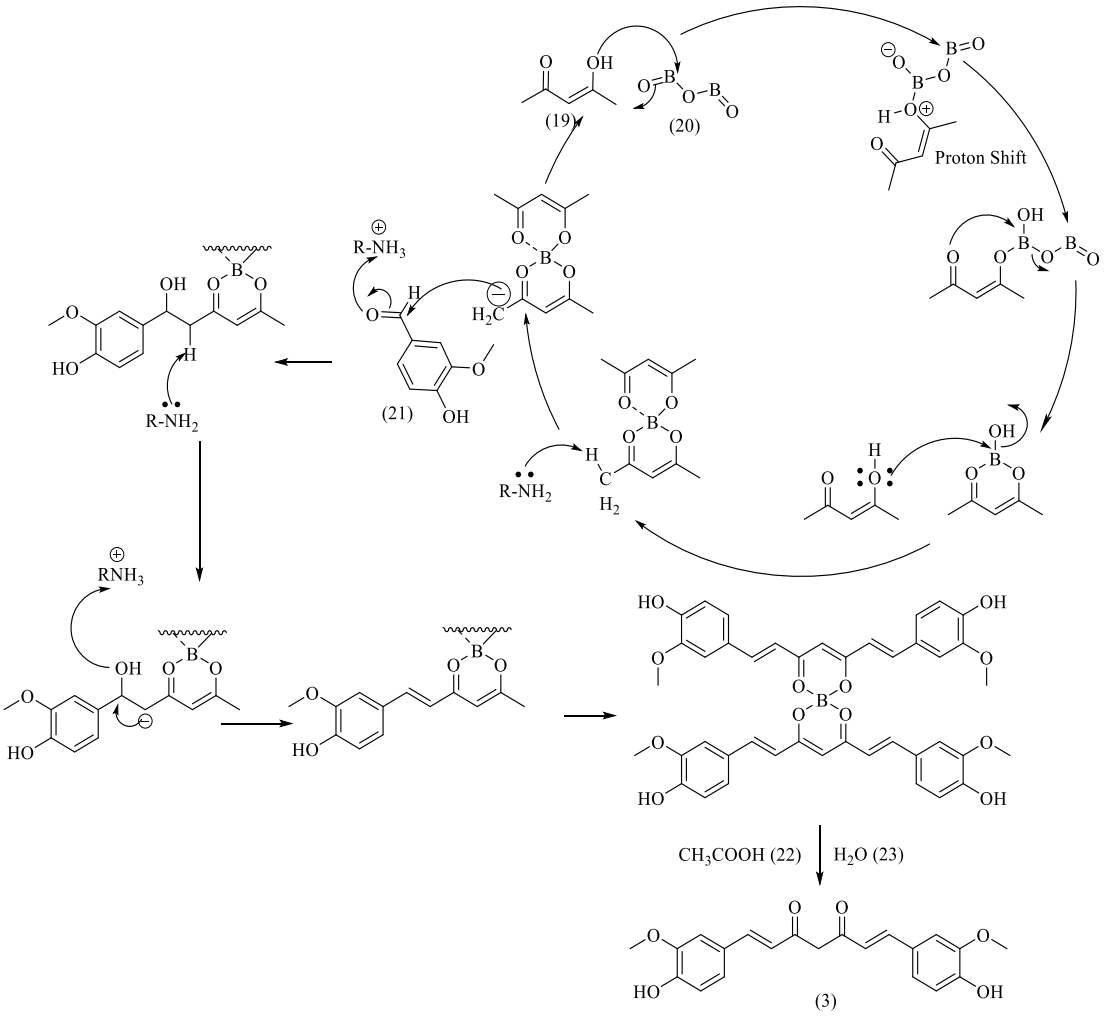

Figure 2.2. Mechanism of the synthesis of curcumin from vanillin.

The synthesis of curcumin mono glucoside **(24)** and di glucoside **(27)** by enzymatic process (almond β-D-glucosidase) [92], *Strophanthus gratus* cell culture [93], aldol condensation reaction [94], and the nucleophilic substitution reaction (S N-2) [95]. However, few of the general and efficient methods used recently for the preparation of curcumin **(3)** and curcumin mono **(24)** and di glucoside **(27)**, are described briefly below.

2.2. (a) Synthesis of curcumin by Aldol condensation with vanillin and acetyl acetone:

Aldol condensation processes for synthesis of curcumin **(3)** has been reported by H.J.J. Pabon [85]. These authors carried out aldol condensation, using n-butyl amine which had a strong catalytic effect. This effect was increased by adding the amine in small portions during the reaction. The best yield of curcumin **(3)** was obtained by using ethyl acetate as a solvent and tri-isopropyl borate (1.5-2 moles) for 1 mole of vanillin **(21)**. (Scheme 2.1).

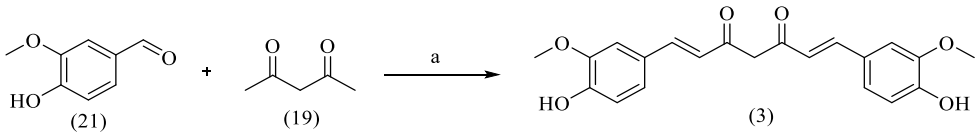

Reagent and condition: (a) Tri-isoproyl borate, n-butyl amine

Scheme 2.1. Synthesis of curcumin.

Babu et al [86] used 1, 2, 3, 4-tetrahydroquinoline, boric acid and DMF at room temprature for 4h. However, 20 % aqueous acetic acid was used for cleaving the Boron complex to give curcumin **(3)** (Scheme. 2.2).

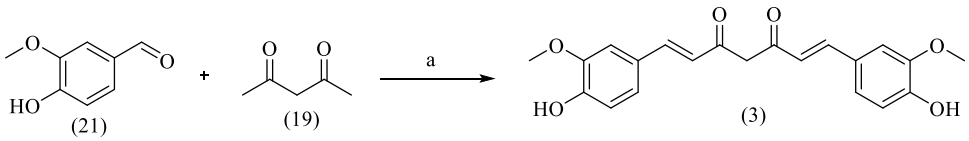

Reagent and condition:(a) DMF, boric acid, tetrahydro quinoline, AcOH, 100°C, 4h, H_2O.

Scheme 2.2. Synthesis of curcumin.

Kulkarni P. S. et al [89] carried out the reaction of acetylacetone **(19)** with calcium hydroxide to make a complex, which inhibited reactive methylene group in acetyl acetone **(19)**. After addition of vanillin **(21)**, the condensation of acetyl acetone-calcium complex with vanillin **(21)** resulted in additional elimination reaction. Subsequent addition of dil. HCl cleaved the Ca complex to give the curcumin **(3)** (Scheme 2.3).

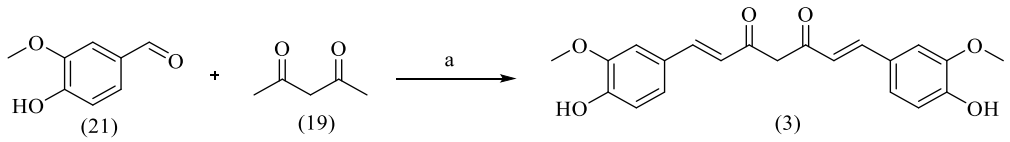

Reagent and condition: (a) $Ca(OH)_2$, 3 Mol, DMF, 110°C, 16h, HCl

Scheme 2.3. Synthesis of curcumin.

2.2. (b) Curcumin glucosides by enzymatic reaction.

Shimoda K. et al. [92-93] synthesized curcumin 4'-*O*-β- D-glucopyranoside **(24)** by almond β- D-glucosidase-catalyzed reverse-hydrolysis in 19% yield. They also used *Strophanthus gratus,* for glucosidation of curcumin **(3)** (Scheme.2.4).

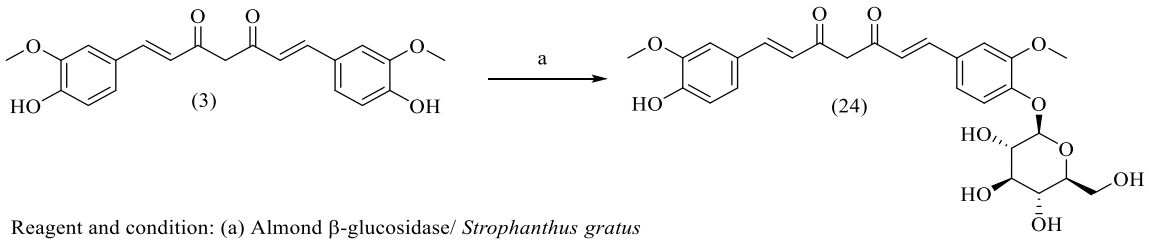

Reagent and condition: (a) Almond β-glucosidase/ *Strophanthus gratus*

Scheme 2.4. Synthesis of curcumin 4'-*O*-β- D-glucopyranoside **(24).**

2.2. (c) Curcumin glucosides synthesized by nucleophilic substitution reaction (SN-2).

Curcumin 4'-*O*-β-D-glucopyranoside **(24)** and curcumin 4,4'-*O*-β-D-diglucopyranosides **(27)** were synthesized from acetobromoglucose **(25)**, which was reacted with vanillin **(21)** followed by nucleophilic substitution reaction with base and phase transfer catalyst, to yield tetra-*O*-acetyl-β-D-glucopyranosylvanillin **(26)**. Tetra-*O*-acetyl-β-D-glucopyranosylvanillin **(26)** underwent aldol condensation with acetylacetone boron trioxide complex to give symmetrical curcumin glucoside and produced unsymmetrical curcumin as major products [94], shown below (Scheme 2.5).

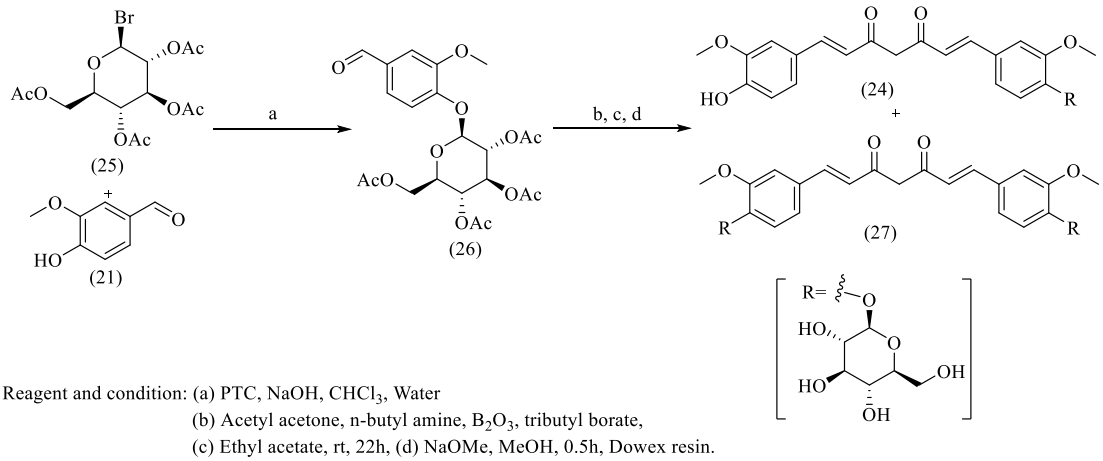

Scheme 2.5. Synthesis of curcumin 4'-*O*-β-D-glucopyranoside **(24)** and curcumin 4,4'-*O*-β-D-diglucopyranosides **(27)**.

2.3. Basis of present work:

As discussed in chapter 1, curcumin **(3)** and several of its derivatives exhibit wide range of biological activities and are key ingredients of many molecular targets of diseases. Therefore, it was thought to develop selective and efficient methods to synthesize curcumin **(3)** and its mono and di glucosides in order to evaluate these for Parkinson's disease (PD). The Phase transfer catalytic efficiency in organic synthesis for certain reactions has also been evaluated. Although there is a significant amount of information available on the synthesis of curcumin **(3)**, considerably less of this is available for the synthesis of its glucosides specifically mono glucoside of curcumin **(24)**. Curcumin **(3)** mitigates varied therapeutic effects through suppression of NF-κB/IκB pathway, c-jun N-terminal kinase, cyclooxygenase 2, Bcl-2 and Bcl-xL and cellular inhibitor of apoptosis protein-1. Keeping in mind the above facts and in continuation of our effort to develop a new generation for cure of Parkinson's disease (PD) we carried out the present work. Curcumin **(3)** crosses the blood brain barrier (BBB) and along with it excess entry of glucose in brain might be helpful in mitigating the effect of PD. Glucose moiety may also enhance the bioavailability of curcumin **(3)** was the concept. Their PTC catalytic efficiency in organic synthesis for certain reactions has also been evaluated.

2.4. Objective of the present work:

The present work describes the synthesis of curcumin **(3),** Curcumin 4'-*O*-β-D-glucopyranoside **(24)** and curcumin 4,4'-*O*-β- D-diglucopyranosides **(27)** by relevant modifications wherever necessary. Phase transfer catalyst (PTC), base and solvents have been changed wherever necessary. Symmetric aldol condensation reaction as well as nucleophilic substitution reaction have been used for their preparation. Subsequently their biological evaluation against Parkinson's disease (PD) has been carried out.

2.5. Materials and Methods:

Commercially available reagent grade chemicals were used as received. All reactions were followed by TLC on Merck, with detection by UV light and/or spraying 20% $KMnO_4$ aqueous solution, PMA, by spraying with an ethanolic H_2SO_4 followed by heating at 120 °C for 10 min. Column chromatography was performed on Silica Gel (100–200 mesh size). IR spectra were recorded as a neat chloroform, methanol solution or KBr palate with a Perkin-Elmer Spectrum RX-1 (4000-450 cm^{-1}) spectrophotometer. The ^{1}H and ^{13}C NMR spectra were recorded on a Bruker 400, 800MH_Z in (Dutreted) chloroform, methanol, dimethylsuphoxide chemical shift values in ppm relative to $SiMe_4$ as internal reference, signals are reported as s (singlet), d (doublet), t (triplet), m (multiplet); *J* in Hz. Mass spectra (LCMS) were performed by the Mass Spectrometer (MODEL).

2.6 . Experimental:

2.6. (a) Chemical synthesis and spectroscopy:

Synthesis of curcumin (3):

A mixture of vanillin **(21)** (60.8 g, 0.4 mol), boric acid (24 g, 0.38 mol), *m*-xylene (13.2 g), acetylacetone **(19)** (20.8 g, 0.21 mol) and n- butyl amine (1.9 ml, 0.02 mol) were dissolved in dimethyl formamide (70 ml) and refluxed in dean stark apparatus under reduce pressure (18 mm Hg) at 58-62°C for 2 h. The mixture of n-butyl amine (0.8 ml, 0.01 mol) in DMF (20 ml) was added to the reaction mixture and refluxed for

2 h. The completion of reaction was checked with TLC. The reaction mixture was diluted with mixture of acetic acid (110 ml) and water (20 ml). This solution was slowly added to the round bottom flask containing 540 ml water and 60 ml acetic acid stirred at 80°C for 2 h, cooled to room temperature and filtered, washed with cold water, and the crude product crystallized from methanol and found pure orange powder curcumin (**3**) [37]. Yellow crystals solid; yield 55 g, 71%; R*f* 0.51 (40% ethyl acetate:hexane) mp.182-183°C); IR (KBr) υmax (cm^{-1}) 3510, 3011, 1601, 1505. ^{1}H NMR (400 MHz, $CDCl_3$) δ 7.59 (d, *J* = 15.8 Hz, 2H), 7.12 (d, *J* = 8.1 Hz, 2H), 7.05 (s, 2H), 6.93 (d, *J* = 8.2 Hz, 2H), 6.48 (d, *J* = 15.8 Hz, 2H), 5.86 (s, 2H), 5.80 (s, 1H), 3.95 (s, 6H). ^{13}C NMR (101 MHz, $CDCl_3$) δ 183.28, 147.87, 146.80, 140.54, 127.72, 122.88, 121.81, 114.85, 109.66, 101.16, 77.33, 77.02, 76.70, 55.98 ppm; HRMS (ESI): Calculated for $C_{21}H_{20}O_6$ $[M+H]^+$: 369.1260, found 369.1292.

2.6. (b) Preparation of 1,2,3,4,6-pentacetyl-β-D-glucopyranose (29):

A mixture of D-glucose (50.0 g, 0.277 mol), acetic anhydride (283 g, 2.77 mol) and sodium acetate (30.0 g, 0.366 mol) were incubated with continuous stirring at 100°C for 5 h. The reaction was checked as described [35] and the product was crystallized from ethanol as white powder (yield 89 g, 82%; mp. 130°C).

2.6. (c) Preparation of 2,3,4,6- tetra-*O*-acetyl 1-bromo- D-glucopyranose (25):

To the solution of 1,2,3,4,6-pentacetyl-β- D-glucopyranose (60.0 g, 0.15 mol) in glacial acetic acid (120 ml), hydrobromic acid (150 ml, 33%) was added. The reaction mixture was incubated with continuous stirring at 5°C for 30 min followed by at room temperature for 5 h. The completion of reaction was checked and the crude product 2,3,4,6-tetra-*O*-acetyl 1-bromo-D-glucopyranose was crystallized from diethyl ether/petroleum ether as white crystalline solid (yield 58.70 g, 92%; mp. 86-88°C).

2.6. (d) Synthesis of 4-*O*-and 4,4′-di-*O*-(2,3,4,6-tetra-*O*-acetyl-D-glucosyl) curcumin (30), (31):

To stirred curcumin (4.08 g, 0.011 mol) in dichloromethane (75 ml), aqueous solution of KOH (75 ml, 15 %) was added followed by addition of benzyl tri butyl ammonium chloride (3.45 g, 0.011 mol), 2,3,4,6-tetra-*O*-acetyl-1-bromo- D-

glucopyranose (11.5 g, 0.02 mol) in dichloromethane (50 ml) and the reaction mixture was stirred for 5h at room temperature (25 ± 1°C).The completion of reaction was checked by TLC. The organic layer was separated and washed with 50 ml (0.1 N) NaOH solution, brine solution, and water, dried over sodium sulphate and concentrated under rotatory. The product obtained was a mixture of 4-*O*-(2,3,4,6-tetra-*O*-acetyl-D-glucosyl) curcumin **(30)** yield 2.5 g (25 %), mp. 86-88°C and 4, 4′-di-*O*-(2,3,4,6-tetra-*O*-acetyl-D-glucosyl) curcumin **(31)**with yield 5 g (44%), mp. 172-174°C. The mixture was separated on silica gel column and eluted with ethyl acetate: hexane (40:60 v/v) gradient [38-39].

4-*O*-(2,3,4,6-tetra-*O*-acetyl-D-glucosyl) curcumin (30):

Orange powder; yield 2.5 g, 25%; R*f* 0.4 (40% ethyl acetate: hexane), mp. 86-88°C; IR (KBr) υmax (cm^{-1}) 3419, 1750. ^{1}H NMR (800 MHz, $CDCl_3$) δ 7.59 (d, *J* = 15.7 Hz, 2H), 7.18–7.03 (m, 6H), 6.53 (d, *J* = 15.7 Hz, 2H), 5.36–4.97 (m, 4H), 4.29 (dd, *J* = 12.3, 5.0 Hz, 2H), 4.18 (dd, *J* = 12.3, 2.5 Hz, 2H), 4.01– 3.68 (m, 6H), 2.21–1.97 (m, 12H). ^{13}C NMR (201 MHz, $CDCl_3$) δ 183.06, 170.57, 170.25, 169.39, 169.31, 150.67, 147.63, 139.96, 131.45, 123.34, 121.56, 119.48, 111.45, 101.64, 100.22, 72.40, 72.00, 71.01, 68.21, 61.81, 56.02, 20.69, 20.61, 20.57 ppm; HRMS (ESI): Calculated for $C_{35}H_{38}O_{15}$ $[M+H]^+$: 699.2211, found 699.2245.

4, 4′- di-*O*-(2,3,4,6-tetra-*O*-acetyl-D-glucosyl) curcumin (31):

Orange powder; yield 5 g, 44%; R*f* 0.4 (40% ethyl acetate: hexane), mp. 172-174°C; IR (KBr) υmax (cm^{-1}) 3450, 1760, 1633. ^{1}H NMR (800 MHz, $CDCl_3$) δ 7.59 (d, *J* = 15.8 Hz, 2H), 7.17– 7.02 (m, 6H), 6.53 (d, *J* = 15.7 Hz, 2H), 5.84 (s, 1H), 5.37–4.97 (m, 10H), 4.24 (dd, *J* = 70.0, 3.8 Hz, 4H), 3.87 (s, 6H), 2.22–1.90 (m, 24H).^{13}C NMR (201 MHz, $CDCl_3$) δ 183.04, 175.20, 170.57, 170.24, 169.38, 169.31, 150.63, 147.60, 139.94, 131.41, 123.30, 121.54, 119.41, 111.43, 101.61, 100.17, 72.37, 71.97, 70.99, 68.19, 61.79, 55.99, 20.66, 20.58, 20.53 ppm; HRMS (ESI): Calculated for $C_{49}H_{56}O_{24}$ $[M+H]^+$: 1029.3162, found 1029.3199.

2.6. (e) Preparation of 4-*O*-(β-D-glucosyl) curcumin (24):

The reaction mixture of 4-*O*-(acetylated glucosyl) curcumin **(30)** (5 g, 0.007 mol) in dry methanol (100 ml), sodium methoxide (1.9 g, 0.03 mol) was added in to

reaction mixture, the solution stirred for 30 min at 0 °C. The completion of reaction was checked with TLC. The reaction mixture was neutralized with Dowex H^+ resin. The resin was filtered and the filtrate was concentrated under rotatory, at 20 °C. The crude product was purified on column chromatography, eluted with dichloromethane: methanol (85:15v/v). (**24**) Bright orange crystalline; yield 3.5g, 92 %; mp. R*f* 0.5 (15% methanol: dichloromethane) mp110–111°C. IR (KBr) υmax (cm^{-1}) 3400, 1629. ^{1}H NMR (800 MHz, Methanol-d_4) δ 7.59 (d, *J*= 15.8 Hz, 1H), 7.30–7.16 (m, 6H), 7.14– 7.10 (s, 1H), 6.83 (d, *J* = 8.2 Hz, 2H), 6.73–6.62 (m, 1H), 4.99 (d, *J* = 7.6 Hz, 1H), 3.96–3.86 (m, 6H), 3.76 (s, 1H), 3.5-3.40 (m, 5H). ^{13}C NMR (201 MHz, Methanol-d_4) δ 184.26, 182.29, 149.56, 149.14, 148.44, 148.00, 141.13, 139.72, 129.93, 127.08, 122.83, 122.38, 122.06, 120.86, 115.94, 115.16, 110.91, 110.29, 100.76, 76.88, 76.42, 73.39, 69.86, 61.05, 55.31, 55.02 ppm; HRMS (ESI): Calculated for $C_{27}H_{30}O_{11}$ $[M+H]^+$: 531.1788, found 531.1823.

2.6. (f) Preparation of 4,4'-*O*-di-(β- D-glucosyl) curcumin (27):

The 4,4'-*O*-di-(β-D-glucosyl) curcumin **(31)** was prepared *via* deacetylation with the help of methanolic solution of sodium methoxide (2.1 g, 0.038 mol) acetylated di glucoside curcumin (4g, 0.0039 mol) at room temperature. And neutralised with acedic dowex resin. Reaction was checked with TLC and the resulting reaction mixutr was purified with column chromatography. The structure was confirmed with the ^{1}H and ^{13}C NMR and LCMS spectra. Dark orange solid; yield 2.5g, 92 %; mp. R*f* 0.5 (20% methanol: dichloromethane) 154–156°C), IR (KBr) υmax (cm^{-1}) 3400, 1629.^{1}H NMR (400 MHz, DMSO-d_6) δ 7.59 (d, *J* = 15.8 Hz, 2H), 7.36 (d, *J* = 15.8 Hz, 2H), 7.25 (d, *J* = 8.4 Hz, 1H), 7.13 (d, *J* = 8.4 Hz, 2H), 6.85 (t, *J* = 15.8 Hz, 1H), 6.11 (d, *J* = 15.8 Hz, 1H), 5.32 (s, 2H), 5.14 (s, 2H), 5.07 (d, *J* = 5.0 Hz, 2H), 4.98 (t, *J* = 12.9 Hz, 2H), 4.59 (t, *J* = 5.3 Hz, 2H), 3.84 (s, 6H), 3.77 (s, 1H), 3.67 (d, *J* = 7.2 Hz, 3H), 3.28 (s, 2H). ^{13}C NMR (101 MHz, DMSO-d_6) δ 183. 24, 149.12, 148.53, 140.33, 128.64, 122.52, 115.10, 111.32, 101.21, 99.65, 77.11, 76.84, 73.12, 69.65, 60.65, 55.76 ppm. HRMS (ESI): Calculated for $C_{33}H_{40}O_{16}$ $[M+H]^+$: 693.2316, found 693.2346.

2.7. Bioassay:

2.7. (a) Cell culture and cell viability:

The N27 dopaminergic cell line used throughout the study was grown and maintained as described [40]. The cells were treated with freshly prepared ROT (prepared in DMSO and subsequently diluted in culture media) for 24 h with or without pretreatment with 4-*O*-(β-D-glucosyl) curcumin **(24)** and curcumin for 24 h. Cell viability was assessed using 3-(4,5-dimethylthiazol-2-yl)-2,5-diphenyltetrazolium bromide (MTT) assay [40] and LDH release assay [41]. After the treatment period, 10 µl of cell lysis solution (2 % Triton X-100) was added to the untreated cells to obtain 100 % cell death.

2.7. (b) Bioavailability of curcumin mono glucoside and curcumin in N27 Cells:

Levels of 4-*O*-(β-D-glucosyl) curcumin **(24)** (CMG) and curcumin (CUR) were estimated using high performance liquid chromatography (HPLC) with UV/Vis detector as described [42]. In brief, the cells treated with and without 4-*O*-(β-D-glucosyl) curcumin **(24)** or CUR were homogenized in 500 µl of ice cold sodium phosphate buffer (0.1 M; pH 6.8) containing 0.1 % EDTA and centrifuged at 2500×g for 10 min at 4 °C. The supernatant was sequentially extracted with methanol, hexane and ethyl acetate fraction. 4-*O*-(β-D-glucosyl) curcumin **(24)** or CUR was concentrated by removing ethyl acetate by vacuum evaporation and the residue was reconstituted in methanol. Twenty microliter of this sample was injected via injector into a C18 column of the HPLC system to separate the curcuminoids. The mobile phase consisting of 50 mM potassium dihydrogen orthophosphate (pH adjusted to 3.5 using orthophosphoric acid): acetonitrile (40:60 v/v) was pumped isocratically at a flow rate of 0.8 ml/ min. The detection was carried out using a UV-Visible detector at 424 nm. The retention time of 4-*O*-(β-D-glucosyl) curcumin (CMG) was 3.65 min while the retention time of bisdemethoxy curcumin, demethoxy curcumin and curcumin (**3**) (CUR) were 8.59, 9.25 and 10.02 min respectively. The Empower™ 3 software was utilized for integration.

2.8. Results & Discussion:

2.8. (a) Synthesis of curcumin and its glucosides:

Synthesis of curcumin was carried out by aldol condensation reaction of vanillin **(21)** and acetyl acetone **(19)** in the presence of n-butyl amine as a catalyst. Boric acid was used for blocking the reactivity of active methylene group in acetyl acetone **(19)**, under reduce pressure. DMF was used as solvent.

Table 2.1. The effect of solvent and pressure on preparation of curcumin **(3)**.

S. No.	Pressure (mm Hg)	Time (h)	Temperature (°C)	Yield (%)
1.	10	4	80	60
2.	15	4	80	63
3.	15	4	90	56
4.	18	4	90	50
5.	**18**	**4**	**58-62**	**71**

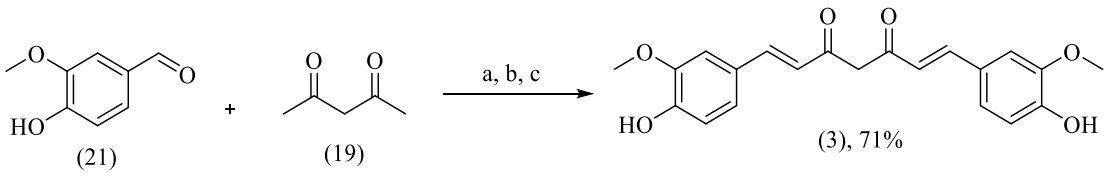

Reagent and condition: (a) n-Butylamine, DMF, *m*-xylene, boric acid, 58-62 °C, 4h
(b) Acetic acid, water, 80 °C, 2h (c) MeOH, reflux, 1h.

Scheme 2.6. Synthesis of curcumin **(3)**.

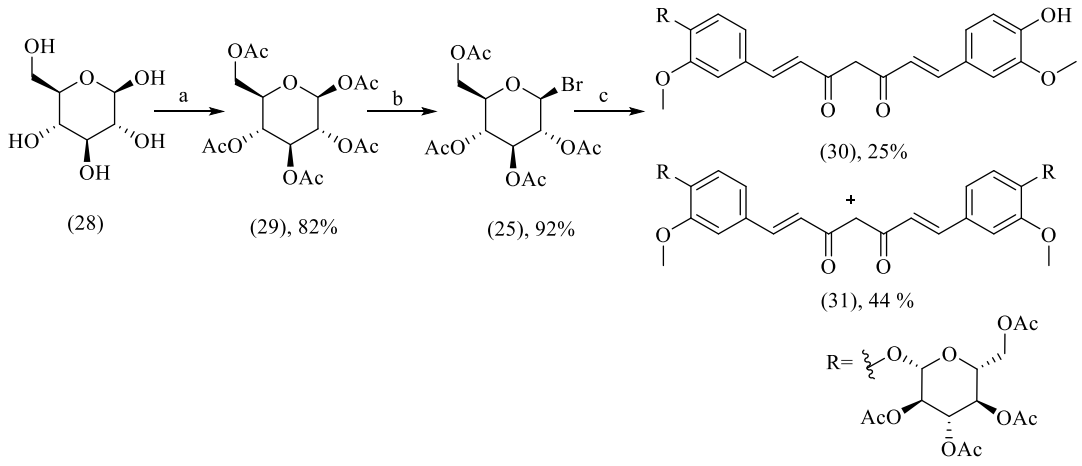

Reagent and condition: (a) Acetic anhydride, sodium acetate, 100 °C, 5h (b) HBr in acetic acid, acetic acid 5 °C, 30 min, rt, 5h (c) Curcumin, KOH, water, DCM, BTBACl, rt, 5h

Scheme 2.7. Synthesis of 4-*O* and 4,4-di-*O*-(2,3,4,6-tetra-*O*-acetyl-D-glucosyl) curcumin (30), (31).

The preparation of 1,2,3,4,6-pentacetyl-β-D-glucopyranose **(29)** was carried out by esterification of readily available D-glucose **(28)**. The latter on reaction with acetic anhydride in presence of sodium acetate gave 1,2,3,4, 6-Pentacetyl-β-D-glucopyranose **(29)**, which on halogenation with hydro bromic acid in glacial acetic acid afforded the corresponding of 2,3,4,6-tetra-*O*-acetyl 1-bromo- D-glucopyranose **(25)** in 92% yields. The bromo glucose ester **(25)** on selective nucleophilic substitution reaction with solution of curcumin in 15 % aqueous KOH, benzyl tributyl ammonium chloride (PTC), dichloromethane resulted in 4-*O*-(acetylated glucosyl)-CUR **(30)** yield (25%), and 4,4-di-*O*-(acetylated glucosyl) CUR **(31)** with yield (44%). The unreacted curcumin was separated with column chromatography.

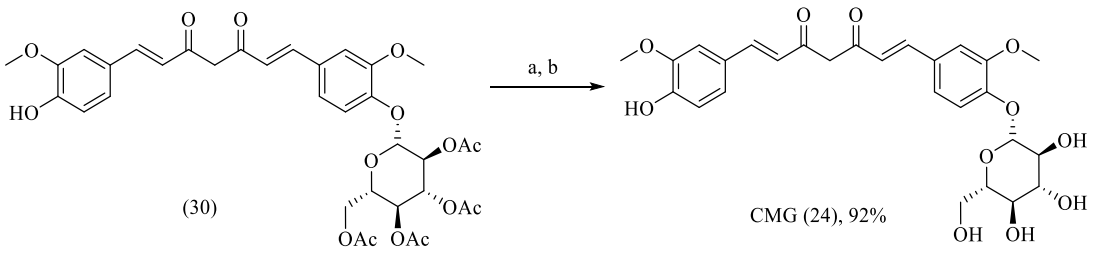

Reagent and condition: (a) NaOMe, MeOH, 0 °C, 30 Min (b) Dowex resin acidic, rt, 10 min.

Scheme 2.8. Synthesis of 4-*O*-(β-D-glucosyl) curcumin (CMG) **(24)**.

The synthesis of curcumin is shown in (Scheme 2.6.) curumin **(3)** was synthesized with vaniline **(21)** and acetyl acetone **(19)** through aldol condensation in presence of n-butyl amine and boric acid. On increasing temperature and reducing the pressure yield of curcumin was relatively reduced. m-Xylene was used for removing the water formed during the whole duration of reaction by making azeotropic mixture, the reaction components were the same as in conventional method, however reaction was carried out under reduced pressure with different solvents and with continuous removal of water during the reaction, thus making the reaction conditions more favourable for improved yield. We optimized condition for better yield of curcumin **(3)** as shown in (table 2.1). Relatively low temperature i.e. 58-62°C and high pressure (18 mm Hg) gave 71% yield. The glucose moiety was synthesized as pentacetate β- D-glucose **(29)** and then converted to acetobromoglucose **(25)** in the scheme 2.7). Curcumin **(3)** in the scheme 2.6) was treated with acetobromoglucose **(25)** to obtain a mixture of 4-*O*- and 4, 4'-di-*O*-(2,3,4,6-tetra-*O*-acetyl-D-glucosyl) CUR (**30** and **31** in the scheme 2.7). These two glucosides were separated on silica gel column and

characterized by ^{1}H NMR and ^{13}C spectra. The 4-*O*-(2,3,4,6-tetra-*O*-acetyl-D-glucosyl)-CUR **(30)** was deacetylated to obtain 4-*O*-(β-D-glucosyl) CUR **(24)** in the (Scheme 2.8), with 92% yield and was characterized by ^{1}H NMR and ^{13}C spectra. The glucoside was characterized as β-glucoside by enzymatic hydrolysis with β-glucosidase from almonds.

2.8. (b) Cytotoxicity of rotenone (ROT) and protective effect of curcumin (CUR) and 4-*O*-(β- D -glucosyl) curcumin (24) (CMG) against cell death:

Treatment of N27 cells with ROT (10-2000 nM) for 24 h caused neuronal death in a dose-dependent manner (Figure 2.3 A). Treatment with 500 nM ROT for 24 h caused 50% cell death and the same concentration was used for future experiments. Cells pre-treated with 4-*O*-(β- D -glucosyl) curcumin **(24)** or CUR (0.25 -5 μM) for 24 h were significantly protected against ROT (500 nM) at 5 μM of 4-*O*-(β-D-glucosyl) curcumin **(24)** and 1 μM of CUR (Figure 2.3 B and 2.3 C). These results were further confirmed by LDH release assay supporting the neuroprotective efficacy of 4-*O*-(β-D-glucosyl) curcumin **(24)** compared to CUR (Figure 2.3 D and 2.3 E).

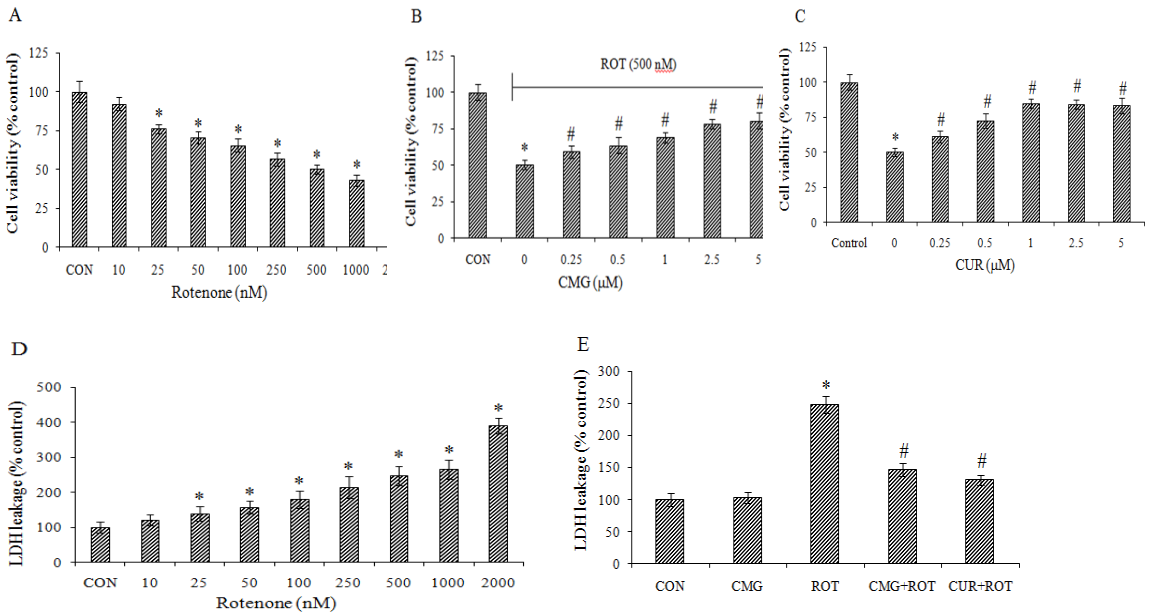

Figure 2.3. Neuronal death of N27 cells with rotenone and neuroprotective effect of curcumin **(3)** and 4-*O*-(β-D-glucosyl) curcumin **(24)**.

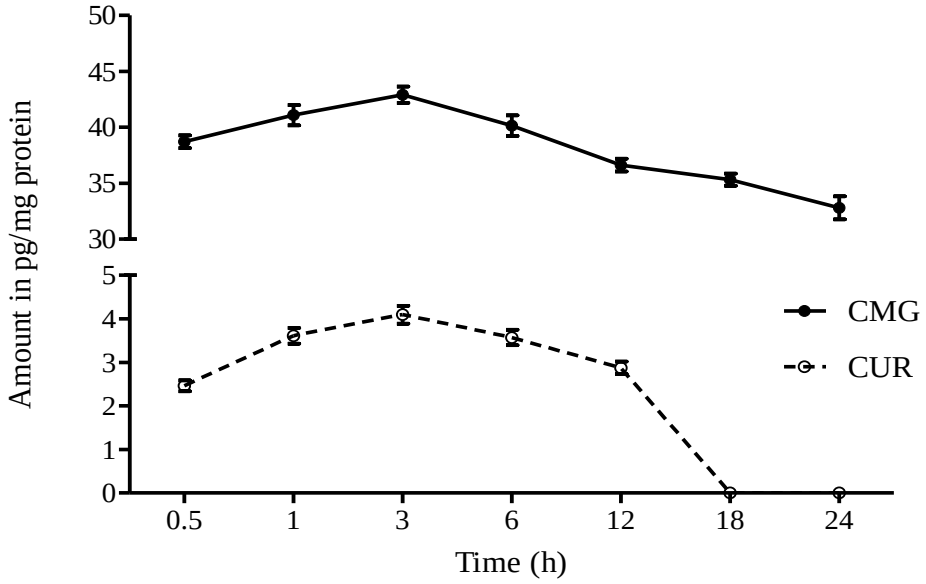

Figure 2.4. Bioavailability of curcumin **(3)** and 4-*O*-(β- D -glucosyl) curcumin **(24)** in N27 dopaminergic neuronal cells.

2.8. (c) Bioavailability of 4-*O*-(β-D-glucosyl) curcumin (24) (CMG) levels within N27 cells:

Next, we compared the bioavailability of 4-*O*-(β-D-glucosyl) curcumin **(24)** and CUR in N27 dopaminergic neuronal cells. N27 cells were treated with 4-*O*-(β-D-glucosyl) curcumin **(24)** and CUR (5 μM each) at different time intervals (0-24 h) followed by quantitation of their intra cellular levels (Figure 2.4). At 30 min time-point, the concentration of 4-*O*-(β-D-glucosyl) curcumin **(24)** and CUR were 38.72 ± 0.99 and 2.46 ± 0.12 pg/mg of protein respectively. The maximum level of CMG was found to be 42.92 ± 1.25 pg/mg protein after 3 h of treatment. While CUR levels drastically decreased after 18 h of treatment, 4-*O*-(β-D-glucosyl) curcumin **(24)** concentration was found to be 35.32 ± 0.93 and 32.80 ± 1.77 after 18 and 24 h of treatment respectively, indicating its increased transport across the cell membrane and availability in N27 cells compared to CUR (Figure 2.4).While curcumin **(3)** displays numerous health benefits, its low bioavailability due to low water solubility and rapid metabolism has been the major impediment in its in vivo application. Phase I clinical trials have shown that curcumin **(3)** exhibited poor oral bioavailability. During curcumin **(3)** metabolism, it undergoes sulfatation, methylation and glucuronidation

and these conjugated metabolites can be found in plasma after curcumin **(3)** injection. These metabolites show reduced bioactivity and are excreted. Consequently, enhancement of curcumin **(3)** bioavailability would be of utmost importance in order to exert therapeutic effects, in vivo.

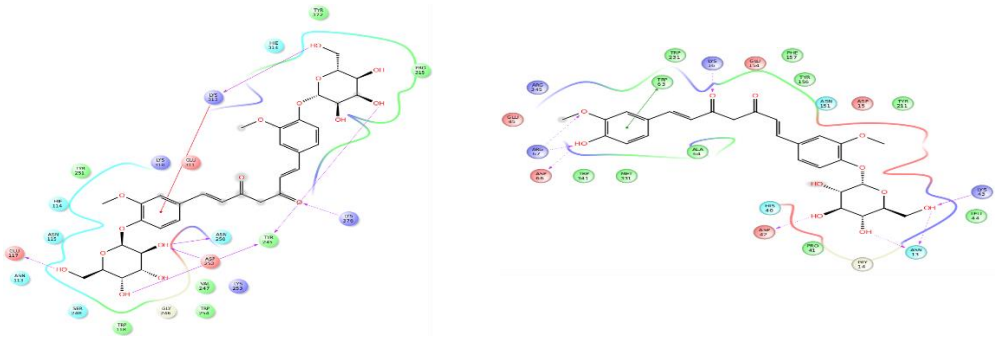

Figure 2.5. Docked conformation of 4,4'-*O*-di-(β-D-glucosyl) curcumin **(27)** and 4-*O*-(β-D-glucosyl) curcumin **(24)** against α-Synuclein (G-Score- -9.2)/ (G-Score -9.5).

Various attempts made to improve the bioavailability of curcumin **(3)** include improved intestinal absorption via absorption enhancers, novel delivery systems such as curcumin nanoparticles, liposomal curcumin or curcumin phospholipid complexes and improving metabolic stability via adjuvants such as piperine to prevent glucuronidation. In the current study, we synthesized curcumin derivative by blocking the phenolic group with glucose, through biodegradable glucosidic bond. Glycosylation improves the bioavailability by better solubility due to increased hydrophilicity and enhanced metabolic stability due to protection of phenolic hydroxyl groups. Previous study on 4-*O*-(β-D-glucosyl) curcumin **(24)** has investigated its effect on the *in vitro* aggregation of alpha synuclein. However, a comprehensive analysis of the neuroprotective properties of curcumin monoglucoside in a cell and fly model has not been conducted so far. Both 4-*O*-(β-D-glucosyl) curcumin **(24)** and 4,4'-*O*-di-(β-D-glucosyl) curcumin **(27)** of curcumin **(3)** were prepared in the current study. This approach could delay the metabolic degradation of curcumin **(3)** along with the accumulation of curcumin **(3)** and the desired ligand in the cell followed by the action of esterases. It is well known that the antioxidant activity of curcumin **(3)** is mainly due to its free phenolics. In silico docking of 4-*O*-(β- D -glucosyl) curcumin **(24)** and 4,4'-*O*-di-(β-D-glucosyl) curcumin **(27)** to the two most important molecular targets of PD viz. α-synuclein and cAbI indicated higher binding energy for 4,4'-*O*-di-(β-D-glucosyl) curcumin **(27)** as compared to 4-*O*-(β-D-

glucosyl) curcumin **(24)** and curcumin **(3)** (Figure 2.5, 6.) However our wet experiments showed that 4-*O*-(β- D -glucosyl) curcumin **(24)** is more active than 4,4'-*O*-di-(β-D-glucosyl) curcumin **(27)**. This can be explained by hypothesizing that although 4,4'-*O*-di-(β-D-glucosyl) curcumin **(27)** is more hydrophilic than 4-*O*-(β-D-glucosyl) curcumin **(24)**, both phenolics are blocked in the former and not readily available to scavenge free radicals necessary for the antioxidant property of curcumin **(3)**. According to literature reports, the water solubility of 4-*O*-(β-D-glucosyl) curcumin **(24)** (CMG) is 230 times higher than curcumin **(3)**. These results are in support with glycosylation of other compounds like genistein, where genistein-7-*O*-α-D-glucopyranoside showed fourfold increase in solubility (358 μM) at 25 °C, compared with genistein (90 μM). In the present study, we have shown the4-*O*-(β-D-glucosyl) curcumin **(24)** bioavailability within N27 cells was ~tenfold more compared to curcumin **(3)**. 4-*O*-(β-D-glucosyl) curcumin **(24)** levels remained high even after 24 h of treatment whereas curcumin **(3)** levels were below the detectable limits after 18 h of treatment (Figure 2.4). Apart from increased hydrophilicity and enhanced metabolic stability due to protection of phenoxyl groups, the cellular uptake could be enhanced since 4-*O*-(β-D-glucosyl) curcumin **(24)** could be taken up via glucose transporters.

2.9. Conclusion:

To summarize, our study demonstrates that 4-*O*-(β-D-glucosyl) curcumin **(24)** (CMG), a bioconjugate of curcumin **(3)** has better bioavailability than curcumin **(3)** itself and protects against rotenone (ROT) induced toxicity *in vitro* and *in vivo* via decreasing ROS level, improving intracellular Glutathione level, preventing dopamine depletion and inhibiting JNK mediated - caspase 3 dependent apoptosis. The advantage of 4-*O*-(β-D-glucosyl) curcumin **(24)** is that while one free phenolic group of curcumin **(3)** contributes to its antioxidant activity, the glucoside moiety attached to the other phenolic helps in enhancing solubility, cellular uptake and bioavailability. According to our knowledge, this is the first report to show that 4-*O*-(β-D-glucosyl) curcumin **(24)** has a protective effect in ROT-based PD models, suggesting that 4-*O*-(β-D-glucosyl) curcumin **(24)** could offer better pharmacokinetics and pharmacodynamics compared to curcumin **(3)** in Parkinson's disease (PD).

2.10. Spectral Data (^{1}H and ^{13}C):

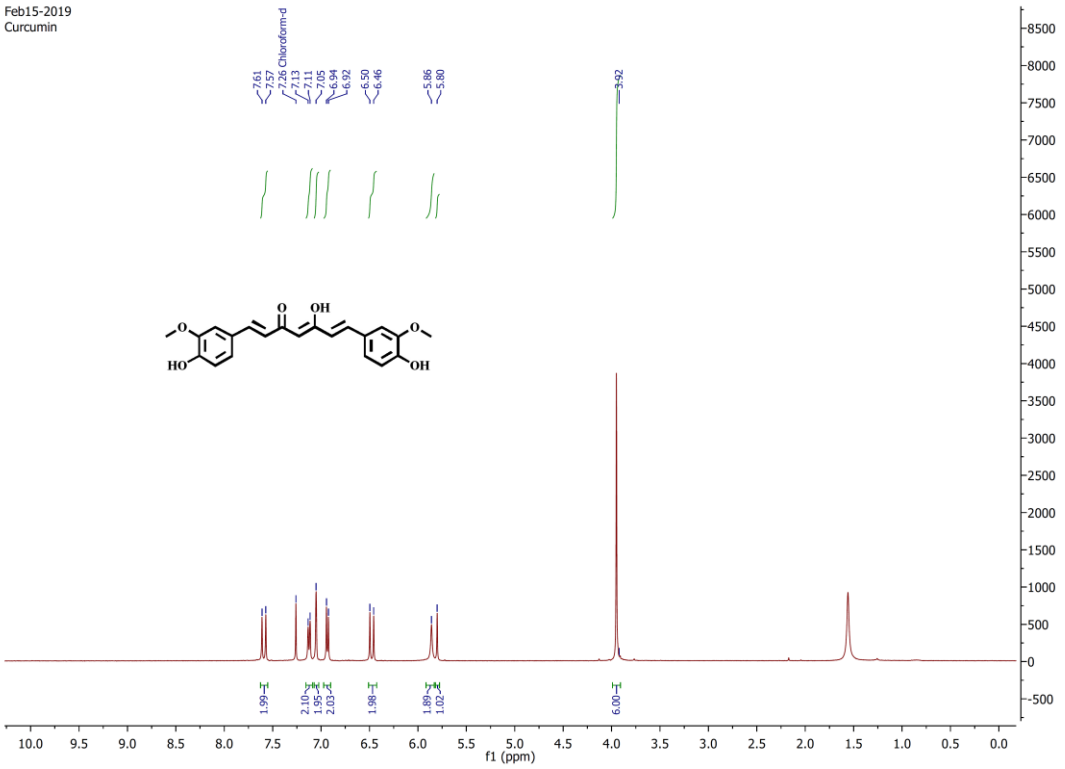

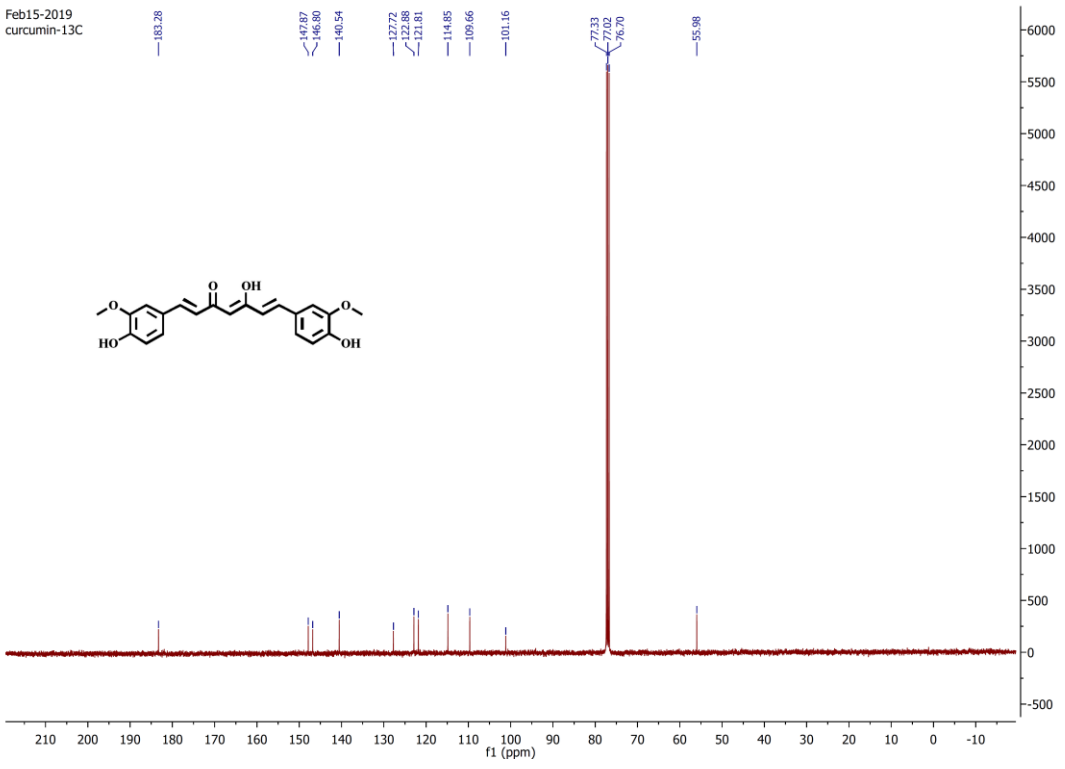

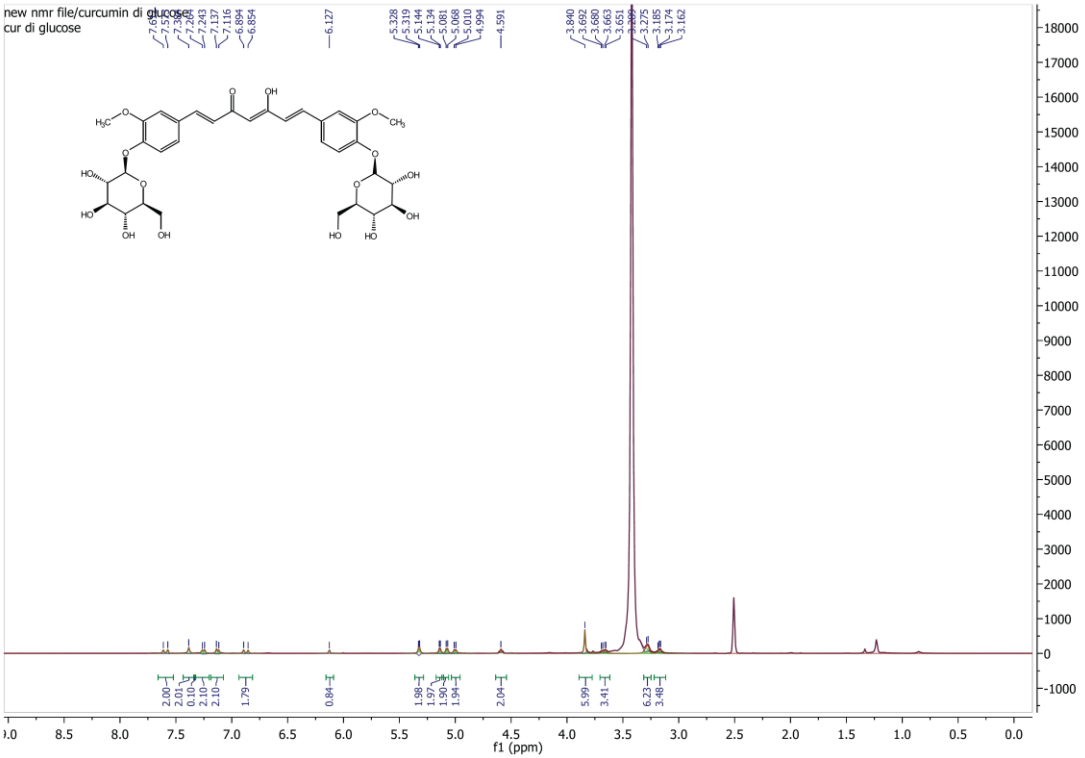
new nmr file/curcumin di glucose
cur di glucose
f1 (ppm)

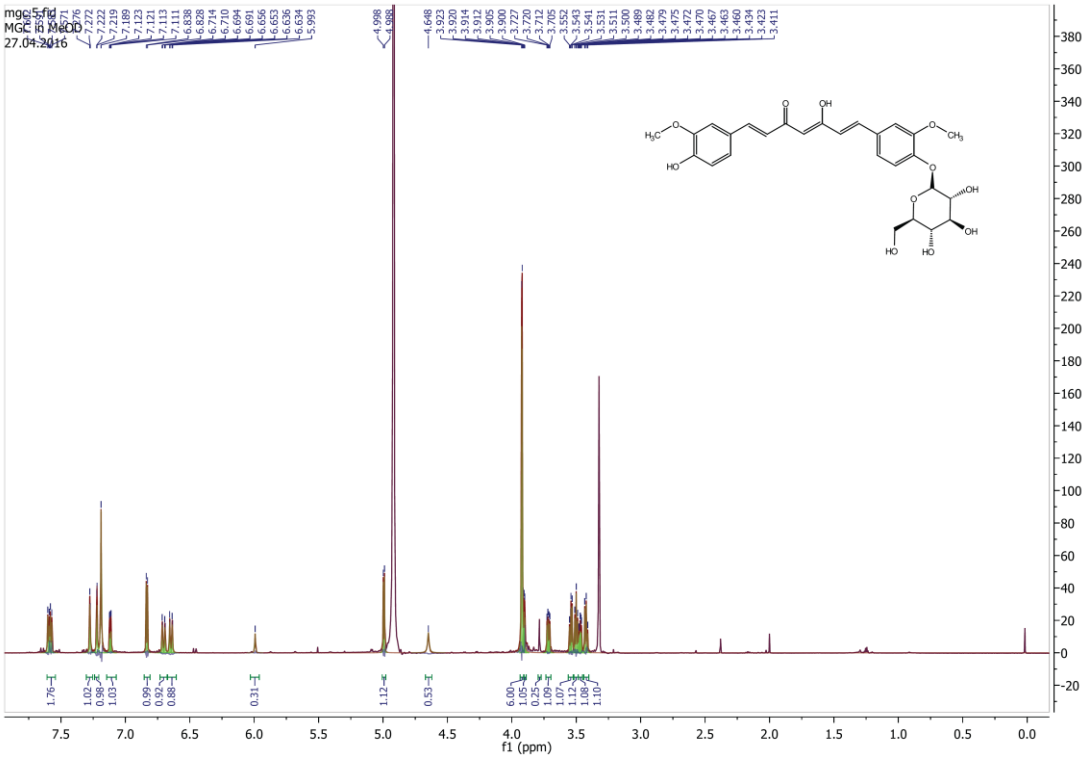
mgc-5.fid
MGC in MeOD
27.04.2016
f1 (ppm)

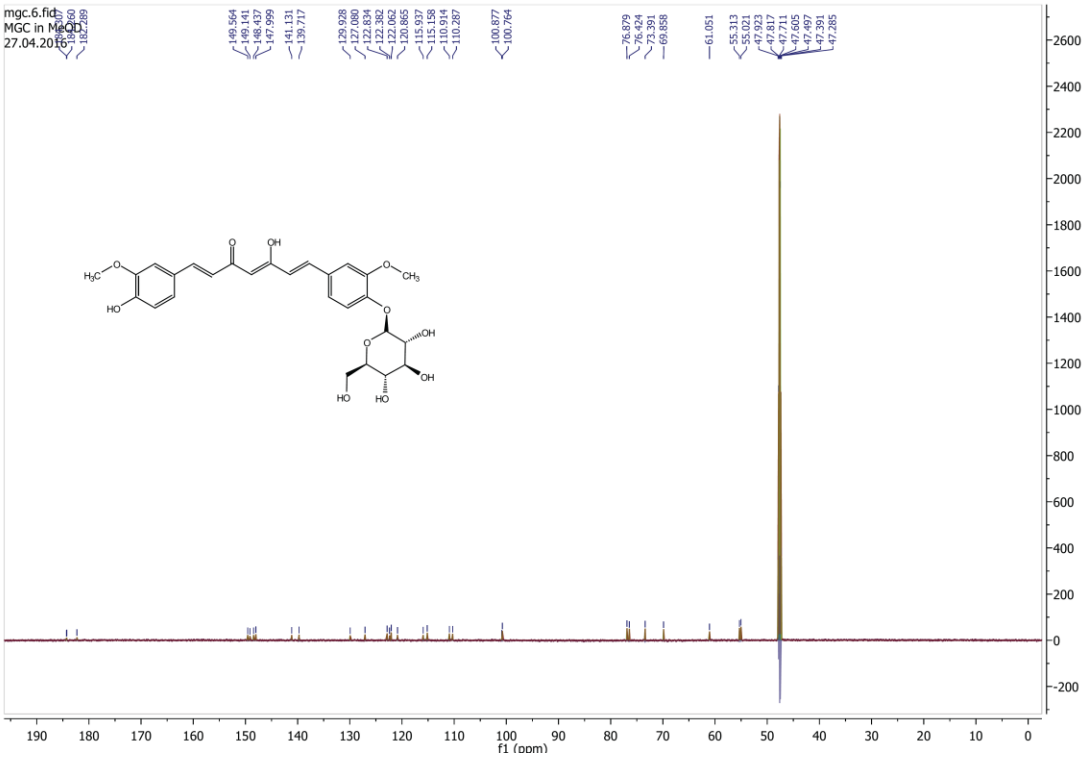
mgc.6.fid
MGC in MeOD
27.04.2016
149.564
149.141
148.437
147.999
141.131
139.717
129.928
127.080
122.834
122.382
122.062
120.865
115.937
115.158
110.914
110.287
100.877
100.764
76.879
76.424
73.391
69.858
61.051
55.313
55.021
47.823
47.817
47.711
47.605
47.497
47.391
47.285
f1 (ppm)

2.11. References:

1. W. Dauer, S. Przedborski, Parkinson's Disease: Mechanisms and Models, Neuron 39 (2003) 889–909.
2. S. Phani, J.D. Loike, S. Przedborski, Neurodegeneration and Inflammation in Parkinson's disease, Parkinsonism and Related Disorders, 18S1 (2012) S207–S209.
3. T. Pringsheim, N. Jette, A. Frolkis, T.D. Steeves, The Prevalence of Parkinson's Disease: A Systematic Review and Meta-analysis, Mov. Disord. Official J. Mov. Disord. Soc. 29 (2014) 1583–1590.
4. C.W. Olanow, D.R. Wakeman, J.H. Kordower, Peripheral Alpha-Synuclein and Parkinson's Disease, Mov. Disord. Official J. Mov. Disord. Soc. 29 (2014) 963–966.
5. L.V. Kalia, S.K. Kalia, α-Synuclein and Lewy pathology in Parkinson's disease, Curr. Opin. Neurol. 28 (2015) 375–381.
6. (a) G.K. Tofaris, A. Razzaq, B. Ghetti, K.S. Lilley, M. G. Spillantini, Ubiquitination of α-Synuclein in Lewy Bodies is a Pathological Event Not Associated with Impairment of Proteasome Function, J. Biol. Chem. 278 (2003) 44405–44411. (b) L. Stefanis, Alpha-Synuclein Aggregation and Synaptic Pathology in Parkinson's disease and Dementia with Lewy Bodies, Neurobiol. Aging 39 (2016). S1–S13.
7. A. Quesada, B.Y. Lee, P.E. Micevych, PI3 Kinase/Akt Activation Mediates Estrogen and IGF-1 Nigral DA Neuronal Neuroprotection Against a Unilateral Rat Model of Parkinson's Disease, Dev. Neurobiol. 68 (2008) 632–644.
8. K. Nakaso, S. Ito, K. Nakashima, Caffeine Activates the PI3K/Akt Pathway and Prevents Apoptotic Cell Death in a Parkinson's Disease Model of SH-SY5Y cells, Neurosci. Lett. 432 (2008) 146–150.
9. Y.M. Wang, Q.F. Cui, W.L. Zhao, J.Y. Zhang, H.Q. Wang, D.O. Oncology, Nrf2/ ARE/HO-1 Signaling Pathway is a New Neuroprotective Target for Parkinson's disease, Basic & Clin. Med. 34 (2014) 1125–1128.

10. T.P. Williamson, Activation of the Nrf2-are Pathway as a Therapeutic Strategy in Parkinson's disease, 2012, Dissertations & Theses - Gradworks.

11. H. Wilms, P. Rosenstiel, J. Sievers, G. Deuschl, L. Zecca, R. Lucius, Activation of Microglia by Human Neuromelanin is NF-κB-dependent and Involves p38 Mitogen-Activated Protein Kinase: Implications for Parkinson's disease, Faseb J. Official Publ. Fed. Am. Soc. Exp. Biol. 17 (2003) 500–502.

12. S.A. Correa, K.L. Eales, The Role of p38 MAPK and Its Substrates in Neuronal Plasticity and Neurodegenerative Disease, J. Signal Transduct. 2012 (2012) 649079.

13. Y. Wu, Y. Shang, S. Sun, H. Liang, R. Liu, Erythropoietin Prevents PC12 Cells from 1-methyl-4-phenylpyridinium Ion-induced Apoptosis via the Akt/GSK- 3b/caspase-3 Mediated Signaling Pathway, Apoptosis 12 (2007) 1365–1375.

14. T. Duka, V. Duka, J.N. Joyce, A. Sidhu, α-Synuclein Contributes to GSK-3β-catalyzed Tau Phosphorylation in Parkinson's Disease Models, Faseb J. Official Publ. Fed. Am. Soc. Exp. Biol. 23 (2009) 2820–2830.

15. M. Golpich, E. Amini, F. Hemmati, N.M. Ibrahim, B. Rahmani, Z. Mohamed, A.A. Raymond, L. Dargahi, R. Ghasemi, A. Ahmadiani, Glycogen synthase kinase-3 beta (GSK-3β) Signaling: Implications for Parkinson's Disease, Pharmacol. Res. 97 (2015) 16–26.

16. C.Y. Kuan, R.E. Burke, Targeting the JNK signaling pathway for stroke and Parkinson's Diseases Therapy, Curr. Drug Targets Cns Neurol. Disord. 4 (2005) 63–67.

17. S. Hunot, M. Vila, P. Teismann, R.J. Davis, E.C. Hirsch, S. Przedborski, P. Rakic, R.A. Flavell, JNK-mediated Induction of Cyclooxygenase 2 is Required for Neurodegeneration in a Mouse Model of Parkinson's Disease, Proc. Natl. Acad. Sci. United States of America 101 (2004) 665–670.

18. K. Noda, T. Kitami, W.P. Gai, F. Chegini, P.H. Jensen, T. Fujimura, K. Murayama, K. Tanaka, Y. Mizuno, N. Hattori, Phosphorylated IκBα is a

Component of Lewy Body of Parkinson's Disease, Biochem. Biophysical Res. Commun. 331 (2005) 309–317.

19. D. Uberti, T. Carsana, S. Francisconi, G.F. Toninelli, P.L. Canonico, M. Memo, A Novel Mechanism for Pergolide-induced Neuroprotection: Inhibition of NFκB Nuclear Translocation, Biochem. Pharmacol. 67 (2004) 1743–1750.

20. D.C. Berwick, K. Harvey, The Importance of Wnt Signaling for Neurodegeneration in Parkinson's Disease, Biochem. Soc. Trans. 40 (2012) 1123–1128.

21. E. Arenas, Wnt Signaling in Midbrain Dopaminergic Neuron Development and Regenerative Medicine for Parkinson's Disease, J. Mol. Cell Biol. 6 (2014) 42–53.

22. M. Xilouri, L. Stefanis, Autophagic Pathways in Parkinson Disease and Related Disorders, Expert Rev. Mol. Med. 13 (2011) 1–21.

23. M. Xilouri, T. Vogiatzi, K. Vekrellis, L. Stefanis, Alpha-Synuclein Degradation by Autophagic Pathways: A Potential Key to Parkinson's Disease Pathogenesis, Autophagy 4 (2008) 917–919.

24. A.W. Willis, Parkinson Disease in the Elderly Adult, Mo. Med. 110 (2013) 406–410.

25. F. Jiang, J. Yang, Y. Zhang, M. Dong, S. Wang, Q. Zhang, F.F. Liu, K. Zhang, C. Zhang, Angiotensin-converting Enzyme 2 and Angiotensin 1-7: Novel Therapeutic Targets, Nat. Rev. Cardiol. 11 (2014) 413–426.

26. T. Fujita, K. Ishihara, S. Yasuda, T. Nakamura, M. Maeda, M. Kobayashi, K. Sahashi, Y. Ikeda, Y. Kumagai, M. Majima, In Vivo Kinetics of Indoxyl Sulfate in Humans and its Renal Interaction with Angiotensin-Converting Enzyme Inhibitor Quinapril in Rats, J. Pharmacol. Exp. Ther. 341 (2012) 626–633.

27. P.K. Li, B. Pandit, D.L. Sackett, Z. Hu, J. Zink, J. Zhi, D. Freeman, R.W. Robey, K. Werbovetz, A. Lewis, A Thalidomide Analogue with In Vitro

Antiproliferative, Antimitotic, and Microtubule-Stabilizing Activities, Mol. Cancer Ther. 5 (2006) 450–456.

28. N. Zhang, S. Ayralkaloustian, T. Nguyen, J. Afragola, R. Hernandez, J. Lucas, J. Gibbons, C. Beyer, Synthesis and SAR of [1,2,4]triazolo[1,5-a]pyrimidines, a Class of Anticancer Agents With a Unique Mechanism of Tubulin Inhibition, J. Med. Chem. 50 (2007) 319–327.

29. D.W. Snyder, N.J. Bach, R.D. Dillard, S.E. Draheim, D.G. Carlson, N. Fox, N.W. Roehm, C.T. Armstrong, C.H. Chang, L.W. Hartley, Pharmacology of LY315920/S-5920, [[3-(aminooxoacetyl)-2-ethyl-1- (phenylmethyl)-1Hindol-4-yl]oxy] Acetate, A Potent and Selective Secretory Phospholipase A2 Inhibitor: A New Class of Anti-inflammatory Drugs, SPI, J. Pharmacol. Exp. Ther. 288 (1999) 1117–1124.

30. R.D. Dillard, N.J. Bach, S.E. Draheim, D.R. Berry, D.G. Carlson, N.Y. Chirgadze, D.K. Clawson, L.W. Hartley, L.M. Johnson, N.D. Jones, Indole Inhibitors of Human Nonpancreatic Secretory Phospholipase A2. 1. Indole-3-acetamides, Cheminform 28 (1997) 5137–5158.

31. J. Goldberg, Q. Jin, Y. Ambroise, S. Satoh, J. Desharnais, K. Capps, D.L. Boger, Erythropoietin Mimetic Derived from Solution Phase Combinatorial Libraries, J. Am. Chem. Soc. 124 (2002) 544–555.

32. E.M. Delorme, S.S. Tian, Preclinical Activity of Eltrombopag (SB-497115), An Oral, Nonpeptide Thrombopoietin Receptor Agonist, Stem Cells 27 (2009) 424–430.

33. G. Kochlamazashvili, C. Henneberger, O. Bukalo, E. Dvoretskova, O. Senkov, P.M.J. Lievens, R. Westenbroek, A.K. Engel, W.A. Catterall, D.A. Rusakov, The Extracellular Matrix Molecule Hyaluronic Acid Regulates Hippocampal Synaptic Plasticity by Modulating Postsynaptic L-type Ca $^{2+}$Channels, Neuron 67 (2010) 116–128.

34. B. Ritz, S.L. Rhodes, L. Qian, E. Schernhammer, J.H. Olsen, S. Friis, L-type Calcium Channel Blockers and Parkinson Disease in Denmark, Ann. Neurology 67 (2010) 600–606.

35. A. Lita, X. Liu, M. Wang, Advances of the Research and Development of New Anti-Parkinson's Disease drugs, Chin. Pharm. Aff. 26 (2012) 629–633.

36. H. Zhang, R. Tong, L. Bai, J. Shi, O. Liang, Emerging Targets and New Small Molecule Therapies in Parkinson's Disease Treatment, Bioorg. Med. Chem. 24 (2016) 1419–1430.

37. T. Huynh, The Parkinson's Disease Market, Nat. Rev. Drug Discov. 10 (2011) 571–572.

38. L. V. Kalia, and A. E. Lang, Parkinson's disease, Lancet, 386 (2015), 896–912.

39. Y. Zhang, Q.Y. Sun, R.H. Yu, The Contribution of GIGYF2 to Parkinson's Disease: a Meta-Analysis, Neurol. Sci. 36 (2015) 2073–2079.

40. K. Li, B. S. Tang, Z. H. Liu, LRRK2 A419V Variant is a Risk Factor for Parkinson's Disease in Asian Population, Neurobiology of Aging 36 (2015) 2908.e11–2908.e15.

41. Z. Yu, T. Wang, J. Xuet, Mutations in the Glucocerebrosidase Gene are Responsible for Chinese Patients with Parkinson's disease, J. Hum. Genet. 60 (2014) 1–6.

42. A. Lwin, E. Orvisky, O. Goker-Alpan, Glucocerebrosidase Mutations in Subjects with Parkinsonism, Molecular Genetics and Metabolism 81 (2004) 70–73.

43. G. Mercado, P. Valde, C. HetZ, An ERcentric view of Parkinson's Disease. Trends Mol Med 19 (2013) 165–175

44. P. Anand, S.G. Thomas, A.B. Kunnumakkara, C. Sundaram, K.B. Harikumar, B. Sung, S.T. Tharakan, K. Misra, I.K. Priyadarsini, K.N. Rajasekharan, B.B. Aggarwal, Biological Activities of Curcumin and its Analogues (Congeners) Made by Man and Mother Nature, Biochem. Pharmacol 76 (2008) 1590–1611.

45. P. Dadhaniya, C. Patel, J. Muchhara, N. Bhadja, N. Mathuria, K. Vachhani, M.G. Soni, Safety Assessment of a Solid Lipid Curcumin Particle Preparation: Acute and Subchronic Toxicity Studies, Food and Chemical Toxicology 49 (2011) 1834–1842.

46. G.P. Lim, T. Chu, F. Yang, W. Beech, S.A. Frautschy, G.M. Cole, The Curry Spice Curcumin Reduces Oxidative Damage and Amyloid Pathology in an Alzheimer Transgenic Mouse, J. Neurosci. 21 (2001) 8370–8377.

47. M. Thiyagarajan, S.S. Sharma, Neuroprotective Effect of Curcumin in Middle Cerebral Artery Occlusion Induced Focal Cerebral Ischemia in Rats. Life Sci 74 (2004) 969–985.

48. F. Yang, G.P. Lim, A.N. Begum, O.J. Ubeda, M.R. Simmons, S. S.Ambegaokar, P. P. Chen, R. Kayed, C.G. Glabe, S.A. Frautschy, G.M. Cole, Curcumin Inhibits Formation of Amyloid Beta Oligomers and Fibrils, Binds Plaques, and Reduces Amyloid *In Vivo*. The Journal of biological chemistry 280 (2005) 5892–5901.

49. M. Grundman, P. Delaney, Antioxidant Strategies for Alzheimer's Disease. Proc. Nutr. Soc. 61 (2002) 191–202.

50. J.M. Ringman, S.A. Frautschy, G.M. Cole, D.L. Masterman, J.L. Cummings, A Potential Role of the Curry Spice Curcumin in Alzheimer's Disease, Curr. Alzheimer Res. 2 (2005) 131–136.

51. D.B. Singh, M.K.Gupta, R.K. Kesharwani, M. Sagar, S. Dwivedi, K. Misra, Molecular drug targets and therapies for Alzheimer's disease, Translational Neuroscience 5 (2014) 203–217.

52. S.J. Kim, T.G. Son, H.R. Park, M. Park, M.-S. Kim, H.S. Kim, H.Y. Chung, M.P. Mattson, J. Lee, Curcumin Stimulates Proliferation of Embryonic Neural Progenitor Cells and Neurogenesis in the Adult Hippocampus. The Journal of biological chemistry 283 (2008) 14497–14505

53. K.I. Priyadarsini, D.K. Maity, G.H. Naik, M.S. Kumar, M.K. Unnikrishnana, J.G. Satav, H. Mohan, Role of phenolic O-H and methylene hydrogen on the free radical reactions and antioxidant activity of curcumin. Free radical biology & medicine 35 (2003) 475–484.

54. Y. Xua, B. Kub, L. Cuic, X. Lib, P.A. Barisha, T.C. Fosterc, W.O. Oglea, Curcumin Reverses Impaired Hippocampal Neurogenesis and Increases

Serotonin Receptor 1A mRNA and Brain-Derived Neurotrophic Factor Expression in Chronically Stressed Rats, Brain Research 1162 (2007) 9–18.

55. R.B. Mythri and M.M. Srinivas Bharath, Curcumin: A Potential Neuroprotective Agent in Parkinson's Disease, Curr. Pharm. Des. 18 (2012) 91–99.

56. R. B. Mythri, G. Harish, S. K. Dubey, K. Misra, M. M. Srinivas Bharath, Glutamoyl Diester of the Dietary Polyphenol Curcumin Offers Improved Protection Against Peroxynitrite-Mediated Nitrosative Stress and Damage of Brain Mitochondria In Vitro: Implications for Parkinson's Disease, Mol. Cell Biochem. 347 (2011) 135–143.

57. R.A. Sharma, A.J. Gescher, W.P. Steward, Curcumin: The Story So Far, Eur. J. Cancer 41 (2005) 1955–1968

58. G. Garcea, D.J. Jones, R. Singh, A.R. Dennison, P.B. Farmer, R.A. Sharma, W.P. Steward, A.J. Gescher, D.P. Berry, Detection of Curcumin and its Metabolites in Hepatic Tissue and Portal Blood of Patients Following Oral Administration, Br. J. Cancer 90 (2004) 1011–1015.

59. M.H. Pan, T.M. Huang, J.K. Lin Comparative Studies on the Suppression of Nitric Oxide Synthase by Curcumin and Its Hydrogenated Metabolites through Down-regulation of IkB Kinase and NFκB Activation in Macrophages, Biochemical Pharmacology 60 (2000) 1665–1676.

60. P. Anand, A.B. Kunnumakkara, R.A. Newman, B.B. Aggarwal, Bioavailability of Curcumin: Problems and Promises. Mol Pharm 4 (2007) 807–818.

61. N.K. Gupta, V.K. Dixit, Development and Evaluation of Vesicular System for Curcumin Delivery. Arch. Dermatol Res. 303 (2011) 89–101.

62. N.K. Gupta, V.K. Dixit, Bioavailability Enhancement of Curcumin by Complexation With Phosphatidyl Choline, J. Pharm. Sci. 100 (2011) 1987–1995.

63. C. Li, Y. Zhang, T. Su, L. Feng, Y. Long, Z. Chen, Silica-coated Flexible Liposomes as a Nanohybrid Delivery System for Enhanced Oral Bioavailability of Curcumin, Int. J. Nanomedicine 7 (2012) 5995–6002.

64. H. Li, N. Zhang, Y. Hao, Y. Wang, S. Jia, H. Zhang, Y. Zhang, Z. Zhang, Formulation of Curcumin Delivery With Functionalized Single-Walled Carbon Nanotubes: Characteristics and Anticancer Effects In Vitro, Drug Deliv. 21 (2014) 379–387.

65. B. Raya, S. Bishtb, A. Maitrad, A. Maitrab, D.K. Lahiri, Neuroprotective and Neurorescue Effects of a Novel Polymeric Nanoparticle Formulation of Curcumin (NanoCurc) in the Neuronal Cell Culture and Animal Model: Implications for Alzheimer's Disease. J. Alzheimers Dis. 23 (2011) 61–77.

66. S. Bisht, G. Feldmann, S. Soni, R. Ravi, C. Karikar, A. Maitra, A. Maitra, Polymeric Nanoparticle-Encapsulated Curcumin ("nanocurcumin"): A Novel Strategy for Human Cancer Therapy, J Nanobiotechnology 5 (2007) 3.

67. W. Tiyaboonchai, W. Tungpradi, P. Plianbangchang, Formulation and Characterization of Curcuminoids Loaded Solid Lipid Nanoparticles. Int. J. Pharm. 337 (2007) 299–306.

68. M.O. Iwunze, D. McEwan, Peroxynitrite Interaction with Curcumin Solubilized in Ethanolic Solution, Cell Mol. Biol. 50 (2004) 749–752.

69. M.H.M. Leung, H. Colangelo, T.W. Kee, Encapsulation of Curcumin in Cationic Micelles Suppresses Alkaline Hydrolysis, Langmuir 24 (2008) 5672–5675.

70. F. Wang, X. Wu, F. Wang, S. Liu, Z. Jia, J. Yang, The Sensitive Fluorimetric Method for the Determination of Curcumin Using the Enhancement of Mixed Micelle. J. Fluoresc. 16 (2006) 53–59.

71. Z. Ma, A. Haddadi, O. Molavi, A. Lavasanifar, R. Lai, J. Samuel1y, Micelles of Poly(ethylene oxide)-b-poly(epsilon-caprolactone) as Vehicles for the Solubilization, Stabilization, and Controlled Delivery of Curcumin, J. Biomed. Mater. Res. A 86 (2008) 300–310.

72. A. Sahu, U. Bora, N. Kasoju, P. Goswami, Synthesis of Novel Biodegradable and Self-Assembling Methoxy Poly(ethylene glycol)-palmitate Nanocarrier for Curcumin Delivery to Cancer Cells, Acta Biomater. 4 (2008) 1752–1761.

73. A. Liu, H. Loua, L. Zhaob, P. Fan, Validated LC/MS/MS Assay for Curcumin and Tetrahydrocurcumin in Rat Plasma and Application to Pharmacokinetic Study of Phospholipid Complex of Curcumin, J. Pharm. Biomed. Anal. 40 (2006) 720–727.

74. M. Bishnoi, K. Chopra, L. Rongzhu, S. K. Kulkarni, Protective effect of curcumin and its Combination with Piperine (bioavailability enhancer) Against Haloperidol-Associated Neurotoxicity: Cellular and Neurochemical Evidence, Neurotox. Res. 20 (2011) 215–225.

75. D. Suresh, K. Srinivasan, Tissue Distribution & Elimination of Capsaicin, Piperine & Curcumin Following Oral Intake in Rats, Indian J. Med. Res. 131 (2010) 682–691.

76. Harish, C. Venkateshappa, R. B. Mythri, S. K. Dubey, K. Mishra, N. Singh, S.Vali, M. M. S. Bharath, Bioconjugates of Curcumin Display Improved Protection Against Glutathione Depletion Mediated Oxidative Stress in a Dopaminergic Neuronal Cell Line: Implications for Parkinson's Disease, Bioorg. Med. Chem. 18 (2010) 2631–2638.

77. B. S. Gadad, P. K. Subramanya, S. Pullabhatla, I. S. Shantharam, K.S. Rao, Curcumin-Glucoside, A Novel Synthetic Derivative of Curcumin, Inhibits α–Synuclein Oligomer Formation: Relevance to Parkinson's Disease, Current Pharmaceutical Design, 18 (2012) 76–84.

78. G.M. Petzinger, B.E. Fisher, S. McEwen, J.A. Beeler, J.P. Walsh, M.W. Jakowec, Exercise-Enhanced Neuroplasticity Targeting Motor and Cognitive Circuitry in Parkinson's Disease. Lancet. Neurol. 12(2013) 716–726.

79. P.L. Wu, M. Lee, T.T. Huang, Effectiveness of Physical Activity on Patients with Depression and Parkinson's Disease: A Systematic Review, PLoS One 12 (2017) e0181515.

80. A. Uhrbrand, E. Stenager, M.S. Pedersen, U. Dalgas, Parkinson's Disease and Intensive Exercise Therapy-A Systematic Review and Meta-analysis of Randomized Controlled Trials, J. Neurol. Sci. 353(2015) 9–19.

81. R. Šumec, P. Filip, K. Sheardová, M. Bareš, Psychological Benefits of Nonpharmacological Methods Aimed for Improving Balance in Parkinson's Disease: A Systematic Review. Behav. Neurol. 2015 (2015) 620674.

82. L. Roeder1, J, T. Costello, S, S. Smith, I, B. Stewart, G.K. Kerr, Effects of Resistance Training on Measures of Muscular Strength in People with Parkinson's Disease: A Systematic Review and Meta-Analysis. PLoS One 10 (2015) e0132135.

83. M.R. RaffertyA, P.N. Schmidt, S. T. Luoc, K. Lid, C. Marrase, T.L. Davis, M. Guttmang, F. Cubillosb, T. Simunih, Regular Exercise, Quality of Life, and Mobility in Parkinson's Disease: A Longitudinal Analysis of National Parkinson Foundation Quality Improvement Initiative Data. J Parkinsons Dis 7 (2017) 193–202.

84. J. Collett, M. Franssen, A. Meaney, D. Wade, H. Izadi, M. Tims, C. Winward, M. Bogdanovic, A. Farmer, H.Dawes, Phase II Randomised Controlled Trial of a 6-month Self-Managed Community Exercise Programme for People with Parkinson's Disease. J. Neurol. Neurosurg. Psychiatry, 88 (2016) 204–211.

85. H.J.J. Pabon, A Synthesis of Curcumin and Related Compounds, Recueil 83 (1964) 379–386.

86. K. V. D. Babu, K. N. Rajasekharan, Simplified Condition For Synthesis of Curcumin I and Other Curcuminoids, Organic Preparations and Procedures International: The New Journal for Organic Synthesis 26 (1994) 674–677.

87. S. Venkateswarlu, M.S. Ramachandra, G.V. Subbaraju, Synthesis and Biological Evaluation of Polyhydroxycurcuminoids, Bioorg. Med. Chem. 13 (2005) 6437–6380.

88. X.Shen, X. Yang, Y. Zhu, X. Liu, H. Wen. Synthesis of [$^{18}O_2$]-curcumin, J. Label Compd. Radiopharm. 57 (2014) 658–659.

89. P.S. Kulkarnib , D.D. Kondhareb , R. Varalaa ,P.K. Zubaidhab, Calcium Hydroxide: An Efficient and Mild Base for One-pot Synthesis of Curcumin and its Analogues, Acta. Chimica. Slovaca 6 (2013) 150–156.

90. C. E. Nichols, D. Youssef, R.G. Harris, A. Jha, Microwave-assisted Synthesis of Curcumin Analogs. Arkivoc 13 (2006) 64–72.

91. M.A. Surati, S. Jauhari, K. R. Desai, A Brief Review: Microwaveassisted Organic Reaction, Archives of Applied Science Research 4 (2012) 645–661.

92. K. Shimoda, H. Hamada, Enzymatic Synthesis and Anti-Allergic Activities of Curcumin Oligosaccharides, *Biochemistry Insights* 3 (2010) 1–5.

93. K. Shimoda, T. Hara, H. Hamada, H. Hamada, Synthesis of Curcumin β-Maltooligosaccharides Through Biocatalytic Glycosylation with Strophanthus gratus Cell Culture and Cyclodextrin Glucanotransferase, Tetra. Lett. 48 (2007) 4029–4032.

94. K. Mohri, Y. Watanabe, Y. Yoshida, M. Satoh, K. Isobe, N. Sugimoto, Y. Tsuda, Synthesis of Glycosylcurcuminoids, Chem. Pharm. Bull. 511 (2003) 268–1272.

95. K.S. Parvathy, P. Srinivas. Ultrasound-assisted Reaction of 2,3,4,6-tetra-O-acetyl-a-D-Glucopyranosyl Bromide with Potassium Salt of Curcumin Under PTC Conditions, Ultrasonics Sonochemistry 15 (2008) 571–577.

Chapter 3

Designing, synthesis, characterization and antibacterial properties of some curcumin analogues

3.1. Introduction:

Curcumin **(3)** the yellow pigment of spice turmeric known as gold molecule is a wonderful lead molecule for developing multi-targeted drugs chemical structure of curcumin **(3)** comprises of diferuloylmethane that has attracted huge attention of the scientific community since it possesses activity against various human aliments. It possesses pharmacological safety and wide range of biological activities such as antibacterial, antineoplastic agent, anti-inflammatory, anti-HIV, anti-viral, anti-diabetic etc. Curcumin **(3)** is one of the most widely researched naturally occurring biologically active compound which is also known to be cytoprotective for healthy human cells. However, its limitation of low bioavailability and water solubility has restricted its medicinal application. A large number of curcumin analogues/derivatives have been synthesized and tested for multiple disorders to overcome this limitation. Different procedures have been adopted for synthesized curcumin analogues by various Chemists [1]. However, expected success has so far evaded the scientists for the lack of knowledge of the exact mechanism of drug action in each case. The QSAR studies of curcumin **(3)** and its derivatives have been reported by several authors but overall conclusive decisions are still unavailable [2-4].

3.1. (a) Analogues of curcumin having antibacterial properties:

The curcumin analogues are well known for their antibacterial properties. FtsZ protein helps in cell division. FtsZ is a homolog of tubulin, the ubiquitous eukaryotic cytoskeletal protein involved in many essential cellular processes including mitosis. FtsZ, a prokaryotic homologue of eukaryotic cytoskeletal protein tubulin has been known as a plausible target. Curcumin inhibits the assembly of FtsZ protofilaments in Bacillus subtilis (B. subtilis) [5]. Curcumin has inhibitory effect on NF-κB activation and as a result on the release of IL-8 and cell scattering which leads to reduction in inflammation of gastric tissue. This effect is the main consequence for presence of H. pylori in stomach .It has been reported that the antibacterial activity of curcumin is due to its membrane damaging property in both Gram positive and Gram negative bacteria [6]. The major target of curcumin is bacterial membrane. In the Gram-negative Bacteria, the cell wall is composed of a single layer of peptidoglycan surrounded by outer membrane. Grampositive Bacteria has thick cell wall (15-80 nm),

consisting of several layers of peptidoglycan. It has been reported for strains of both *Staphyloccocus aureus* (Gram positive) and *Psuedomonas aeruginosa* (Gram negative) bacteria [7]. The bacteria are able to prompt 'human-like' surfactant proteins on their own or that primers and antibodies to human surfactant proteins distinguish the bacterial proteins and genes [8]. The results suggested the existence of a new group of bacterial surfactant proteins and DNA.

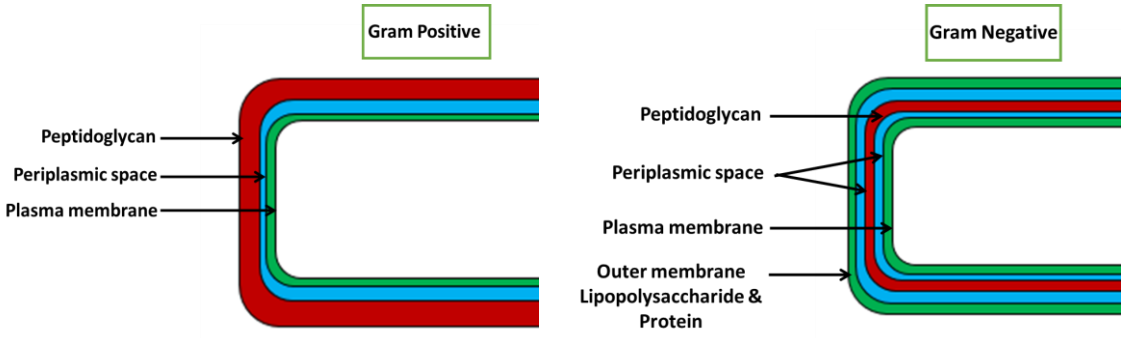

Figure 3.1. Cell wall structure of gram positive and gram negative bacteria.

These proteins can also be the feasible target for curcumin and analogues. In view of the multiple targets reported in literature for antibacterial activity of curcumin and analogues, we decided to design, prepare and test a dozen analogues based on their binding to specific key target proteins inhibiting cell wall formation in both Gram positive and Gram negative bacteria. If cell wall damage is the only criteria for activity both Gram positive and Gram negative pathogens should show similar activity [9]. However, our results show that besides this parallel mechanisms involving different targets are working simultaneously.

The monomeric MipZ protein of *Caulobacter vibrioides* (similar to *Pseudomonas aeruginosa*) and Pyruvate kinase (PK) of *Staphylococcus aureus* are key regulators in the lysis of bacterial cells. MipZ belongs to the Mrp/MinD family of P loop ATPases, the proteins that act as nucleotide-dependent molecular switches. MipZ directly interferes with FtsZ polymerization, thereby restricting FtsZ ring formation to mid cell, the region of lowest MipZ concentration. The cellular localization of MipZ thus serves the dual function of positioning the FtsZ ring and delaying formation of the cell division apparatus until chromosome segregation has initiated. This phenomenon makes it an important target for antibacterial drug

discovery. Pyruvate kinase enzyme structure complex with FBP, PG, Mn^{2+} and K^{+}, the enzyme present in *S. aureus* is involved basically in the catalyzing final steps of glycolysis and thus cell wall formation [10]. This enzyme converts phosphoenolpyruvate (PEP) and ADP to pyruvate and ATP respectively. This reaction is a committed step leading to either anaerobic fermentation or oxidative phosphorylation of pyruvate kinase. PK can thus be called the control point of glycolysis and finely tunes the biochemical reaction pathway which makes it an important target for the antibacterial drug discovery.

3.1. (b) Pharmacology of antibacterial drugs:

(i) Molecular organization of bacteria: Atomic association of bacterial cell divider is in charge of its unbending nature. Albeit distinctive types of microorganisms have diverse cell divider structures, practically all microbes contain one specific macromolecule that is explicit to that specific microscopic organisms. This macromolecule is known as peptidoglycan and comprises of two noteworthy sub-units; the spine or glycan parcel comprises of two diverse amino sugars N-acetyl muramic corrosive and N-acetyl glucosamine. The peptide bit of the atom comprises of a chain of a few distinctive amino acids that are appended to every one of N-acetylmuramic corrosive in the glycan bit of the particle. Albeit just a couple of the 20 basic amino acids typically found in regular proteins happen in peptidoglycan and its definite sythesis changes from one to other microscopic organisms. One regular amino corrosive diamino pimelic corrosive, which is identified with amino corrosive lysine, is found in no other living being in nature aside from in certain bacterial cell dividers. Likewise numerous amino acids in bacterial cell divider are of D-setup while those in eukaryotic proteins are of L-arrangement.

(ii) Gram negative and gram positive microscopic organisms: Multiple proteins are associated with the readiness of the cell dividers, which can be differentially focused by various medication particles going about as inhibitors, accordingly cell divider development is restrained. Gram negative microbes are encompassed by two layers, the external film works as a productive porousness boundary containing lipolysaccharides (LPS) and porin. Gram-positive bacteria having lipid bilayer cell film of the majority of the Gram-positive microscopic organisms is secured by a permeable peptidoglycan layer.

(iii) Bacterial mechanisms of antibiotic resistance: Several mechanism have developed in microscopic organisms which meet them with anti infection opposition. These mechanism can synthetically adjust the anti-microbial, render it latent through physical expulsion from change target site with the goal that it isn't perceived by the anti-microbial. The most well-known mode is enzymatic inactivation of the anti toxin. A current cell compound is changed to respond with the anti-toxin so that it is never again influences the microorganism. An elective procedure used by numerous microorganisms is the adjustment of the anti microbial target site. These and different components are appeared in the going with (Table 3.1).

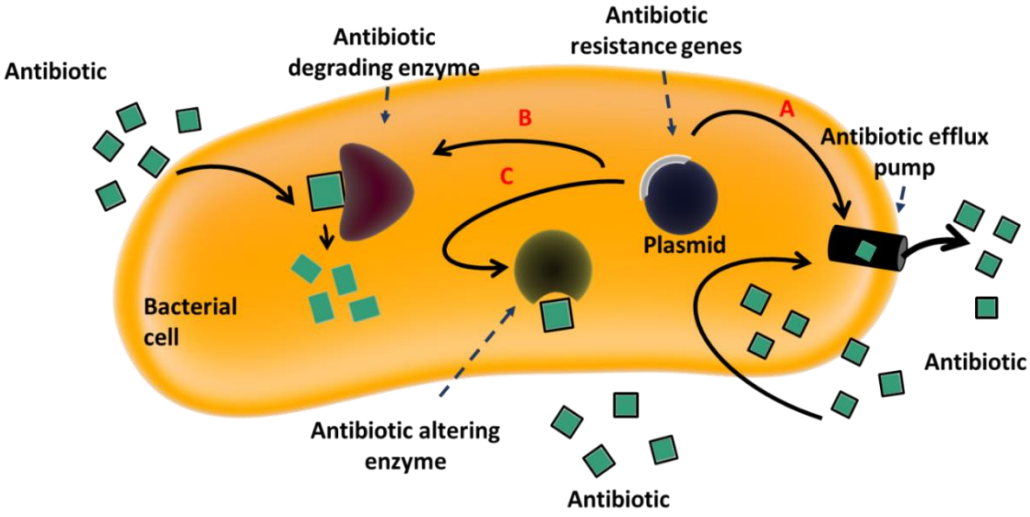

Figure 3.2. Mechanism of antibiotic resistance in bacteria.

Table 3.1. Different modes of antibiotic drug resistance.

Antibiotic drug	**Mode of resistance**
Chloramphenicol	Low acceptance into cell
Tetracycline	Active efflux from the cell
β–lactams,Erythromycin, Lincomycin	Excludes or reduces binding of antibiotic to cell target
β-lactams,Aminoglycosides, Chloramphinacol	Enzymatic cleavage or modification to inactive antibiotic molecule
Sulfonamides,Trimethoprim	Metabolic bypass of withdrawn reaction
Sulfonamides,Trimethoprim	Overproduction of antibiotic target(titration)

(iv) The acquisition and spread of drug resistance in bacteria: The advancement of resistance is inescapable after the presentation of another medication/anti infection. Starting rates of protection from new medications are typically on the request of 1%. Nonetheless, present day employments of anti-infection agents have caused an enormous increment in the quantity of safe microscopic organisms. Indeed, inside 8-12 years after wide spread use, strains impervious to different medications become across the board. Different medication safe strains of certain microscopic organisms have achieved the extent that practically no anti-microbials are accessible for treatment. Anti-microbial opposition in microorganisms might be an innate quality of the creature for example it's regular nature for survival (for example a specific sort of cell dividers structure) that renders it normally safe or it might be gained by methods for transformation in its own DNA or securing of opposition presenting DNA from another source.

(v) Vertical gene transfer: The spontaneous mutation frequency for antibiotic resistance is of the order of regarding 10^{-8}-10^{-9}. This suggests that one in each 108-109 bacterium in associate degree infection can develop resistance through the method of mutation. In *E. coli*, it's been calculable that antibiotic resistance is nonheritable at the speed of roughly 10^{-9} onceexposed to high concentration of antibiotic. though mutation is incredibly rare event, the in no time rate of growth of bacterium and therefore the absolute range of cells earned means it doesn't take long before resistance is developed duringa population. Once the resistance genes have developed, theyare transferred onto all the bacteria's issue throughout deoxyribonucleicacid replication. Thiscanbe called vertical cistron transfer or vertical evolution. The method is strictly a matter of Darwinian evolution driven by principles of natural selection aspontaneousmutation with in the microorganism body imparts resistance to a member of the microorganism population. Within the selective setting of the antibiotic, the wild sort (non mutants) ar killed and therefore the resistant mutant is allowed to grow and flourish.

3.2. (a) Earlier methods of preparation of curcumin analogues:

A large number of approaches leading to the synthesis of curcumin **(3)** derivatives have been developed. The synthesis of isoxazole, N-substituted pyrazoles,

pyrimidine-2(1H)-thione and pyrimidine ring in the molecular scaffold of curcumin **(3)** is well reported [11]. The synthesis of 4,4'-*O*-di (N-phthaloyl-glycinoyl)-curcumin through base catalyzed esterification is reported by our research group [12]. Reduction of diketo group present in curcumin is reported to obtain (1E, 6E)-1,7-bis(4-hydroxy-3-methoxyphenyl) hepta-1,6-diene-3,5-diol [13]. The nucleophilic substitution reaction of phenolic hydroxyl group of curcumin and tetra acetyl bromoglucose to yield the glycosidic link [14] halide phosphate ester [15], and sulfonat [16] has also been done. However, few of the general and efficient methods used recently for the preparation of curcumin derivatives are described briefly below.

3.2. (b) Biginelli type reaction of curcumin with hydroxyl amine, hydrazine, urea and thiourea:

Basically Biginelli reaction has been reported for the synthesis of 3,4 dihydropyrimidin-2(1H)-ones from diketoester aldehyde and urea. The oxazole, pyrazoles, pyrimidine, pyrimidine-2(1H)-thione derivatives of curcumin **(3)** have been prepared as depicted in (Scheme 3.1).

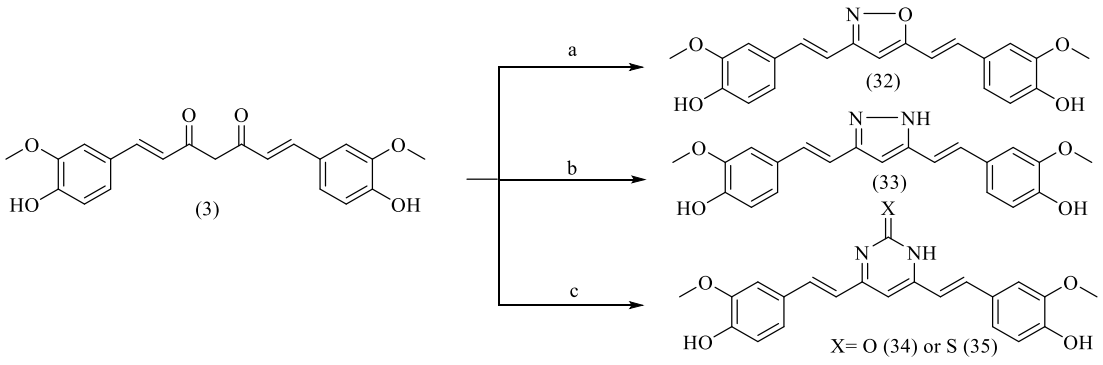

Reagent and condition: (a) NH_2OH, pyridine, EtOH, Reflux, 48h, (b) $NH_2.NH_2$, AcOH, rt, 48h
(c) AcOH, Urea/Thiourea, Reflux, 12h.

Scheme 3.1. Preparation of curcumin analogs with hydroxyl amine, hydrazine, urea and thiourea.

The diketone functionality of curcumin **(3)** was cyclized to the corresponding derivatives of curcumin **(3)** by refluxing it with hydroxylamine hydrochloride and pyridine in ethanol for 48 h. The curcumin **(3)** was cyclized to its corresponding pyrazoles derivative by hydrazine hydrate and acetic acid at room temperature for

48h. Urea and thiourea derivatives of curcumin **(3)** were prepared by refluxing curcumin **(3)**, urea/thiourea in acetic acid for 12h.

3.2. (c) *In situ* formation of *O*-alkyl/aryl phosphatesphosphates:

In 2018, W. Kozak and S. Demkowicz et al [15] described the reaction of trimethyl and triethylphosphites with phenols in the presence of iodine to give the corresponding dialkylarylphosphates (Scheme 3.2).

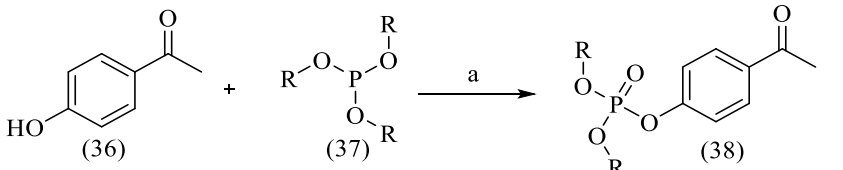

Reagent and condition: (a) I_2, Pyridine, DCM

Scheme: 3.2

3.2 (d) Synthesis of 4, 4-*O*-di glycinoyl curcumin:

In 2005, S. Mishra et al [12] described the reaction of acyl chloride and 10% NaOH, with curcumin **(3)** to give corresponding 4, 4-*O*-di glycinoyl curcumin **(39)**. (Scheme 3.3)

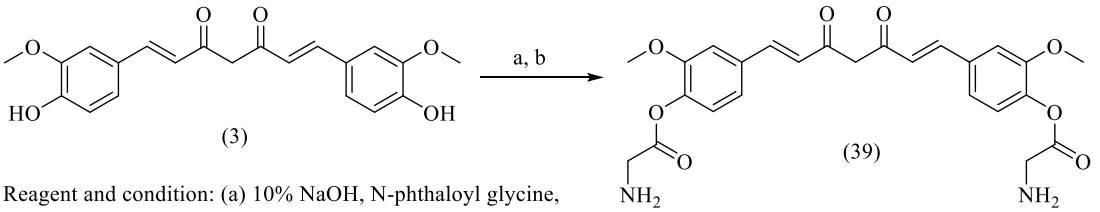

Reagent and condition: (a) 10% NaOH, N-phthaloyl glycine, 6h, 0- rt, (b) NH_3 pyridine, 1 min.

Scheme 3.3

3.2. (e) Carbodiimide coupling reaction:

Reaction between carboxylic acids **(40)** and phenols **(41)** in DCC/EDC, in presence of DMAP, DCC/EDC activate the acid group for formation of intermediate *O*-acyl -isoureas which react with phenolic group to form urea and ester. Carboxylic acids have tendency to form ketenes on treatment with DCC/EDC preferably acylate hydroxyl groups in the presence of base. [17] (Scheme 3.4)

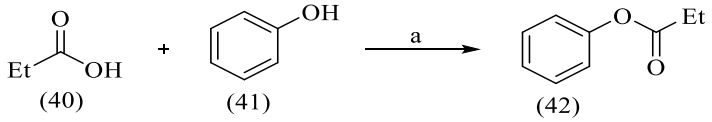

Reagent and condition: (a) DCC/EDC, DMAP

Scheme 3.4

3.3. Basis of the present work:

As discussed in the introduction part of chapter two, curcumin **(3)** analogues are well known for their antibacterial properties. It was thought and synthesized curcumin derivatives and also prepared the fine particles of curcumin. We think about the target protein of bacteria like FtsZ protein helps in cell division. FtsZ is a homolog of tubulin, the ubiquitous eukaryotic cytoskeletal protein involved in many essential cellular processes including mitosis. FtsZ, a prokaryotic homologue of eukaryotic cytoskeletal protein tubulin has been known as a plausible target. Keeping in mind the above facts and in continuation of our effort to develop a new generation for cure of bacterial infection, we carried out the present work. Curcumin **(3)** inhibits the assembly of FtsZ protofilaments in *Bacillus subtilis (B. subtilis)*. Sulfonate and phosphonate moiety may also enhance the bioavailability of curcumin **(3)** was the concept. Their PTC, DCC, DMAP, TEA and EDCHCl catalytic efficiency in organic synthesis for certain reactions has also been evaluated.

3.4. Objectives of the research work:

In the past few decades, curcumin **(3)** based analogues have attracted remarkable attention from the synthetic community, and extensive efforts have been made towards syntheses of these fascinating molecules. Although a large number of synthetic approaches have been reported, a unified and divergent approach with viability on a gram scale synthesis still represents an attractive goal. Therefore, we planned a synthetic route for these curcumin **(3)** based analogues that would render an opportunity to access these natural products analogues in adequate amount enabling to explore their antibacterial properties and their mode of action.

3.5. Material and Methods:

Commercial reagents and solvents were purified. Thin layer chromatography (TLC) was performed using silica gel 60 F254 pre-coated plates, which were visualized by UV fluorescence or by staining with iodine and alcoholic solution of phosphomolybodic acid. Column chromatography was performed on a silica gel (100-200 mesh) column. ^{1}HNMR spectra were recorded on bruker 400 ultra shield (400 MHz for ^{1}H and 101 MHz for ^{13}C, respectively) and bruker 800 ultra shield plus (800 MHz and 201 MHz for ^{1}H and ^{13}C, respectively) instruments in $CDCl_3$, CD_3OD and $DMSOd_6$. Chemical shifts (δ) are given in parts per million (ppm) using TMS (δ = 0.00) as the internal standard. Coupling constant (*J*) values are given in Hertz (Hz) with multiplicity [(s) singlet, (d) doublet (t) triplet, (dd) doublet of doublet, (dt) doublet of triplet (td) triplet of doublet, (m) multiplet]. HRMS (high resolution mass spectra) were performed on Agilent Technologies 6530 Accurate-Mass Q-TOF LC/MS using the electron spray ionization (ESI) technique. The software's used for computational studies were AutoDock 4.2.6 for docking and scoring. The active sites were predicted using DoGSiteScorer web server for finding binding sites. For wet laboratory testing the pathogenically active bacterial strains were obtained from NCCS Pune through Tezas Microbiology Laboratory, Allahabad.

3.6. Experimental:

3.6. (a) Molecular docking:

Structural modifications such as protein preparation, RMSD calculation of proteins and binding site identification were performed through *in silico* methods. The 3-D structure of proteins MipZ and Pyruvate kinase were downloaded from Research Collaboration for Structural Bioinformatics (RCSB), with the particular pdb id's 2XIT and 1A3W. The structure of 2XIT refers to crystal structure of monomeric MipZ of Caulobacter vibrioides (similar to Pseudomonas aeruginosa) the protein contains two chains (A, B) and all 294 amino acids. The crystal structure of pyruvate kinase complex with FBP,PG, MN2+ and K+ with 1A3W (pdb id) refers to Staphylococcus aureus, the structure contains two chains(A,B) and 500 amino acid molecules, the ligands in the structure are bound to both the chains.

The docking procedure has been performed *in-silico* and the active sites were predicted using AutoDock and DoGSiteScorer for the proteins. Autodock and DoGSiteScorer [18] were used to predict the binding cavity. The DoGSiteScorer is a specialized pocket finding tool. It estimates pocket on the protein surface solely based on the protein heavy atom coordinates depending on their special overlap with any protein atom. The simple score is basically calculated by a linear combination of three properties like pocket volume, enclosure and lipophilic character further SVM is added for druggability predictions. The binding cavity dimensions for 1A3W were X (21.4765), Y (-15.064), Z (25.1785) and for the protein 2XIT the dimensions were X (-11.674), Y (-0.4305), Z (49.6347).

Using simple 2D chemical structure editor and visualization tool ChemDraw new variant analogs of curcumin were designed changing the side chains. After active site prediction molecular docking was performed with the 2D structures of curcumin analogs against both the proteins in the specific co-ordinates of the pocket through AutoDock [19]. AutoDock is very effective software for protein-ligand docking. AutoDock calculates free energy scoring function based on the linear regression analysis, the AMBER force field.

The designed ligand molecules were synthesized by unambiguous methods, characterized by ^{1}H NMR and ^{13}C spectra. Curcumin salt was prepared for enhancing the solubility in most solvents. Curcumin **(3)** and one of the elevene analogues prepared were nanotized as well in order to enhance their activity. All compounds were tested on culture plates of *S. aureus* and *P. aeruginosa* for sensitivity, their MIC values and IC_{50} values were calculated. The results obtained have indicated that besides glycolysis i.e. cell wall damaging effect, other antibacterial mechanisms also appear to be operational.

3.6. (b) Chemical synthesis and spectroscopy:

(i) Synthesis of 4,4'-((1E,1'E)-isoxazole-3,5-diylbis(ethene-2,1-diyl)) bis(2 methoxyphenol. (32): A mixture of curcumin **(3)** (368 mg, 1 mmol), hydroxylamine hydrochloride (280 mg, 4.0 mmol) and pyridine (0.3 ml, 4.2 mmol) in ethanol (50 ml) was refluxed for 6 h. Recation was checked with TLC. The resulting reaction mixture

was concentrated under reduced pressure. The residue was diluted with ethyl acetate (50 ml) and washed with water (100 ml). The organic layer was separated and concentrated. Crude product crystallized with ethanol to give pure product (**32)**.

(32) (Light brown solid; yield 325 mg, 89%); R*f* 0.51(30% ethyl acetate: hexane); mp 160-162 °C; IR (KBr) υmax (cm^{-1}) 3248, 3011, 1636; ^{1}H NMR (400 MHz, DMSO-d_6) δ 9.39 (d, *J* = 29.1 Hz, 2H), 7.35 – 7.24 (m, 4H), 7.14 – 7.01 (m, 4H), 6.86 (s, 1H), 6.81 (dd, *J* = 8.1, 2.9 Hz, 2H), 3.85 (s, 6H). ^{13}C NMR (101 MHz, DMSO-d_6) δ 168.82, 162.72, 148.44, 136.91, 135.25, 127.80, 127.46, 122.14, 121.80, 116.05, 113.10, 110.81, 110.54, 98.34, 56.14. ppm; HRMS (ESI): Calculated for $C_{21}H_{19}NO_5$ $[M+H]^+$: 366.1263, found 366.1299.

(ii) Synthesis of 4,4'-((1E,1'E) -(1H-pyrazole-3,5-diyl) bis(ethene-2,1-diyl))bis(2-methoxyphenol) (33), 4,6-bis((E)-4-hydroxy-3-methoxystyryl)pyrimidin-2(1H)-one. **(34), 4, 6-bis ((E)-4-hydroxy-3-methoxystyryl) pyrimidine-2(1H)-thione (35).**

A mixture of curcumin **(3)** (368 mg,1 mmol), hydrazine/urea/ thiourea (4 mmol) was added in flask containing glacial acetic acid (15 ml) and reaction mixture was refluxed for 6 h. Reaction was checked with TLC. The resulting reaction mixture was concentrated under reduced pressure and diluted with ethyl acetate (50 ml), washed with water. The organic layer was separated and dried with sodium sulphate and concentrated. Crude product was recrystallized with ethanol, to give pure crystals.

(33) (Brown solid; yield 335 mg, 92%); R*f* 0.49 (35% ethyl acetate: hexane); mp 212-214 °C; IR (KBr) υmax (cm^{-1}) 3248, 3012, 1645, 1583,1361; ^{1}H NMR (400 MHz, DMSO-d_6) δ 12.83 (s, 1H), 9.40 (d, *J* = 30.3 Hz, 1H), 9.17 (d, *J* = 51.4 Hz, 1H), 7.34 – 7.26 (m, 2H), 7.19 – 7.02 (m, 4H), 6.97 (dd, *J* = 20.4, 7.6 Hz, 2H), 6.86 (s, 1H), 6.84 – 6.75 (m, 2H), 6.63 (s, 1H), 3.84 (d, *J* = 4.6 Hz, 6H). ^{13}C NMR (101 MHz, DMSO-d_6) δ 168.82, 162.72, 148.44, 136.91, 135.25, 127.62, 121.98, 116.03, 113.10, 111.10, 108.70, 99.79, 98.33, 56.86, 55.02. ppm; HRMS (ESI): Calculated for $C_{21}H_{20}N_2O_4$ $[M+H]^+$: 365.1423, found 365.1469.

(34) (Brown solid; yield 340 mg, 86%); R*f* 0.5 (50 % ethyl acetate: hexane); mp 102-104°C; IR (KBr) υmax (cm^{-1}) 3285,3033, 1655,1622,1558,1375; ^{1}H NMR (400

MHz, DMSO-d_6) δ 9.66 (s, 2H), 7.56 (d, *J* = 15.8 Hz, 2H), 7.33 (s, 2H), 7.16 (d, *J* = 8.1 Hz, 2H), 6.83 (d, *J* = 8.1 Hz, 2H), 6.76 (d, *J* = 15.8 Hz, 2H), 6.07 (s, 1H), 3.85 (s, 6H). ^{13}C NMR (101 MHz, DMSO-d_6) δ 183.68, 149.82, 148.46, 141.18, 126.81, 123.60, 121.56, 116.17, 111.81, 101.31, 56.16.ppm; HRMS (ESI): Calculated for $C_{22}H_{20}N_2O_5$ $[M+H]^+$: 393.1372, found 393.1407.

(35) (Dark brown solid; yield 305 mg, 74%); R*f* 0.5 (50 % ethyl acetate: hexane); mp 112-114°C; IR (KBr) υmax (cm^{-1}) 3270, 3030, 1637, 1578, 1377, 1028; ^{1}H NMR (400 MHz, DMSO-d_6) δ 9.68 (d, *J* = 18.4 Hz, 1H), 9.35 (d, *J* = 26.3 Hz, 1H), 7.55 (d, *J* = 15.8 Hz, 2H), 7.44 – 7.30 (m, 2H), 7.27 (d, *J* = 3.0 Hz, 1H), 7.14 (t, *J* = 10.9 Hz, 2H), 7.08 – 7.02 (m, 1H), 6.81 (dd, *J* = 16.6, 6.8 Hz, 2H), 6.74 (s, 1H), 6.07 (s, 1H), 3.85 (s, 6H). ^{13}C NMR (101 MHz, DMSO-d_6) δ 183.68, 149.82, 148.46, 141.18, 126.80, 123.60, 121.56, 116.16, 111.80, 101.29, 56.13. ppm; HRMS (ESI): Calculated for $C_{22}H_{20}N_2O_4S$ $[M+H]^+$: 409.1144, found 409.1179.

(iii) Synthesis of (1E, 6E)-1,7-bis(4-hydroxy-3-methoxyphenyl) hepta-1,6-diene-3,5-diol . **(43).** The curcumin **(3)** (368 mg, 1 mmol) was soluble in dry methanol (50) at 0 ºC and stirred for 0.5 h, followed by addition of sodium borohydride (84 mg, 2.2 mmol). The reaction was stirred for 25 h, at room temperature, reaction checked by TLC, the resulting reaction mixure was concentrated and transferred in water (100ml) and product was extracted with ethyl acetate. Separated organic layer was dried over sodium sulphate, concentrated under rotatory. The crude product was recrystallized with ethyl acetate, to give the pure product **(43)**, Dark orange Oil; yield 187 mg, 50% R*f* 0.3 (45 % ethyl acetate: hexane); (KBr) υmax (cm^{-1}) 3392, 1598, 1514, 1037, ^{1}H NMR (400 MHz, $CDCl_3$): 7.71 (2H, m) 7.60 (2H, d, *J* = 15.7 Hz), 7.15 (2H, m), 6.94 (1H, d, *J*=15.7Hz), 6.53 (1H, d, *J* = 2 Hz), 4.30 (4H, s), 3.97(6H, s), 2.83 (2H, m); ^{13}C NMR (100.1 MHz, ($CDCl_3$) δ 154.25, 146.35, 143.45, 133.18, 120.68, 120.65, 115.20, 111.06, 67.44, 55.67, 40.87. ppm. HRMS (ESI): Calculated for $C_{21}H_{24}O_6$ $[M+H]^+$: 373.1573, found 373.1609.

(iv) Synthesis of 4, 4'-*O*- di (N-phthaloyl-glycinoyl)-curcumin. **(44):**

To stirred of N-phthaloyl glycine (451 mg, 2.2 mmol), (EDC.HCl) 1-ethyl-3-(3-dimethylaminopropyl) carbodiimide hydrochloride (633 mg, 3.2 mmol) and

dimethylaminopyridine (402 mg, 3.2 mmol) in dry dichloromethane was at 0°C, for 30 min. Curcumin **(3)** (368 mg. 1 mmol) dissolved in dry dichloromethane (15 ml) was added in to the reaction mixture and it was stirred at room temprature for 12 h. After complet of the reaction, the reaction mixture was concentrated under rotatory. Crude product crystallized from dichloromethane, to give the pure product **(44)** (Dark orange solid; yield 610 mg, 82 %); R*f* 0.5 (45 % ethyl acetate: hexane); mp 152-154°C; (KBr) υmax (cm^{-1}) 3492, 1715, 1598, 1035, ^{1}H NMR (400 MHz, $CDCl_3$): 7.91 (8H, m) 7.79 (2H, d, *J*= 1.9 Hz), 7.60 (2H, d, *J* = 15.7 Hz), 7.45 (2H, d, *J*= 2 Hz), 7.21(2H, dd, *J*= 8.3 Hz), 7.15 (2H, m), 6.94 (1H, d, *J*=15.7Hz), 6.53 (1H, d, *J* = 2 Hz), 5.30 (4H, m), 3.97(6H, s); ^{13}C NMR (100.1 MHz, ($CDCl_3$) δ 183.14, 169.31, 154.25, 146.35, 143.45, 133.18, 127.11,124.31, 123.91, 120.68, 120.65, 110.20, 59.71, 56.21, 40.87. ppm. HRMS (ESI): Calculated for $C_{41}H_{30}N_2O_{12}$ $[M+H]^+$: 743.1799, found 743.1833.

(v) Synthesis of 4, 4'-*O*-dimethyl sulfonate curcumin (45):

To stirring mixture of curcumin **(3)** (368 mg, 1 mmol), triethyl amine (0.42 ml, 3 mmol) in dry tetrahydrofuran (25 ml) at under argon atmosphere at 0 °C, methyl sulphonyl chloride (0.17 ml, 2.2 mmol) was added and stirred at room temperature for 12 h. The reaction was checked with TLC. The resulting reaction mixture was concentrated under rotatory. Crude product was purified with column chromatography using hexane: ethyl acetate (7:3) as eluent, to give the pure product 4,4'-*O*-dimethyl sulfonyl curcumin **(45)** (Orange solid, yield 400 mg, 76%); R*f* 0.4 (30% ethyl acetate: hexane), mp 165-167 °C; IR (KBr) υmax (cm^{-1}) 3412, 1720, 1646, 1564, 1444, 1218; ^{1}H NMR (400 MHz, $CDCl_3$) δ 7.62 (d, *J* = 15.8 Hz, 2H), 7.34 (d, *J* = 8.3 Hz, 2H), 7.24 – 7.13 (m, 4H), 6.61 (d, *J* = 15.8 Hz, 2H), 5.90 (s, 1H), 3.96 (s, 6H), 3.29 – 3.20 (m, 6H). ^{13}C NMR (101 MHz, $CDCl_3$) δ 182.94, 151.74, 139.43, 135.22, 125.07, 121.00, 112.14, 102.17, 56.12, 38.57, 30.33.ppm. HRMS (ESI): Calculated for $C_{23}H_{24}O_{10}S_2$ $[M+H]^+$: 525.0811, found 525.0852.

(vi) Synthesis of 4-*O*-(2, 3, 4, 6-tetra-*O*-acetyl-D-glucosyl) curcumin (30):

To stirring solution of curcumin **(3)** (368 mg, 1mmol) in dichloromethane (50 ml), aqueous solution of KOH (50ml, 15%) was added at room temprature during 15 min, followed by addition of benzyl tributyl ammonium chloride (312mg, 1mmol). The

solution of 2,3,4,6-tetra-*O*-acetyl-1-bromo-D-glucopyranose **(25)** (1g, 2.4 mmol) in dichloromethane (25 ml) was added into the reaction mixture, and stirred for 8h at room tempareture, reaction was checked by TLC. Organic layer was separated from resulting reaction mixture, and organic layer washed with 50 ml of (0.1 N) NaOH solution, brine solution, and water. Separated organic layer was dried over sodium sulphate, concentrated under high vacuum. The product purified with silica gel column chromatography using ethyl acetate: hexane (2:3) as eluent, to give pure 4-*O*-(2,3,4,6-tetra-*O*-acetyl-D-glucosyl) curcumin. (**30**) Orange powder; yield 180mg; 25%; R*f* 0.4 (40% ethyl acetate: hexane), mp. 86-88°C; IR (KBr) υmax (cm^{-1}) 3419, 1750. ^{1}H NMR (800 MHz, $CDCl_3$) δ 9.90 (s, 1H), 7.59 (d, *J* = 15.7 Hz, 2H), 7.14 – 7.07 (m, 4H), 6.53 (d, *J* = 10.0 Hz, 1H), 5.84 (s, 1H), 5.35 – 5.28 (m, 3H), 5.21 – 5.14 (m, 1H), 5.06 – 5.00 (m, 1H), 4.28 (dt, *J* = 13.3, 6.7 Hz, 1H), 4.18 (dd, *J* = 12.3, 2.3 Hz, 4H), 3.91 – 3.78 (dt, 6H), 2.23 – 1.90 (m, 12H). ^{13}C NMR (201 MHz, $CDCl_3$) δ 183.14, 169.96, 150.75, 147.71, 140.04, 131.53, 123.42, 121.64, 119.56, 111.53, 101.71, 100.30, 72.28, 71.09, 68.28, 61.88, 56.09, 20.64.ppm. HRMS (ESI): Calculated for $C_{35}H_{38}O_{15}$ $[M+H]^+$: 699.2211, found 699.2245.

(vii) Synthesis of 4-*O*-diethyl phosphonyl-curcumin and 4, 4'-*O*-diethyl phosphonyl curcumin. **(46)-(47).**

To stirring solution of triethyl phosphite (500 mg, 3mmol) in dichloromethane (25ml) at 0 ºC, iodine (751mg, 2.9 mmol) was added into the reaction mixture and stirred for 5 minutes. The colorless solution was allowed to warm at room temperature. The phosphorylation agent was added drop wise into the solution of curcumin **(3)** (368 mg, 1mmol), pyridine (0.3ml, 4.1 mmol) in dichloromethane (25ml) and stirred at room temprature for 3h. Reaction was checked by TLC. The resulting reaction mixure was concentered under reduced pressure. The reaction mixture was diluted with dichloromethane (50ml), washed with water, separated organic layer dride over sodium sulphate and concentrated in vacuo. Mixture was separated on silica gel column chromatography using ethyl acetate: hexane (2:3) as eluent, to give pure **(46)** (Orange solid; yield 150 mg, 29%); R*f* 0.4 (40% ethyl acetate: hexane), mp. 98-100°C; IR (KBr) υmax (cm^{-1}) 3401, 2926, 1627, 1588, 1468, 1270, 1214, ^{1}H NMR (400 MHz, $CDCl_3$) δ 7.75 – 7.49 (m, 2H), 7.32 (dd, *J* = 8.2, 1.3

Hz, 1H), 7.16 – 7.02 (m, 3H), 6.95 – 6.87 (m, 2H), 6.64 – 6.38 (m, 2H), 5.88 – 5.78 (s, 1H), 4.37 – 4.21 (m, 4H), 3.95 (s, 3H), 3.92 (s, 3H), 1.44 – 1.34 (m, 6H). ^{13}C NMR (101 MHz, $CDCl_3$) δ 184.51, 181.84, 150.89, 148.17, 146.94, 141.23, 139.29 ,132.87, 127.43, 124.00, 123.07, 121.61, 121.07, 114.94, 111.68, 109.70, 101.57, 64.79, 55.96, 16.09.ppm. HRMS (ESI): Calculated for $C_{25}H_{29}O_9P$ $[M+H]^+$: 505.1549, found 505.1581.

(47) (Orange solid; yield 300mg, 46%); R*f* 0.5 (50% ethyl acetate: hexane), mp. 121-123°C; IR (KBr) υmax (cm^{-1}) 3468, 2925, 1630, 1465;^{1}H NMR (400 MHz, $CDCl_3$) δ 7.60 (d, *J* = 15.8 Hz, 2H), 7.36 – 7.29 (m, 2H), 7.17 – 7.08 (m, 4H), 6.55 (d, *J* = 15.8, Hz, 2H), 5.87 (s, 1H), 4.32 – 4.18 (m, 8H), 3.95 – 3.91 (m, 6H).1.42 – 1.36 (m, 12H). ^{13}C NMR (101 MHz, $CDCl_3$) δ 183.11, 150.92, 141.41, 139.88, 132.72, 124.02, 121.62, 121.20, 111.73, 101.78, 64.7, 56.01, 16.09.ppm. HRMS (ESI): Calculated for $C_{29}H_{38}O_{12}P_2$ $[M+H]^+$: 641.1838, found 641.1858.

(viii) Synthesis of fine particle of curcumin and isoxazole curcumin.

Curcumin **(3)** / isoxazole curcumin (100 mg) dissolved in DMSO (10 ml) was slowly added into the boiling mili Q water (100 ml) during 1h. Cooled at room tempareture and reaction mixture was sonicated for 1h. After sonication reaction mixture was centrifuged for 2h at 5000 rpm. Supernatant water was decanted, the fine particles of the product were dried in hot air oven.

3.7. Bioassay:

3.7. (a) *In vitro* testing for antibacterial activity.

Based on the in silico results we further continued to check the activity of the compounds against bacterial gram negative strain (*Pseudomonas aeruginosa*) and gram positive strains (*Staphylococcus aureus*).

3.7. (b) Bacterial cultures:

The standard strains of *Pseudomonas aeruginosa* (MCC 3081) and *Staphylococcus aureus* (MCC 2408) were procured from National Centre for Cell

Science (NCCS) Pune. For revitalization, freeze-dried bacteria were sub-cultured in Brain Heart Infusion (BHI, Himedia Laboratories, Mumbai) broth and incubated at 37˚C for 24 h. These strains were tested for their purity, morphological and biochemical characteristics and maintained by periodical subculturing on Nutrient agar (Himedia Laboratories, Mumbai) slants for both *Pseudomonas aeruginosa* and *Staphylococcus aureus.*

3.7. (c) Inoculum preparation:

Pseudomonas aeruginosa and *Staphylococcus aureus* was plated separately. Single colony was transferred and incubated with agitation at 37˚C for 24 h. *Pseudomonas aeruginosa* and *Staphylococcus aureus* cells were harvested by centrifugation (4000 × g, 15 min) at 4˚C. Pelleted cells in centrifuge tube were washed with 2 volumes of sterile saline solution (NSS, 0.85% NaCl) and re-suspended in it until a McFarland standard of 0.5 was achieved. The bacterial growth was quantified as per method of ICMSF and the cell density adjusted approximately to 1x105 colony forming units (cfu/ml) of bacterial suspension. Fresh inoculum was prepared for each experiment.

3.7. (d) MIC calculation:

The synthesized compounds were soluble in DMSO at various serial dilution concentrations starting from 1M and further diluted into 0.1, 0.01, 0.001, 0.0001M concentrations. And we have calculated MIC accordingly the standard National Committee for Clinical Laboratory Standards microdilution methods (NCCLS 2000), and the values were measured by a determination of the--optical density of bacterial cell at a wavelength of 600 nm. MICs were determined by broth dilution technique [20]. The nutrient soup, which contained logarithmic in order to two fold diluted amounts of test compound and controls was inoculated with approximately 1 × 105 c.f.u./ml of actively dividing bacteria cells. The cultures have been incubated for 24 h at 37 °C and the growth was monitored visually and spectrophotometrically. The lowest concentration (the highest dilution) need to arrest the growth of bacteria was observed as minimum inhibitory concentration (MIC). The chloramphenicol is used as standard drug against the synthesized compounds

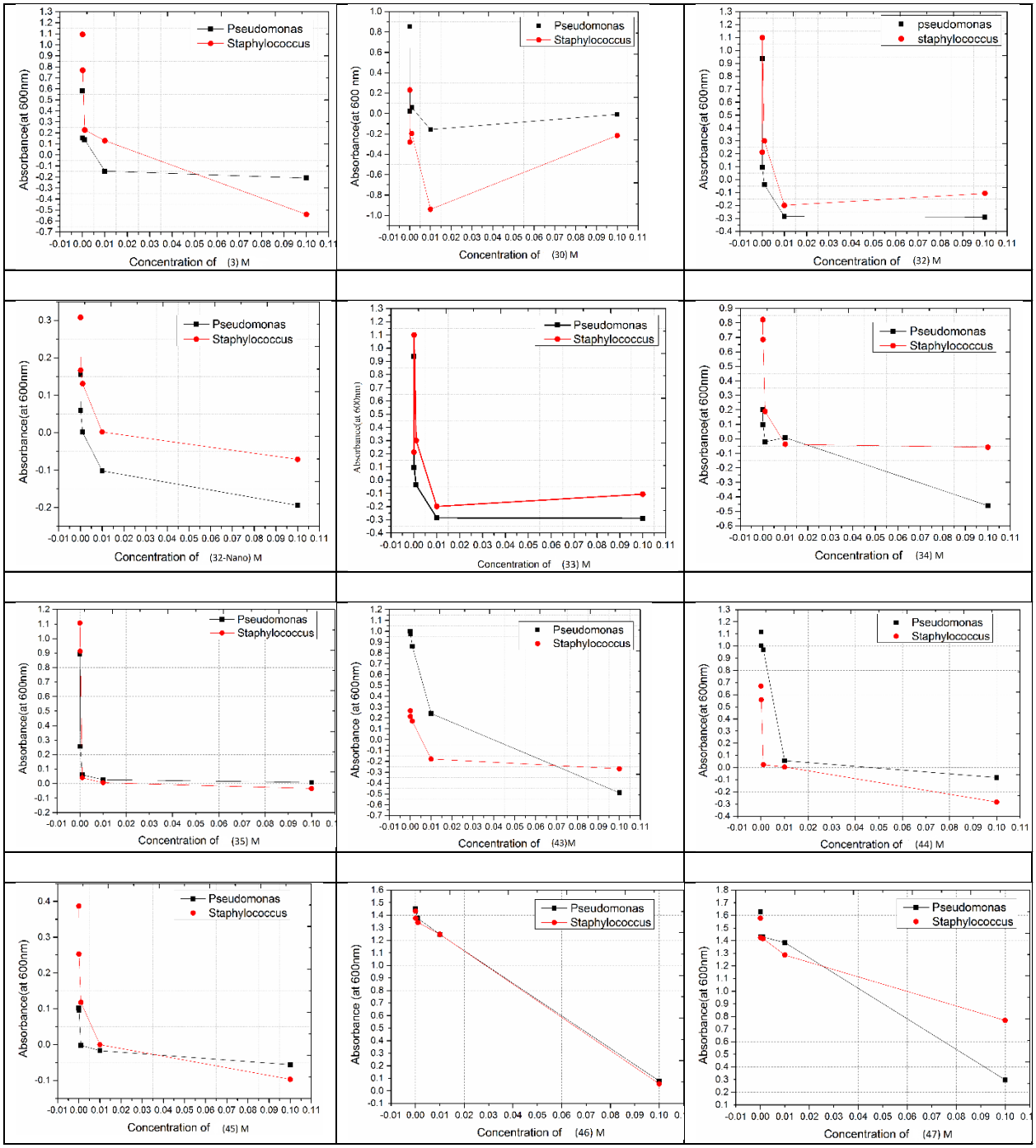

Figure 3.3. Graphs showing absorbance against molar concentration of compounds (**32**)-(**47**) against *Styphylococcus aureus* and *Pseudomonas arigunosa*.

Table 3.2. MIC/ IC_{50} values and binding energies of curcumin **(3)** and its analogues with MipZ and Pyruvate kinase proteins of *Pseudomonas aeruginosa* and *Staphylococcus aureus* respectively.

Compounds	MIC S. aureus Unit-M	MIC P. aeruginosa Unit-M	IC_{50} (Gram+ve) Unit-M	IC_{50} (Gram -ve) Unit-M	Binding scores P. aeruginosa	Binding scores S. aureus
(32-Nano)	0.0007	0.01	0.503	0.055	-9	-8
(32)	0.0002	0.003	0.050	0.051	-9	-8
(33)	0.0003	0.004	0.050	0.052	-8.8	-8.1
(34)	0.0006	0.003	0.0503	0.051	-9.5	-8.7
(35)	0.01	0.01	0.05	0.05	-9.4	-8.5
(46)	0.1	0.1	0.08	0.08	-8.6	-7.4
(47)	0.0	0.1	0.0	0.08	-7.9	-5.4
(45)	0.0004	0.01	0.0502	0.05	-7.5	-8.5
(44)	0.01	0.01	0.05	0.05	-10.5	-6.2
(30)	0.0004	0.005	0.050	0.052	-1.8	-9.2
(43)	0.05	0.04	0.07	0.07	-8.4	7.8
(3)	0.05	0.025	0.075	0.0625	-8	-4

3.7. (e) IC_{50} (Half of maximum inhibitory concentration):

In order to calculate the IC_{50} (50% of minimum inhibitory concentration), the intercept and slope were calculated from the graph using Python-2.7script through formulae Y= MX + C. In the following graphs (Fig.3.3) the Y-axis represents the value of absorbance of the remaining supernatant solutions of various serial concentrations of ligands used, the initial concentration marked at X-axis of the compound. The MIC and IC_{50} values of curcumin **(3)**, Sodium salt of curcumin, nano curcumin and curcumin analogues have been tabulated in (Table 3.2).

3.8. Results and Discussion:

3.8. (a) Curcumin analogues/derivatives:

Despite important therapeutic window and mechanism of action, the therapeutic utility of curcumin **(3)** is limited because of its fast metabolism, poor absorption and low bioavailability under physiological conditions. It is believed that active methylene group and the ketone moiety are responsible for its fast metabolism.

In order to overcome this problem and to improve its pharmacokinetics properties, we studied several synthetic modifications on the carbonyl, active methylene group and side functionalities on aromatic rings.

Nitrogen and sulfur containing heterocyclic moieties such as pyrazoles, pyrimidines and thio pyrimidines containing derivatives are well known for their broad-spectrum of pharmacological properties such as antimicrobial, anti-inflammatory, analgesic, enzyme inhibition, antioxidant, and anticancer. These scaffolds have important role in drug designing as important pharmacophore. Therefore towards the synthetic goal, we focused on incorporating isoxazole, N-substituted pyrazoles, pyrimidine-2(1H)-thione and pyrimidine ring in the molecular scaffold of curcumin **(3)**. Based on the *in-silico* analysis we executed the chemical synthesis, *in-vitro* analysis and validation of the obtained results.

The first objective of this work was to synthesize a series of curcumin **(3)** derivatives (**32), (34)**, (**35), (44), (45), (30), (46),** and (**47**) followed by their evaluation as antimicrobial agents against Gram-positive and Gram-negative bacteria. A series of curcumin **(3)** derivatives has been synthesized that contain isoxazole, pyrazole, thiazole, thione, attached to the carbonyl functionality and phthalimide along with their phosphate, sulphate and glucoside fragment attached to the hydroxyl group in the aromatic part of curcumin **(3)**.

Towards the synthetic goal, we began with the synthesis of compound **(32)**. The reaction of curcumin **(3)** with hydroxylamine hydrochloride in dry ethanol and 10 mol % of pyridine furnished **(32)** in 89% yields. Following the synthesis of other analogues, the reaction of hydrazine hydrate, with curcumin **(3)** in glacial acetic acid gave **(33)** in 92% yield. Under similar conditions the reaction of curcumin **(3)** with urea and thiourea accomplished **(34)** and **(35)** respectively 86% and 74% yield. (Scheme 3.5). To synthesize compound **(43)** the unsaturated di keto group of curcumin **(3)** was by reduced by reported protocol [12], where curcumin **(3)** was treated with sodium borohydride to furnish the corresponding 3,5 diol in **(43)** in yield 50% shown in Scheme 3.6. The result was confirmed with ^{1}H NMR spectroscopy. The next task was to synthesize di N-phthaloyl glycine ester of curcumin **(44)** which was done by coupling of carboxylic group of phthaloyl glycine with hydroxyl group curcumin in 2:1 molar ratio, in dimethyl amino pyridine and

EDC. The yield of compound **(44)** 82% and results were supported by ^{1}H NMR and ^{13}C NMR spectra (Scheme3.7).

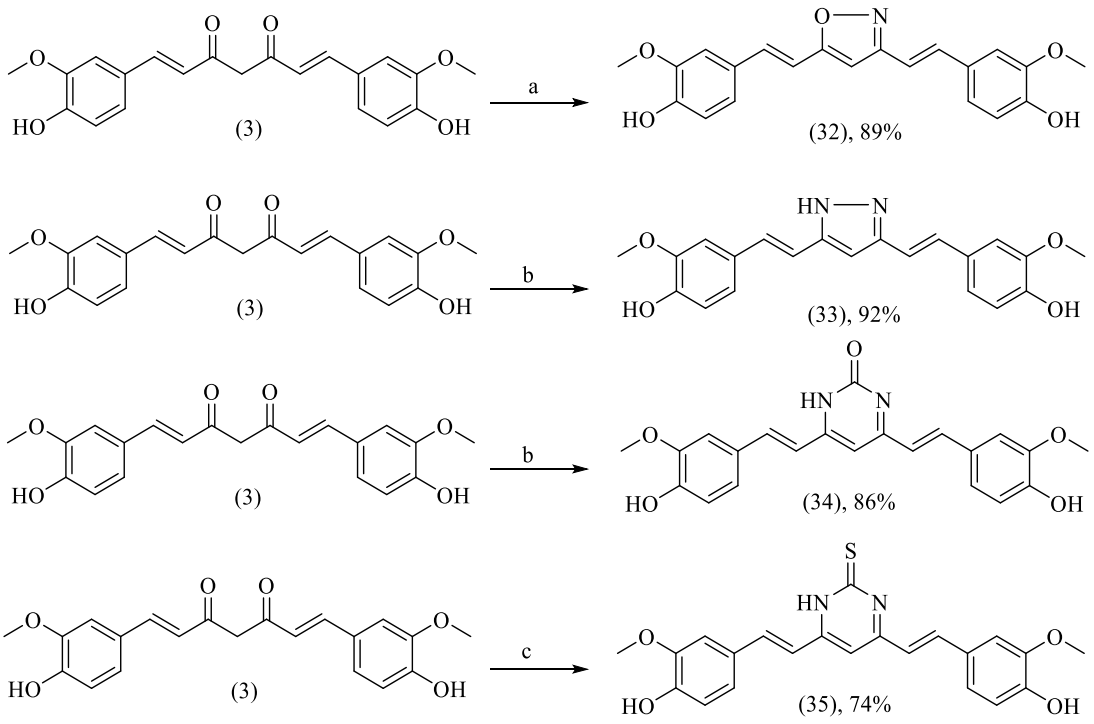

Reagent and condition: (a) $NH_2OH.HCl$, Pyridine, EtOH, 80°C, 6h; (b) Urea/NH_2NH_2, AcOH, 110°C, 4h
(c) Thiourea, AcOH, 110, 7h.

Scheme 3.5. Synthesis of compounds **(32)-(35).**

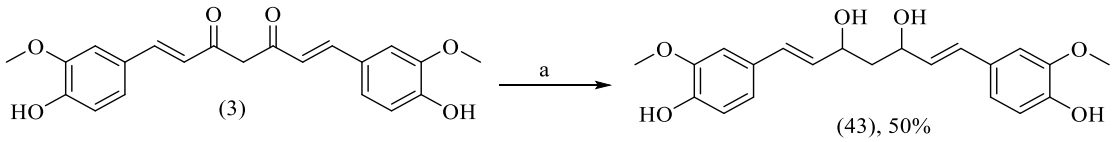

Reagent and condition: (a) $NaBH_4$, MeOH, 12h, rt.

Scheme 3.6. Synthesis of compound **(43).**

To begin with the synthesis of **(45)**, curcumin was treated with methyl suphonyl chloride in the presence of triethylamine (TEA) to bring out the nucleophilic substitution on phenolic group of curcumin. The product yield were calculated 76% and **(45)** confirm with ^{1}H NMR and ^{13}C NMR spectra.Proceeding synthesis of title compound **(30)** curcumin was treated with bromo tetra acetyl glucose in the presence of BTBAC to carried out the nucleophilic substitution on phenolic group of curcumin resulting in a mixture of di and mono tetra acetyl glucose curcumin. The mixture of compound **(30)** was purified with column chromatography with yield of **(30)** yield

25% and **(30)** confirm with ^{1}H NMR and ^{13}C NMR spectra .(Scheme 3.7) To synthesized compounds **(46)** and **(47)**, we were treated curcumin with phosphorylating agent (mixture of triethyl phosphite and iodine) and the presence of triethylamine (TEA) to achieve a mixture of **(46)** and **(47)**, and were purified with column chromatography, yield respectively 29%, 46%, show (scheme 3). We were prepared the fine particles of curcumin **(3)** and **(32)** by the reported protocol [22].

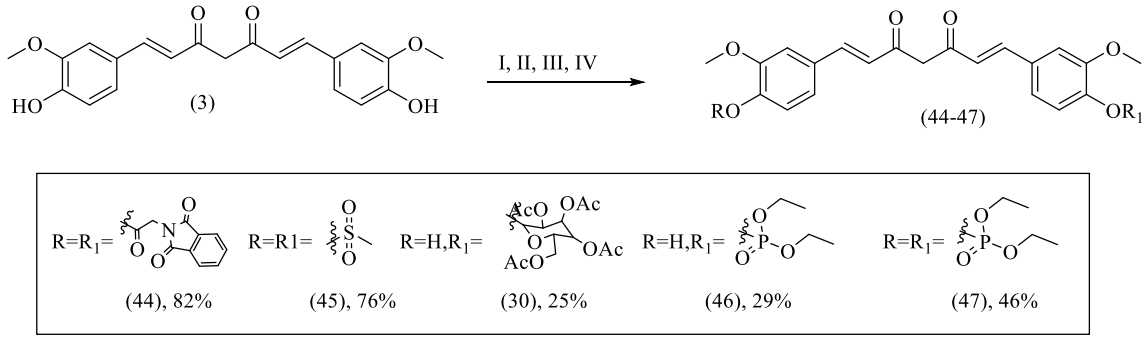

Reagent and condition:
(I) DMAP, EDC.HCl, DCM, 0°C, 0.5 h, rt, 12 h,
(Il) TEA, THF, 0 °C, 0.5 h, rt, 12 h, (lll) BTBAC, DCM, 15 min., rt, 8 h
(lV) DCM, 0 °C, 5 min, pyridine, rt, 3 h.

Scheme 3.7. Synthesis of compounds **(44)-(47)**.

3.8. (b) Biological assay:

In the present study, we have taken maximum concentration (0.1 molar) of all synthesized derivatives of curcumin, which was serially diluted in order to calculate MIC and IC_{50} values of each compound. The optical density of un-inoculated and inoculated broth was noted and adjusted as error against all readings taken. At 0.1 molar concentration, the absorption values recorded after complete lysis of bacteria are suggested of their respective activities against both the Gram positive (*Staphylococcus aureus*) and Gram negative (*Pseudomonas aeruginosa*) bacteria. The shown graphs given above we can arrange these compounds in the following order with respect to relative activities towards both Gram positive (*Staphylococcus aureus*) and Gram negative (*Pseudomonas aeruginosa*) bacteria**.**

(46)>(35)>(45)>(44)>(30)>(3-Nano)>(32)>(43)>(32-Nano)>(3)>(33)>(47)>(34).

The **(46)** and **(47)** activities was equal **(3)**, (**30), (45)** and **(44)** are relatively more active towards Gram positive bacteria while (**47), (32-Nano)**, (**32), (34), (3-Nano), (43)** and **(33)** are more active towards Gram negative bacteria. The activity of **(30)** appears to be least towards both Gram positive and Gram negative bacteria which

may be due to a tetra acetyl glucose group attached at the phenolic function of curcumin causing not free any functional group for binding. The IC_{50} of chloramphenicol against *Pseudomonas aeruginosa* was 0.002M and 0.00001M for *Staphylococcus aureus*, which is considerably less in comparison to the synthesized compounds. These compounds can serve as better antibacterial alternatives, as now days the microbes became resistant to antibiotics due to their unselective use.

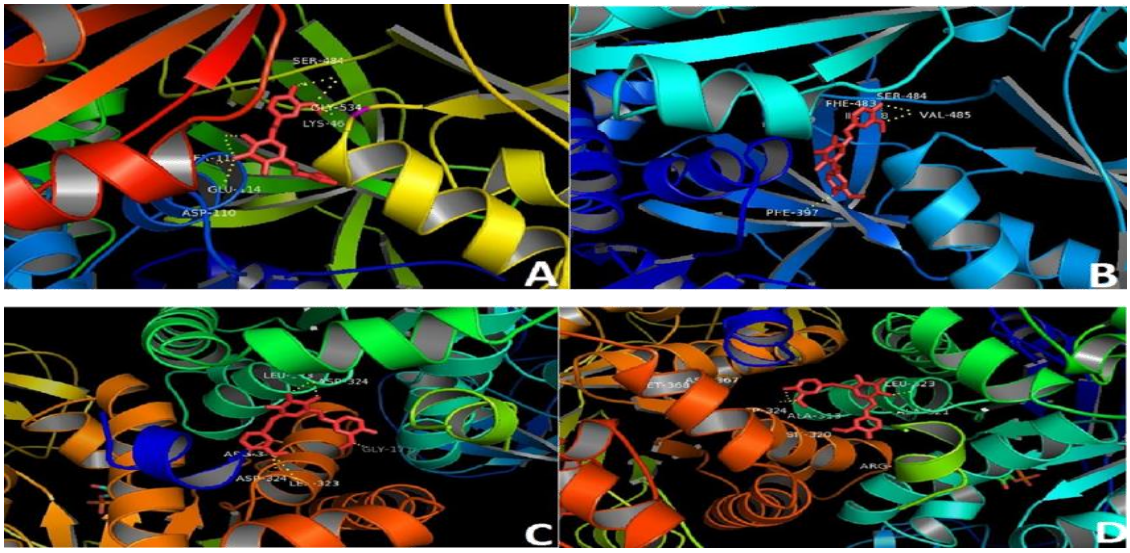

Figure 3.4. (A) and (C) show 3D interaction of **(34)** with 2XIT and 1A3W respectively while (B) and (D) represent **(35)** thione with2XIT and 1A3W respectively.

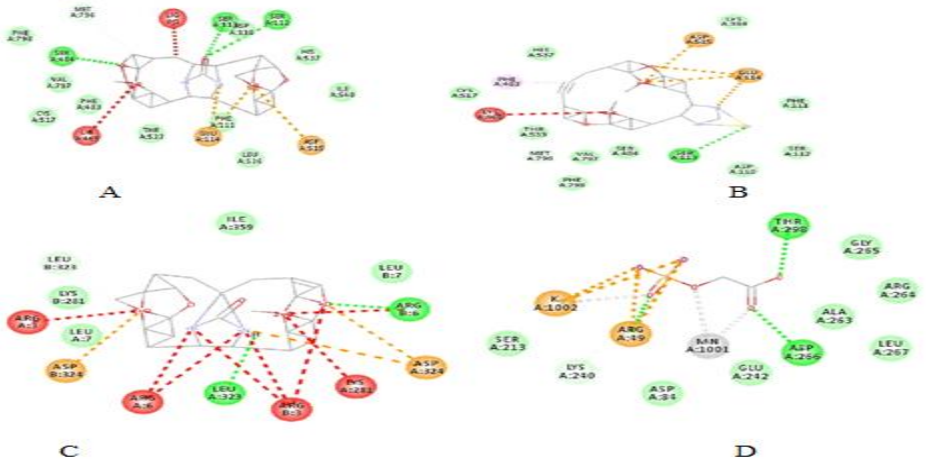

Figure 3.5. (A) and (C) show 2D interaction diagram of **(34)** with 2XIT and 1A3W respectively while (B) and (D) represent interaction of **(35)** with 2XIT and 1A3W respectively.

Since the cell wall structure of Gram positive and Gram negative bacteria is different and cell wall degeneration takes place due to inhibition of proteins of glycolytic pathway, it is evident that the amount of lysis of bacteria must differ in both with the same concentration of the ligand [23]. Therefore, in case of **(46)** and **(35)** it appears that some alternate mechanism is operating. This may be due to the presence of Sulphur in **(35)** and phosphate group in **(46)** which may preferably interact with bacterial surface proteins or DNA. The question arises why **(47)** i.e. the diphosphate of curcumin does not behave in a similar fashion. The binding energies in this case are comparatively much less than the monophosphate, indicating conformational strain in the molecule hindering docking. All the remaining molecules besides **(46)** and **(35)** have difference in relative activities, indicating that the mechanism operating is partly by membrane degeneration and partly by alternate mechanisms depending on the relative affinities of their substituents with bacterial surface moieties. Curcumin **(3)**, **(30)** [4-*O*-(2,3,4,6-tetra-*O*- acetyl-D-glucosyl curcumin], **(45)** [4,4'-*O*-dimethyl sulfonate curcumin] and (**44)** [4,4'-*O*-di (N-phthaloyl-glycinoyl)-curcumin] being more active towards Gram positive bacteria can prove to be most effective antibacterial drugs , since there are very few anti bacterials for Gram positive bacteria in the market. Curcumin **(3)** appears to have better activity for *S. aureus* than *P. aeruginosa*, while its sodium salt has almost equivalent activity while curcumin in nano form is more active for *P. Aeruginosa* than *S.aureus.* Therefore curcumin **(3)** can be taken in different forms according to the nature of infection. However, the MIC and IC_{50} values suggest preferable use of Sodium salt which may be due to its enhanced water solubility.Interestingly, we could observe variation in binding scores with the different analogs that were designed by introduction of different side chains. It was observed in the 2D interactions that the compounds receiving lower and better binding scores have favorable number of H-bonds which makes the combination more stable. The 3D interactions with best result were observed in case of compounds **(32)** and **(34)** with the respective protein 2XIT and 1A3W and have been presented below in the Fig-3.4 and their 2D interactions are illustrated in Fig-3.5. The 3D representation Fig3.4-(A, B) illustrates the combination of **(34)** and **(35)** with monomeric MipZ. The yellow dotted lines represent the H-Bonds between protein and ligand through specific amino acids. The 2D structure also shows that both compounds share the same pocket for binding containing following

common amino acids compound **(34)** and **(35)** with Pyruvate kinase enzyme respectively were such as SER484, the 2D structure of **(34)** and **(35)** with Pyruvate kinase has common LEU323, ASP324, ASP367 amino acids.

3.9. Conclusion:

From the results obtained it can be concluded that curcumin **(3)** analogues with the linker between two aromatic rings substituted with nitrogen containing heterocyclic rings e.g. isoxazole, pyrazole, thiazole, thione can prove to be much better drugs for antibacterial activity. Such molecules along with substituents like phosphate or sulphate substituted at one of the two phenolic hydroxyls of curcumin can prove to be potent anti-inflammatory agents due to their multi-targeted effects. These compounds **(34)**, **(35)** appear to act by some alternate mechanism too e.g. inhibiting cell division in addition to degradation of bacterial cell wall.

3.10. Spectral Data (^{1}H and ^{13}C):

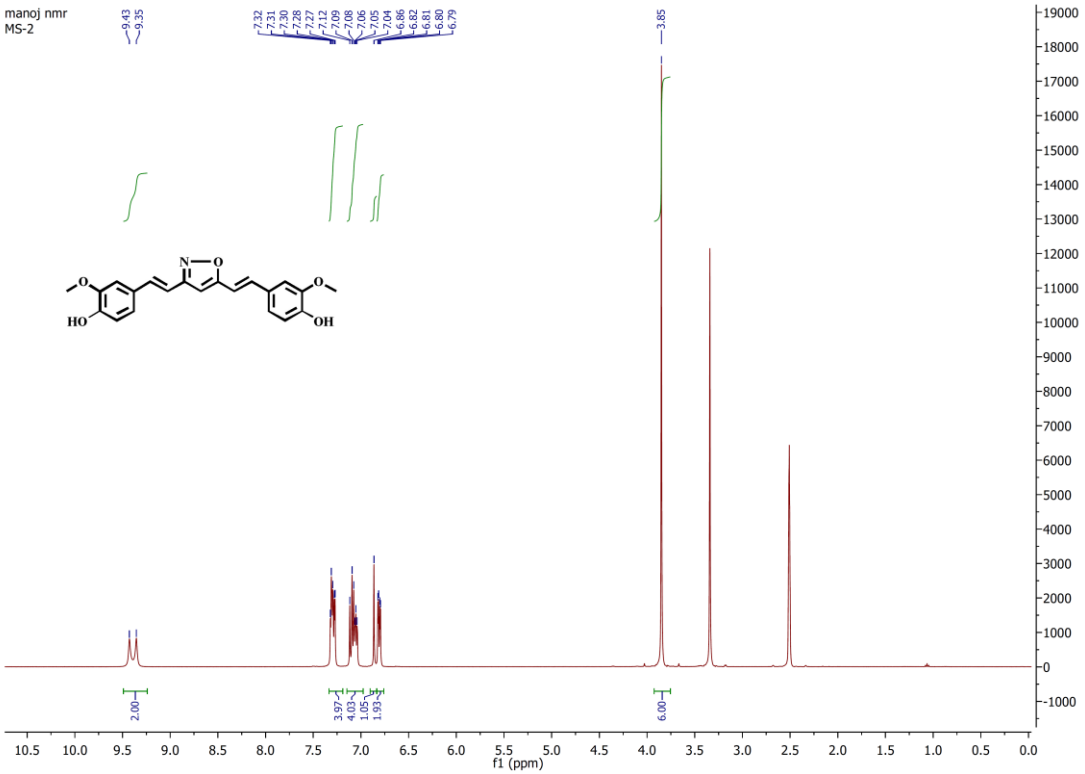

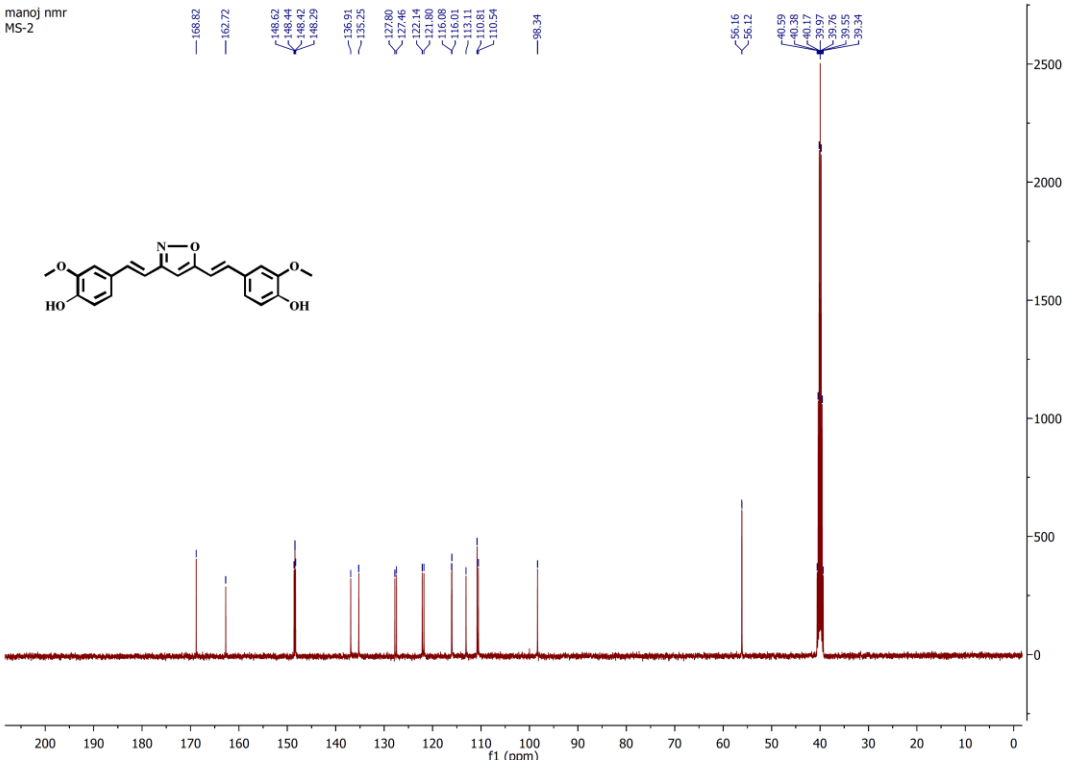

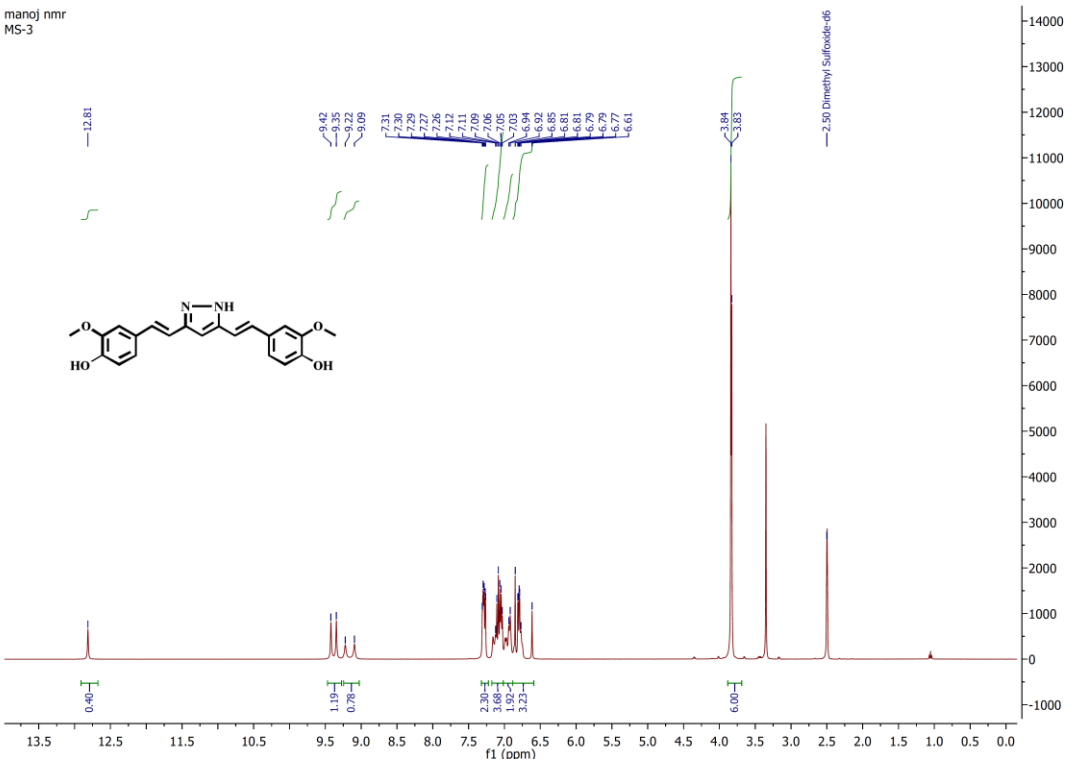
manoj nmr
MS-3
12.81
9.42
9.35
9.22
9.09
7.31
7.30
7.29
7.27
7.26
7.12
7.11
7.09
7.06
7.05
7.03
6.94
6.92
6.85
6.81
6.81
6.79
6.79
6.77
6.61
3.84
3.83
2.50 Dimethyl Sulfoxide-d6
0.40
1.19
0.78
2.30
3.68
1.92
3.23
6.00
f1 (ppm)

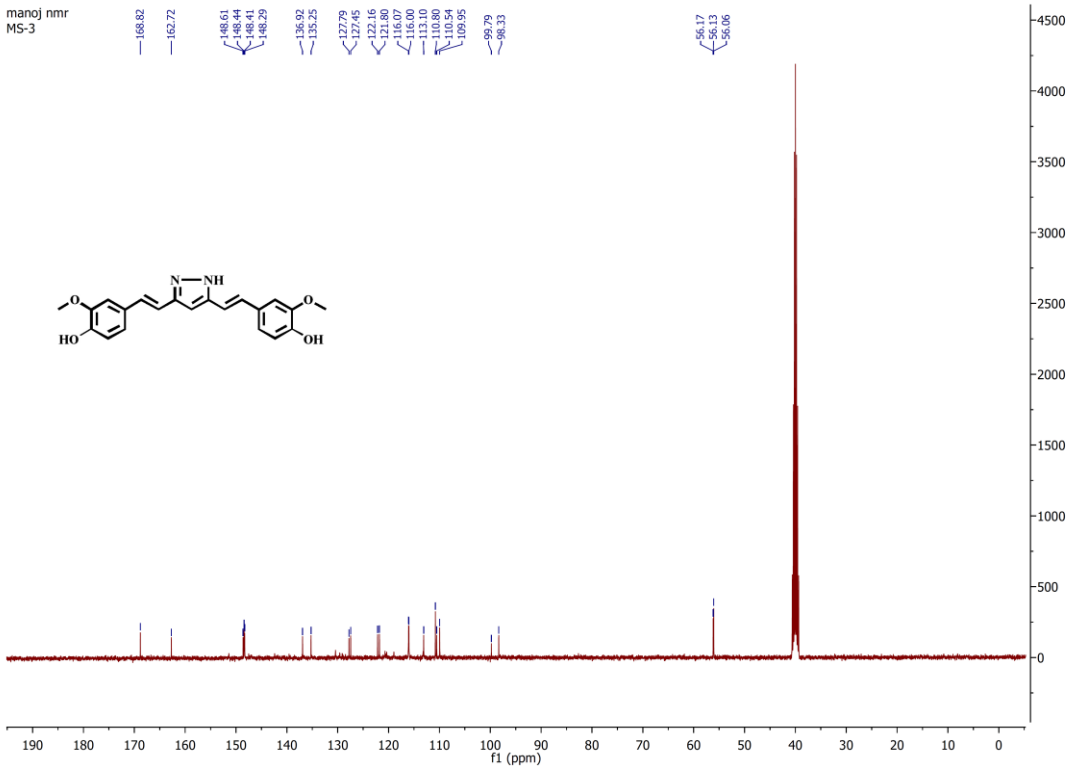
manoj nmr
MS-3
168.82
162.72
148.61
148.44
148.41
148.29
136.92
135.25
127.79
127.45
122.16
121.80
116.07
116.00
113.10
110.80
110.54
109.95
99.79
98.33
56.17
56.13
56.06
f1 (ppm)

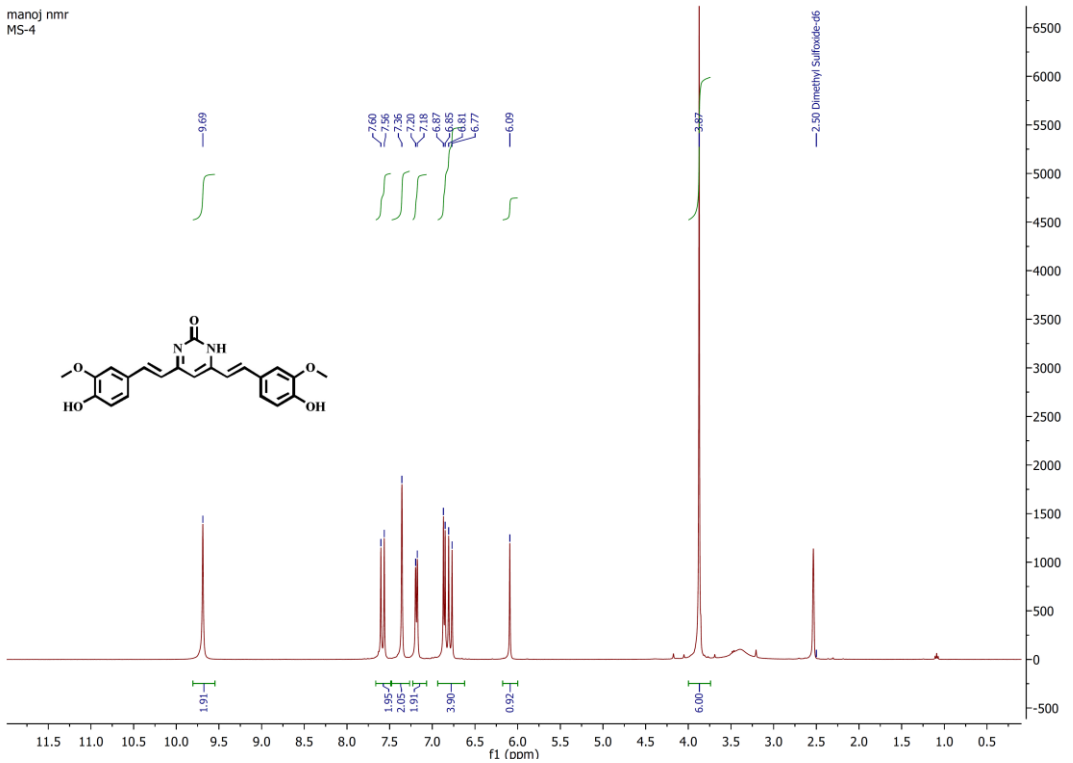
manoj nmr
MS-4
9.69
7.60
7.56
7.36
7.20
7.18
6.87
6.85
6.81
6.77
6.09
3.87
2.50 Dimethyl Sulfoxide-d6
1.91
1.95
2.05
1.91
3.90
0.92
6.00
f1 (ppm)

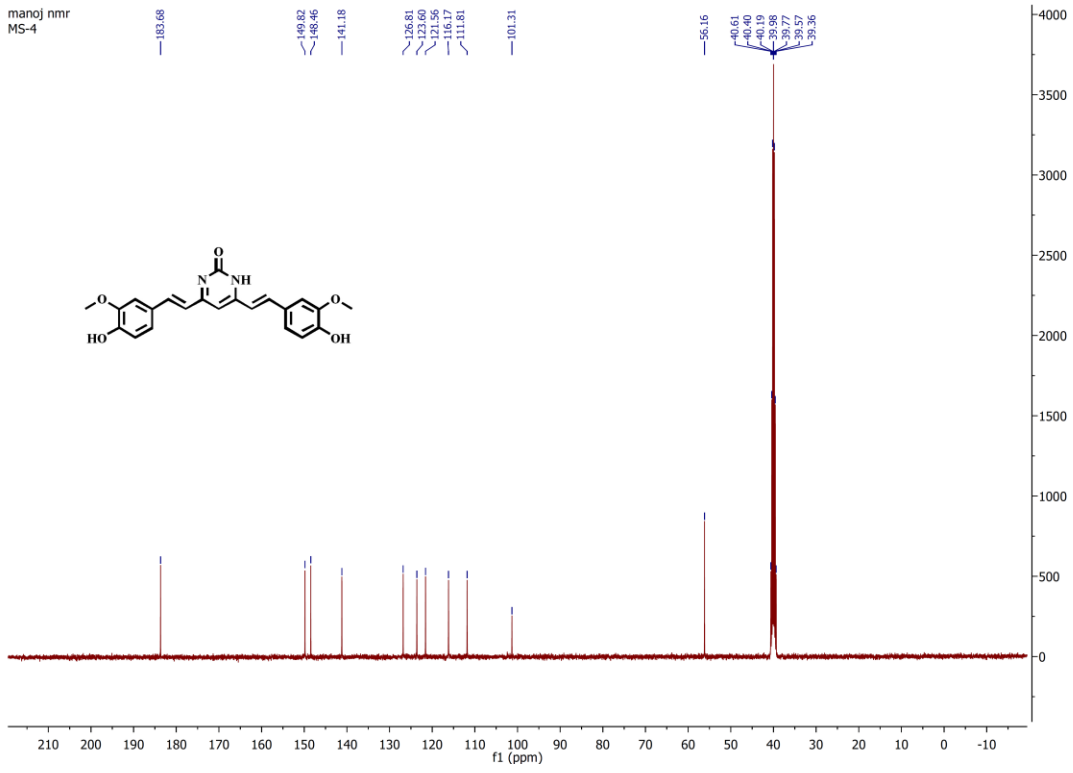
manoj nmr
MS-4
183.68
149.82
148.46
141.18
126.81
123.60
121.56
116.17
111.81
101.31
56.16
40.61
40.40
40.19
39.98
39.77
39.57
39.36
f1 (ppm)

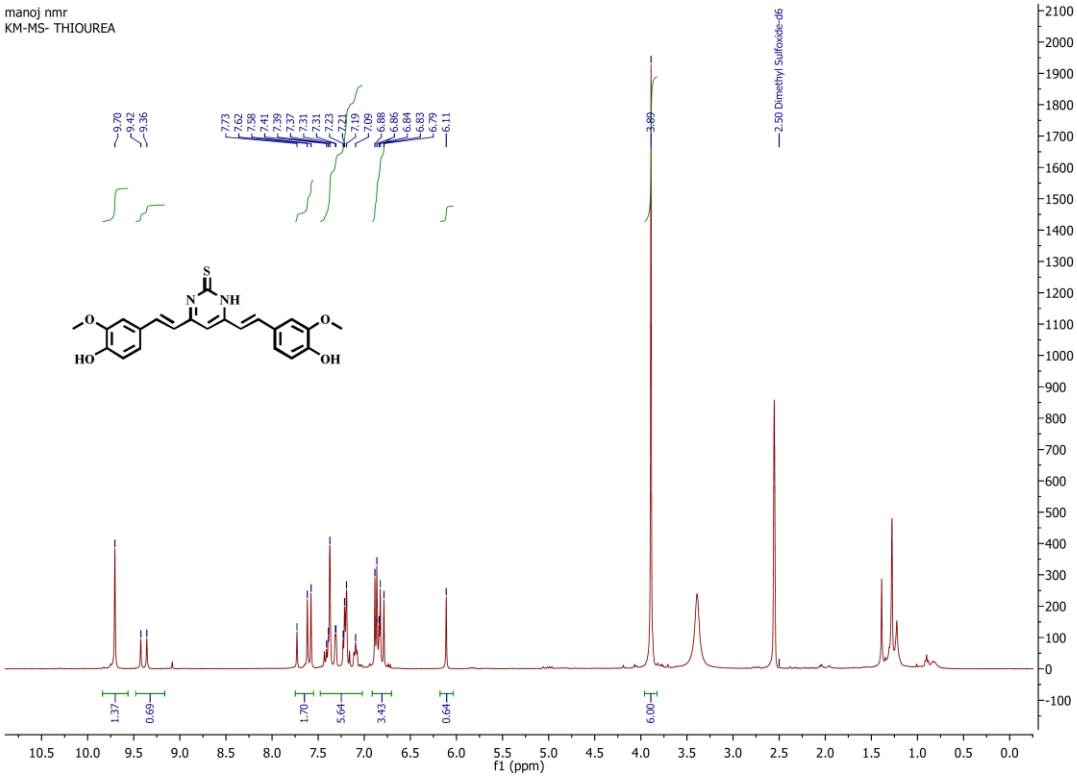
manoj nmr
KM-MS- THIOUREA
9.70
9.42
9.36
7.73
7.62
7.58
7.41
7.39
7.37
7.31
7.31
7.23
7.21
7.19
7.09
6.88
6.86
6.84
6.83
6.79
6.11
3.89
2.50 Dimethyl Sulfoxide-d6
1.37
0.69
1.70
5.64
3.43
0.64
6.00
f1 (ppm)

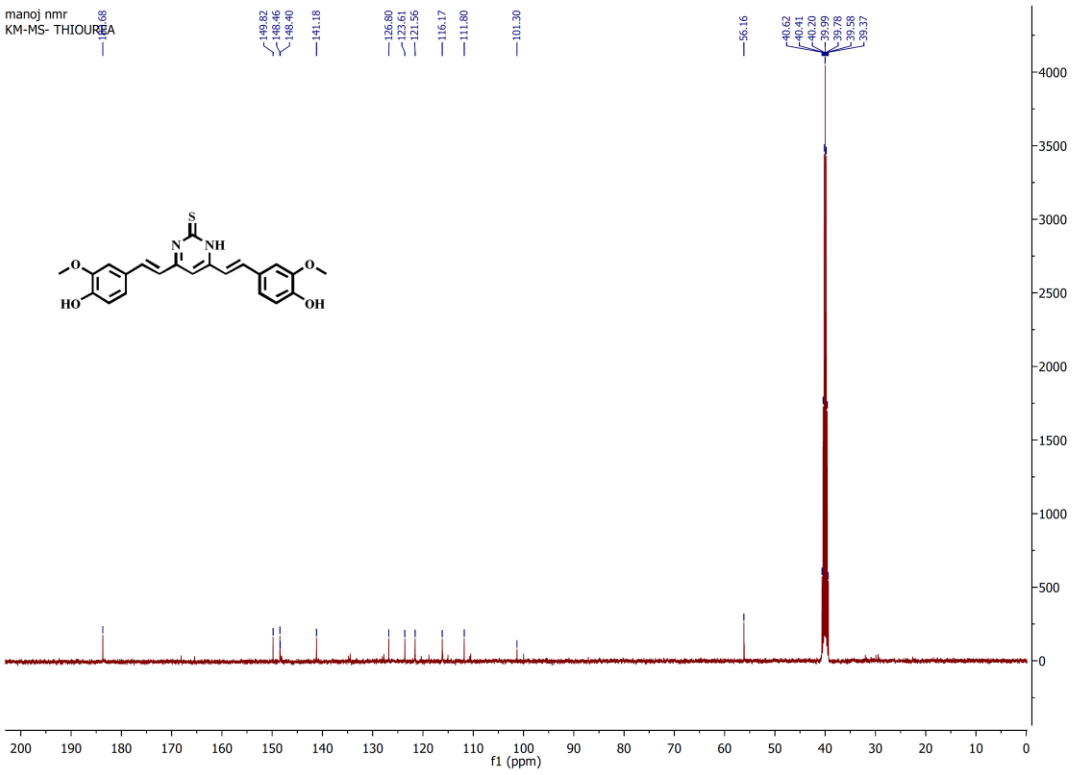
manoj nmr
KM-MS- THIOUREA
168
149.82
148.46
148.40
141.18
126.80
123.61
121.56
116.17
111.80
101.30
56.16
40.62
40.41
40.20
39.99
39.78
39.58
39.37
f1 (ppm)

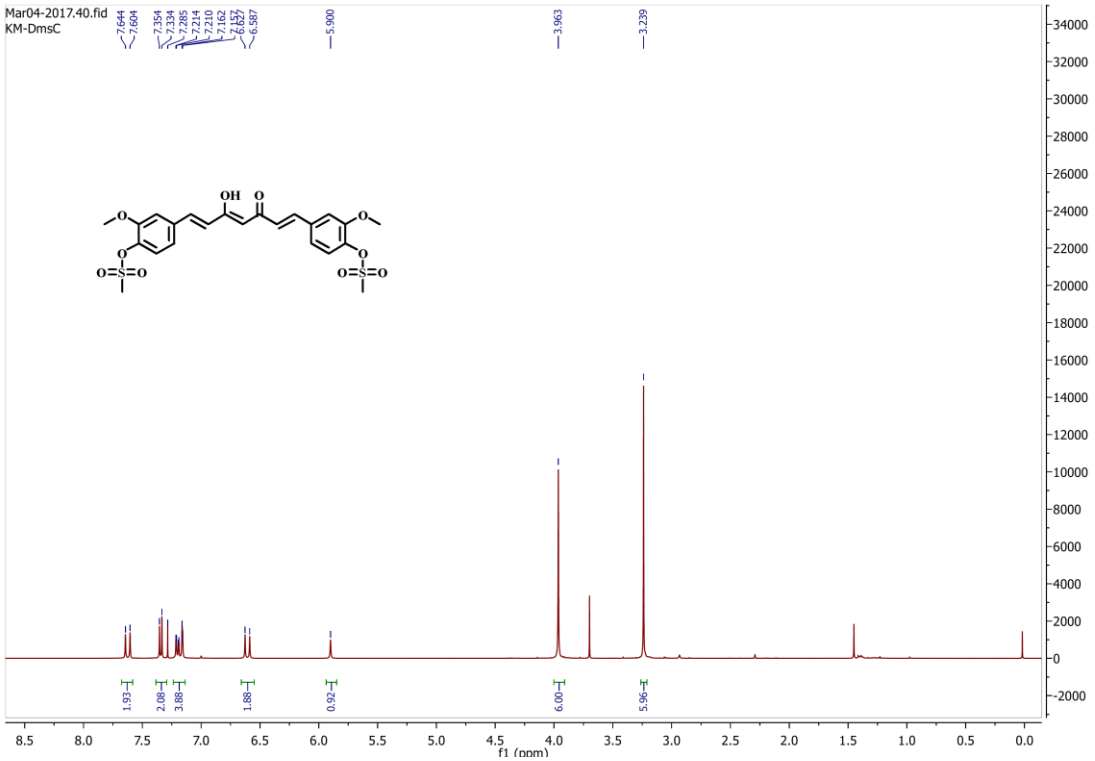
Mar04-2017.40.fid
KM-DmsC
7.644
7.604
7.354
7.334
7.285
7.214
7.210
7.162
6.587
5.900
3.963
3.239
OH
O
O
O
O
O=S=O
O=S=O
1.93
2.08
3.88
1.88
0.92
6.00
5.96
f1 (ppm)

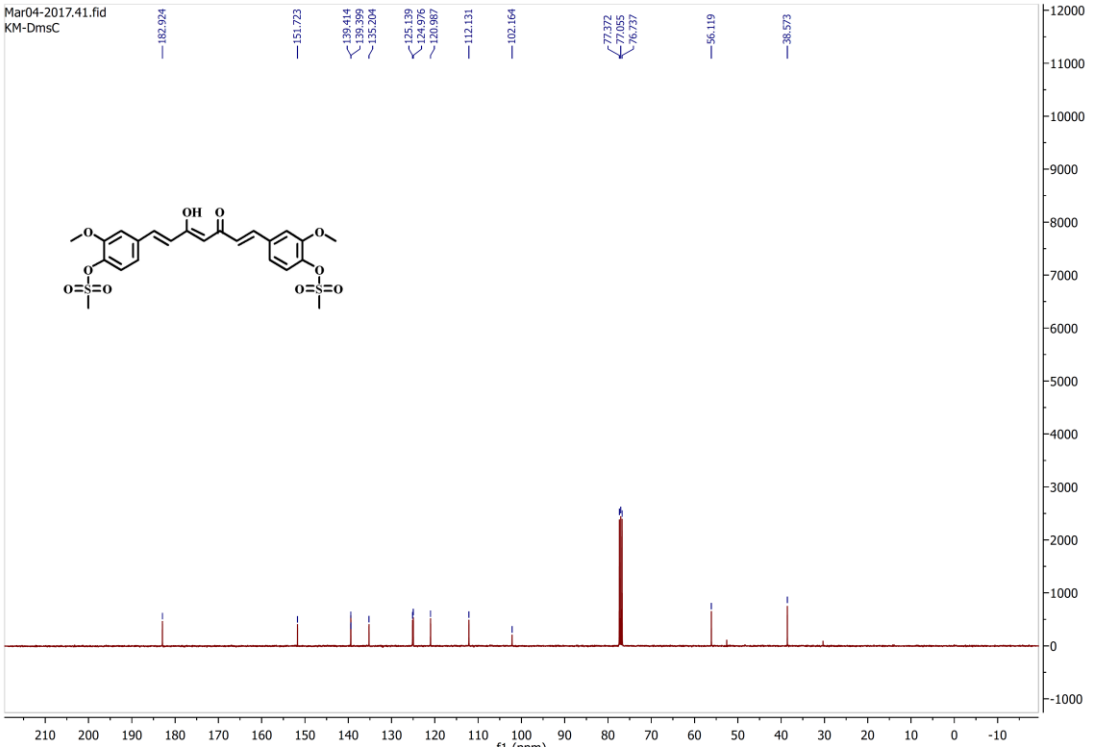
Mar04-2017.41.fid
KM-DmsC
182.924
151.723
139.414
139.399
135.204
125.139
124.976
120.987
112.131
102.164
77.372
77.055
76.737
56.119
38.573
OH
O
O
O
O
O=S=O
O=S=O
f1 (ppm)

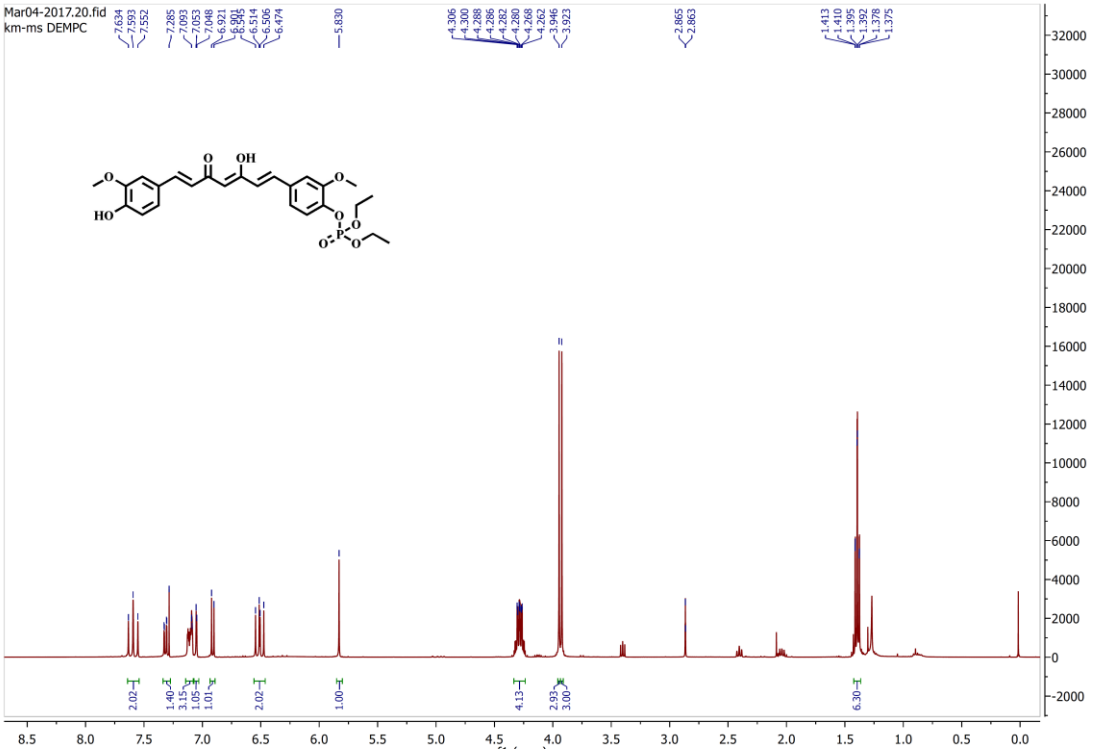
Mar04-2017.20.fid
km-ms DEMPC
7.634
7.593
7.552
7.285
7.093
7.053
7.048
6.921
6.905
6.514
6.506
6.474
5.830
4.306
4.300
4.288
4.286
4.282
4.280
4.268
4.262
3.946
3.923
2.865
2.863
1.413
1.410
1.395
1.392
1.378
1.375
O
OH
HO
O
O
O
O
O
P
2.02
1.40
3.15
1.05
1.01
2.02
1.00
4.13
2.93
3.00
6.30

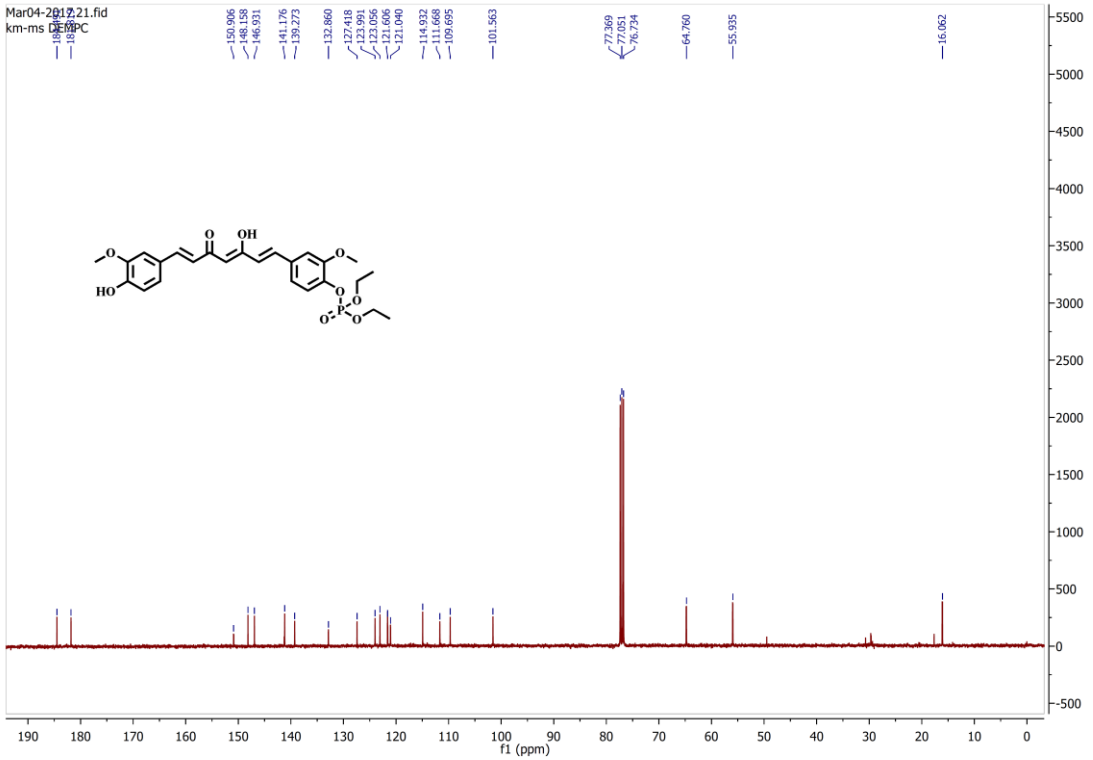
Mar04-2017.21.fid
km-ms DEMPC
150.906
148.158
146.931
141.176
139.273
132.860
127.418
123.991
123.056
121.606
121.040
114.932
111.668
109.695
101.563
77.369
77.051
76.734
64.760
55.935
16.662
O
OH
HO
O
O
O
O
O
P
f1 (ppm)

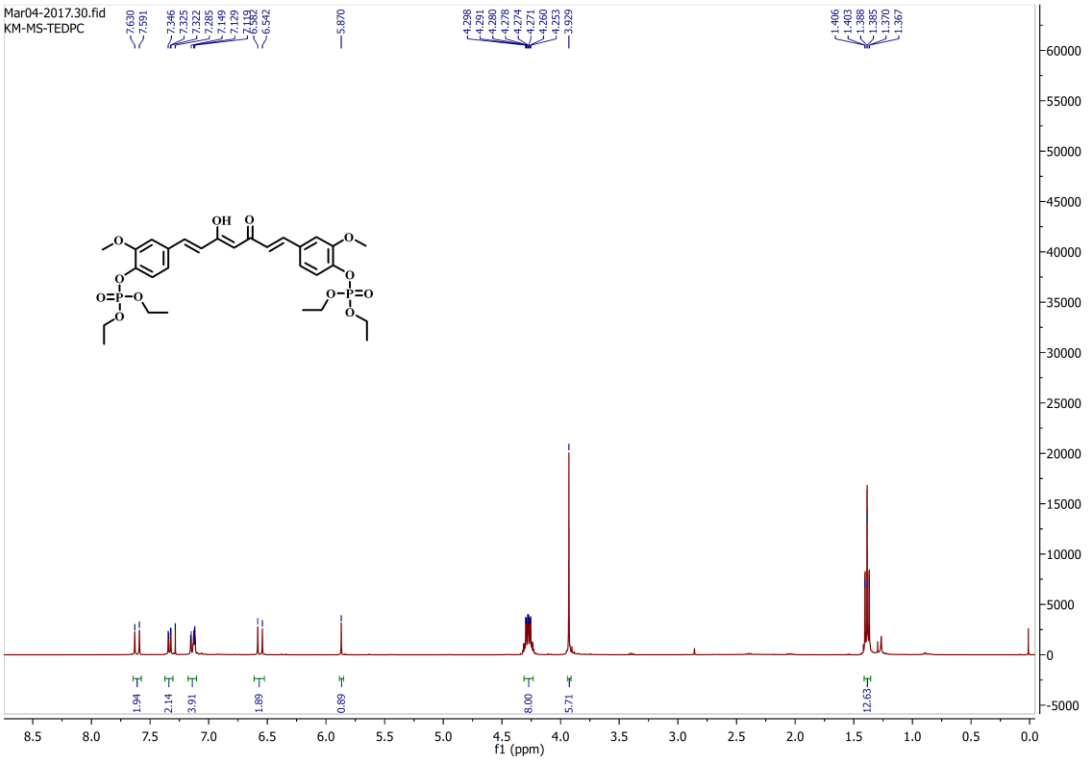
Mar04-2017.30.fid
KM-MS-TEDPC
f1 (ppm)

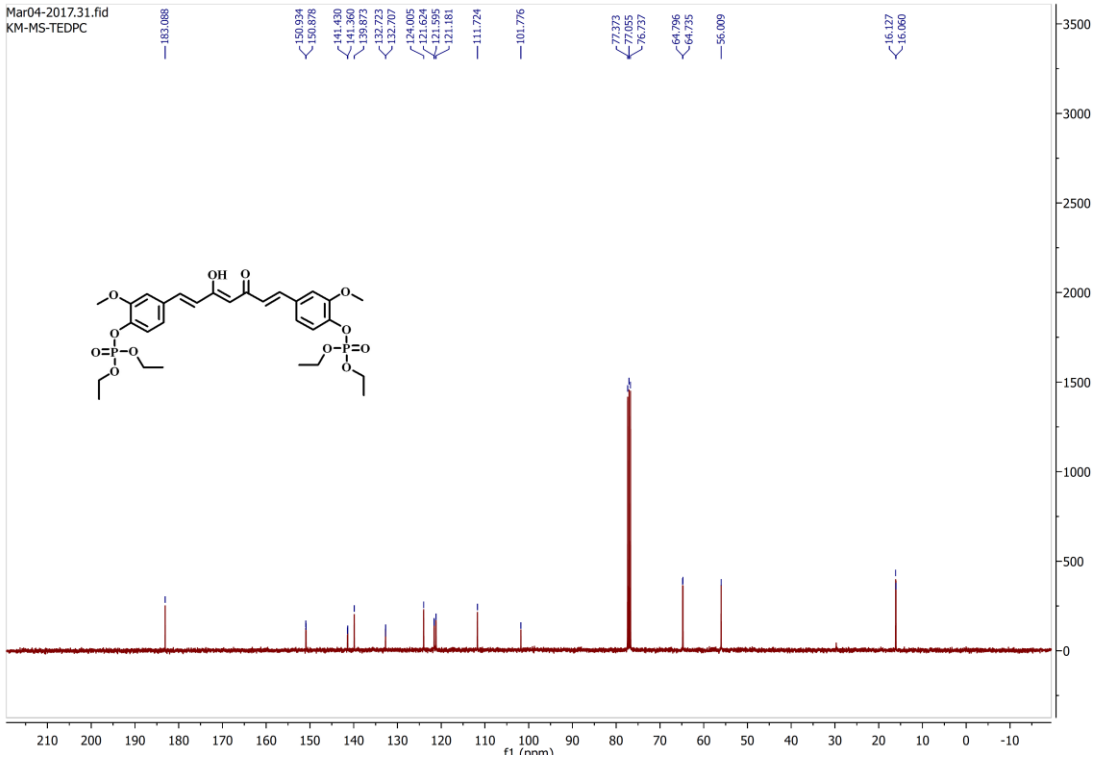
Mar04-2017.31.fid
KM-MS-TEDPC
f1 (ppm)

3.10. References:

1. O.A. Hamed, N. Mehdawi, A.A. Taha, E.M. Hamed, M.A. Al-Nuri, A.S. Hussein, Synthesis and Antibacterial Activity of Novel Curcumin Derivatives Containing Heterocyclic Moiety, IJPR 12 (2013) 47–56.
2. N. Zhou, Y. Xu, X. Liu, Y. Wang, J. Peng, X. Luo, Combinatorial Pharmacophore-Based 3D-QSAR Analysis and Virtual Screening of FGFR1 Inhibitors, Int. J. Mol. Sci. 16 (2015) 1340–13426
3. K.S. Bhullar, A. Jha, D. Youssef, H. Rupasinghe, Curcumin and Its Carbocyclic Analogs: Structure-Activity in Relation to Antioxidant and Selected Biological Properties, Molecules 18 (2013) 5389–404.
4. R. Satpathy, R. Guru, R. Behera, Computational QSAR Analysis of some Physiochemical and Topological Descriptors of Curcumin Derivatives by using Different Statistical Methods, J. Chem Pharm. Res. 2 (2010) 344–50.
5. D. Rai, J.K. Singh, N. Roy, D. Panda, Curcumin Inhibits FtsZ Assembly: An Attractive Mechanism for its Antibacterial Activity, Biochem. J. 410 (2008) 147–155.
6. P. Tyagi, M. Singh, H. Kumari, A. Kumari, K. Mukhopadhyay, Bactericidal Activity of Curcumin I is Associated with Damaging of Bacterial Membrane, Plos one 10 (2015) e0121313.
7. S.Z. Moghadamtousi, H.A. Kadir, P. Hassandarvish, H. Tajik, S. Abubakar, K. Zandi, A Review on Antibacterial, Antiviral, and Antifungal Activity of Curcumin, BioMed Research International 2014 (2014) 186864.
8. L. Bräuer, M. Schicht, D. Worlitzsch, T. Bensel, R.G. Sawers, F. Paulsen, Staphylococcus aureus and Pseudomonas aeruginosa Express and Secrete Human Surfactant Proteins, PloS one 8 (2013) e53705.
9. H. Komatsuzawa, T. Fujiwara, H. Nishi, S. Yamada, M. Ohara, N. McCallum, The Gate Controlling Cell Wall Synthesis in Staphylococcus aureus. Molecular microbiology 53 (2004) 1221–1231.
10. M. Thanbichler, L. Shapiro, MipZ, A Spatial Regulator Coordinating Chromosome Segregation with Cell Division in Caulobacter, Cell 126 (2006) 147–62.
11. M. Ahmed, M.A. Qadir, A. Hameed, M. Imran, M. Muddassar, Screening of Curcumin-Derived Isoxazole, Pyrazoles, and Pyrimidines for their Anti-

inflammatory, Antinociceptive, and, Cyclooxygenase-2, Inhibition, Chem. Biol. Drug Des. 91 (2018) 0338–343.

12. S. Mishra, U. Narain, R. Mishra, K. Misra. Design, Development and Synthesis of Mixed Bioconjugates of Piperic Acid-Glycine, Curcumin-Glycine/Alanine and Curcumin–Glycine-Piperic Acid and their Antibacterial and Antifungal Properties, Bioorg. Med. Chem. 13 (2005) 1477–1486.
13. B. Zeynizadeh, S. Yahyaei, A Mild and Convenient Method for the Reduction of Carbonyl Compounds with $NaBH_4$ in the Presence of Catalytic Amounts of $MoCl_5$, Bull. Korean Chem. Soc. 24 (2003) 1664–1671.
14. M. Pandareesh, M. Shrivash, H.N. Kumar, K. Misra, M.S. Bharath, Curcumin Monoglucoside Shows Improved Bioavailability and Mitigates Rotenone Induced Neurotoxicity in Cell and Drosophila Models of Parkinson's Disease, Neurochem. Res. 41 (2016) 3113–3128.
15. W. Kozak, J. Rachon, M. Daśko, S. Demkowicz, Selected Methods for the Chemical Phosphorylation and Thiophosphorylation of Phenols. Asian J. Org. Chem. 7 (2018) 314–23.
16. R. Yamgar, S. Sawant, Developing a Commercially Viable Process for an Active Pharmaceutical Ingredient, Challenges, Myths and Reality in the Art of Process Chemistry, The Open Process Chemistry Journal 5 (2013) 1–10.
17. R. Shelkov, M. Nahmany, A. Melman, Selective Esterifications of Alcohols and Phenols Through Carbodiimide Couplings, Org. Biomol. Chem. 2 (2004) 397–401.
18. T.A. Halgren, Identifying and Characterizing Binding Sites and Assessing Druggability, J. Chem. Inf. Model 49 (2009) 377–389.
19. G.M. Morris, R. Huey, W. Lindstrom, M.F. Sanner, R.K. Belew, D.S. Goodsell, AutoDock4 and AutoDockTools4: Automated Docking with Selective Receptor Flexibility, Journal of Computational Chemistry 30 (2009) 2785–2791.
20. M. C. Arendrup, J. Guinea, M. Cuenca-Estrella, J. Meletiadis, J. W. Mouton, K. Lagrou, S. J. Howard, Method for the Determination of Broth Dilution Minimum Inhibitory Concentrations of Antifungal Agents for Conidia forming Moulds, Clin. Microbiol Infect. 14 (2008) 982.

21. S.-Y. Teow, K. Liew, S.A. Ali, A.S.-B. Khoo, S.-C. Peh, Antibacterial Action of Curcumin against Staphylococcus aureus: A Brief Review, Journal of Tropical medicine. 2016 (2016) 2853045.
22. Bhawana, R. K. Basniwal, H. S. Buttar, V. K. Jain, Nidhi Jain, Curcumin Nanoparticles: Preparation, Characterization, and Antimicrobial Study, J. Agric. Food Chem. 59 (2011) 2056–2061.
23. S.-Y. Teow, K. Liew, S.A. Ali, A.S.-B. Khoo, S.-C. Peh, Antibacterial Action of Curcumin against Staphylococcus aureus: a Brief Review, J. Trop. Med. 2016 (2016) 2853045.

Chapter 4

Designing and synthesis of flavonoid derivatives for modulatory effect on flagellation of Candida albicans

4.1. Introduction:

The Fungal kingdom contains an entire assorted variety of life forms. Around one lakh twenty thousand species have been recorded till date the contagious fungi is found in filamentous form. Basically the organisms are eukaryotes, unicellular as well as multicellular structures and their cell divider contains chitin [1]. The methods of multiplication are sexual as well as orgamic (asexual). The pathogenic and opportunistic organisms have turned into a major risk of contaminations and pathogenesis. Sharp parasites are the most perilous class since it can misuse the advantage of immunocompromised conditions. Further these strains are exceptionally safe to medicine. In the present investigation, we have basically centred on a standout amongst the most sharp growth fungi i.e. *Candida albicans* which is present in human biome and exceedingly sedate safe in nature. Before diving into the points of interest of the *C albicans* let us examine *Candida* species briefly in a more extensive range.

4.1. (a) *Candida Species* and their significance in fungal world:

Candida species have a place with ascomycetes and are diploid hereditarily.Around two hundred species of *Candida* are known out of which *C. albicans, C. dubliniensis, C. glabrata, C. krusei, C. parap-silosis, and C. tropicalis. H. capsulatum, A. fumigatus, and C. neoformans* are notable for their existence in soil and human biome [2]. These are chiefly present endogenously at various areas of human biome, for example, gastrointestinal tract, butt, oral pits and vaginal cavity [3]. Nearly half of the sound human populace is the bearer of amiable type of *C. albicans.*

C. albicans is a safe commensal of human biome in yeast shape for most part found in skin and gastrointestinal cavity. It is a polymorphic life form and can experience morphological changes between the yeast shape (with adjusted cells and little girl buds that physically discrete from the mother cell), the pseudohyphal frame (comprising of chains of cells with various degrees of stretching that still show tightening influences among adjacent cells), and the genuine hyphal shape (comprising of long cylinders with parallel sides and no choking influences) [4]. Michail S. Lionakis, Medical Mycology, 2018, 56, S1–S159. Hyphal shape

expansion makes it obtrusive and it can enter tissues. These polymorphic changes cause disturbances in the immunocompromised patients. *Candida albicans* is a noteworthy human pathogen and a standout amongst the most vital reason for contagious disease in people [5].

Generally *C.albicans* separates through sprouting process mitotically. The chains of these buds associated with the source are called mycelium. The joints that are different from one another or from other hyphal cells connecting them are frequently called chlamydospores. In case there should arise an occurrence of immunocompromised conditions it changes into hyphal shape. There are few conditions like pH, oxygen, carbon dioxide, or glucose which can trigger the dimorphic change of *Candida* from yeast to hyphal shape [6]. There are numerous components that characterize the intrusiveness of *C. albicans*, however the primary and the underlying driver known is the hyphal development (Figure 4.1).

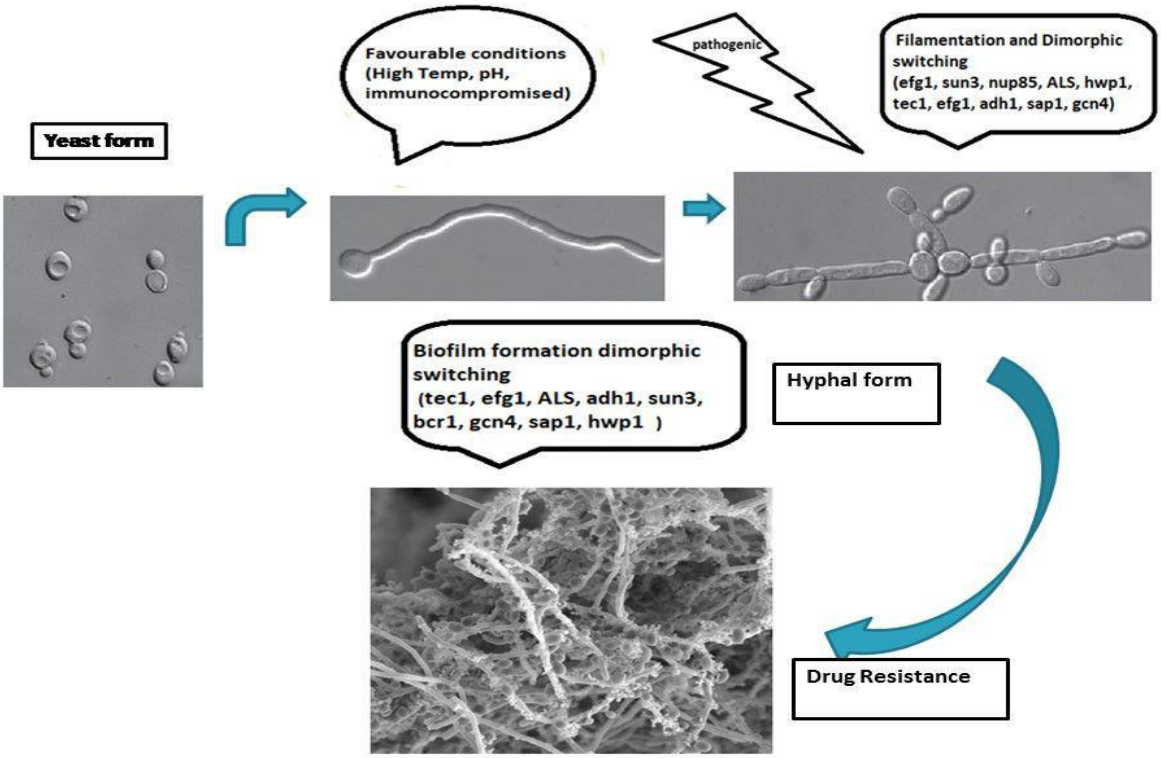

Figure 4.1. Biological flow of *Candida albicans.*

The healing facilities and restorative establishments are additionally experiencing the *Candida* contaminations since 90s [7]. Nosocomial circulation system contaminations up to 8–15 % are caused by *Candida species.* The

immunocompromised patients who are experiencing malignancy, diabetes, HIV and long haul anti-toxin treatment are the simple unfortunate casualties. Other than this the essential anti-infection treatment can likewise quicken the outgrowth of *C. albicans*. Oral and vaginal thrushes are extremely normal and relatively 90% of the considerable number of ladies experience the ill effects of vaginal disease at least ones throughout their life. In the good conditions the mucosal obstructions can be disturbed, and it can likewise hurt alternate organs through foundational contaminations. *Candida* is profoundly hereditarily altered to pathogenic form in basic pH and remains beneficial in acidic pH since the gut and the vaginal pH is acidic [8].

C. albicans cannot be for all time expelled from the human biome and nature. Moreover, protection from the presently accessible enemy of parasitic prescriptions is rising [9-10]. This circumstance makes contagious diseases a noteworthy general wellbeing concern, and in this way novel enemy of parasitic medication targets are of extraordinary intrigue. Most of *Candida* drugs including azoles target cell film or cell divider combination. Therefore, recognizable proof of option of physiological pathways that influences pathogenicity and qualities associated with the yeast to hyphae change is an essential objective for the improvement of new antifungal operators. Several factors are known as the centre elements in charge of destructiveness and pathogenicity in *C. albicans*. From quite a few examinations it has been discovered that the main driver of destructiveness in *Candida* is hyphal development. The non-filamentous strains of *C. albicans* are non-harmful in nature [11].

Hyphal shapes are more cement and emit a lot of hydrolytic catalysts. The non-hyphal type of *Candida* is non-pathogenic in nature. When stage is transformed it can harm the macrophages and neutrophils. Hyphal type of *Candida* remains no more a cooperative animal group and can connect with the host tissue to result into profound entrance in anyorgan/tissue. There are set of qualities and transcriptional factors which act at various stages to help the dimorphic progress and that mirrors the shortcoming of the safe arrangement of the human body. A delayed anti-toxin treatment gives appropriate supplement to expansion and further eliminates microbes, consequently the parity of microorganisms is aggravated, and *Candida* gets space for

outgrowth [12]. Biofilm is the exopolysaccharides kept around the filamentous development of *C. albicans*. Biofilm state is again more harmful stage than hyphal. Amid this stage there is high creation of couple of chemicals like proteinases, phospholipases, and adhesins etc. Fluconazole or other commercial azoles have very little power for entering these polysaccharide-based biofilms [13]. The pathogenicity of *C. albicans* is immensely affected by biofilm arrangement and alternate pathways. Additionally, biofilm development expands the defencelessness for expanding the strength of *Candida* getting to be destructive

4.1. (b) System of pathogenicity in *candida albicans:*

The pathogenicity in *Candida species* is caused by few factors, for example, hyphal growth as mentioned earlier. Different traits can be recorded as advertisement e.g., interchange Glyoxalate pathway, hydrolytic chemicals, phospholipases etc. [14]. The progress of yeast to hyphal shape is called dimorphism. The two structures are critical, however hyphal frame is one more obtrusive for human species. The steps of biofilm development have been shown in the (figure 4.2).

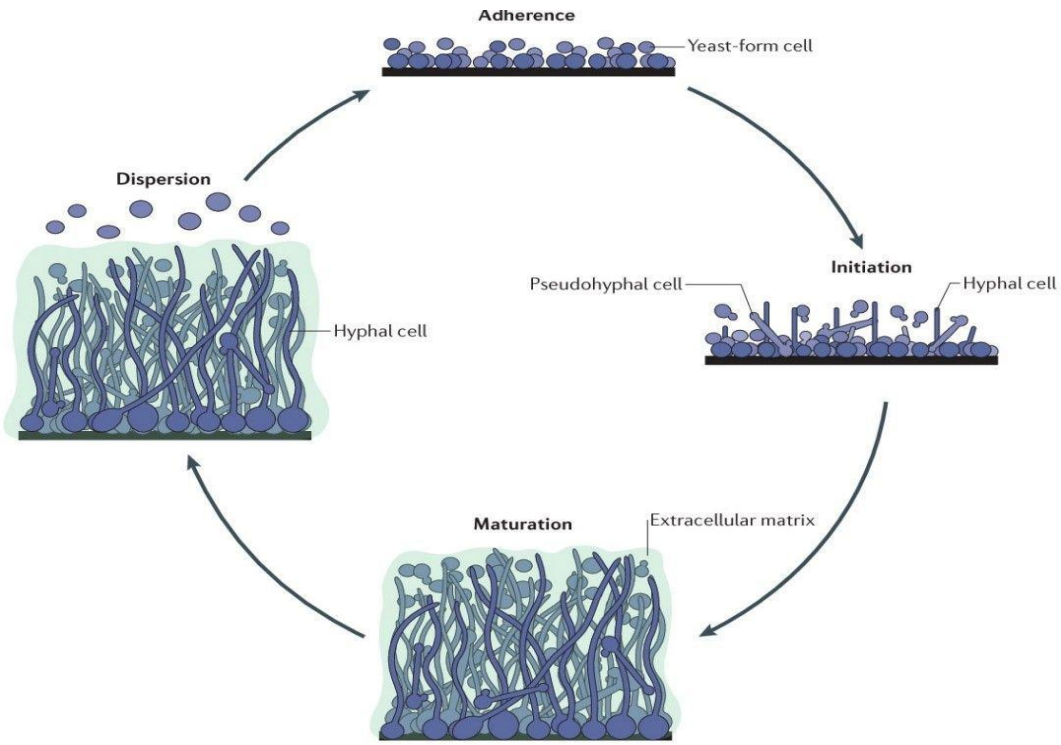

Figure 4.2. Diagrammatic representation of steps in biofilm formation.

The proteins related with hyphae arrangement are predominantly hyphal divider protein (Hwp1), agglutinin-like grouping protein (Als3) as well as some chemicals like discharged aspartic proteases (Sap4, Sap5 and Sap6). In the hyphal frame the species is more cement in nature, therefore to multiply and infiltrate other organs bond is essential. Adhesins like the agglutinin-like grouping (ALS) proteins from the class Als1–7 and Als9 have been discovered coding for glycosylphosphatidylinositol (GPI)- connected cell surface glycoproteins. Biofilm development is a piece of the consecutive procedure of pathogenicity. At the point when the hyphal development gets completely populated the polysaccharides gets filled into the spaces between the hyphal dividers. These shape a layer basically through the amassing of extracellular grid material which moves toward becoming biofilm. The greater part of the realized medications can't infiltrate this entry. The significantly included controllers is warm stun protein Hsp90. Hsp90 downregulation causes the event of Ras1-pka pathway.

Further hydrolytic proteins, for example, emitted hydrolases help in promoting adhesion and hyphal development. The class of these chemicals, i.e. proteases, phospholipases and lipases improve the proficiency of additional cell supplement securing and along these lines give insusceptibility to *C. albicans.*

The primary goal of this examination has been to discover the main drivers of *Candida albicans* getting to be pathogenic and sedate safe. Further our point was to locate the better and more secure approach to restrain the pathogenesis in light of the fact that the ordinary yeast frame *Candida* is non-obtrusive and is a vital piece of our biome.

The optional contaminations because of harmful strain can be averted by restraint or constriction of pathways that prompt destructiveness. These causes are mainly filamentation, white hazy stage change and biofilm arrangement. This happens through the commitment of numerous components, for example, hereditary, transcriptional, ecological etc. Along these lines, coming down to the real actualities we can take four foremost pathways occurring in various cell organelles of *C. albicans*, for example, glyoxalate pathway, Ras1-pka pathway, Ergosterol pathway

and flagging pathways. Further the key components which can possibly influence most extreme pathways have been recorded underneath:

Efg1: Efg1 protein is a major regulator of cell wall dynamics in *Candida albicans* as revealed by DNA microarrays and represents improved filamentous development [15]. Efg1 was transcriptional controller of the switch between two heritable states, first is the opaque and second is the white states. Efg1 is associated with numerous collaborations, for example, stretch obstruction, Ras1 pka pathway, and white hazy stage change and biofilm arrangement. It's a transcriptional figure connecting numerous pathways and causes hypoxial biofilm formation. The investigation of the Efg1 quality established that a pointed Efg1 articulation level smothers development of genuine hyphae [16]. Efg1 is essential for articulation of all hyphal-explicit qualities, and Tec1overexpression has been appeared to re-establish filamentous development in an Efg1/Efg1 freak [17].

2QZX: It is secreted Aspartic Proteinase (Sap5) from *Candida albicans* Sap5 has been taken as the second target. Sap5 is a class of hydrolytic compounds. Different classes of compounds take an interest during the time spent destructiveness and attack. The weakening of hydrolytic proteins if there should arise an occurrence of *candida* decreases harmfulness [18]. Proteolytic movement is a critical harmfulness factor. Additionally, the hydrolytic compounds principally Sap5 contribute for appropriation and defeating of remaining host hindrances and disease. Sap5 being a critical hydrolytic chemical non-liable to have comparable homology in human and is a potential focus of pathogenicity in *C. albicans*.

Erg11: Ergosterol biosynthesis pathway happens in the cell layer of C albicans. For the most part the medications accessible in the market against *Candida* development is the class of azoles chiefly fluconazole. The key factor of this pathways is Erg11. Erg11 principally encodes for the catalyst Cytochrome P450 lanosterol 14a-demethylase [19]. The restraint of this protein can straightforwardly influence the pathways prompting cellulase layer harm in *Candida*. The vast majority of the azole tranquilize targets Erg11 however as of late Candida has created sedate protection from azoles because of the change in Erg11. Thus, the objectivehas been taken to discover different inhibitors having preferred partiality over azoles.

Glyoxylate pathway: Glyoxylate pathway usually known as TCA (Tri carboxylic corrosive) is a fundamental metabolic pathway occurring in *C. albicans*, since it is basic for it to make due in supplement restricted host specialties and unfavourable host conditions. This pathway happens in three cell organelles, for example, cytoplasm, mitochondria and peroxisome as shown in (Fig 4.3) [20]. There are course of responses happening however couple of chemicals like N-myristoyltransferase and Isocitrate lyase (ICL) are the centre compounds in charge of the pathways. Here, we have focused on N-myristoyltransferase for the hindrance of the pathway. Glyoxylate pathway has non-homologs with warm blooded creatures which makes it an exceptionally protected and vital target.

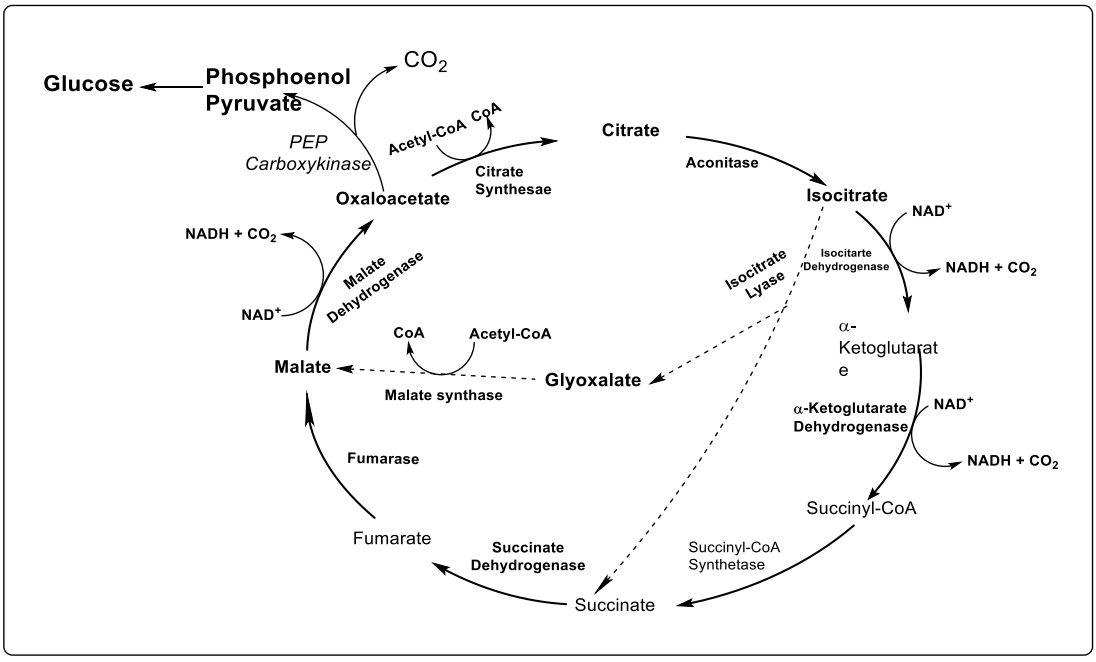

Figure 4.3. Glyoxylate pathway in *Candida albicans.*

4.2. Earlier methods of preparation of polyphenols:

Several synthetic routes of coumarins, chalcon, derivatives of curcumin and acetylation of quercetin has been reported since last few years, however peachmann condensation, claisen-schmidt condensation, acylation, aldol condensation reaction and their application are well known. Some references are site in this series for their synthesis including solid support catalyst Yb $(OTf)_3$ promoted coupling of phenols and propiolic acids to coumarins [21], sulfuric acid [22], base catalysed synthesis of chalcons [23], Pyridine mediated acetylation of quercetin with and acetic anhydride

along with dichloromethane as a solvent [24], gives tetaracetyl quercetin, underwent controlling of temperature [25].

4.2. (a) Coumarin synthesis by $Yb(OTf)_3$ promoted coupling of phenols and propiolic acids.

S. Genovese et al [21] have reported solvent-free synthesis of coumarin derivatives in which resorcinol **(48)** reacts propiolic acids **(49)** in the presence of hydrate 10%mol as the catalyst under microwave irradiation.

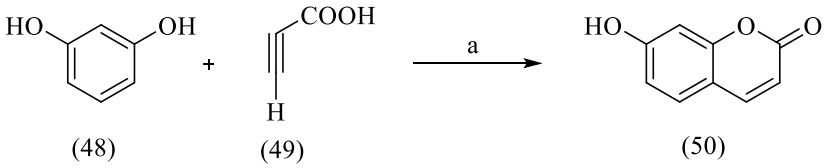

(48) (49) (50)

Reagent and condition: (a) $Yb(OTf)_3$, MW, 2 min.

Scheme 4.1

4.2. (b) Couamrin synthesis by Pechmann condensation reaction.

H.A. Aisa et al [22], have described the coupling reaction of resorcinol **(48)** with malic acid **(51)** in sulfuric acid to give coumarin **(50)**, at 120 °C for 4h.

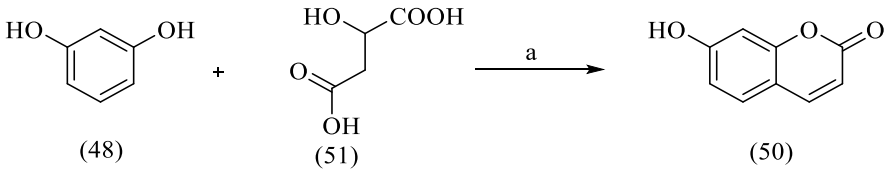

(48) (51) (50)

Reagent and condition: (a) H_2SO_4, 120°C, 4h

Scheme 4.2

4.2. (c) Chalcone synthesis by Claisen-Schmidt condensation.

S. Anwar et al [23], have reported the synthesis of chalcone **(54)**, start with acetophenone **(52)** and aldehyde under basic medium aqueous KOH at rt., good to high yield.

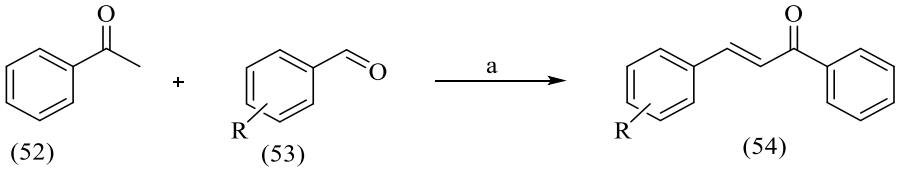

Reagent and condition: (a) EtOH, Aq. KOH, 12-24h

Scheme 4.3

4.2. (d) Acetylation of quercetin.

Y.H. Zhen et al [24], have described, pyridine base mediated acetylation of quercetin **(5)** at 85 °C for 10 minutes to give penta acetyl quercetin derivative **(55)**.

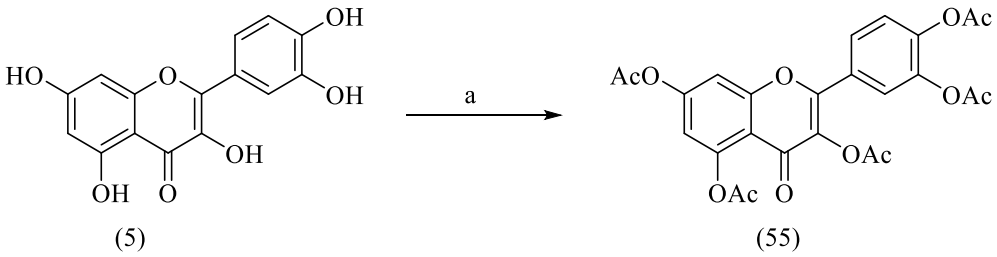

Reagent and condition: (a) Ac_2O, pyridine, rt, 2h, 85 °C, 10 min.

Scheme 4.4

4.2. (e) Selective acetylation of quercetin.

C. Paradisiet et al [25], have reported acetylation of quercetin **(5)** under control reaction temperature with decrement of molar concentration of acetic anhydride helps to achieve tetra acetyl quercetin derivatives.

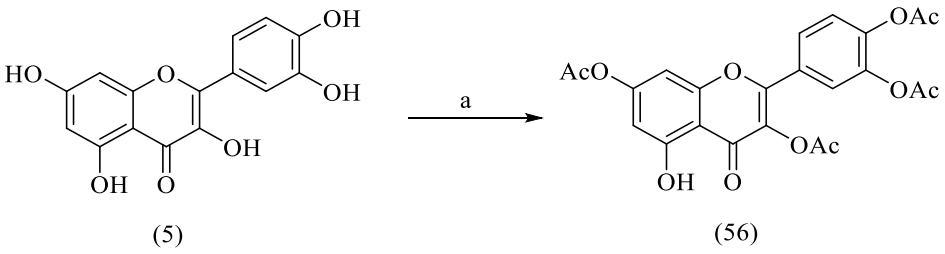

Reagent and condition: (a) Ac_2O, pyridine, DCM, rt, 3h

Scheme 4.5

4.3. Basis of the present work:

In the present study we have targeted *in-silico* all the above mentioned targets with a class of polyphenols such as flavonoids, coumarins, chalcones and curcumin analogs. Chalcones are precursor compounds for flavonoids biosynthesis in plants, and they can also be synthesized in laboratory. Chalcones have a wide spectrum of biological activities including anticancer, antiprotozoal, antiviral, antioxidative, antibacterial, antihelmintic, insecticidal amoebicidal, and immunosuppressive. We have been modified in their structure has proven useful for the development of new medicinal agents and having improved potency and lesser toxicity and good pharmacological actions. Chalcones and coumarins have nearby relationship with flavones, tetralones and aziridines. Flavonoids are present in plants as pigments and secondary metabolites and also as conjugates with many other natural compounds [26-28]. These have are antioxidant properties. In the present scenario these have evolved as important lead molecules. Flavonoids possess multiple anti-bacterial, anti-cancerous and anti-fungal properties.

Curcumin **(3)**, the yellow pigment of spice turmeric is a polyphenol. In vitro, curcumin **(3)** inhibits certain epigenetic enzymes (the histone deacetylases: HDAC1, HDAC3, HDAC8), transcriptional co-activator proteins [29]. Its derivatives wide range of biological activities such anticancer, antiprotozoal, antiviral, antioxidative, antibacterial, antihelmintic, insecticidal amoebicidal, and anti-inflammatory activities which makes these compounds as special attraction for investigation. All these compounds are less toxic than synthetic drugs and contain biofilm degrading capacity. Hence, curcumin **(3)** derivatives do have better potential over known commercial azole antifungal drugs. One of these analogues of curcumin **(3)** i.e. 1,7-di(1H-indol-3yl) hepta1,6-diene-3,5-dione **(58)** has been used for therapy of varies cancers [30]. The difluoro boron complex has been used for cyanide ion sensing ability [31]. It can inhibit proliferation of various cancer cell lines (A549, K562, SW480) as compared to curcumin **(3)** and it induced theactivation of caspase-3,8,9 followed by down regulation of cyclin D1. More details about curcumin **(3)** have been given in chapters 2 and 3.

4.4. Object of the present work:

The objective of the present work is to designing, synthesized, characterization and discover new herbal based antifungal compounds precisely for preventing filamentation growth in *Candida* species. These compunds are decrease pathogenicity, would be non-toxic and may be solve the problem of drug resistance as well as replace the toxic azoles in market.

4.5. Material and Methods:

In the present study all the proteins were either downloaded from RCSB or modelled by I-Tasser using the sequences of particular strains of the species that have to be considered for further *in-vitro* studies. The strains were provided by the school of life sciences, JNU. The software's used for *in-silico* examination was Schrodinger and its have more modules with the help of prediction of ADME properties. All the media and solvents used for *in-vitro* studies were purchased from Sigma Aldrich.

All chemicals, reagents and Duterated solvents were purchased from Sigma Aldrich and Merck Checked reactions of TLC plates (Aluminium silicagel coted) and it's purchased from Merck. ^{1}H NMR, ^{13}C NMR. Spectrum w recorded on a Bruker 400 MHz spectrometer, at 400 MHz and 100 MHz for ^{1}H and ^{13}C respectively. Chemical shifts (δ) values and tetramethylsilane (TMS) is used as an internal standard in during of spectrum analysis. All the ^{1}H and ^{13}C spectra were reported, value of coupling constant (*J*) was reported in Hz. The spots reaction mixture was visualized in UV chamber, and stain with solution of PMA, KMnO4. Charring of it is with heat gun. Purification of products was carried out by silica gel column chromatography (100-200) mesh size.

The study began with the screening of targets for C *albicans*. The targets were sorted based on the pathways that lead to virulence in *C albicans*. The pathogenicity and drug resistance in *C albicans* has become a serious problem in the present scenario. The whole methodology has been divided in three steps and shown as a flow chart in Fig. 4.4.

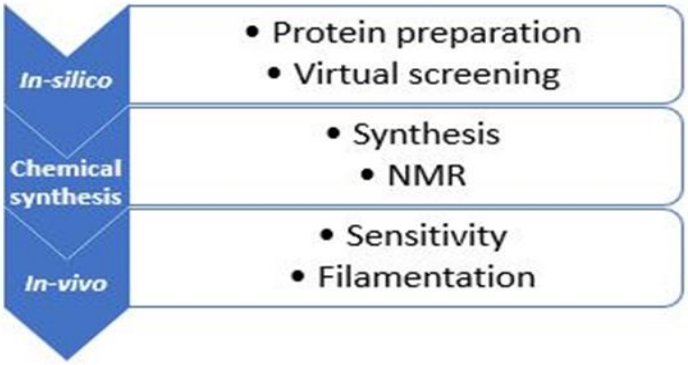

Figure 4.4. Flow chart of methodology.

4.6. Experimental:

4.6. (a) *In silico* studies, the protein modelling and preparation:

The protein targets N-myristoyl transferase and SAP5 protein structures were downloaded from RCSB (Research Collaboration for Structural Bioinformatics). N-myristoyl transferase protein pdb file has been downloaded from RCSB, pdb id-1IYK contains two chains A, B and 392 amino acids with two distinct inhibitors i.e. myristoyl-COA and peptidic inhibitor (p1). Sap5 (Secreted Aspartyl Proteinase5) protein pdb file has been downloaded from RCSB, pdb id-2QZX, containing macromolecule Candidapepsin-5, two chains A, B and 342 amino acids [32]. Sap5 was differs from Sap1-3 by its electrostatic overall charge as well as concluded structural conformation of its entry to the active site cleft. Design of inhibitors specific for Sap5 should focus on the S4 and S3 pockets, which expressively differ from Sap1-3 in size and electrostatic charge. Saps were show controlled regulation and expression for the individual stages of the infection process.

Efg1 and Erg11 protein has been modelled using I-Tasser online server. The protein sequence of *C. albicans* strain SC5314 was downloaded from NCBI [33]. I-TASSER server is an online stage which is uses meta stringing way to deal with find comparative creases and formats. The persistent pieces expelled from the PDB layouts are gathered into full length models by means of replica-exchange trade Monte Carlo recreations with the stringing unaligned areas is worked through abinitio demonstrating. In situations where no suitable format is recognized by LOMETS, I-

TASSER assembles the entire structure by abinitio demonstrating. The low free vitality states are distinguished by SPICKER through bunching the recreation traps. The quality of the models was assessed using the DOPE (Discrete Optimized Protein Energy) method. The mode with the lowest DOPE score was selected as the best model over the same query sequence. Thereafter, the Ramachandran distribution plots were plotted for these two best initial models, and the one with better performance was selected for further validation by Verify 3D. All the protein structures were prepared in Protein Prep module of Schrodinger [34]. It modifies the non-bonded atoms and stabilizes the protein by removing extra water molecules. After the energy minimization, the proteins were ready for virtual screening.

4.6. (b) Ligand library preparation:

The ligand library was prepared by collecting the different analogs of polyphenols. The molecules belonging to classes of coumarins, flavonoids and curcumin analogs were collected from data bases and the ligand molecules were stabilized and prepared in LigPrep module of Schrodinger. The module stabilizes the molecules based on Lipinski rule.

4.6. (c) Virtual screening and docking:

All the ligand libraries were docked in the specific pockets of the proteins. The binding sites of proteins were located using SiteMap module of Schrodinger [35]. SiteMap has proven algorithm for binding site identification and it generally proposes three to five active sites based on the volume and position. The best possible pocket was considered for further protocol.

Virtual screening was carried out in Glide [36]. Glide provides a rational workflow for virtual screening from HTVS to SP to XP, enriching the data at every level such that only an order of magnitude fewer compounds need to be studied at the next higher accuracy level. Glide assembles the programs highly configured to analyse large amount of data accurately.

Based on the activity of compounds such as docking scores and No of H-bonds in the protein ligand interaction the best compounds were sorted. The compounds Chalcone

(54), Coumarin **(50)**, quercetin tetraacetate **(56)**, quercetin pentaacetate **(55)** and (1E,6E)-1,7-di(1H-indol-3-yl) hepta-1,6-dience-3,5-dione) **(58)** were screened based on their docking score, interaction with protein amino acids and their common affinity with all the protein targets. These compounds were synthesised in the laboratory using unambiguous methods and further tested *in-vivo* for their sensitivity.

4.6. (d) Chemical synthesis and spectroscopy:

(i) Synthesis of 7-Hydroxy-2H-chromen-2-one4 (50).

A mixture of resorcinol **(48)** (2.8 g, 25 mmol), malic acid **(51)** (4 g, 29 mmol) and conc. sulfuric acid (10 ml) was stirred at room tempareture for 1 h. The reaction mixture was heated to100°C and stirred for another 3 h. After cooling to r.t, ice water (50 g) was added to the reaction mixture and stirred for 0.5 h. The reaction mixture was filtered and dried to afford compound as white solid (Scheme 4.6). Crude product was purified with column chromatography, make elution gradient was ethyl acetate: hexane (5:5). **(50)** (Light orange solid, yield 2.9g, 71%); R*f* 0.49 (50% ethyl acetate: hexane); mp 230–231°C. IR (KBr) υmax (cm^{-1}) 3429, 1627, 1236, 833; ^{1}H NMR (400 MHz, DMSO-d_6) δ 10.57 (s, 1H), 7.96 – 7.92 (m, 1H), 7.53 (d, *J* = 8.5 Hz, 1H), 6.82 – 6.74 (m, 1H), 6.72 (d, *J* = 2.2 Hz, 1H), 6.21 (d, *J* = 9.5 Hz, 1H). ^{13}C NMR (101 MHz, DMSO-d_6) δ 161.77, 160.90, 155.97, 145.00, 130.19, 113.59, 111.88, 111.75, 102.63.ppm. HRMS (ESI): Calculated for $C_9H_6O_3$ $[M+H]^+$: 163.0317, found 163.0347.

(ii) Synthesis of *E* chalcone (54).

The synthesis of title compound **(54)** was conducted according to procedure described and slightly modified [37].To the stirred solution of sodium hydroxide (2.2g, 0.05 mol) in aq.ethanol (EtOH: H_2O 50:2 ml) at 0 ºC a solution of benzaldehyde **(53)** (7.2g, 0.06 mol) and acetophenone **(52)** (6.8g, 0.05 mol) in ethanol (50 ml) was added during 10 min. The reaction mixture was stirred for 12 h and reaction followed with TLC. The resulting reaction mixture was, diluted with water (200 ml). The obtained precipitate of chalcone **(54)** was filtered and washed with cold water, product (Scheme 4.7) weight was 10g.

(54) (Light green solid; yield 10g, 71%); R*f* 0.3 (5% ethyl acetate: hexane); mp 56–57°C. IR (KBr) υmax (cm^{-1}) 3052, 1627, 1604, 1574; ^{1}H NMR (800 MHz, $CDCl_3$) δ 8.04 (d, *J* = 7.2 Hz, 1H), 7.83 (d, *J* = 15.7 Hz, 1H), 7.65 (dd, *J* = 6.4, 2.7 Hz, 2H), 7.59 (t, *J* = 7.3 Hz, 1H), 7.56 (s, 1H), 7.54 (s, 1H), 7.52 (t, *J* = 7.7 Hz, 2H), 7.45 – 7.41 (m, 3H). ^{13}C NMR (201 MHz, $CDCl_3$) δ 190.58, 144.88, 138.23, 134.90, 132.84, 130.60, 129.00, 128.67, 128.55, 128.50, 122.09, 77.25.ppm. HRMS (ESI): Calculated for $C_{15}H_{12}O$ $[M+H]^+$: 209.0888, found 209.0917.

(iii) Synthesis of quercetin tetra acetate 4-(3,7-diacetoxy-5-hydroxy-4-oxo-4H-chromen-2-yl)-1,2-phenylene diacetate (56).

To the stirred solution of quercetin **(5)** (1g, 3.3 mmol) in dichloromethane (100 ml), 2-5 drops of pyridine were added followed with acetic anhydride (3.3 ml, 32 mmol). Reaction mixture was stirred at room temperature for 24 h and the resulting reaction mixture was purified with column chromatography. Elution was made with gradient of ethyl acetate: hexane (39:61), and to give correnponding pure product (**56**) (Scheme 4.8).

Light yellow solid; yield 650 mg, 43%; R*f* (39 % ethyl acetate: hexane); mp 246-248°C; IR (KBr) υmax (cm^{-1}) 3119, 3022, 2935, 1749, 1711; ^{1}H NMR (400 MHz, $CDCl_3$) δ 12.10 (s, 1H), 7.83 – 7.67 (m, 2H), 7.45 – 7.29 (m, 1H), 6.86 (d, *J* = 2.0 Hz, 1H), 6.61 (d, *J* = 2.0 Hz, 1H), 2.43 – 2.27 (m, 12H). ^{13}C NMR (101 MHz, $CDCl_3$) δ 176.29, 168.21, 167.84, 167.76, 161.75, 156.37, 155.96, 144.66, 142.27, 132.23, 127.58, 126.57, 124.05, 108.83, 105.57, 101.19, 21.21, 20.70, 20.43. ppm. HRMS (ESI): Calculated for $C_{23}H_{18}O_{11}$ $[M+H]^+$: 471.0849, found 471.0880.

(iv) Synthesis of quercetin pentacetate (2-(3, 4-diacetoxyphenyl)-4-oxo-4H-chromene-3,5,7-triyl triacetate) (55).

The synthesis of title compound **(55)** was conducted according to procedure described and slightly modified [38]. To the stirred solution of quercetin **(5)** (1 g, 3.3 mmol) in acetic anhydride (10 ml, 98 mmol), pyridine (1-3 ml) was added and the mixture refluxed for 2h and reaction checked with TLC. The resulting reaction mixture was diluted with water (200 ml). The productwas extracted with ethyl acetate, concentrated under reduced pressure. The product (Scheme 4.8) was purified with

silica gel column chromatography. Elution was done with gradient of ethyl acetate: hexane (40:60). The pure product obtained was 1g **(55).**

White solid; yield 1g, 62 %; R*f* 0.5 (40% ethyl acetate: hexane); mp 190-192°C IR (KBr) υmax (cm^{-1}) 3120, 3023, 1749, 1711; ^{1}H NMR (400 MHz, $CDCl_3$) δ 7.72 (dd, *J* = 8.5, 2.1 Hz, 1H), 7.69 (d, *J* = 2.0 Hz, 1H), 7.36 (s, 1H), 7.34 – 7.33 (m, 1H), 6.88 (d, *J* = 2.2 Hz, 1H), 2.43 (s, 3H), 2.35 – 2.33 (m, 12H).^{13}C NMR (151 MHz, $CDCl_3$) δ 170.07, 169.29, 167.90, 167.86, 167.84, 156.89, 154.30, 153.82, 150.45, 144.41, 142.24, 134.10, 127.81, 126.46, 123.96, 123.88, 114.81, 113.92, 109.01, 21.20, 21.06, 20.69, 20.53.ppm. HRMS (ESI): Calculated for $C_{25}H_{20}O_{12}$ $[M+H]^+$: 513.0955, found 513.0998.

(v) Synthesis of 1,7-di(1H-indol-3-yl) hepta-1,6-diene-3,5-dione (58).

The synthesis of title compound (**58)** was conducted according to procedure described and slightly modified [39]. To the stirred mixture of acetyl acetone **(19)** (250 mg, 2.5 mmol) and boron trioxide (130 mg, 1.8 mmol) in argon atmosphere a solution of indole-3-carboxaldehyde **(57)** (725 mg, 5 mmol) in 35 ml of absolute ethyl acetate was added at rt during 15 min. Tributyl borate (5 ml, 18.5 mmol) was added in the reaction mixture and n-butyl amine (0.05ml,0.47 mmol) dissolved in ethyl acetate (5 ml) was added dropwise and mixture stirred for 20 hr at room temperature. Reaction was checked with TLC. The resultin reaction mixure was concentrated under reduced pressure and crude product (Scheme 4.9) diluted with 200 mL methanol, refluxed for 4h. The reaction mixture was again concentrated under reduced pressure. Crude product was finally purified with column chromatography, elution was made with gradient of ethylacetate: hexane (45:55). The pure product **(58)** was obtained 700 mg.

(58) Red solid; yield 700 mg, 79 %; R*f* 0.48 (45% ethyl acetate: hexane); mp 208-210°C IR (KBr) υmax (cm^{-1}) 3320, 1749, 1711; ^{1}H NMR (800 MHz, DMSO-d_6) δ 11.81 (s, 2H), 7.98 (dd, *J* = 10.4, 5.3 Hz, 2H), 7.93 (d, *J* = 2.7 Hz, 2H), 7.85 (dd, *J* = 16.0, 4.7 Hz, 2H), 7.47 (t, *J* = 7.3 Hz, 2H), 7.23 – 7.16 (m, 4H), 6.62 (d, *J* = 15.9 Hz, 2H), 5.89 (s, 2H). ^{13}C NMR (201 MHz, DMSO-d_6) δ 204.26, 194.65, 181.16, 137.98, 135.50, 133.39, 123.06, 121.12, 120.65, 117.07, 113.13, 112.45, 100.26. ppm. HRMS (ESI): Calculated for $C_{23}H_{18}N_2O_2$ $[M+H]^+$: 355.1368, found 355.1400.

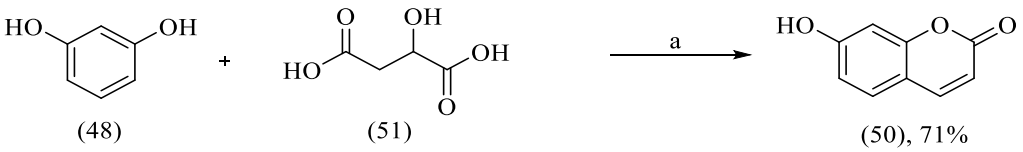

(48) (51) (50), 71%

Reagent and Condition: (a) H_2SO_4, rt, 1h, 100 °C, 3h.

Scheme 4. 6. Synthesis of 7-Hydroxy-2H-chromen-2-one **(50).**

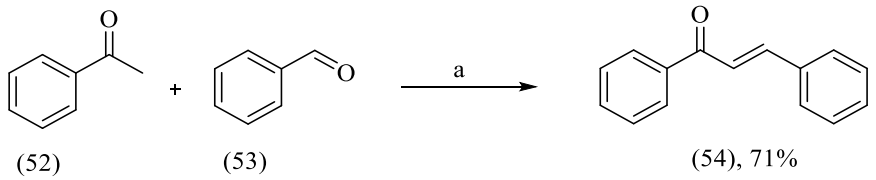

(52) (53) (54), 71%

Reagent and condition: (a) Methenol, NaOH, rt, 12h.

Scheme 4.7. Synthesis of E-chalcone **(54).**

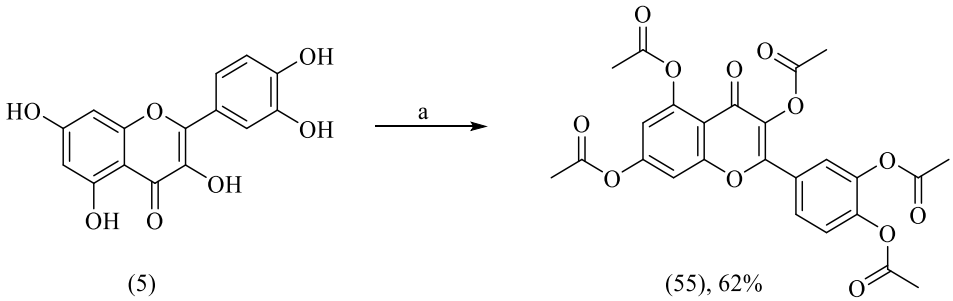

(5) (55), 62%

Reagent and condition: (a) Acetic anhydride, Pyridine, 100 °C, 2h

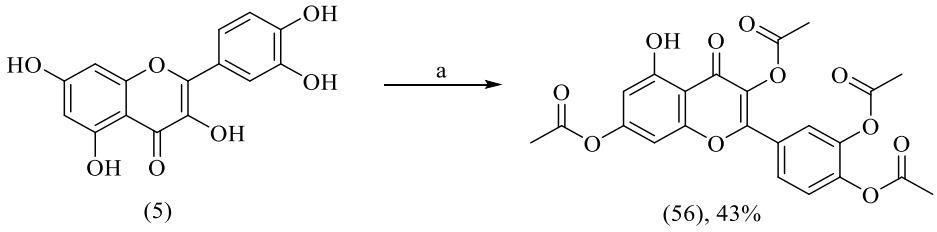

(5) (56), 43%

Reagent and condition: (a) DCM, Acetic anhydride, Pyridine, rt, 24h

Scheme 4.8. Synthesis of pentacetate quercetin **(55)** and tetracetate quercetin **(56).**

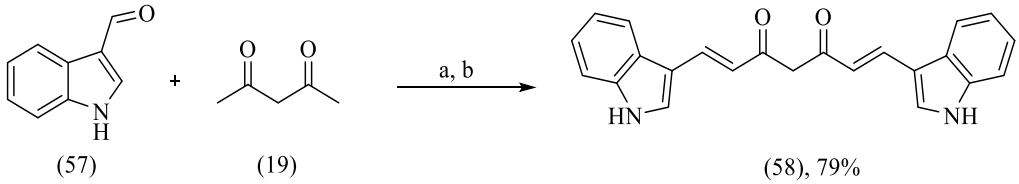

(57) (19) (58), 79%

Reagent and condition: (a) acetyl acetone, boron trioxide, rt, 15 min.
(b) Ethyl acetate, n-butylamin, tributylborate, rt, 20h.

Scheme 4.9. Synthesis of 1,7-di(1H-indol-3-yl)hepta-1,6-diene-3,5-dione **(58).**

4.7. Bioassay:

4.7. (a) *In vivo* studies:

The affectability of mixes was tried *in-vivo*. Candidanian strain SC5314 was taken for examination. The wild strain was tried separately first to watch the conduct for typical development and filamentation. The mixes were broken up in DMSO to make their molar arrangements. Further the wild sort strain fit for filamentation SC5314 was tried in 96 well plate techniques with standard fluconazole. The dissolvable media utilized was RPMI, it is one the most flawless media utilized in affectability test. The plates were kept at 37 °C hatching 24 hours. The settled hasten of *Candida* cells was unmistakable in the wells which demonstrated less or no action. To get the exactness, the OD of the plate was taken to additionally figure the IC_{80} esteems. The procedure was rehashed multiple times to guarantee the exact affectability of the mixes. The molarity of the most dynamic well (MIC) and 80% of control well (IC_{80}) was determined [40].The process was done with around eight mixes and the impressive action was found in around five of them. These mixes were additionally tried for filamentation.

Filamentation test was performed further to approve whether the mixes are indicating action with the picked targets naturally or not. The filamentation test was performed in creepy crawly media at pH 4.5 and 37 °C at 220 rpm. It gives the strain best condition for filamentation. The filamentation was seen at a few time interims 1.5hrs, 3hrs, 5hrs, 7hrs and 12 hrs. Cells were imaged by DIC microscopy. The aggravated that demonstrate less or no development of fibers ought to focus on the pathways identified with Ras1 pka pathway, glyoxylate pathway and hydrolytic catalysts. Generally if there is coagulates and still no filamentation that would allude to erg11 pathway as the compound will follow up on the cell layers and the organelles will coagulate together without film.

4.8. Results and Discussion:

4.8. (a) *In silico* studies:

The compounds that were found to have better affinity with all four targets were 7-hydroxy-2H-chromen-2-one (Coumarin) **(50)**, (E)-1,3-diphenylprop-2-en-1-one (Chalcone) **(54)**, 2-(3,4-diacetoxyphenyl)-4-oxo-4H-chromene-3,5,7-triyltriacetate (Quercetin pentaacetate) **(55)**, 4-(3,7-diacetoxy-5-hydroxy-4-oxo-4H-chromen-2-yl)-1,2-phenylene diacetate (Quercetin tetraacetate) **(56)**, (1E,6E)-1,7-di(1H-indol-3yl) hepta-1,6-diene-3,5-dione **(58)**, 2-(2,4-Difluorophenyl)-1,3-bis(1H-1,2,4-triazol-1-yl) propan-2-ol (Fluconazole).

The most of H-bonds were occupied in the regions of phenyl ring. This shows the relevance of phenolic groups in polyphenols and justifies their interaction with most of the target proteins. The 2D interaction of respective compounds with amino acids in protein's active site have been tabulated (Table 4.1). The detailed interaction and docking diagram have also been represented in Fig-(4.5- 4.17).

Table 4.1. Docking score, H-bonds of ligands docked with protein targets showing amino acids in active sites.

Protein Target	Compound	Docking Score	H-Bonds	Amino acids in active site
N-myristoyl transferase	Coumarin **(50)**	-5.541	1, GLY429	Charged(-ve) ASP428; Charged(+ve) LYS433; Hydrophobic MET427, LEU220, PRO426, PRO214, ILE431; Polar THR221, THR222
	Pentaacetate Quercetin **(55)**	-5.368	4, LYS436, SER214, PHE414	Charged (-ve) ASP432, ASP412; Charged (+ve) LYS433, LYS436; Hydrophobic ILE431, PHE414, ILE111; Polar THR221, THR222, SER214, GLY429
ERG11	Chalcone **(50)**	-7.825	3, TYR118, HIE377, SER378	Hydrophobic PHE228, MET508, LEU376, VAL509, PHE380, TYR64, TYR132, LEU121, TYR118; Polar HIE377, SER378, THR122
	Tetraacetate	-6.676	1,	Charged (+ve) LYS:A90, HEM1;

Protein Target	Compound	Docking Score	H-Bonds	Amino acids in active site
	Quercetin **(56)**		PHEA:233	Hydrophobic LEU:A87, TYR:A64, PRO:A230, ILE:A231, PHE:A380, PHE:A233, ILE:A379, TYR:A32,LEU:A376, VAL:A510, TYR:A505; Polar SER:A506, SER:A378, SER:A233, THR:A311
	Coumarin **(50)**	-6.349	GLYA:303	Charged (-ve) HEM1; Hydrophobic ILE:A304, ILE:A31, TYR:A132, LEU:A376; Polar THR:A311
SAP5	Chalcone **(54)**	-5.484	SERA:180, LYSB:271	Charged (-ve) ARG:B204, LYS:B271; Charged (+ve) ASP:B263; Hydrophobic PRO:A275, TYR:A180, VAL:A274, VAL:A330, PRO:A329; Polar SER:B259, SER:A313, THR:B261, SER:A180, SER:B273
	Pentaacetate Quercetin **(55)**	-6.069	THRB:261, LYSB:271, LYSA:271	Charged (-ve) ARG:B20, LYS:A331, LYS:B271, LYS:A271; Charged(+ve) GLU:A278, ASP:A263, ASP:B263; Hydrophobic PRO:A275, VAL:A274, PRO:B329,PRO:A329, TYR:A332, VAL:A274; Polar SER:B259, THR:B261, SER:A273, SER:A313
	Tetraacetate Quercetin **(56)**	-6.233	THRB:261, LYSB:271, THRA:261	Charged (-ve) LYS:A331, ARG:B204, LYS:B271; Charged (+ve) GLU:A278, ASP:B263; Hydrophobic

Protein Target	Compound	Docking Score	H-Bonds	Amino acids in active site
				PRO:A275,VAL:A261, PRO:B275,PRO:B329, ILE:B272, VAL:A274, TYR:A332, PRO:A329; Polar SER:B259, SER:A313, SER:B273, THR:A261, SER:A273, SER:A180
Efg1	Chalcone **(54)**	-4.651	MET272	Charged (-ve) ARG254, LYS242, LYS275, LYS268; Hydrophobic VAL227, LEU258, MET272; Polar ASN245,HIE273, THR241
	Tetraacetate Quercetin **(56)**	-3.314		Charged (-ve) ARG251, , ARG254, LYS242, LYS275, LYS268; Charged (+ve) ASP255; Hydrophobic VAL227, LEU258, MET272; Polar SER228, ASN245, HIE273, ASN239,THR241

Quercetin pentaacetate **(55),** Quercetin tetraacetate **(56)** and coumarin **(50)** have been found active in all four targets illustrating their high affinity. Fluconazole which is an already known marketed drug for antifungal treatment has been reported with many side effects. Including fluconazole many azoles are very toxic for human biome. In last few years *Candida species* has also shown drug resistance against azole compounds. In such scenario polyphenols appear to show promising results and also they are non-toxic.

These naturally occurring compounds also proved their activity *in vitro*. The results of their sensitivity and effect on filamentation are shown in Table 4.2. Only the compounds that have made combination with more than one target were selected for in-vivo analysis. The first target molecule N-myristoyl transferase had made combination with coumarin **(50)** and quercetin penta acetate **(55)** with the respective docking score -5.541 and -5.368. Mainly amino acids forming H-bonds were GLY429

and (LYS436, SER214, PHE414) respectively. The second target ERG11 i.e. one of the lead target of ergosterol pathway. Mainly makes combination with all types of azoles. However, in the experiments conducted for the present research, few polyphenols were also found making combination such as chalcone **(54)**, quercetin tetraacetate **(56)** and coumarin **(50)** with the respective docking scores -7.825, -6.676 and -6.349. The amino acid making H-bonds in case of each respective compound were (TYR118, HIE377, SER378) Chalcone, (PHE: A233) quercetin tetraacetate **(56)** and (GLY:A303) Coumarin **(50)**

Table 4.2. Compound sensitivity and inhibition of *Candida albicans* filamentation with SC5314.

Compound Name	**Compound IUPAC**	**IC_{80}(µM)**	**Filamentation**
Coumarin **(50)**	7-hydroxy-2H-chromen-2-one	20	++
Chalcone **(54)**	(E)-1,3-diphenylprop-2-en-1-one	10	++++
Pentaacetate Quercetin **(55)**	2-(3,4-diacetoxyphenyl)-4-oxo-4H-chromene-3,5,7-triyl triacetate	5	+++
Tetraacetate Quercetin **(56)**	4-(3,7-diacetoxy-5-hydroxy-4-oxo-4H-chromen-2-yl)-1,2-phenylene diacetate	8	++
Di indol-1,6-diene-3,5-dione **(58)**	(1E,6E)-1,7-di(1H-indol-3yl) hepta-1,6-diene-3,5-dione	5	+++
Fluconazole	2-(2,4-Difluorophenyl)-1,3-bis(1H-1,2,4-triazol-1-yl) propan-2-ol	2	_

The third target SAP5 had potential combination with Chalcone, Quercetin pentacetate and Quercetin tetracetate with the respective docking scores -5.484, -6.069 and-6.349. The respective binding site H-bonding amino acids were (SERA:180, LYS:B271) Chalcone, (THR:B261, LYS:B271 and LYS:A271) quercetin pentacetate and (THR:B261, LYS:B271, THR:A261) Quercetin tetracetate . The last target protein Efg1 was found making combination with Chalcone and Quercetin tetracetate with respective docking scores -4.651 and -3.314.

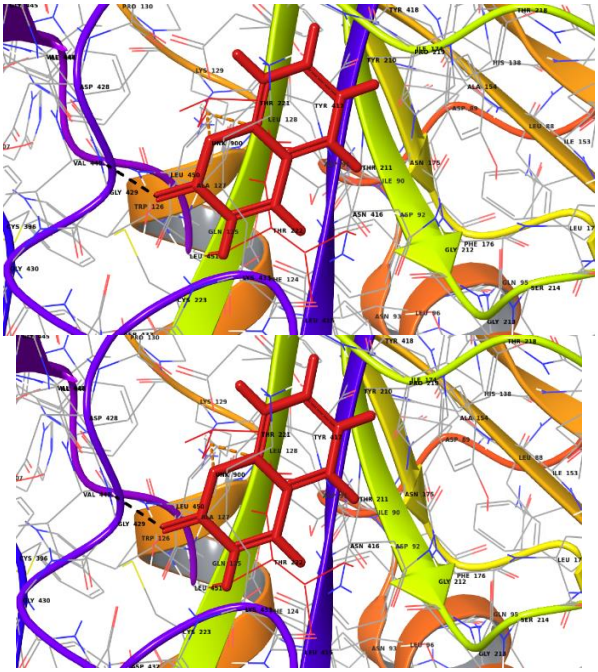

Figure 4.5. Showing 3D docking interaction of 1IYK with coumarin **(50)** and quercetin penta acetate **(55).**

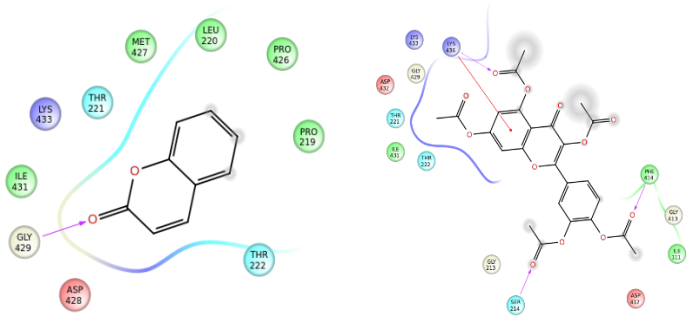

Figure 4.6. 2D interaction diagrams of coumarin **(50)** and quercetin penta acetate **(55)** with N-myristoyl transferase.

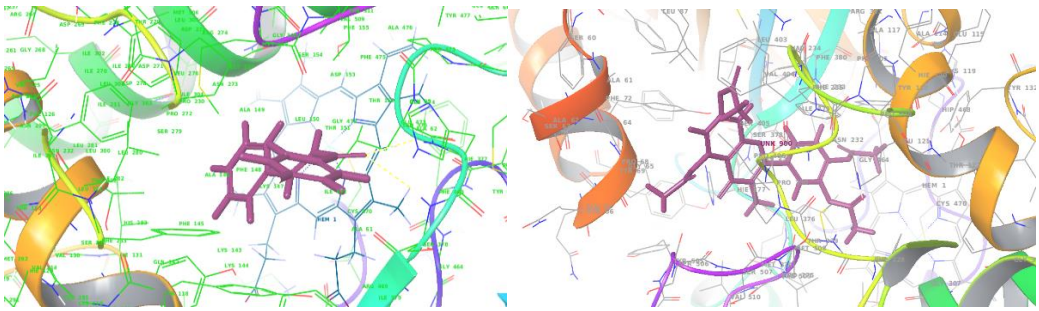

Figure 4.7. Showing 3D docking interaction Erg11 with chalcone **(54)** and quercetin tetra acetate **(56).**

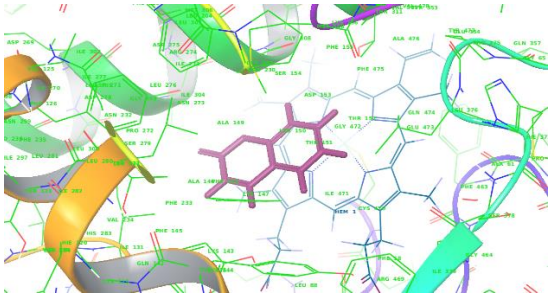

Figure 4.8. Showing 3D docking interaction Erg11 with coumarin **(50).**

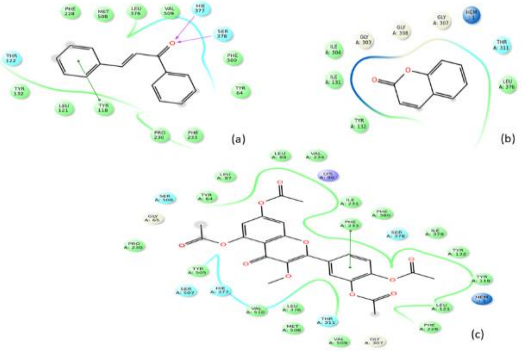

Figure 4.9. 2D interaction diagrams of (a) chalcone **(54)** (b) coumarin **(50)** and (c) quercetin tetra acetate **(56)** with Erg11.

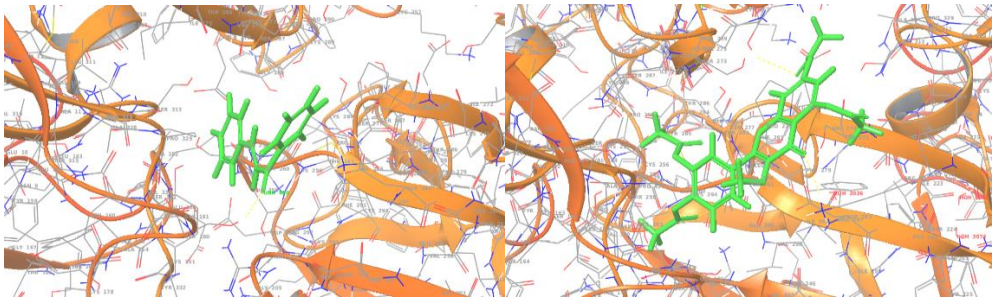

Figure 4.10. Showing 3D docking interaction of chalcone **(54)** and quercetin tetra acetate **(56)** with SAP5.

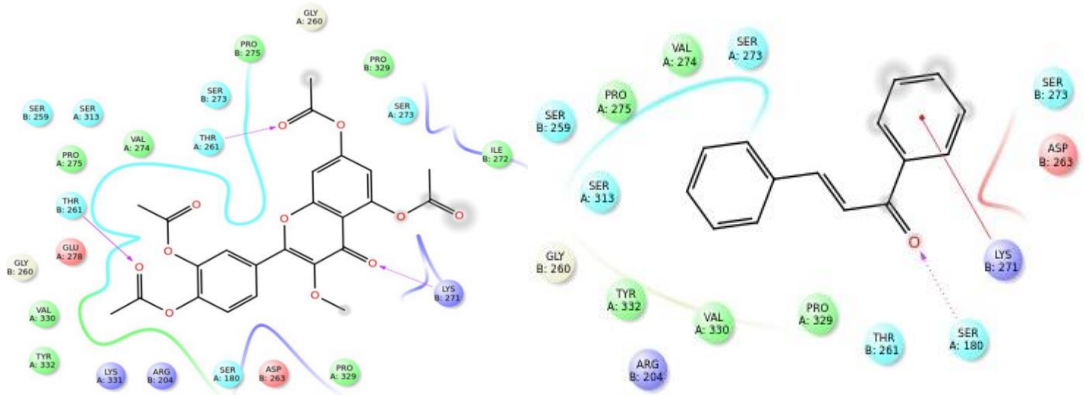

Figure 4.11. 2D interaction diagrams of chalcone **(54)** and quercetin tetra acetate **(56)** with SAP5 respectively.

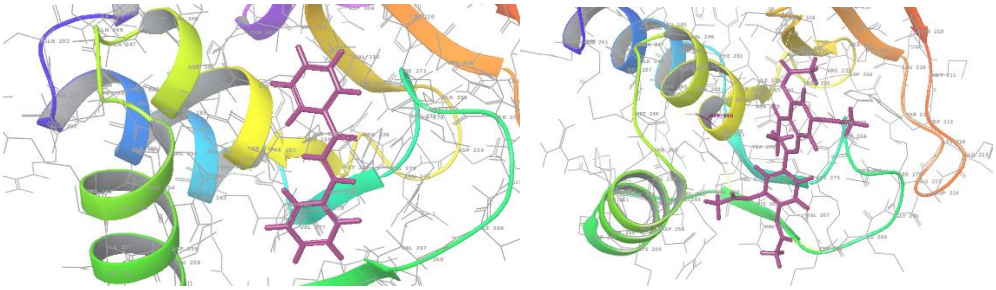

Figure 4.12. Showing 3D docking interaction of chalcone **(54)** and quercetin tetra acetate **(56)** with Efg1.

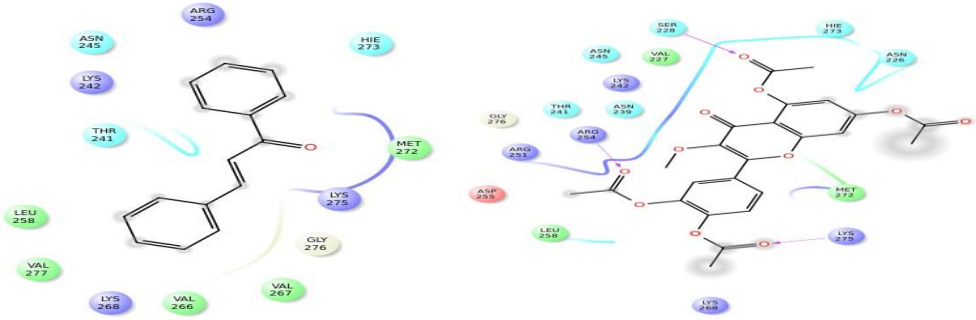

Figure 4.13. Showing 3D docking interaction chalcone **(54)** and quercetin tetra acetate **(56)** with Efg1 respective.

4.8. (b) *In-vitro* studies:

The azoles mostly target Ergosterol pathway which did not show effect on the filamentation instead they cause cell death. While in this present study the compounds that have shown significant results with filamentation and have shown sensitivity in C*andida* growth. As we can see that chalcones might have not shown higher sensitivity as compared to Fluconazole but is giving better effect with filamentation [Fig 4.18 (a), (b) and (c)]. The yeast form of *C albicans* is non-pathogenic and thus polyphenols show a better way to solve the problem of pathogenicity caused by *C albicans*. quercetin pentacetate, quercetin tetracetate and coumarins have been found active in all four targets illustrating their high affinity. Fluconazole which is an already known marketed drug for antifungal treatment has been reported with many side effects. Including fluconazole many azoles are very toxic for human biome. In such scenario polyphenols seem to show promising results and also, they are non-toxic.These naturally occurring compounds also proved their activity *in vitro*. The

polyphenols are naturally occurring antioxidants and can also be synthesised in laboratory. It has relevance in both ways as a drug or a supplement to help body in making a balance of biome. These will prove as betterand safe alternative medicines in case of drug resistance of commercial azoles. As azoles mostly target Ergosterol pathway which did not show effect on the filamentation instead they cause cell death. While here the synthesized compounds that have been taken in our study have shown significant results with filamentation and also shown sensitivity in candida growth.

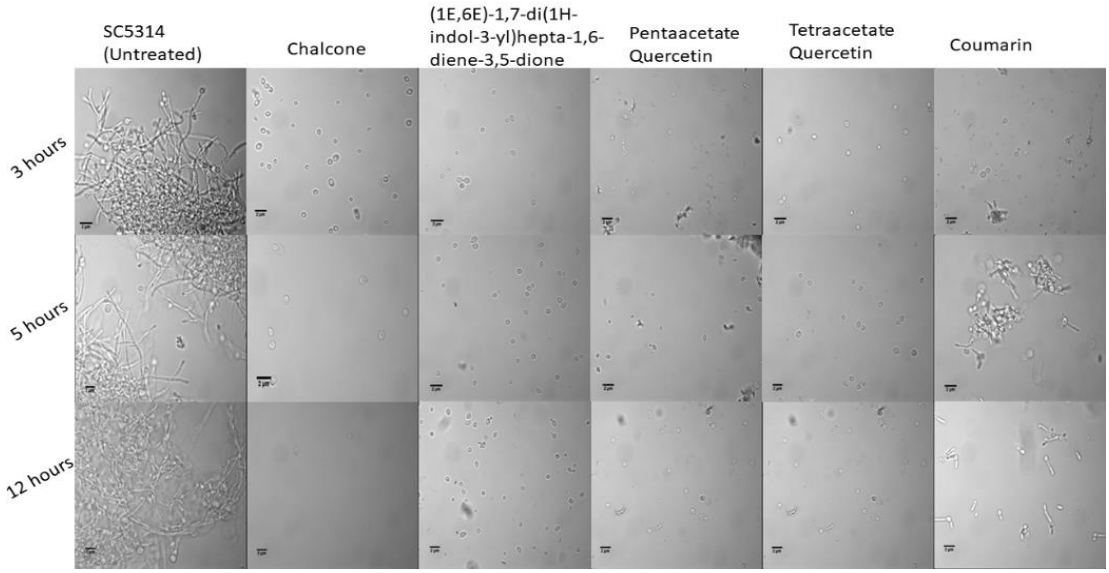

Figure 4.14. Showing the multiple filamentation growth of SC5315 *candida albicans* untreated strain against the same with our proposed lead molecule.

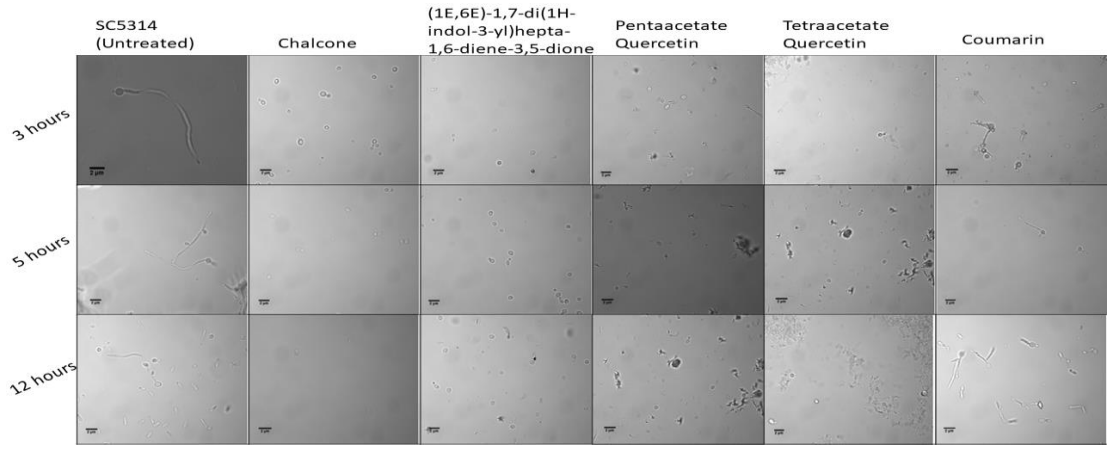

Figure 4.15. Showing the filament length growth of SC5315 *Candida albicans* untreated strain against the same with our proposed lead molecules.

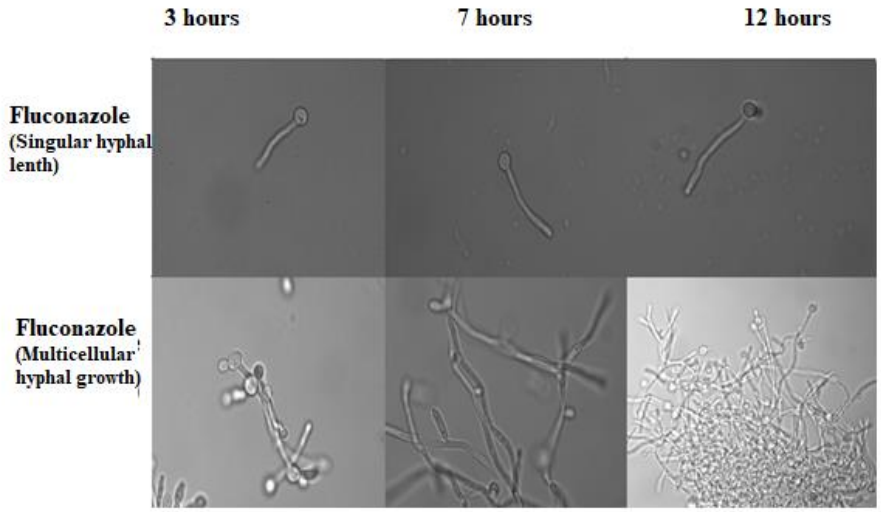

Figure 4.16. Representing the filament length and complex growth in *Candida albicans* treated with fluconazole.

4.9. Conclusion:

In the present scenario immergence of fungal infections has become a global problem. The gene alteration in *C. albicans* has controlled to imbalance in human biome. In addition, the drug resistance and biofilm formation has made it a big concern to human health. In the present study naturally occurring compound based non toxic solution has been worked out. Since the experiments have been conducted on targets in main pathways leading to emergence of pathogenicity in *C. albicans*, it can be considered as a more prominent solution. Further all results have been validated *in-vitro* and polyphenols viz. quercetin acetates, *E*-Chalcone **(54)** 7-hydroxy coumarin **(50)** and (1E,6E)-1,7-di(1H-indol-3yl) hepta-1,6-diene-3,5-dione **(58)** (a curcumin analogue) have proved to be the safe alternative of toxic azoles. The polyphenols are naturally occurring antioxidants and can also be synthesised in laboratory. It has relevance in both ways as a drug or a supplement to help body in making a balance of biome. These will prove as better and safe alternative medicines in case of drug resistance of commercial azoles.

4.10. Spectral Data (^{1}H and ^{13}C):

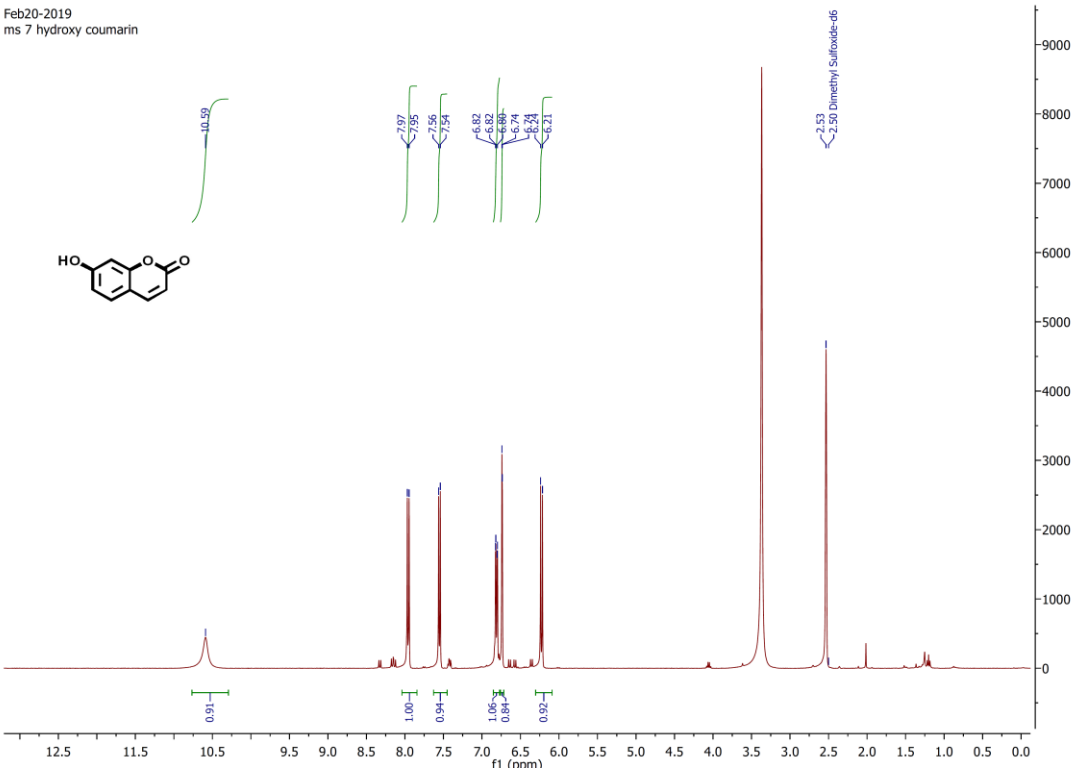

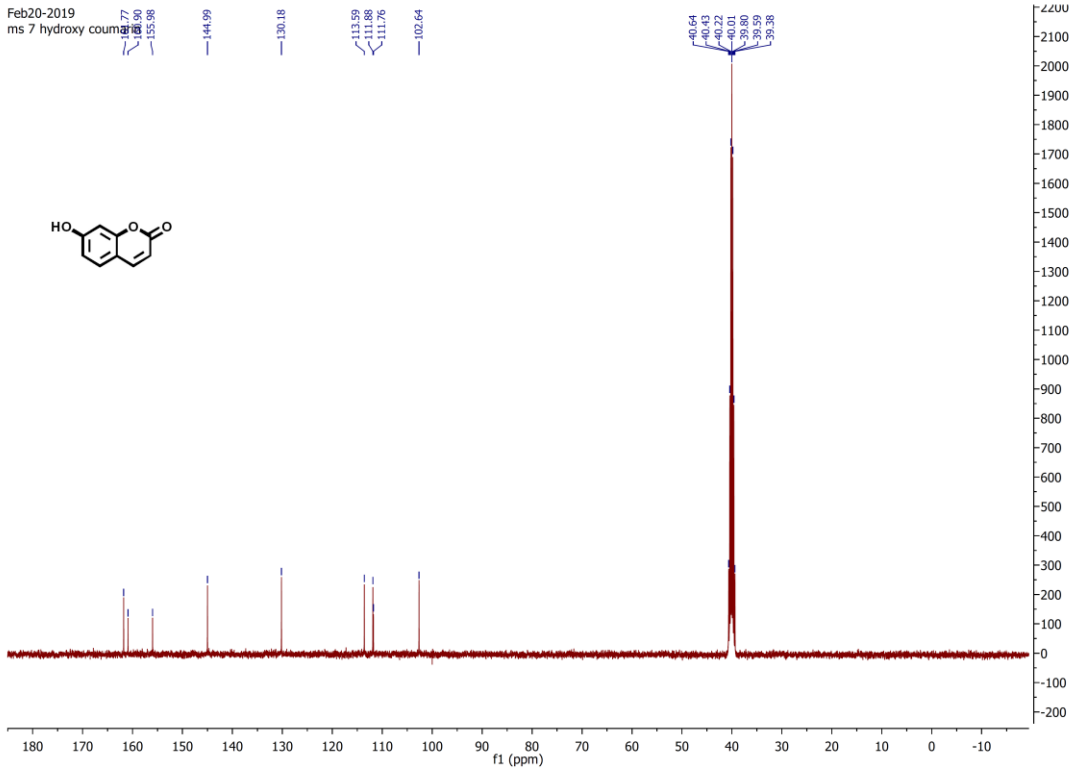

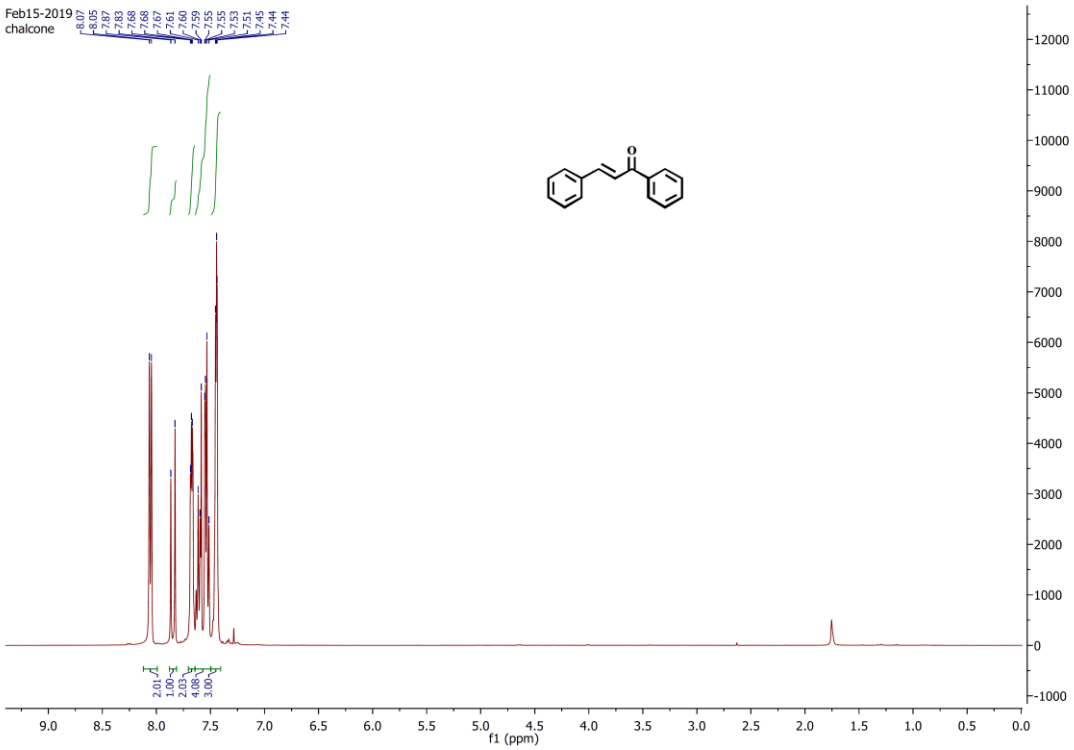
Feb15-2019
chalcone
8.07
8.05
7.87
7.83
7.68
7.68
7.67
7.61
7.60
7.59
7.55
7.55
7.53
7.51
7.45
7.44
7.44
2.01
1.00
2.03
4.08
3.00
f1 (ppm)

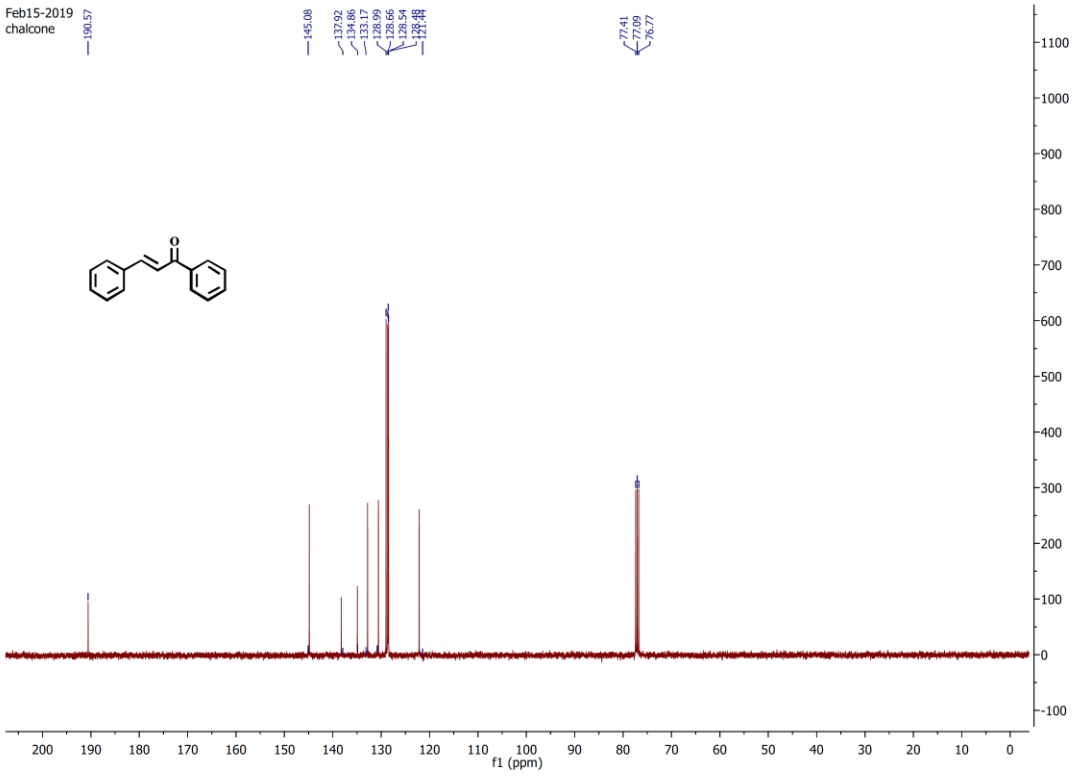
Feb15-2019
chalcone
190.57
145.08
137.92
134.86
133.17
128.99
128.66
128.54
121.44
77.41
77.09
76.77
f1 (ppm)

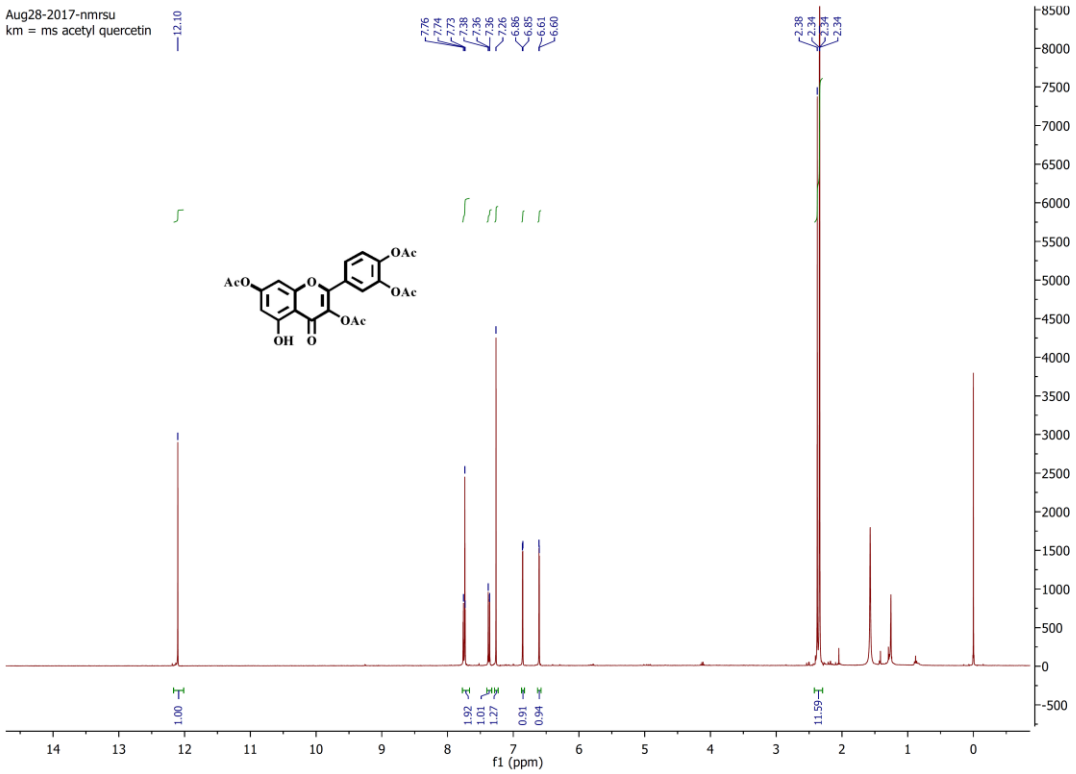
Aug28-2017-nmrsu
km = ms acetyl quercetin
12.10
7.76
7.74
7.73
7.38
7.36
7.36
7.26
6.86
6.85
6.61
6.60
2.38
2.34
2.34
2.34
OAc
AcO
OAc
OAc
OH
O
1.00
1.92
1.01
1.27
0.91
0.94
11.59
f1 (ppm)

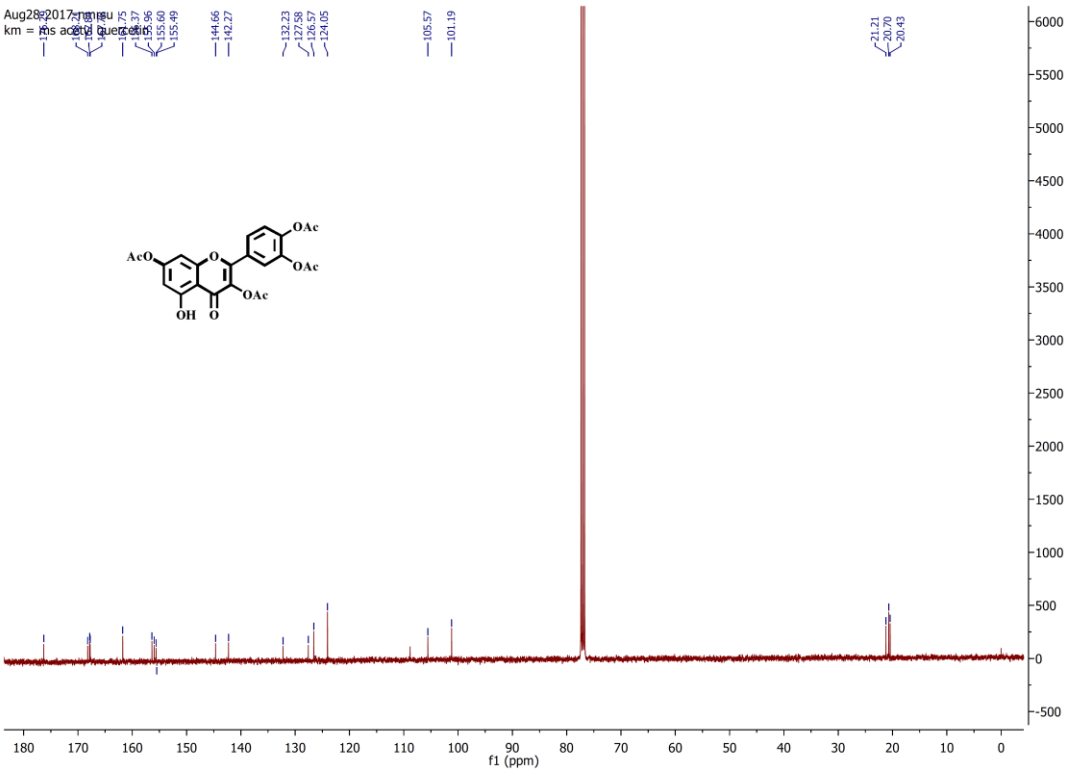
Aug28-2017-nmrsu
km = ms acetyl quercetin
144.66
142.27
132.23
127.58
126.57
124.05
105.57
101.19
21.21
20.70
20.43
OAc
AcO
OAc
OAc
OH
O
f1 (ppm)

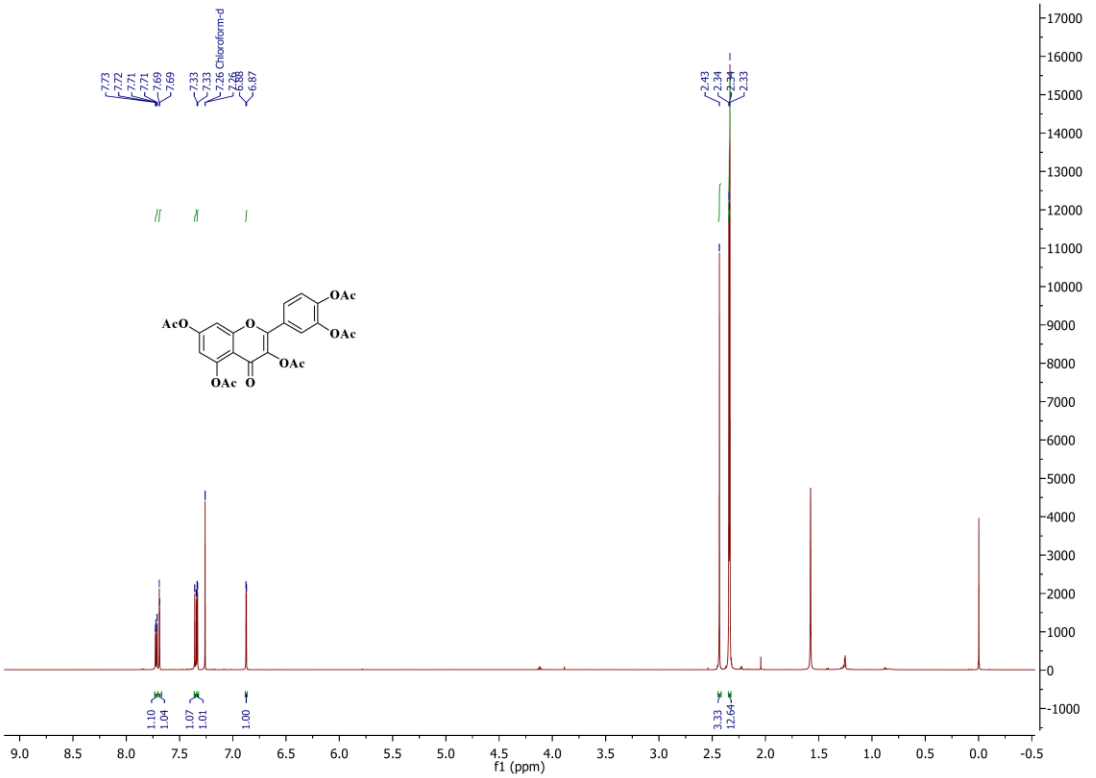
7.73
7.72
7.71
7.71
7.69
7.69
7.33
7.33
7.26 Chloroform-d
6.88
6.87
2.43
2.34
2.34
2.33
AcO
OAc
OAc
OAc
OAc O
1.10
1.04
1.07
1.01
1.00
3.33
12.64
f1 (ppm)

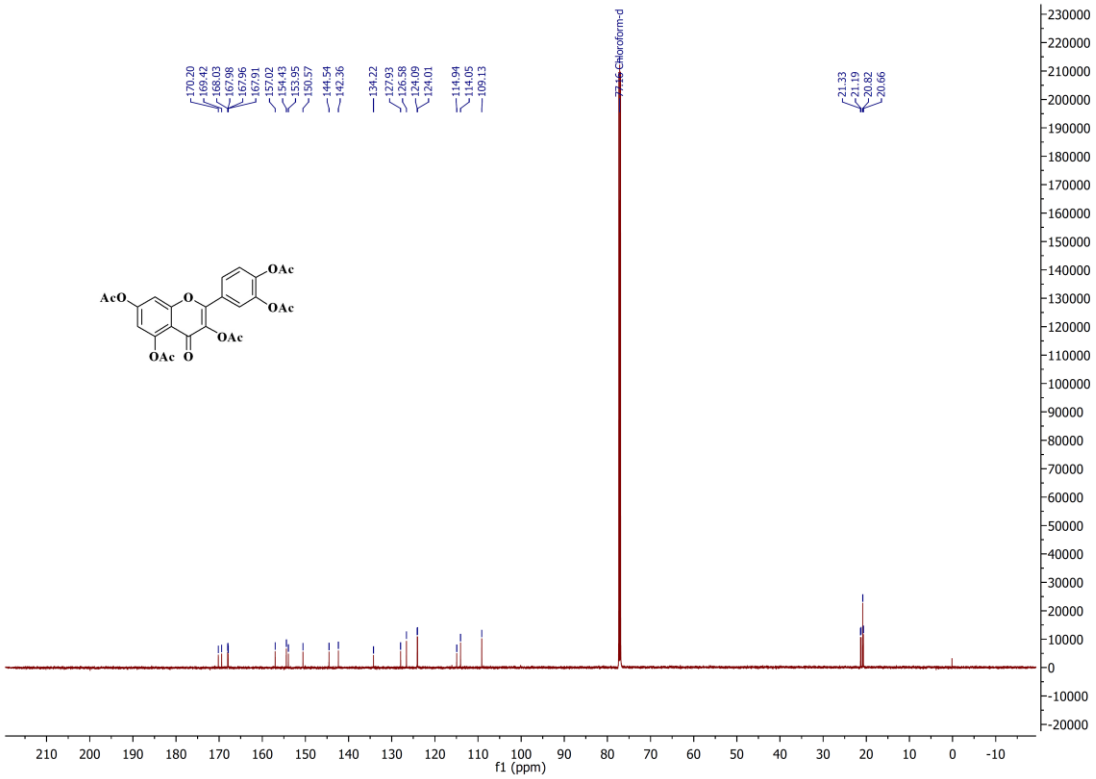
170.20
169.42
168.03
167.98
167.96
167.91
157.01
154.43
153.95
150.57
144.54
142.36
134.22
127.93
126.58
124.09
124.01
114.94
114.05
109.13
77.16 Chloroform-d
21.33
21.19
20.82
20.66
AcO
OAc
OAc
OAc
OAc O
f1 (ppm)

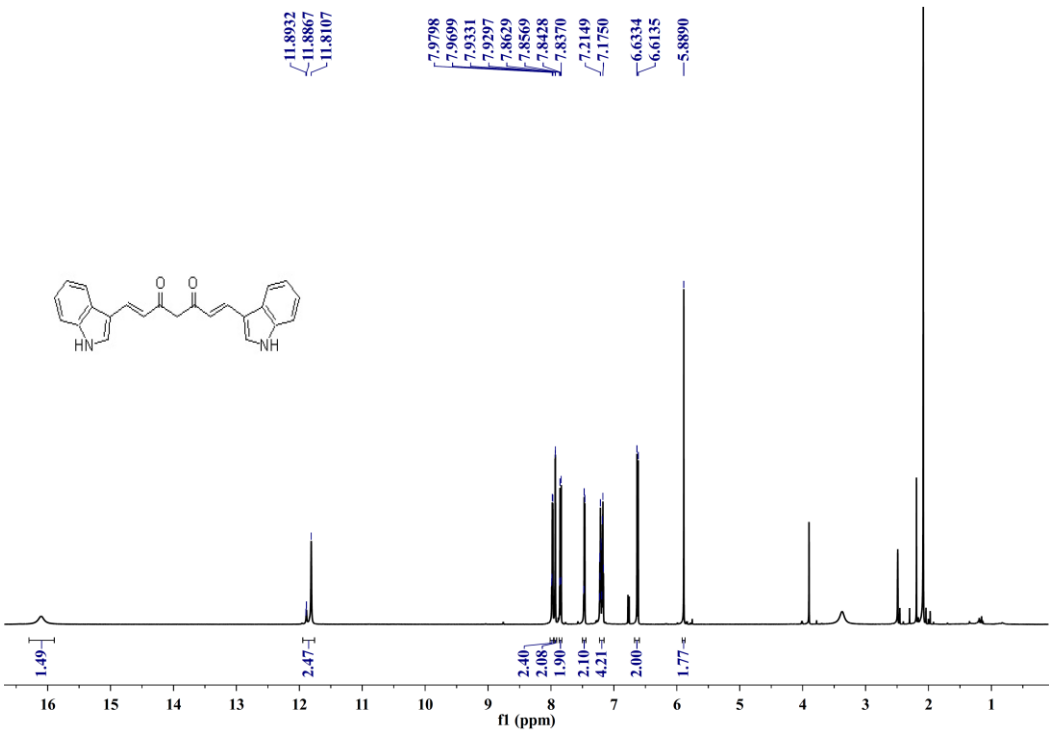
11.8932
11.8867
11.8107
7.9798
7.9699
7.9331
7.9297
7.8629
7.8569
7.8428
7.8370
7.2149
7.1750
6.6334
6.6135
5.8890
O
O
HN
NH
1.49
2.47
2.40
2.08
1.90
2.10
4.21
2.00
1.77
16 15 14 13 12 11 10 9 8 7 6 5 4 3 2 1
f1 (ppm)

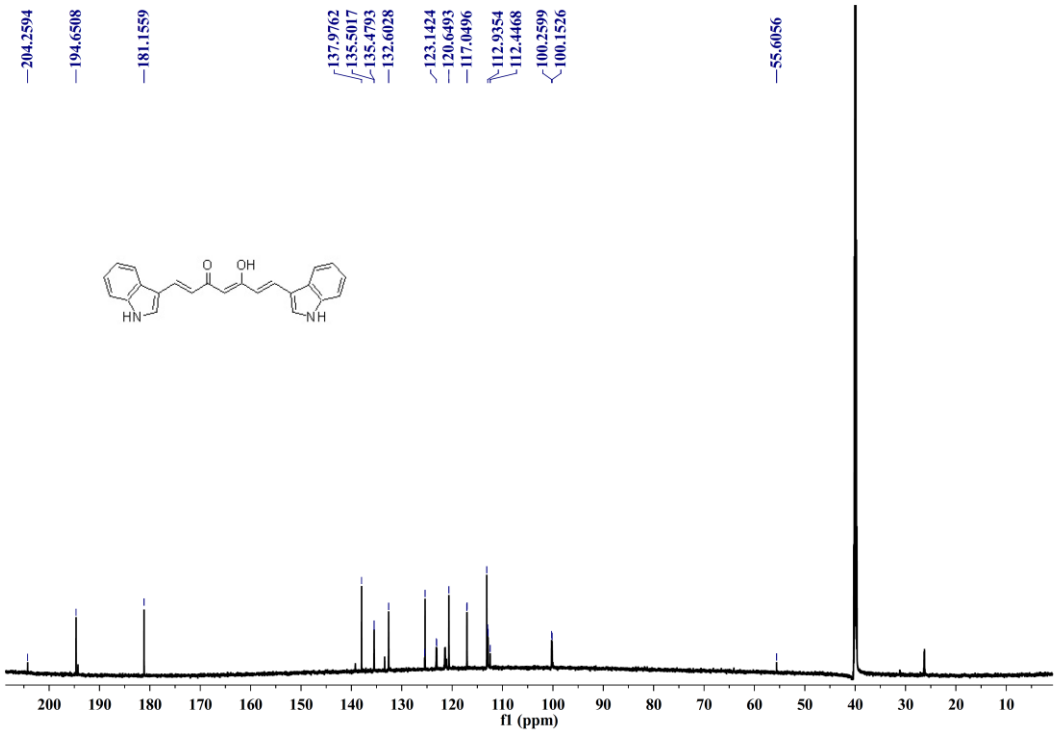
204.2594
194.6508
181.1559
137.9762
135.5017
135.4793
132.6028
123.1424
120.6493
117.0496
112.9354
112.4468
100.2599
100.1526
55.6056
O
OH
HN
NH
200 190 180 170 160 150 140 130 120 110 100 90 80 70 60 50 40 30 20 10
f1 (ppm)

4.11. References:

1. D. Gozalbo, P. Roig, E. Villamon, M.L. Gil, Candida and Candidiasis: The Cell Wall as a Potential Molecular Target for Antifungal Therapy, Current Drug Targets – Infectious Disorders 4 (2004) 117–135.
2. T.K. Kourkoumpetis, G.C. Velmahos, P.D. Ziakas, E. Tampakakis, Manolakaki, J.J. Coleman, E. Mylonakis, The Effect of Cumulative Length of Hospital Stay on the Antifungal Resistance of Candida Strains Isolated from Critically Ill Surgical Patients, Mycopathologia 171 (2011) 85–91.
3. F.L. Mayer, D. Wilson, B. Hube, Candida albicans pathogenicity mechanisms, Virulence 4 (2013) 119–128.
4. T.E. Zaoutis, J. Argon, J. Chu, J.A. Berlin, T.J. Walsh, C. Feudtner, The Epidemiology and Attributable Outcomes of Candidemia in Adults and Children Hospitalized in the United States: A Propensity Analysis, CID 41 (2005) 1232–1239.
5. B. Alexandra, Hyphal Growth in Human Fungal Pathogens and Its Role in Virulence, International Journal of Microbiology 2012 (2011) 11–22.
6. D.R. Littman, E.G. Pamer, Role of the Commensal Microbiota in Normal and Pathogenic Host Immune responses, Cell Host & Microbe 10 (2011) 311–323.
7. K. Klimesova, Z.J. Zakostelska, H. Tlaskalova-Hogenova, Oral Bacterial and Fungal Microbiome Impacts Colorectal Carcinogenesis, Frontiers in Microbiology 9 (2018) 774–787.
8. K.W. Nickerson, A.L. Atkin, J.M. Hornby, Quorum Sensing in Dimorphic Fungi: Farnesol and Beyond, APPL. ENVIRON. MICROBIOL 72 (2006) 3805–3813.
9. P.Vandeputte, S. Ferrari, A.T. Coste, Antifungal Resistance and New Strategies to Control Fungal Infections, International Journal of Microbiology 2012 (2011) 26–52.
10. A. Vermes, H.J Guchelaar, J. Dankert, Flucytosine: A Review of its Pharmacology, Clinical Indications, Pharmacokinetics, Toxicity and Drug Interactions, Journal of Antimicrobial Chemotherapy 46 (2000) 171–179.
11. H.J. Lo, J.R. Köhler, B. DiDomenico, D. Loebenberg, A. Cacciapuoti, G.R. Fink, Nonfilamentous C. albicans Mutants Are Avirulent, Cell 90 (1997) 939–949.

12. M.A. Jabra-Rizk, W.A. Falkler, T.F. Meiller, Fungal Biofilms and Drug Resistance, Emerging Infectious Diseases 10 (2004) 14–19.
13. B. Wächtler, D. Wilson, K. Haedicke, F. Dalle, B. Hube, From Attachment to Damage: Defined Genes of Candida albicans Mediate Adhesion, Invasion and Damage during Interaction with Oral Epithelial Cells, PloS one 6 (2011) 17046.
14. G. Cotter, K. Kavanagh, Adherence Mechanisms of Candida albicans, British Journal of Biomedical Science 57 (2000) 241–249.
15. K. Sohn, C. Urban, H. Brunner, S. Rupp, EFG1 is a Major Regulator of Cell wall Dynamics in Candida albicans as Revealed by DNA Microarrays, Molecular Microbiology 47 (2003) 89–102.
16. V.R. Stoldt, A. Sonneborn, C.E. Leuker, J.F. Ernst, Efg1p, an Essential Regulator of Morphogenesis of the Human Pathogen Candida albicans, is a Member of a Conserved Class of bHLH Proteins Regulating Morphogenetic Processes in Fungi, The EMBO Journal 16 (1997) 1982–1991.
17. H. Liu, Co-regulation of Pathogenesis with Dimorphism and Phenotypic Switching in Candida albicans, a Commensal and a Pathogen, Int. J. Med. Microbiol. 292 (2002) 299–311.
18. M. Schaller, C. Borelli, H.C. Korting, B. Hube, Hydrolytic Enzymes as Virulence Factors of Candida albicans, Mycoses 48 (2005) 365–377.
19. J.C. Loper, Cytochrome P450 Lanosterol 14α-Demethylase (CYP51): Insights from Molecular Genetic Analysis of the ERG11 Gene in Saccharomyces Cerevisiae. J Steroid Biochem. Molec. Biol. l43 (1992) 1107–1116.
20. L. Tao, Y. Zhang, S. Fan, C.J. Nobile, G. Guan, G. Huang, (2017) Integration of the tricarboxylic acid (TCA) cycle with cAMP Signaling and Sfl2 Pathways in the Regulation of CO2 Sensing and Hyphal Development in Candida albicans, PLoS Genetics 13 (2017) 1–31.
21. 1. S. Fiorito, F. Epifano, V.A. Taddeo, S. Genovese, Ytterbium triflate Promoted Coupling of Phenols and Propiolic acids Synthesis of Coumarins, Tetrahedron Letters 57 (2016) 2939–2942.
22. 2. C. Niu, G. Xian, P. Gen, L.J. Dou, L.F. Nie, H. Himit, M. Kabas H.A. Aisa, Synthesis and Biological Evaluation of Furocoumarin Derivatives on Melanin

Ynthesis in Murine B16 cells for the Treatment of Vitiligo, Bioorg. Med. Chem. 24 (2016) 5960–5968.

23. 3. M.R. Ahmad, V. G. Sastry, N. Bano, S. Anwar, Synthesis of Novel Chalcone Derivatives by Conventional and Microwave irradiation Methods and Their Pharmacological activities, Arabian journal of chemistry 9 (2016) S931–S935.
24. 4. X.R. Baoa, H. Liaob, J. Qub, Y. Sunb, X. Guob, E.X. Wangb, Y.H. Zhen, Synthesis, Characterization and Cytotoxicity of Alkylated Quercetin Derivatives, Iranian Journal of Pharmaceutical Research 15 (2016) 329–335.
25. 5. A. Mattarei, L. Biasutto, F. Rastrelli, S. Garbisa, E. Marotta, M. Zoratti, C. Paradisi, Regioselective O-Derivatization of Quercetin via Ester Intermediates. An Improved Synthesis of Rhamnetin and Development of a New Mitochondriotropic Derivative, Molecules 15 (2010) 4722–4736.
26. L. Bo, W. Jun, Z. Wenxuan, L. Zhongwen, Z.W. Qi Song, Synthesis and Biological Activity of Salinomycin Hydroxamic acid Conjugates, Bioorganic & Medicinal Chemistry Letters 27 (2017) 1624–1629.
27. Z. Nowakowska, A Review of Anti-infective and Anti-inflammatory Chalcones. European Journal of Medicinal Chemistry 42 (2007) 125–137.
28. A. Mattarei, L. Biasutto, F. Rastrelli, S. Garbisa, E. Marotta, M. Zoratti, C. Paradisi, Regioselective O-Derivatization of Quercetin via Ester Intermediates. An Improved Synthesis of Rhamnetin and Development of a New Mitochondriotropic Derivative, Molecules 15 (2010) 4722–-4736.
29. K.M. Nelson, J.L. Dahlin, J. Bisson, J. Graham, G.F. Pauli, M.A. Walters (2017) The Essential Medicinal Chemistry of Curcumin: Miniperspective, Journal of Medicinal Chemistry 60 (2017) 1620–1637.
30. O. Edna, T. Alsalim, B. Saeed, E.M.S. Mohamed, K. Onat, S.Hanna, E. Thomas, Modulation of P-glycoprotein Activity by Novel Synthetic Curcumin Derivatives in Sensitive and Multidrug-Resistant T-cell Acute Lymphoblastic Leukemia Cell Lines, Toxicology and Applied Pharmacology 305 (2016) 216–233.
31. S. Sogabe, M. Masubuchi, K. Sakata, T.A. Fukami, K. Morikami, Y. Shiratori, Crystal Structures of Candida albicans N-Myristoyltransferase with Two Distinct Inhibitors, Chemistry & Biology 9 (2002) 1119–1128.

32. C. Borelli, E. Ruge, J.H. Lee, M. Schaller, A. Vogelsang, M. Monod, H.C. Korting, R. Huber, K. Maskos, X-ray Structures of Sap1 and Sap5: Structural Comparison of the Secreted Aspartic Proteinases from Candida albicans, Proteins 72 (2008) 1308–1319.
33. J. Yang, R. Yan, A. Roy, D. Xu, J. Poisson, Y. Zhang, The I-TASSER Suite: Protein Structure and Function Prediction, Nature Methods 12 (2015) 7–8.
34. G.M. Sastry, M. Adzhigirey, T. Day, R. Annabhimoju, W. Sherman, Protein and Ligand Preparation: Parameters, Protocols, and Influence on Virtual Screening Enrichments, J. Comput. Aid. Mol. Des. 27 (2013) 221–234.
35. T.A. Halgren, Identifying and Characterizing Binding Sites and Assessing Druggability, J. Chem. Inf. Model. 49 (2009) 377–389.
36. R.A. Friesner, R.B. Murphy, M.P. Repasky, L.L. Frye, J.R. Greenwood, T.A. Halgren, P.C. Sanschagrin, D.T. Mainz, Extra Precision Glide: Docking and Scoring Incorporating a Model of Hydrophobic Enclosure for Protein-Ligand Complexes, J. Med. Chem. 49 (2006) 6177–6196.
37. S. Zixing, L. Xinxiang, H. Lin, X.H. Hu, New Observation on a Class of Old Reactions: Chemoselectivity for the Solvent-Free Reaction of Aromatic Aldehydes with Alkylketones catalyzed by a Double-Component Inorganic Base System, Science China Chemistry 53 (2010) 1095–1101.
38. N. Handler, W. Jaeger, H. Puschacher, K. Leisser, T. Erker, Synthesis of Novel Curcumin Analogues and their Evaluation as Selective Cyclooxygenase-1 (COX-1) Inhibitors, Chemical and pharmaceutical bulletin 55 (2007) 64–71.
39. S.A. Sufi, L.N. Adigopula, S.B. Syed, V. Mukherjee, M.S. Coumar, H.S.P. Rao,R. Rajagopalan, In-silico and in-vitro Anti-cancer Potential of a Curcumin Analogue (1E,6E)-1, 7-di (1H-indol-3-yl) hepta-1, 6-diene-3, 5-dione, Biomedicine & Pharmacotherapy 85 (2017) 389–398.
40. G. Christopher, P.U. Pierce, T. Sushma, L. Jose, R. Lopez, A 96 Well Microtiter Plate-based Method for Monitoring Formation and Antifungal Susceptibility Testing of Candida albicans Biofilms, Journal of Visualized Experiments 44 (2010) 2287.

Chapter 5

Synthesis of stereospecific substituted aryl/alkyl oximes and studies of their inhibitory effect on different cancer cell lines

5.1. Introduction:

Oximes are chemical compounds, with the general formula RR'C=NOH, where R is an organic side chain and R' may be hydrogen (forming aldoxime), or another organic group (forming a ketoxime) (Fig. 5.1). . Oximes have been known for more than 100 years. Methylglyoxime was the first oxime chemically synthesized in 1882 by the German chemists Victor Meyer and Alois Janny [1, 2] (Fig. 5.2).

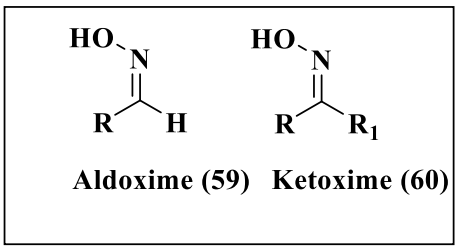

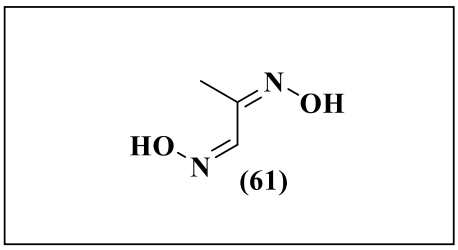

Figure 5.1. Structures of aldoxime and ketoxime. **Figure 5.2.** Methylglyoxime.

Oximes are generally prepared by the reaction of hydroxylamine with aldehydes or ketones. This reaction usually gives mixture of the two cis-trans isomeric forms of oximes. Oximes show geometrical isomerism i.e. occur in two forms syn (*Z* form) and anti (*E* form) .The *Z* or *E* configuration is determined by the position of the lone pair on nitrogen with respect to the alkyl or aryl group. That is, *Z* configuration is one in which the lone pair on nitrogen and the alkyl or aryl group are in the same side, while, in *E* configuration, they are on opposite sides.

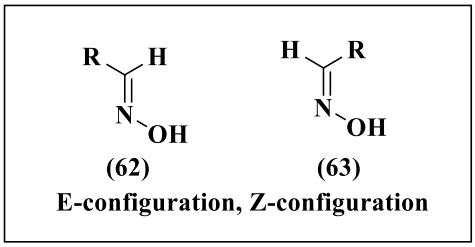

Figure 5.3. Cis-trans isomerism in oximes.

5.1. (a) Biological activity of oximes:

Some oximes occur in two interconvertable isomers, *E* and *Z*, (Fig 5.3). However, biological activities of these isomers depend on the structural conformation

of target sites. Oximes and derivatives are involved in various biological activities such as growth regulation, plant defense, pollinator attraction, and plant communication with the neighboring environment. The oxime derivatives have property of quenching reactive oxygen species (ROS) and storage of compounds for reduced nitrogen that can be released on demand by the activation of endogenous turnover pathways. Chemically synthesized bioactive oximes and derivatives have been used in Agro and Pharmaceutical industries [3].

5.1. (b) Oximes and cancer therapy:

Cancer is an overwhelming global health problem, now the second leading cause of death in the United States. It is predicted to surpass heart diseases as the main cause of death in future [4]. Breast cancer is a leading cause of premature death worldwide; in the United States, it was estimated to cause more than 40,000 deaths in 2014 [5]. Breast cancer is classified according to its expression of estrogen receptor (ER), progesterone receptor (PR), and/or human epidermal growth factor receptor (Her2/neu) and current therapies target these receptors [6]. Triple-negative breast carcinoma is a heterogeneous subset of tumors defined only by their aggressive nature and the absence of the estrogen receptors (ER). Its poor overall prognosis reflects not only its inherent aggressiveness but also the lack of targeted therapies [7]. As approximately one million breast cancers are diagnosed each year and about 15% are Triple-negative breast carcinoma, there is a clear and urgent need for new therapies.

Following are some important examples of oximes, their derivatives or oximino groups present in molecules, which have shown remarkable anti-proliferative activities. The hydroximino group at position 6 in B ring or position 17 of cholesterol type side chain of steroid derivatives (Fig. 5.4) is found to be biologically cytotoxic to various cancer cell lines such as Sk-Hep-1, H- 292, PC-3 and Hey-1B cells. Therefore, biological activity of a steroidal oxime was significantly dependent on the location of the hydroximino group and the type of a side chain at position 17 on the core structure of steroid [8]**.** Hydroximino androstene derivatives show the antineoplastic activity [9]. Dimethylation of alkannin oxime derivative, displays significant anticancer activity also good cellular selectivity and thus is considered as a promising antineoplastic agent for colorectal carcinoma and melanoma. However, its

potent cytotoxicity is not closely related with reactive oxygen species and bioreductive alkylation [10].

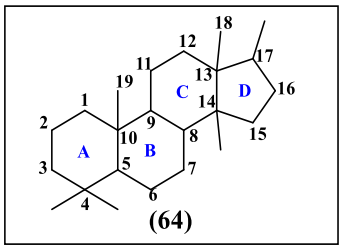

Figure 5.4. Steroid ring system (hydroximino group at position 6 of B-ring or in the side chain at position 17 have antiproliiferative properties against cancer).

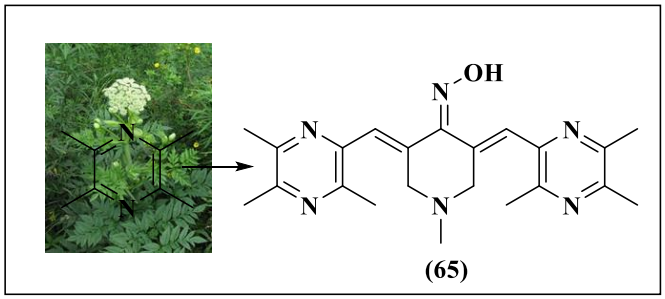

Figure 5.5. BRAFV600E, FAK and EGFR-TK kinases as inhibitors of tubulin polymerization.

The derivatives of indirubin 3-oximes inhibits actinomycin D-induced nuclear transport of YB-1 and suppresses the activation of MDR1 gene expression in the human hepatocellular carcinoma cell line HepG2, as well as indirubin 3'-oxime and actinomycin D in combination increase the anticancer effect on HepG2 cells line [11]. The steroidal oximes are showing antiproliferative activity *in vitro* as compared to the activity observed in Diosgenin. The antiproliferative activity of steroidal oximes increases 2.3–2.8 times due to the oxime group present in the spiroketalic side chain [12]. A series of α, β-unsaturated cyclohexanone oxime derivatives bearing different substitutions and ligustrazine (Tetramethyl pyrazine) incorporation were investigated *in vitro* for their antiproliferative effect on five different human cancer cell lines. The, β-unsaturated cyclohexanone oxime derivatives exhibited the strongest antiproliferative activity. BRAFV600E, FAK and EGFR-TK kinases have been discovered as inhibitors of tubulin polymerization (Fig 5.5) [13]. Indirubin 3-oxime (Indox) (Fig.5.6 a) an indigo alkaloid, was found to exhibit potent antitumor activities on various types of cancer cells. However, its modulatory effects on human neuroblastoma and the underlying mechanisms remain poorly understood. It inhibits cell cycle-related kinases such as cyclin dependent kinases and glycogen synthase kinase-3β. The conjugation of oxirane, a protein reactive component, enhanced the

cytotoxic activity of Indox, as determined from the IC_{50} value of indirubin 3-(O-oxiran-2-ylmethyl) oxime Epoxide and Indox derivatives contain one or two halogen element or a methoxy group on the aromatic ring of the Indox. The bromine-substitution at the 5-position on Indox derivative having bromine on the aromatic ring was efficient for improving anticancer activity [14]. 5-bromoindirubin 3'-(O-oxiran-2-ylmethyl) oxime (Figure 5.6 b) was the best anticancer agent in both short- (24 h) (IC_{50}: 0.67 μM) and extended-duration (72 h) cultures.

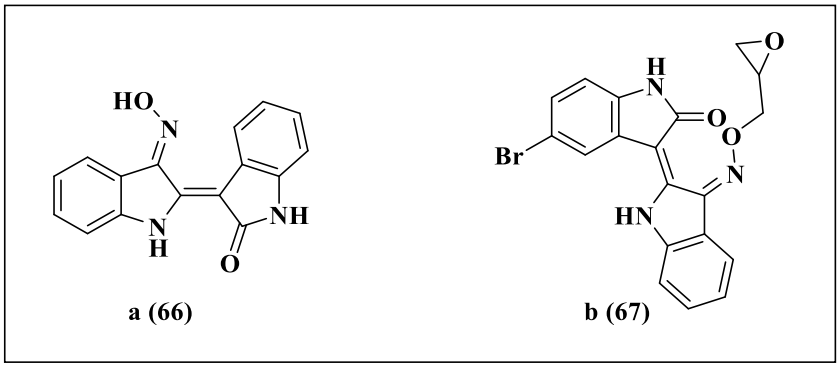

Figure 5.6. Indirubin 3-oxime (Indox) [a] and 5-bromoindirubin 3'-(O-oxiran-2-ylmethyl) oxime [b].

The sulfur containing shikonin oxime derivatives have shown in *vitro* cytotoxic activity against HCT-15, MGC-803, Bel7402, MCF-7 cancer cells and HSF cell lines. Sulfur-containing shikonin oxime derivatives exhibited potent cytotoxic activity selectively towards HCT-15 cells and did not display apparent toxicity to the normal HSF cells, some of which were more or rather effective to the parent compound against HCT-15, MGC-803 and Bel7402 cells lines [15]. The QSAR models pointed out that the internal electronic environment of α, β-unsaturated carbonyl-based compounds, oxime and oxime ether analogues have correlation with their antitumor activity. And another specific combination of acceptor, donor with each other and with certain atoms at specific distances have key role in deciding the antitumor activity [16]. Chemokines are a large family of structurally related chemoattractive cytokines, which have four conserved cysteines forming two disulfide bonds, and act through seven transmembrane spanning receptors coupled to heterotrimeric GTP binding proteins (G-protein-coupled receptors). Chemokines were thought to be signaling molecules that attract leukocytes to sites of inflammation; however, CXC chemokine ligand (CXCL)12 [also known as stromal cell derived

factor (SDF)-1α and pre-β cell growth stimulating factor (PBSF)] is the first member that was shown to be critical for developmental processes, including hematopoiesis (1), cardiogenesis (1-3), vascular formation (2), and neurogenesis (3), as well as the maintenance of tissue stem cells (4). CXCL12. CXCR4 are the physiological receptors for SDF-1. The interaction between CXCL12and CXCR4 leads to the activation of various intracellular signaling transduction pathways and downstream effectors that mediate cell survival, proliferation, migration, and adhesion. CXCR4 is highly expressed in various types of cancers, breast cancer [17], prostate cancer[18-19], lung cancer [20-21] are associated with chemotaxis, invasion, angiogenesis, and cell proliferation contributing tumorigenesis and cancer progression. A potential mechanism of CXCR4's involvement in tumor dissemination and metastasis is through promoting its trans endothelial migration at the primary site. The main goal of our drug discovery program is to identify novel substituted oxime scaffolds for research and treatment of cancer. Consequently; increasing interest has been devoted to the design and discovery of more effective anticancer agents in current medicinal chemistry [22-29].

5.2. Earlier methods for synthesis of oximes:

A large variety of synthetic approaches leading to the synthesis of oximes and its derivatives have been reported. However, the most common and widely used method, is the nucleophilic addition of hydroxylamine to aldehydes or ketones. The highly stereoselective conversion of aldehydes and ketones to their corresponding oximes with hydroxylamine hydrochloride was catalyzed by copper sulphate and potassium carbonate [30]. IBX (2-Iodo benzoic acid) induced procedures are reported for the generation of imines from secondary amines under mild conditions and in notably high yields [31].The benzyl alcohol was oxidised with prepared oxidant 3,6-bis(triphenylphosphonium)cyclohexene dichromate, (BTPCT) to obtain the benzaldehyde oxime [32]. Benzyl alcohol has also been oxidized with air, ionic liquid and microwave irradiation [33].Methyl arenes, NBS, oxidant, and dimethyl formamide have been used to afford oximes [34]. Oxidation with 2,2,6,6-tetramethylpiperidin-1-yloxy Radical (TEMPO) catalyzed aerobic oxidation of hydroxylamine and alkoxyamine to oximes and oxime ethers has been reported[35], by base and solvent mediated decomposition of tosylhydrazones, highly selective synthesis of N-alkyl substituted hydrazones, dialkylidenehydrazines, and oximes has been achieved [36], primary amine, $InCl_3$, TEMPO, O_2 [37], Aryl alcohol protected

with TMS and oxidant gave the oximes [38]. However, few of the general and efficient methods used recently for the preparation of oximes are described briefly below.

5.2. (a) Synthesis by the Nucleophilic Substitution reaction:

Mixture of *Z* and *E* isomers of 4-chlorobenzaldoxime **(69-70)** was produced via nucleophilic attack of hydroxylamine by the using K_2CO_3 / $CuSO_4$. By the effect of catalysts different orientation of product was formed. K_2CO_3 catalyst affords Z isomer while $CuSO_4$ catalyst affords E isomer. Both isomers have different physical and biological activities (Scheme 5.1).

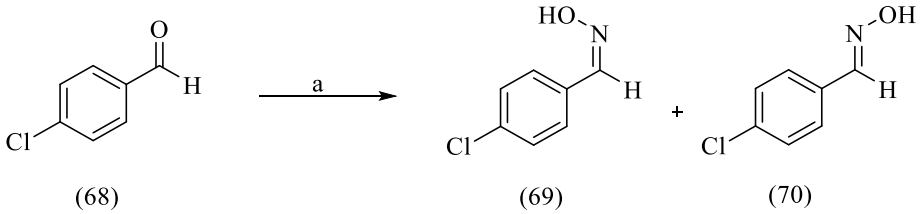

(68) (69) (70)

Reagent and condition: (a) Catalyst, 90°C

Scheme 5.1. Synthesis of *Z* and *E* isomers of 4-chlorobenzaldoxime.

5.2. (b) By the oxidation of primary/secondary amines with 2-iodoxybenzoic acid [IBX]:

IBX-mediated reactions accompanied with direct oxidation of primary and secondary amine compounds to furnish their respective oxime, via single electron transfer (SET) mechanism and hydrolyzed counterparts to respective carbonyl compounds (Scheme 5.2).

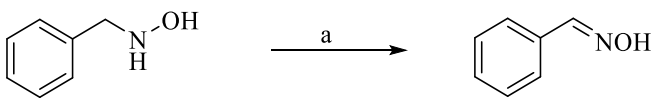

(71) (72)

Reagent and condition: (a) IBX (3.1 eq.), DMSO, 30 min

Scheme 5.2. 2-iodoxybenzoic acid mediated synthesis of oximes.

5.2. (c) By the oxidation of benzyl alcohol:

A mixture of the benzyl alcohol **(73)** and oxidant equimolar ratio were grinded in a mortar for 5 min at an ambient temperature and hydroxyl amine hydrochloride was added into the reaction mixture at same temperature for 35 min. to give oxime derivatives (Scheme 5.3).

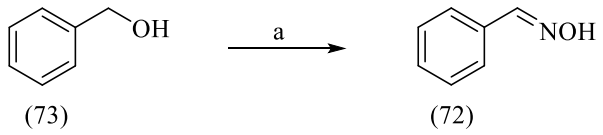

(73) (72)

Reagent and condition: (a) BTPCD, rt, 35 min

Scheme 5.3. Synthesis of oximes by oxidation of benzyl alcohol.

5.2. (d) By the microwave irradiation method:

The oximes have been synthesized from alcohols with hydroxylamine hydrochloride using 1-methylimidaziloum nitrate, [Hmim][NO_3] in ionic liquid under microwave irradiation (Scheme 5.4).

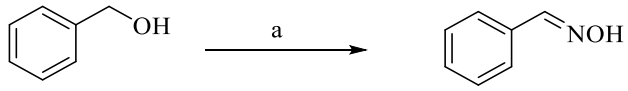

(73) (72)

Reagent and condition: (a) [HMIM][NO_3], MW (80w), air

Scheme 5.4. Synthesis of oximes from aromatic alcohols.

5.2. (e) Oxime preparation by Wohl–Ziegler reaction:

NBS reacts with benzoyl peroxide to generate bromide radical followed by reacting with methyl benzene to gives dibromomethylbenzene which returns to react with hydroxyl amine hydrochloride in presence of TEA in DMF as a solvent to afford benzaldehyde oxime **(72)** (Scheme 5.5).

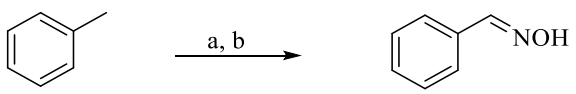

(74) (72)

Reagnt and condition: (a) NBS, benzoyl peroxide, (b) NH_2OH, DMF, TEA

Scheme 5.5. Preparation of oximes by Wohl–Ziegler reaction.

5.2. (f) By oxidation of alkoxyamine with 2,2,6,6-Tetramethylpiperidin-1-yloxy radical [TEMPO]:

Benzyl bromides has been directly transformed to oxime via in situ alkoxyamine formation by a nucleophilic substitution reaction of oxygen radical via TEMPO mediated oxidation along with hydrogen abstraction (Scheme 5.6).

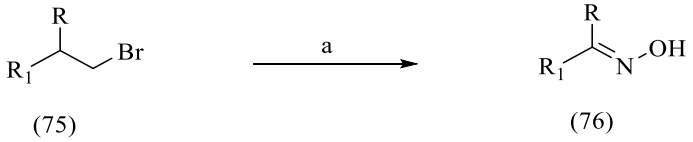

(75) (76)

Reagent and condition: (a) Oxident, BTF, 80°C R=H, R_1= Bn

Scheme 5.6. Synthesis of oximes by oxidation of alkoxyamines.

5.2. (g) By the decomposition of tosylhydrazones:

Base mediated decomposition reactions of tosylhydrazone, in presence nitromethan and DMSO as a solvent yielded oxime. The reaction mixture was heated at 110 ^{0}C with stirring for 16 h to give oxime derivatives (Scheme 5.7).

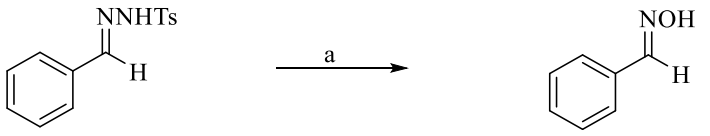

(77) (72)

Reagent and condition: (a) NaOH, 10 eq. CH_2NO_3, DMSO, 110^{o}C, 16h

Scheme 5.7. Preparation of oximes by decomposition of tosylhydrazones.

5.2. (h) By oxidation of amines with $InCl_3$:

Aerobic oxidation of primary amines to oximes is carried out in presence of mild oxidizing agent TEMPO/acetaldoxime along with $InCl_3$ as catalyst at 100 $^{\circ}$C (Scheme 5.8)

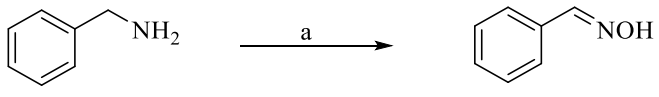

(78) (72)

Reagent and condition: (a) $InCl_3$, (5 Mol%), toluene, O_2, 100°C, 4h

Scheme 5.8. Preparation of oximes by oxidation of amines.

5.2. (i) Oxidation of silyl protected benzyl alcohol:

Oxidative conversion of silyl ether of benzyl alcohol to oxime has been described using trichloroisocyanuric acid (TCCA) with catalytic amount hydroxylamine hydrochloride under solvent-free conditions (Scheme 5.9).

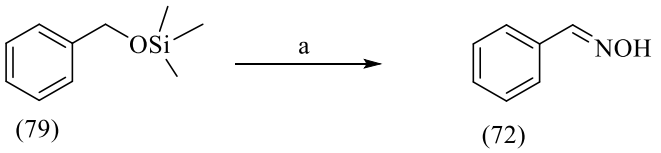

(79) (72)

Reagent and condition: (a) TCCA (5 Mol%), NH_2OH, sovent free, 100 °C

Scheme 5.9. Preparation of oximes by oxidation of silyl protected benzyl alcohol.

5.3. Basis of present work:

The main hindrance in the successful tumor chemotherapy includes the development of resistance in tumor cells against cytotoxic agents and the failure in discovery of novel anticancer agents possessing multi target approach. Due to the structural irrelativeness of this resistance to cytostatics, it was termed multidrug resistance (MDR), which is categorized by a reduced responsiveness to cytotoxic agents. So far, researchers have been struggling to overcome or circumvent multidrug resistance (MDR) in cancer. Drugs which efficiently target drug-resistant tumors are the need of the hour. In spite of massive research endeavours and rapid progress made, there is an increasing demand for new therapies as ever. It is vital to find new targets and novel multifunctional agents for cancer treatment due to MDR developed by cancer cells.

5.4. Objective of present work:

On the basis of our earlier findings, we have synthesized 18 substituted aromatic oximes. These oximes have been prepared by a novel stereospecific method which was discovered accidently and yields mainly Z isomer. Oximes have anticancer potential on human cancer cell lines. Among these, the 3 most active compounds were selected as precursors for additional synthesis to their oxime derivatives. The 3 most potent among all 18 compounds were synthesized for anticancer mechanistic studies

for their effects on CXCL-12, CXCR-4, VEGF and VEGFR-2 and were tested *in vitro* to reverse MDR developed by cancer cells.

5.5. Materials and Methods:

All chemicals, reagents and solvents used in this study were purchased from Merck analytical grade and Sigma Aldrich Chemical. Bruker 400 instruments were used to record ^{1} H NMR spectra and A Bruker FT-101MHz instrument was used to record ^{13}C NMR spectra with TMS as internal standard. Chloroform-D and DMSO-d_6 were used as solvents. Coupling constants (*J*) were assessed in hertz (Hz) and spin multiples are given as s (singlet), d (double), t (triplet), q (quartet), m (multiplet). The mass spectral measurements (HRMS) were recorded over a range of 40-1000 m/z.with an electrospray ionization (ESI) interface.

5.6. Experimental:

5.6. (a) General Procedure for the preparation of α, β-unsaturated compounds (80, 88-105):

A mixture of aldehyde (10 mmol), ethyl cyanoacetate (10.1 mmol) and sodium ethoxide (20 mol %) in 25 ml ethanol was refluxed at 80-85 °C for 1-2h and room temprature for 2-8 h. The progress of the reaction was checked by TLC. The resulting reaction mixture was directly charged onto silica gel column and eluted with a mixture of ethyl acetate: n-hexane to afford pure olefin, yield 83-95%. All the products were prepared by using the same procedure. The olefinic products thus obtained were characterized by comparison of their ^{1}H NMR, ^{13}C NMR and mass spectra.

Ethyl (*E*)-2-cyano-3-phenylacrylate (80): White solid; yield 1.88 g, 94 %; R*f* 0.48 (5% ethyl acetate: hexane); mp 50-52°C IR (KBr) υmax (cm^{-1}) 3030, 2979, 2223, 1749, 1711; ^{1}H NMR (400 MHz, $CDCl_3$) δ 8.26 (s, 1H), 8.00 (dt, *J* = 3.6, 2.5 Hz, 2H), 7.60 – 7.46 (m, 3H), 4.39 (q, *J* = 7.1 Hz, 2H), 1.41 (t, *J* = 7.1 Hz, 3H). ^{13}C NMR (101 MHz, $CDCl_3$) δ 162.52, 155.09, 133.34, 131.49, 131.10, 129.31, 115.52, 103.03, 77.37, 77.05, 76.73, 62.77, 14.18. ppm. HRMS (ESI): Calculated for $C_{12}H_{11}NO_2$ $[M+H]^+$: 202.0790, found 202. 0827.

Ethyl (*E*)-2-cyano-3-(4-hydroxyphenyl) acrylate(88): White solid; yield 1.89 mg, 85 %; R*f* 0.48 (20% ethyl acetate: hexane); mp 180-182°C IR (KBr) υmax (cm^{-1}) 3120, 2554, 2226, 1774; ^{1}H NMR (800 MHz, DMSO-d_6) δ 10.84 (s, 1H), 8.23 (s, 1H), 7.99 (d, *J* = 7.5 Hz, 2H), 6.95 (d, *J* = 7.9 Hz, 2H), 4.28 (q, *J* = 7.1 Hz, 2H), 1.29 (t, *J* = 7.0 Hz, 3H). 13C NMR (201 MHz, DMSO-d_6) δ 163.39, 163.08, 155.16, 134.47, 122.99, 116.95, 116.85, 97.48, 62.42, 40.31, 40.26, 40.20, 40.15, 40.05, 39.95, 39.84, 39.74, 39.63, 14.51, ppm. HRMS (ESI): Calculated for $C_{12}H_{11}NO_3$ $[M+H]^+$: 218.0739, found 218. 0777.

Ethyl (*E*)-2-cyano-3-(2-hydroxyphenyl) acrylate (89) White solid; yield 1.90 g, 85 %; R*f* 0.48 (20% ethyl acetate: hexane); mp 170-172°C IR (KBr) υmax (cm-1) 3029, 2954, 2228, 1799, 1711;^{1}H NMR (400 MHz, $CDCl_3$) δ 8.55 – 8.54 (m, 1H), 7.65 (ddd, *J* = 15.7, 7.8, 1.5 Hz, 2H), 7.39 – 7.32 (m, 2H), 4.43 (q, *J* = 7.1 Hz, 2H), 1.42 (t, *J* = 7.1 Hz, 3H). ^{13}C NMR (101 MHz, CDCl3) δ 163.08, 156.75, 155.18, 148.63, 134.35, 129.51, 124.86, 118.33, 117.89, 116.80, 77.38, 77.06, 76.75, 62.01, 14.24.ppm. HRMS (ESI): Calculated for $C_{12}H_{11}NO_3$ $[M+H]^+$: 218.0739, found 218. 0789.

Ethyl (*E*)-2-cyano-3-(3,4-dihydroxyphenyl)acrylate(90): White solid; yield 1.9 g, 84%; R*f* 0.48 (25% ethyl acetate: hexane); mp 191-193°C IR (KBr) υmax (cm-1); 3031, 2979, 2224, 1726, 1607; ^{1}H NMR (400 MHz, DMSO-d_6) δ 10.30 (s, 1H), 9.61 (s, 1H), 8.06 (s, 1H), 7.59 (d, *J* = 2.2 Hz, 1H), 7.34 (dd, *J* = 8.4, 2.1 Hz, 1H), 6.84 (d, *J* = 8.3 Hz, 1H), 4.22 (q, *J* = 7.1 Hz, 2H), 1.22 (t, *J* = 7.1 Hz, 3H). ^{13}C NMR (101 MHz, DMSO-d_6) δ 163.21, 155.43, 152.56, 146.31, 127.43, 123.42, 116.93, 116.89, 116.46, 97.04, 62.35, 40.63, 40.42, 40.21, 40.01, 39.80, 39.59, 39.38, 14.53.ppm; HRMS (ESI): Calculated for $C_{12}H_{11}NO_4$ $[M+H]^+$: 234.0688, found 234. 0716.

Ethyl (*E*)-2-cyano-3-(2-methoxyphenyl)acrylate(91): Light yellow solid; yield 1.9 g, 83 %; R*f* 0.48 (10% ethyl acetate: hexane); mp 80-82°C IR (KBr) υmax (cm^{-1}); 3029, 2221, 1726, ^{1}H NMR (400 MHz, $CDCl_3$) δ 8.75 (s, 1H), 8.28 (dd, *J* = 7.9, 1.6 Hz, 1H), 7.51 (ddd, *J* = 8.8, 7.4, 1.6 Hz, 1H), 7.06 (t, *J* = 7.6 Hz, 1H), 6.98 – 6.94 (m, 1H), 4.38 (q, *J* = 7.1 Hz, 2H), 3.91 (s, 3H), 1.40 (t, *J* = 7.1 Hz, 3H). ^{13}C NMR (101 MHz, $CDCl_3$) δ 162.83, 159.24, 149.79, 134.96, 129.38, 120.97, 120.75, 115.90, 111.17, 102.42, 77.36, 77.04, 76.72, 62.49, 55.76, 14.19.ppm; HRMS (ESI):

Calculated for $C_{13}H_{13}NO_3$ $[M+H]^+$: 232.0895, found 232. 0926.

Ethyl (*E*)-2-cyano-3-(3,4-dimethoxyphenyl)acrylate(92): Light yellow solid; yield 2.4 g, 91 %; R*f* 0.5 (20% ethyl acetate: hexane); mp 138-140°C IR (KBr) υmax (cm^{-1}); 3022, 2221, 1745**;** ^{1}H NMR (400 MHz, $CDCl_3$) δ 8.16 (s, 1H), 7.81 (d, *J* = 2.1 Hz, 1H), 7.48 (dd, *J* = 8.5, 2.0 Hz, 1H), 6.95 (d, *J* = 8.4 Hz, 1H), 4.38 (q, *J* = 7.1 Hz, 2H), 3.97 (d, *J* = 4.9 Hz, 6H), 1.40 (t, *J* = 7.1 Hz, 3H). ^{13}C NMR (101 MHz, $CDCl_3$) δ 163.14, 154.72, 153.70, 149.31, 127.90, 124.64, 116.38, 111.68, 110.96, 99.44, 77.34, 77.23, 77.03, 76.71, 62.48, 56.17, 56.08, 14.23.ppm; HRMS (ESI): Calculated for $C_{14}H_{15}NO_4$ $[M+H]^+$: 262.1001, found 262. 1037.

Ethyl (*E*)-2-cyano-3-(3,4,5-trimethoxyphenyl)acrylate(93): Light yellow solid; yield 2.49 g, 84%; R*f* 0.48 (20% ethyl acetate: hexane); mp 156-158°C IR (KBr) υmax (cm^{-1}); 2982, 2941, 2221, 1722; ^{1}H NMR (400 MHz, $CDCl_3$) δ 8.52 (s, 1H), 8.12 (d, *J* = 9.0 Hz, 1H), 6.71 (d, *J* = 9.0 Hz, 1H), 4.29 (q, *J* = 7.1 Hz, 2H), 3.89 (d, *J* = 12.0 Hz, 6H), 3.79 (s, 3H), 1.31 (t, *J* = 7.1 Hz, 3H). ^{13}C NMR (101 MHz, $CDCl_3$) δ 163.11, 158.47, 154.87, 149.01, 141.84, 125.02, 118.65, 116.38, 107.65, 100.16, 77.41, 77.09, 76.78, 62.35, 62.12, 60.92, 56.25, 14.20.ppm; HRMS (ESI): Calculated for $C_{15}H_{17}NO_5$ $[M+H]^+$: 292.1107, found 292. 1147.

Ethyl (*E*)-2-cyano-3-(4-hydroxy-methoxyphenyl)acrylate(94): Bright green solid; yield 2.18 g, 86%; R*f* 0.39 (20% ethyl acetate: hexane); mp 109-110°C IR (KBr) υmax (cm^{-1}); 2982, 2911, 2222, 1729; ^{1}H NMR (400 MHz, $CDCl_3$) δ 8.07 (s, 1H), 7.77 (d, *J* = 2.0 Hz, 1H), 7.32 (dd, *J* = 8.4, 2.0 Hz, 1H), 6.94 – 6.91 (m, 1H), 6.24 (s, 1H), 4.30 (q, *J* = 7.1 Hz, 2H), 3.91 (s, 3H), 1.32 (t, *J* = 7.1 Hz, 3H). ^{13}C NMR (101 MHz, $CDCl_3$) δ 163.18, 154.91, 150.90, 146.86, 128.83, 124.28, 116.47, 114.95, 111.19, 98.99, 77.37, 77.06, 76.74, 62.48, 56.17, 14.24.ppm; HRMS (ESI): Calculated for $C_{13}H_{13}NO_4$ $[M+H]^+$: 248.0845, found 248. 0879.

Ethyl (*E*)-2-cyano-3-(4-fluorophenyl) acrylate (95): White solid; yield 2.0 g, 92%; R*f* 0.5 (10% ethyl acetate: hexane); mp 94-96°C IR (KBr) υmax (cm^{-1}); 3421, 3053, 3035, 2226, 1717; ^{1}H NMR (400 MHz, $CDCl_3$) δ 8.22 (s, 1H), 8.06 – 8.01 (m, 2H), 7.23 – 7.17 (m, 2H), 4.39 (q, *J* = 7.1 Hz, 2H), 1.40 (t, *J* = 7.1 Hz, 3H). ^{13}C NMR (101 MHz, $CDCl_3$) δ 166.70, 164.14, 162.42, 153.52, 133.66, 133.56, 127.88, 127.85,

116.84, 116.62, 115.46, 102.60, 102.58, 77.36, 77.25, 77.04, 76.73, 62.82, 14.16.ppm; HRMS (ESI): Calculated for $C_{12}H_{10}FNO_2$ $[M+H]^+$: 220.0696, found 220. 0729.

Ethyl (*E*)-3-(4-bromophenyl)-2-cyanoacrylate (96): White solid; yield 2.6 g, 94%; R*f* 0.5 (10% ethyl acetate: hexane); mp 99-101°C IR (KBr) υmax (cm^{-1}); 3083, 3055, 2223, 1719; ^{1}H NMR (400 MHz, $CDCl_3$) δ 8.19 (s, 1H), 7.88 – 7.83 (m, 2H), 7.67 – 7.62 (m, 2H), 4.39 (q, *J* = 7.1 Hz, 2H), 1.40 (t, *J* = 7.1 Hz, 3H). ^{13}C NMR (101 MHz, $CDCl_3$) δ 162.25, 153.54, 132.70, 132.26, 130.28, 128.29, 115.28, 103.65, 77.37, 77.05, 76.73, 62.92, 14.16.ppm; HRMS (ESI): Calculated for $C_{12}H_{10}BrNO_2$ $[M+H]^+$: 279.9895, found 279. 9762.

Ethyl (*E*)-3-(3-chlorophenyl)-2-cyanoacrylate (97): White solid; yield 2.24 g, 95%; R*f* 0.5 (10% ethyl acetate: hexane); mp 87-89°C IR (KBr) υmax (cm^{-1}); 3417, 3065, 2983, 2228, 1715; ^{1}H NMR (400 MHz, $CDCl_3$) δ 8.18 (s, 1H), 7.94 – 7.89 (m, 1H), 7.53 (ddd, *J* = 8.1, 1.9, 1.1 Hz, 1H), 7.46 (t, *J* = 7.8 Hz, 1H), 4.40 (q, *J* = 7.1 Hz, 2H), 1.41 (t, *J* = 7.1 Hz, 4H). 13C NMR (101 MHz, CDCl3) δ 162.01, 153.22, 135.35, 133.07, 130.83, 130.56, 128.66, 114.96, 104.67, 77.39, 77.08, 76.76, 63.00, 14.15.ppm; HRMS (ESI): Calculated for $C_{12}H_{10}ClNO_2$ $[M+H]^+$: 236.0400, found 236. 0372.

Ethyl (*E*)-3-(2-chlorophenyl)-2-cyanoacrylate (98): White solid; yield 2.25 g, 96%; R*f* 0.5 (5% ethyl acetate: hexane); mp 86-88°C IR (KBr) υmax (cm^{-1}); 3442, 2985, 2225, 1732; 1609; ^{1}H NMR (400 MHz, $CDCl_3$) δ 8.69 (s, 1H), 8.24 (dd, *J* = 7.8, 1.5 Hz, 1H), 7.53 – 7.38 (m, 3H), 4.41 (q, *J* = 7.1 Hz, 2H), 1.41 (t, *J* = 7.1 Hz, 3H). ^{13}C NMR (101 MHz, $CDCl_3$) δ 161.82, 151.17, 136.45, 133.69, 130.35, 129.90, 129.87, 127.48, 114.83, 106.20, 77.38, 77.06, 76.74, 62.97, 14.15.ppm; HRMS (ESI): Calculated for $C_{12}H_{10}ClNO_2$ $[M+H]^+$: 236.0400, found 236. 0363.

Ethyl (*E*)-2-cyano-3-(o-tolyl)acrylate (99): Transparent liquid; yield 1.98 g, 92%; R*f* 0.5 (5% ethyl acetate: hexane); IR (KBr) υmax (cm^{-1}); 3406, 3077, 2986, 2221, 1800, 1738, 1715; ^{1}H NMR (400 MHz, $CDCl_3$) δ 8.57 (s, 1H), 8.14 (d, *J* = 7.7 Hz, 1H), 7.42 (td, *J* = 7.5, 1.1 Hz, 1H), 7.35 – 7.25 (m, 2H), 4.39 (q, *J* = 7.1 Hz, 2H), 2.45 (s, 3H), 1.41 (t, *J* = 7.1 Hz, 3H). ^{13}C NMR (101 MHz, $CDCl_3$) δ 162.46, 153.37, 139.70, 132.78, 131.00, 130.61, 128.62, 126.73, 115.38, 104.53, 77.37, 77.05, 76.73, 62.74,

19.86, 14.17.ppm; HRMS (ESI): Calculated for $C_{13}H_{13}NO_2$ $[M+H]^+$: 216.0946, found 216. 0978.

Ethyl (*E*)-2-cyano-3-(4-(dimethylamino) phenyl) acrylate (100): White solid; yield 2.28 g, 93%; R*f* 0.5 (10% ethyl acetate: hexane); mp 123-125°C IR (KBr) υmax (cm^{-1}); 2986, 2917, 2210, 1705, 1613; ^{1}H NMR (400 MHz, $CDCl_3$) δ 8.07 (s, 1H), 7.96 – 7.92 (m, 2H), 6.71 – 6.67 (q, *J*=7.1, 2H), 4.37 – 4.31 (m, 2H), 3.11 (s, 6H), 1.37 (t, *J* = 7.1 Hz, 3H). ^{13}C NMR (101 MHz, $CDCl_3$) δ 164.33, 154.58, 153.58, 134.07, 119.39, 117.61, 111.50, 94.07, 77.36, 77.04, 76.72, 61.91, 40.03, 14.31.ppm; HRMS (ESI): Calculated for $C_{14}H_{16}N_2O_2$ $[M+H]^+$: 245.1212, found 245. 1250.

Ethyl (*E*)-2-cyano-3-(naphthalen-1-yl) acrylate(101): Ligh green solid; yield 2.25 g, 90%; R*f* 0.5 (10% ethyl acetate: hexane); mp 78-80°C IR (KBr) υmax (cm^{-1}); 2981, 2224, 1724, 1601, 1571; ^{1}H NMR (400 MHz, $CDCl_3$) δ 9.10 (s, 1H), 8.34 (dd, *J* = 15.8, 9.3 Hz, 1H), 8.03 (dd, *J* = 7.9, 6.0 Hz, 2H), 7.92 (td, *J* = 8.5, 2.5 Hz, 2H), 7.65 – 7.54 (m, 2H), 4.48 – 4.41 (q, *J*=7.2, 2H), 1.44 (t, *J* = 7.1 Hz, 3H). ^{13}C NMR (101 MHz, $CDCl_3$) δ 162.36, 152.84, 133.53, 133.46, 131.69, 129.19, 128.34, 128.27, 127.84, 126.85, 125.45, 122.89, 115.44, 105.80, 77.41, 77.09, 76.77, 62.88, 14.24, 13.75.ppm; HRMS (ESI): Calculated for $C_{16}H_{13}NO_2$ $[M+H]^+$: 252.0946, found 252. 0984.

Ethyl (*E*)-2-cyano-3-(1H-indol-3-yl) acrylate(102): Ligh brown solid; yield 2.15 g, 90%; R*f* 0.5 (20% ethyl acetate: hexane); mp 168-170°C IR (KBr) υmax (cm-1); 3258, 2215, 1680, 1574, 1591; ^{1}H NMR (400 MHz, $CDCl_3$) δ 9.71 (s, 1H), 8.64 (dd, *J* = 7.0, 3.2 Hz, 1H), 8.62 (s, 1H), 7.84 – 7.78 (m, 1H), 7.53 – 7.47 (m, 1H), 7.35 – 7.27 (m, 2H), 4.38 (q, *J* = 7.1 Hz, 2H), 1.41 (t, *J* = 9.0, 5.3 Hz, 3H). ^{13}C NMR (101 MHz, $CDCl_3$) δ 163.94, 163.01, 146.67, 135.78, 131.05, 127.45, 124.12, 122.58, 118.26, 118.23, 113.20, 112.38, 111.07, 94.48, 62.02, 14.33.ppm; HRMS (ESI): Calculated for $C_{14}H_{12}N_2O_2$ $[M+H]^+$: 241.0899, found 241. 0933.

Ethyl (*E*)-2-cyano-3-(furan-2-yl) acrylate(103): Ligh yellow solid; yield 1.7 g, 89%; R*f* 0.5 (10% ethyl acetate: hexane); mp 81-83°C IR (KBr) υmax (cm^{-1}); 3129, 3038, 2222, 1715, 1620; ^{1}H NMR (400 MHz, $CDCl_3$) δ 8.04 (s, 1H), 7.77 (d, *J* = 1.6 Hz, 1H), 7.42 (d, *J* = 3.7 Hz, 1H), 6.69 – 6.67 (m, 1H), 4.38 (q, *J* = 7.1 Hz, 2H), 1.40

(t, *J* = 7.1 Hz, 3H). ^{13}C NMR (101 MHz, $CDCl_3$) δ 162.60, 148.78, 148.24, 139.48, 121.67, 115.34, 113.84, 98.71, 77.34, 77.03, 76.71, 62.58, 14.17.ppm; HRMS (ESI): Calculated for $C_{10}H_9NO_3$ $[M+H]^+$: 192.0582, found 192. 0619.

Ethyl (*E*)-2-cyano-3-(4-((dimethylcarbamothioyl)oxy)-3-methoxyphenyl)acrylate (104): White solid; yield 3.0 g, 91%; R*f* 0.5 (40% ethyl acetate: hexane); mp 189-191°C IR (KBr) υmax (cm^{-1}); 2939, 2221, 1725, 1683, 1464; ^{1}H NMR (400 MHz, $CDCl_3$) δ 8.22 (s, 1H), 7.85 (d, *J* = 2.0 Hz, 1H), 7.52 – 7.48 (m, 1H), 7.19 – 7.17 (m, 1H), 4.40 (q, *J* = 7.1 Hz, 2H), 3.92 (s, 3H), 3.48 (s, 3H), 3.38 (s, 3H), 1.42 (t, *J* = 7.1 Hz, 3H). ^{13}C NMR (101 MHz, $CDCl_3$) δ 186.74, 162.50, 154.27, 152.16, 146.72, 130.11, 125.63, 124.93, 115.69, 113.45, 102.46, 77.40, 77.08, 76.76, 62.76, 56.20, 43.42, 38.93, 14.19.ppm; HRMS (ESI): Calculated for $C_{16}H_{18}N_2O_4S$ $[M+H]^+$: 335.0987, found 335. 1023.

Ethyl (*E*)-2-cyano-4-methylpent-2-enoate (105): Transparent liquid; yield 1.25 g, 74%; R*f* 0.5 (2% ethyl acetate: hexane); IR (KBr) υmax (cm^{-1}); 2226, 1613, 1444; ^{1}H NMR (400 MHz, $CDCl_3$) δ 7.46 (d, *J* = 10.6 Hz, 1H), 4.31 (q, *J* = 7.1 Hz, 2H), 3.00 (dhept, *J* = 10.7, 6.6 Hz, 1H), 1.36 (t, *J* = 7.1 Hz, 3H), 1.16 (d, *J* = 6.6 Hz, 6H). ^{13}C NMR (101 MHz, $CDCl_3$) δ 169.12, 161.46, 113.54, 107.57, 77.38, 77.07, 76.75, 62.41, 31.59, 21.23, 14.07.ppm; HRMS (ESI): Calculated for $C_9H_{13}NO_2$ $[M+H]^+$: 168.0946, found 168. 0982.

5.6. (b) Synthesis of *Z* oximes:

General procedure: To the stirred sodium carbonate (632 mg, 5.9 mmol), hydroxylamine hydrochloride (414mg, 5.9 mmol), water (2.5 ml), and the solution of substituted ethyl (E)-2-cyano-3-phenylacrylate (4.9 mmol), methanol (22.5 ml) was added in the reaction mixture and reflux for 1h. Reaction was checked with TLC, the resulting mixture was purified with column chromatography elution ingredients hexane: ethyl acetate (90:5), yield 84-94%.

(*Z*)-benzaldehyde oxime (81). Yellow gel; yield 556mg, 92%; R*f* 0.39 (5 % ethyl acetate : hexane); IR (KBr) υmax (cm^{-1}); 3446, 1956, 1893, 1633, 1488, 1304, 1211; 1H NMR (400 MHz, $CDCl_3$) δ 8.76 (s, 1H), 8.17 (s, 1H), 7.60 – 7.54 (m, 2H), 7.41 –

7.36 (m, 3H).^{13}C NMR (101 MHz, $CDCl_3$) δ 150.42, 131.92, 130.13, 128.83, 127.08, 77.06.ppm; HRMS (ESI): Calculated for C_7H_7NO $[M+H]^+$: 122.0528, found 122.0600.

(*Z*)-4-hydroxybenzaldehyde oxime (109). White solid; yield 450mg, 83.9%; R*f* 0.4 (20% ethyl acetate : hexane); mp 104-106°C; IR (KBr) υmax (cm^{-1}); 3434,2066, 1632, 1515, 1448; ^{1}H NMR (800 MHz, DMSO-d_6) δ 10.83 (s, 1H), 9.73 (s, 1H), 7.99 (s, 1H), 7.39 (d, *J* = 8.6 Hz, 2H), 6.77 (d, *J* = 8.6 Hz, 2H). ^{13}C NMR (201 MHz, DMSO-d_6) δ 159.00, 148.34, 128.41, 124.48, 116.00, 40.24, 40.14, 40.03, 39.93, 39.82, 39.72, 39.62, 38.02.ppm; HRMS (ESI): Calculated for $C_7H_7NO_2$ $[M+H]^+$: 138.0477, found 138.0532.

(*Z*)-3,4-dihydroxybenzaldehyde oxime (110). Brown solid; yield 401mg, 77%; R*f* 0.5 (50% ethyl acetate : hexane); mp 125-127°C; IR (KBr) υmax (cm^{-1}); 3420, 1628, 1599, 1445; ^{1}H NMR (400 MHz, DMSO-d_6) δ 10.71 (s, 1H), 9.15 (s, 1H), 9.03 (s, 1H), 7.82 (d, *J* = 24.7 Hz, 1H), 6.97 (d, *J* = 1.9 Hz, 1H), 6.74 (dd, *J* = 8.2, 1.9 Hz, 1H), 6.66 (d, *J* = 8.1 Hz, 1H). ^{13}C NMR (101 MHz, DMSO-d_6) δ 148.59, 147.40, 145.93, 124.91, 119.71, 115.98, 113.04, 40.52, 40.31, 40.11, 39.90, 39.69, 39.48, 39.27.ppm; HRMS (ESI): Calculated for $C_7H_7NO_3$ $[M+H]^+$: 154.0426, found 154.0459.

(*Z*)- 4-methoxybenzaldehyde oxime (111). Pale yellow solid; yield 550mg, 85.6%; R*f* 0.5 (20% ethyl acetate : hexane); mp 60-62°C; IR (KBr) υmax (cm^{-1}); 3315, 1606, 1514, 1249; ^{1}H NMR (400 MHz, $CDCl_3$) δ 9.25 (s, 1H), 8.11 (s, 1H), 7.53 – 7.48 (m, 2H), 6.92 – 6.87 (m, 2H), 3.81 (s, 3H) ^{13}C NMR (101 MHz, $CDCl_3$) δ 161.08, 150.02, 128.59, 124.59, 114.30, 77.09, 55.36.ppm; HRMS (ESI): Calculated for $C_8H_9NO_2$ $[M+H]^+$: 152.0633, found 152.0667.

(*Z*)-3-methylbenzaldehyde oxime (112). Transparent liquid; yield 560mg, 89%; R*f* 0.5 (10% ethyl acetate : hexane); IR (KBr) υmax (cm^{-1}); 3391, 1626, 1490, 1457, 1226; ^{1}H NMR (400 MHz, $CDCl_3$) δ 8.57 (d, *J* = 13.2 Hz, 1H), 8.43 (s, 1H), 7.68 – 7.64 (m, 1H), 7.28 (td, *J* = 7.4, 1.4 Hz, 1H), 7.24 – 7.17 (m, 2H), 2.43 (s, 3H). ^{13}C NMR (101 MHz, $CDCl_3$) δ 149.30, 136.84, 130.87, 130.22, 129.88, 126.72, 126.27, 77.36, 77.05, 76.73, 19.77.ppm; HRMS (ESI): Calculated for C_8H_9NO $[M+H]^+$:

136.0685, found 136.0758.

(*Z*)-3, 4-dimethoxybenzaldehyde oxime (113). White solid; yield 598mg, 86%; R*f* 0.5 (20% ethyl acetate : hexane); mp 92-94°C; IR (KBr) υmax (cm^{-1}); 3448, 3083, 2962, 1601, 1583; ^{1}H NMR (400 MHz, $CDCl_3$) δ 8.55 (s, 1H), 8.11 (s, 1H), 7.24 (d, *J* = 1.9 Hz, 1H), 7.05 (dd, *J* = 8.3, 1.9 Hz, 1H), 6.89 – 6.86 (m, 1H), 3.92 (s, 6H). ^{13}C NMR (101 MHz, $CDCl_3$) δ 150.82, 150.24, 149.30, 124.82, 121.73, 110.76, 107.99, 77.39, 77.07, 76.75, 55.94, 55.89ppm; HRMS (ESI): Calculated for $C_9H_{11}NO_3$ $[M+H]^+$: 182.0739, found 182.0802.

(*Z*)- 2,3,4-trimethoxybenzaldehyde oxime (114). White crystalline solid; yield 635mg, 88%; R*f* 0.49 (25% ethyl acetate : hexane); mp 97-99°C; IR (KBr) υmax (cm^{-1}); 3409, 1595, 1499, 1298; ^{1}H NMR (400 MHz, $CDCl_3$) δ 8.56 (b, 1H), 8.29 (s, 1H), 7.35 (d, *J* = 8.8 Hz, 1H), 6.63 (d, *J* = 8.8 Hz, 1H), 3.84 (s, 3H), 3.82 (s, 3H), 3.81 (s, 3H). ^{13}C NMR (101 MHz, $CDCl_3$) δ 155.29, 152.69, 146.29, 142.17, 121.45, 118.63, 107.88, 77.05, 61.72, 60.95, 56.08.ppm; HRMS (ESI): Calculated for $C_{10}H_{13}NO_4$ $[M+H]^+$: 212.0845, found 212.0917.

(*Z*)-4-hydroxy-3-methoxybenzaldehyde oxime (115). Pale yellow solid; yield 550mg, 85%; R*f* 0.45 (30% ethyl acetate : hexane); mp 125-127°C; IR (KBr) υmax (cm^{-1}); 3207, 1769, 1593, 1521, 1427, 1278; ^{1}H NMR (400 MHz, DMSO-d_6) δ 10.86 (s, 1H), 9.36 (s, 1H), 8.00 (s, 1H), 7.17 (d, *J* = 1.5 Hz, 1H), 6.98 (dd, *J* = 8.1, 1.6 Hz, 1H), 6.79 (d, *J* = 8.1 Hz, 1H), 3.78 (s, 3H). ^{13}C NMR (101 MHz, DMSO-d_6) δ 148.50, 148.42, 148.26, 124.88, 120.93, 115.89, 109.59, 55.89, 39.93.ppm; HRMS (ESI): Calculated for $C_8H_9NO_3$ $[M+H]^+$: 168.0582, found 168.0627.

(*Z*)-1-naphthaldehyde oxime (116). Light green solid; yield 600mg, 88%; R*f* 0.5 (15% ethyl acetate : hexane); mp 100-102°C; IR (KBr) υmax (cm^{-1}); 3385, 3060, 1614,1510, 1444, 1240; ^{1}H NMR (800 MHz, DMSO-d_6) δ 11.49 (s, 1H), 8.79 (s, 1H), 8.67 (d, *J* = 8.4 Hz, 1H), 7.96 (t, *J* = 9.2 Hz, 2H), 7.80 (d, *J* = 7.0 Hz, 1H), 7.57 (ddd, *J* = 23.4, 15.1, 7.4 Hz, 3H). ^{13}C NMR (201 MHz, DMSO-d_6) δ 148.31, 133.49, 130.01, 129.73, 128.79, 128.66, 127.01, 126.93, 126.20, 125.56, 124.75, 39.62, 39.51, 39.40.ppm; HRMS (ESI): Calculated for $C_{11}H_9NO$ $[M+H]^+$: 172.0684, found 172.0745.

(*Z*)-4-fluorobenzaldehyde oxime (117). White crystalline solid; yield 580mg, 92%; R*f* 0.36 (10% ethyl acetate : hexane); mp 88-90°C; IR (KBr) υmax (cm^{-1}); 3262, 3017, 1882, 1608, 1595, 1474; ^{1}H NMR (400 MHz, $CDCl_3$) δ 8.12 (s, 1H), 7.82 (s, 1H), 7.60 – 7.53 (m, 2H), 7.12 – 7.04 (m, 2H) , ^{13}C NMR (101 MHz, $CDCl_3$) δ 165.06, 162.57, 149.30, 128.94, 128.86, 128.16, 116.09, 115.87, 77.35, 77.03, 76.71.ppm; HRMS (ESI): Calculated for C_7H_6FNO $[M+H]^+$: 140.0433, found 140.0490.

(*Z*)-2-chlorobenzaldehyde oxime (118). White crystalline solid; yield 580mg, 88%; R*f* 0.36 (10% ethyl acetate : hexane); mp 74-76°C; IR (KBr) υmax (cm^{-1}); 3017, 1554, 1485, 1429, 1320; ^{1}H NMR (400 MHz, $CDCl_3$) δ 8.58 (s, 1H), 8.31 – 8.22 (m, 1H), 7.82 (dd, *J* = 7.7, 1.8 Hz, 1H), 7.41 – 7.38 (m, 1H), 7.32 (ddd, *J* = 9.8, 5.7, 2.0 Hz, 1H), 7.29 – 7.24 (m, 1H). ^{13}C NMR (101 MHz, $CDCl_3$) δ 147.60, 133.97, 132.03, 131.01, 129.95, 129.81, 129.77, 127.16, 127.03, 126.55, 77.34, 77.03, 76.71.ppm; HRMS (ESI): Calculated for C_7H_6ClNO $[M+H]^+$: 156.0138, found 156.0192.

(*Z*)-3-chlorobenzaldehyde oxime (119). White crystalline solid; yield 581mg, 88%; R*f* 0.36 (10% ethyl acetate : hexane); mp 71-73°C; IR (KBr) υmax (cm^{-1}); 3299, 1596, 1494, 1399 1318; ^{1}H NMR (400 MHz, $CDCl_3$) δ 8.18 (d, *J* = 1.7 Hz, 1H), 8.10 (s, 1H), 7.59 (q, *J* = 1.6 Hz, 1H), 7.44 (dt, *J* = 7.3, 1.3 Hz, 1H), 7.36 (dt, *J* = 3.5, 1.5 Hz, 1H), 7.34 – 7.29 (m, 1H). ^{13}C NMR (101 MHz, $CDCl_3$) δ 149.19, 134.87, 133.75, 130.04, 126.85, 125.27, 77.35, 77.03, 76.71.ppm; HRMS (ESI): Calculated for C_7H_6ClNO $[M+H]^+$: 156.0138, found 156.0200.

(*Z*)-4-bromobenzaldehyde oxime (120). White crystalline solid; yield 480mg, 90%; R*f* 0.36 (10% ethyl acetate : hexane); mp 116-118°C; IR (KBr) υmax (cm^{-1}); 3212, 1634, 1444, 1258; ^{1}H NMR (400 MHz, $CDCl_3$) δ 8.27 (s, 1H), 8.10 (s, 1H), 7.55 – 7.49 (m, 2H), 7.46 – 7.39 (m, 2H).^{13}C NMR (101 MHz, $CDCl_3$) δ 149.43, 132.06, 130.87, 128.46, 124.32, 77.36, 77.04, 76.72.ppm; HRMS (ESI): Calculated for C_7H_6BrNO $[M+H]^+$: 199.9633, found 199.9679

(*Z*)-*O*-(4-((hydroxyimino) methyl)-3-methoxyphenyl) dimethyl carbamothioate (121). White crystalline solid; yield 840mg, 90.71%; R*f* 0.5 (30% ethyl acetate : hexane); mp 128-130°C; IR (KBr) υmax (cm^{-1}); 3418, 2940, 1626, 1599, 1541, 1508; ^{1}H NMR (400 MHz, $CDCl_3$) δ 8.71 (s, 1H), 8.12 (s, 1H), 7.28 (d, *J* = 1.7 Hz, 1H),

7.11 (dd, *J* = 8.2, 1.8 Hz, 1H), 7.06 (d, *J* = 8.1 Hz, 1H), 3.84 (s, 3H), 3.45 (s, 3H), 3.35 (s, 3H). ^{13}C NMR (101 MHz, $CDCl_3$) δ 187.43, 151.90, 149.78, 144.31, 130.78, 124.33, 120.59, 109.87, 77.45, 77.14, 76.82, 56.07, 43.43, 38.84.ppm; HRMS (ESI): Calculated for $C_{11}H_{14}N_2O_3S$ $[M+H]^+$: 255.0725, found 255.0798.

(*Z*)-4-(dimethylamino)benzaldehyde oxime (122), Light yellow crystalline solid; yield 500mg, 86%; R*f* 0.5 (10% ethyl acetate : hexane); mp 149-151°C; IR (KBr) υmax (cm^{-1}); 2920, 1797, 1613, 1600, 1528, 1448; ^{1}H NMR (400 MHz, $CDCl_3$) δ 8.79 (s, 1H), 8.06 (s, 1H), 7.45 (d, *J* = 8.8 Hz, 2H), 6.68 (d, *J* = 8.8 Hz, 2H), 2.99 (s, 6H). ^{13}C NMR (101 MHz, $CDCl_3$) δ 151.56, 150.45, 128.34, 119.64, 111.95, 77.08, 40.25.ppm; HRMS (ESI): Calculated for $C_9H_{12}N_2O$ $[M+H]^+$: 165.0950, found 165.1008.

(*Z*)-2-nitrobenzaldehyde oxime (123). Light yellow crystalline solid; yield 598mg, 85%; R*f* 0.4 (20% ethyl acetate : hexane); mp 110-112°C; IR (KBr) υmax (cm^{-1}); 3291, 1570, 1521, 1485, 1447; ^{1}H NMR (400 MHz, $CDCl_3$) δ 8.69 (s, 1H), 8.12 (s, 1H), 8.07 (dd, *J* = 8.2, 1.1 Hz, 1H), 7.92 (dd, *J* = 7.8, 1.5 Hz, 1H), 7.69 – 7.62 (m, 1H), 7.56 (ddd, *J* = 8.2, 7.6, 1.5 Hz, 1H). ^{13}C NMR (101 MHz, $CDCl_3$) δ 147.08, 133.58, 130.44, 128.83, 127.16, 124.88, 77.35, 77.03, 76.72.ppm; HRMS (ESI): Calculated for $C_7H_6N_2O_3$ $[M+H]^+$: 167.0378, found 167.0448.

(Z)-4-nitrobenzaldehyde oxime (124). Light yellow crystalline solid; yield 571mg, 85%; R*f* 0.49 (20% ethyl acetate : hexane); mp 110-112°C; IR (KBr) υmax (cm^{-1});3434, 2056, 1605, 1440, 1350; ^{1}H NMR (400 MHz, $CDCl_3$) δ 8.27 (d, J = 8.6 Hz, 2H), 8.23 (s, 1H), 7.98 (s, 1H), 7.77 (d, J = 8.6 Hz, 2H). ^{13}C NMR (101 MHz, $CDCl_3$) δ 148.51, 148.40, 138.16, 127.68, 124.08, 77.35, 77.03, 76.72.ppm; HRMS (ESI): Calculated for $C_7H_6N_2O_3$ $[M+H]^+$: 167.0378, found 167.0449.

(*Z*)-4-((hydroxyimino) methyl) benzonitrile (125). Bright needle crystalline solid; yield 574mg, 89%; R*f* 0.5 (15% ethyl acetate : hexane); mp 115-117°C; IR (KBr) υmax (cm^{-1}); 3430, 2221, 1655, 1534, 1445, 1258; ^{1}H NMR (400 MHz, DMSO-d_6) δ 11.74 (s, 1H), 8.24 (s, 1H), 7.86 (d, *J* = 6.7 Hz, 2H), 7.78 (d, *J* = 1.7 Hz, 2H). ^{13}C NMR (101 MHz, DMSO-d_6) δ 147.59, 138.08, 133.14, 127.48, 119.17, 111.84, 40.59, 40.38, 40.17, 39.96, 39.75, 39.54, 39.33.ppm; HRMS (ESI): Calculated for $C_7H_6N_2O_3$ $[M+H]^+$: 147.0480, found 147.0514.

(*Z*)-1H-indole-3-carbaldehyde oxime (126). Light yellow solid; yield 359 mg, 85%; R*f* 0.5 (30% ethyl acetate : hexane); mp 200-202°C; IR (KBr) υmax (cm-1); 3400, 1622, 1538, 1457, 1421, 1283; ^{1}H NMR (400 MHz, DMSO-d_6) δ 11.40 (s, 1H), 10.52 (s, 1H), 8.29 (s, 1H), 8.00 (d, *J* = 7.9 Hz, 1H), 7.63 (d, *J* = 2.7 Hz, 1H), 7.45 – 7.41 (m, 1H), 7.20 – 7.15 (m, 1H), 7.13 – 7.07 (m, 1H). ^{13}C NMR (101 MHz, DMSO-d_6) δ 145.09, 137.35, 128.85, 124.71, 122.75, 121.94, 120.50, 112.24, 110.09, 40.59, 40.38, 40.17, 39.97, 39.76, 39.55, 39.34.ppm; HRMS (ESI): Calculated for $C_9H_8N_2O$ $[M+H]^+$: 161.0637, found 161.0687.

(*Z*)- heptanal oxime (127). Isolation condition, Hexane: ethyl acetate (9:1), Liquid; yield 400mg, 46%; R*f* 0.5 (10% ethyl acetate : hexane); IR (KBr) υmax (cm-1); 1612, 1528, 1457, 1411, 1213; ^{1}H NMR (400 MHz, $CDCl_3$) δ 7.95 (s, 1H), 6.72 (t, *J* = 5.5 Hz, 1H), 2.38 (td, *J* = 7.5, 5.5 Hz, 2H), 1.54 – 1.44 (m, 2H), 1.39 – 1.25 (m, 6H), 0.92 – 0.87 (m, 3H). ^{13}C NMR (101 MHz, $CDCl_3$) δ 153.02, 77.34, 77.23, 77.03, 76.71, 31.51, 29.04, 26.02, 24.97, 22.53, 14.03.ppm; HRMS (ESI): Calculated for $C_7H_{15}NO$ $[M+H]^+$: 130.1154, found 130.1187.

5.7. Bioassay:

The RPMI & DMEM media, trypsin, antibiotic-antimycotic (Ab/Am) solution, sodium bicarbonate, HEPES and MTT dye were purchased from Sigma-Aldrich, India. The fetal bovine serum was obtained from Gibco-BRL, India. The 96-well plates, T-25 and T-75 flasks were procured from Nunc, Thermo-Fisher Scientific, and India. DMSO and ethanol were purchased from Merck Pvt. Ltd., India. The compounds were tested against a set of cell lines including MCF-7, A431, A549, PC-3, HepG2, MDAMB-231, L-132, NCIH-520, NCIH-460 procured from the National Centre for Cell Science (NCCS), Pune, India. The anti-proliferative potential of the synthesized compounds was evaluated by employing MTT assay and the experiments were performed by following the method reported previously [39]. In brief, the cells were grown in a CO2 incubator at 37°C and 85% humidity in media supplemented with 1 % Ab/Am and 10 % FBS. Experimentally, the cells were seeded in a 96-well flat bottom plate and incubated for 24h. After incubation, the cells were treated with compounds at different concentrations (0.4-50µg/mL) and further incubated for 24 h.

Table 5.1. IC_{50} (μ Mol) values of synthesized oximes for tested cell lines.

S.No.	A-431	A-549	L-132	NCIH-460	NCIH-520	PC-3	HepG-2	MDA-MB-231	MCF-7
81	-	-	-	-	-	-	-	-	-
109	-	-	-	-	-	-	-	-	-
110	9.11±1.54	22.83±1.52	37.84±1.27	8.63±0.15	19.18±2.99	15.13±2.02	21.02±1.75	23.84±0.50	21.34±1.51
111	-	-	-	-	-	-	-	-	-
112	-	-	-	-	-	-	-	-	-
113	10.24±0.90	12.53±0.96	44.26±0.39	9.42±0.39	16.15±0.69	14.94±0.91	16.44±0.29	17.66±0.67	18.75±3.39
114	-	-	-	-	-	-	-	-	-
115	12.25±0.40	24.49±1.27	28.69±0.86	22.29±1.08	-	18.39±2.10	-	21.76±0.94	23.09±3.73
116	-	-	-	-	-	-	-	-	-
117	-	-	-	-	-	-	-	-	-
118	40.80±1.55	-	-	-	-	-	-	-	-
119	-	-	-	-	-	-	-	-	-
120	-	-	-	-	-	-	-	-	-
121	-	-	-	-	-	-	-	-	-
122	-	-	-	-	-	-	-	-	-
123	-	-	-	-	-	-	-	-	-
Flavanone	-	-	-	-	-	-	-	-	-
Tam.	2.49±0.37	2.28±0.03	9.03±0.38	5.35±0.28	6.37±0.21	2.82±0.11	5.28±0.21	7.82±0.20	2.26±0.19

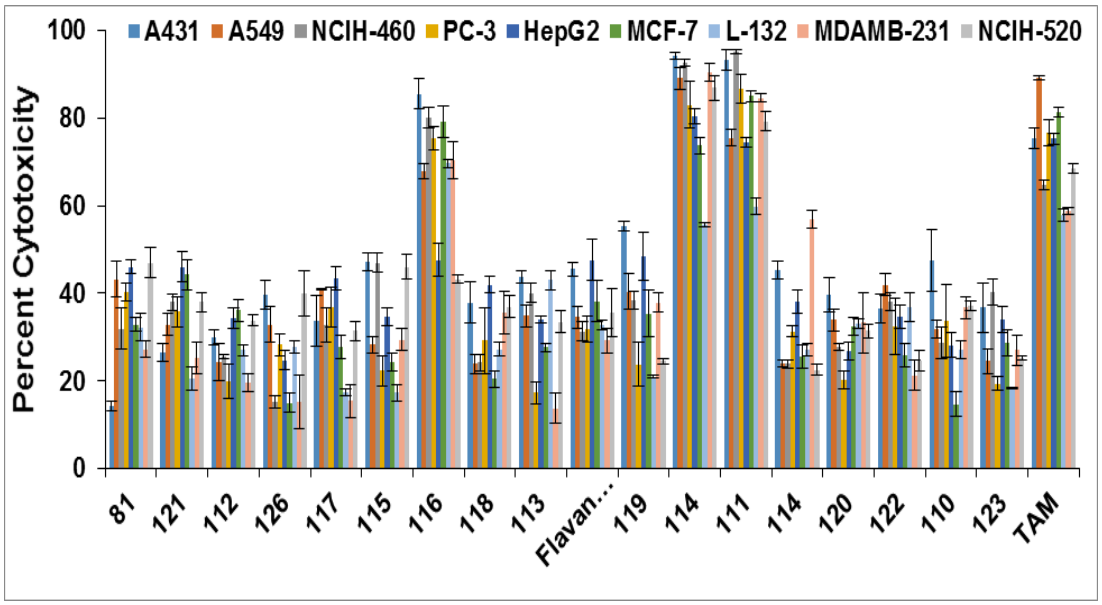

Figure 5.7. Percentage Cytotoxicity of synthetic oximes **(81)....(126)**, flavanone and standard drug tamoxifen.

The MTT dye was added and then plate was incubated for 4 h at 37°C in dark. After that, the dye was removed and DMSO was added to dissolve the formazan crystals followed by recording of absorbance at 570nm. Tamoxifen was used as a standard. The percent cytotoxicity and inhibitory concentration (IC_{50}) was calculated as reported previously [40] (Fig.5.7). Among all the synthesized compounds, compound **(114)** showed maximum growth inhibition in all the tested cancer cell lines (range of IC_{50} 9.42 ± 0.39-18.75 ± 3.39 µg/mL) but it also showed moderate toxicity for normal cell line (L-132) with an IC_{50} value of 44.26 ± 0.39 µg/mL (Table 5.1). Compound **(111)** showed toxicity against all the tested cancer cell lines (range of IC_{50} 8.63 ± 0.15-23.84 ± 0.50 µg/mL) as well as in normal cell line (IC_{50} 37.84 ± 1.27 µg/mL). Compound **(116)** inhibits the growth of skin, lung and breast cancer cell lines (12.25 ± 0.40-24.49 ± 1.27 µg/mL) but slightly altered the growth of the squamous carcinoma and hepatic carcinoma with the percent inhibition of 43.23 ± 1.03 and 47.58 ± 3.68 respectively at the highest tested concentration (50µg/mL).

5.8. Result and Discussion:

We have developed a novel method of synthesis of stereoselective oximes

(mainly *Z* isomer) through direct conversion of substituted aryl/alkyl cyano esters to aryl/alkyl oximes. The alkene-bridged ethyl cyano arylacrylate compounds undergo unexpected C-C bond cleavage with the associated loss of the ethyl cyanoacetate group by Michael addition of hydroxylamine to a benzylidene cyanoacetate followed by a retro Knoevenagel reaction (1, 3 proton shift) without transition-metal catalysis. Besides this the significant advantage of the present method is the formation of stereoselective oximes (Mainly *Z* –form) since this form is known to be biologically active (Scheme 5.10).Substituted aldehydes were condensed with ethyl cyanoacetate (Scheme 5.13) using Sodium ethoxide as catalyst. Different bases were used as standard, but sodium ethoxide was found to give maximum yields under optimal conditions (Table 5.2).

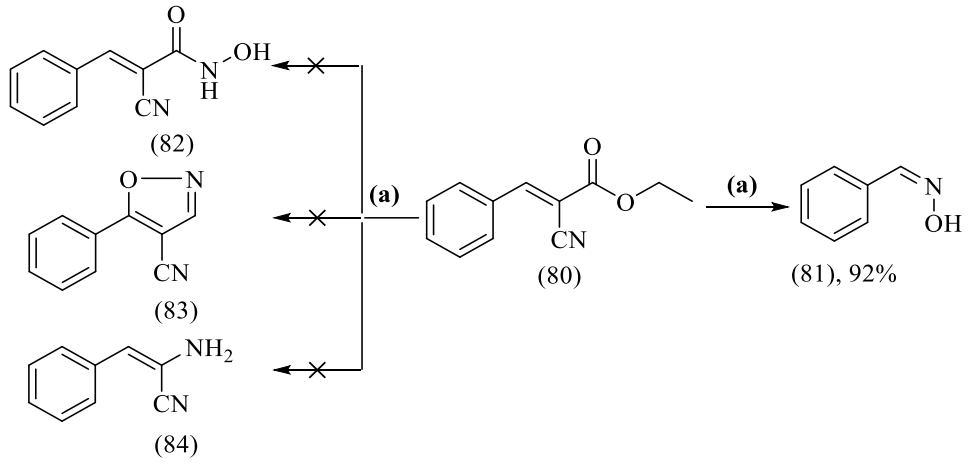

Reagent and condition: (a) $NH_2OH.HCl$, Na_2CO_3, H_2O, MeOH, 100 °C, 1h

Scheme 5.10. Formation of oxime due to C-C bond cleavage.

We wish to highlight our findings on the sodium ethoxide mediated condensation of active methylene group, such as ethyl cyanoacetate and with aromatic, 2 furaldehyde, 1H-indole-3-carbaldehyde and aliphatic aldehydes (isobutyraldehyde). In this study, sodium ethoxide has been employed as a novel, mild and efficient base for carbon-carbon bond formation. Therefore, the reaction with ethyl cyanoacetate in the presence of 20 mol % of sodium ethoxide at 80-90 °C (oil bath temperature) resulted in the formation of ethyl (*E*)-2-cyano-3- phenylacrylate in (78) 94% yield in ethanol.

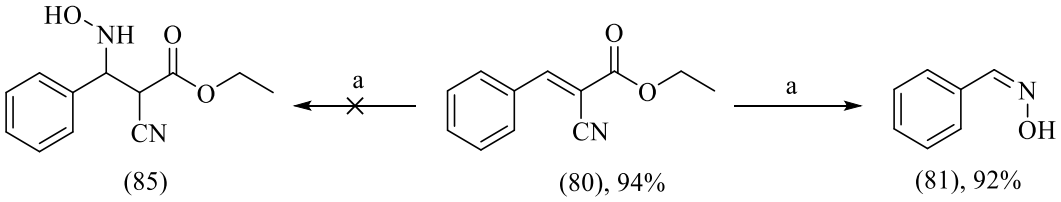

(85) (80), 94% (81), 92%

Reagent and condition: (a) $NH_2OH.HCl$, Na_2CO_3, H_2O, MeOH, 100 °C, 1h.

Scheme 5.11. Unexpected formation of benzyl oxime **(81).**

In a similar method, a wide range of substrates including aromatic, aliphatic and heterocyclic aldehydes i.e. furfural, and indole-3-carboxaldehyde react proficiently with ethyl cycanoacetate under similar reaction conditions to give the corresponding olefins (Scheme 5.13).

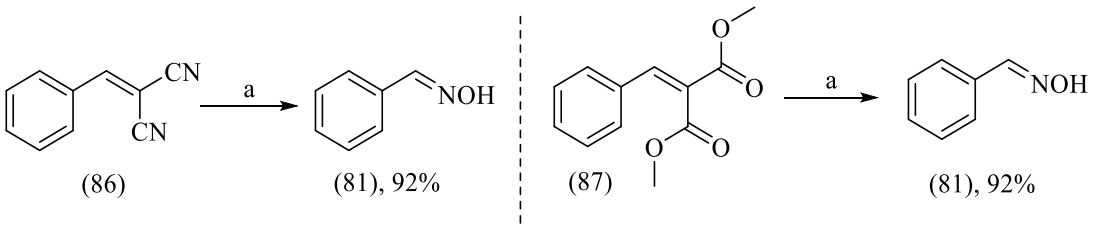

(86) (81), 92% (87) (81), 92%

Reagent and condition: (a)NH_2OH-HCl, Na_2CO_3, Water/MeOH, 100 °C, 1h

Scheme 5.12. Benyloxime **(81)** from benylidene malononitrile **(86)** and dimethyl-2-benzylidene malonate **(87).**

The reaction proceeds smoothly with 20 mol % of sodium ethoxide in ethanol. Sodium ethoxide acts as a base to induce the reaction. The reaction is highly stereoselective, affording α, β-ethylenic compounds in excellent yields, with an *E*-geometry. The progress of these reactions was monitored with ^{1}HNMR. Both electron-rich and electron-deficient aldehydes worked well, giving high yields of products. Electron-deficient aldehydes gave relatively higher yields of olefins than their electron- rich counterparts (Table 5.3).

The comparative yields of olefins from aldehydes were in the following sequence, Aromatic>Heterocyclic>Aliphatic. It is noteworthy to mention that salicylaldehyde afforded the corresponding chrome derivative in 85% yield. In the absence of base, the reaction does not proceed under similar conditions even after a

longer time (~10 h). Furthermore, this method failed to give the desired olefinic products from ethyl cyanoacetate and benzaldehyde. With an increase in reaction temperature to 100 °C, for 1h only **(80)** was isolated. A chemical reaction involving loss of ethyl cyanoacetate group by C−C bond cleavage, by the Michael type addition of hydroxylamine hydrochloride has not been reported previously.

Table 5.2. Optimization of reaction conditions for ethyl (*E*)-2-cyano-3-phenylacrylate **(80)**.

Entry	Base (20 Mol %)	Solvent	Time/h	Temperature ºC	Yield %
1.	Pyridine	MeOH	1	70	30
2.	Pyridine	EtOH	1	80	35
3.	Piperidine	MeOH	1	70	30
4.	Piperidine	EtOH	1	80	40
5.	Triethyl amine	MeOH	1	70	40
6.	Triethyl amine	EtOH	1	80	45
7.	NaOEt	MeOH	1	70	70
8.	**NaOEt**	**EtOH**	**1**	**80**	**94**
9.	*n*-butyl amine	MeOH	1	70	78
10.	*n*-butyl amine	EtOH	1	80	80
11.	NaOEt	Water	1	80	20
12	NaOEt	Water/EtOH	1	80	36
13	NaOMe	EtOH	1	80	88

Another example of electron withdrawing group loss was observed when aqueous hydroxylamine hydrochloride was reacted with other similar substrates (Scheme 5.12). The screening of different solvents revealed that the solvent plays an important role in this reaction. Particularly, methanol: water (9:1) was the only efficient solvent for the formation of oximes, while no reaction occurred in other solvents (Table 5.4, entries, 1– 6). Moreover, the effect of the reaction temperature was also examined, and it was found that a temperature of 100 °C was optimal for this reaction (Table 5.4, entries, and 7–12). Although methanol: water (9:1) was the best choice for this reaction, other solvents such as ethanol: water and DMSO: water were

also effective, however affording the products with slightly reduced yields (Table 5.4, entries 8–12). The Screening of various bases as catalysts (Table 5.5, entries, 1- 7) show that these play an important role in this reaction.

Table 5.3. Synthesized ethyl (*E*)-2-cyano-3-aryl/alkyl acrylate with yield.

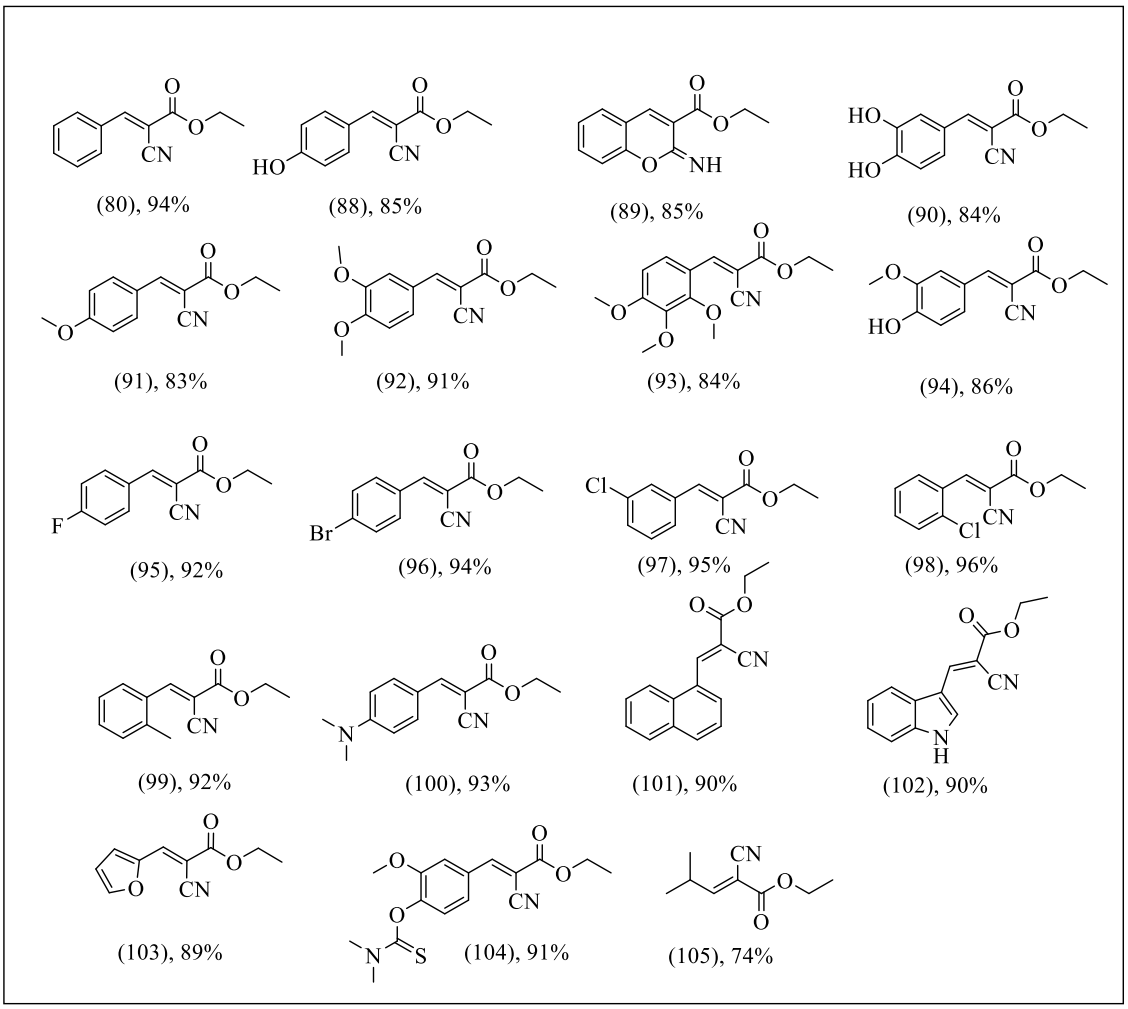

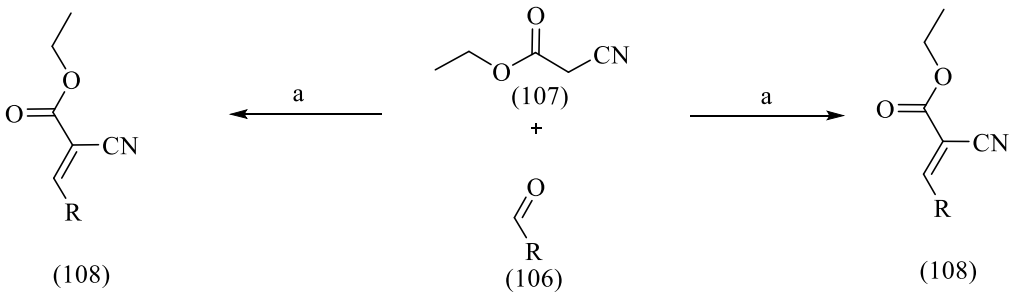

R = Substituted aryl/ furaldehyde,1H-indole-3-carbaldehyde and isobutyraldehyde

Reagent and condition: (a) NaOEt (20 Mol%), EtOH, rt, 3-8 h or EtOH, reflux,1h

Scheme 5.13. Synthesis of ethyl (E)-2-cyano-3-aryl/alkyl acrylate.

Table 5.4. Impact of solvent on yield of oximes.

S. No.	**Base**	**Time (h)**	**Solvent**	**Temperature ^{0}C**	**Yield (%)[b]**
1.	Na_2CO_3	1	MeOH	60	-
2.	Na_2CO_3	1	EtOH	70	-
3.	Na_2CO_3	1	THF	70	-
5.	Na_2CO_3	1	DMF	100	-
6.	Na_2CO_3	1	DMSO	100	-
7.	**Na_2CO_3**	**1**	**MeOH/Water[a]**	**100**	**92**
8.	Na_2CO_3	1	EtOH / Water[a]	100	86
9.	Na_2CO_3	1	THF/Water[a]	100	56
10.	Na_2CO_3	1	DMF/Water[a]	100	57
11.	Na_2CO_3	1	DMSO/Water[a]	100	67
12.	Na_2CO_3	1	Water	100	45
13.	Na_2CO_3	4	MeOH/Water[a]	rt	90

Table 5.5. Impact of base on yield of oximes.

S.No.	**Base**	**Time (h)**	**Temperature (°C)**	**Solvent : water (9:1)**	**Yield (%)**
1.	DABCO	1	100	MeOH : Water	68
2.	TEA	1	100	MeOH : Water	66
3.	K_2CO_3	1	100	MeOH : Water	90
4.	**Na_2CO_3**	**1**	**100**	**MeOH : Water**	**92**
5.	DBU	1	100	MeOH : Water	88
6.	NaOH	1	100	MeOH : Water	75
7.	KOH	1	100	MeOH : Water	74

With the increase of pKa value yield of **(81)** decreased (Table 5.5, entries, 1-7) therefore sodium carbonate and potassium carbonate gave better conversion of stereoselective oximes. Further optimization of the results showed that optimum amount of base i.e. 1.1 equivalent gave (Table 5.5, entries 1–7) excellent yield. Additionally, the reaction was less efficient while proceeding in only water (Table 5.4, entry 12). The scope of reaction was assessed by using other substrates under similar condition (Fig 5.9) to yield corresponding stereoselective oximes (*Z*-isomer) followed by carbon –carbon bond cleavage.

Table 5.6. Synthesized oximes with yield in percentage.

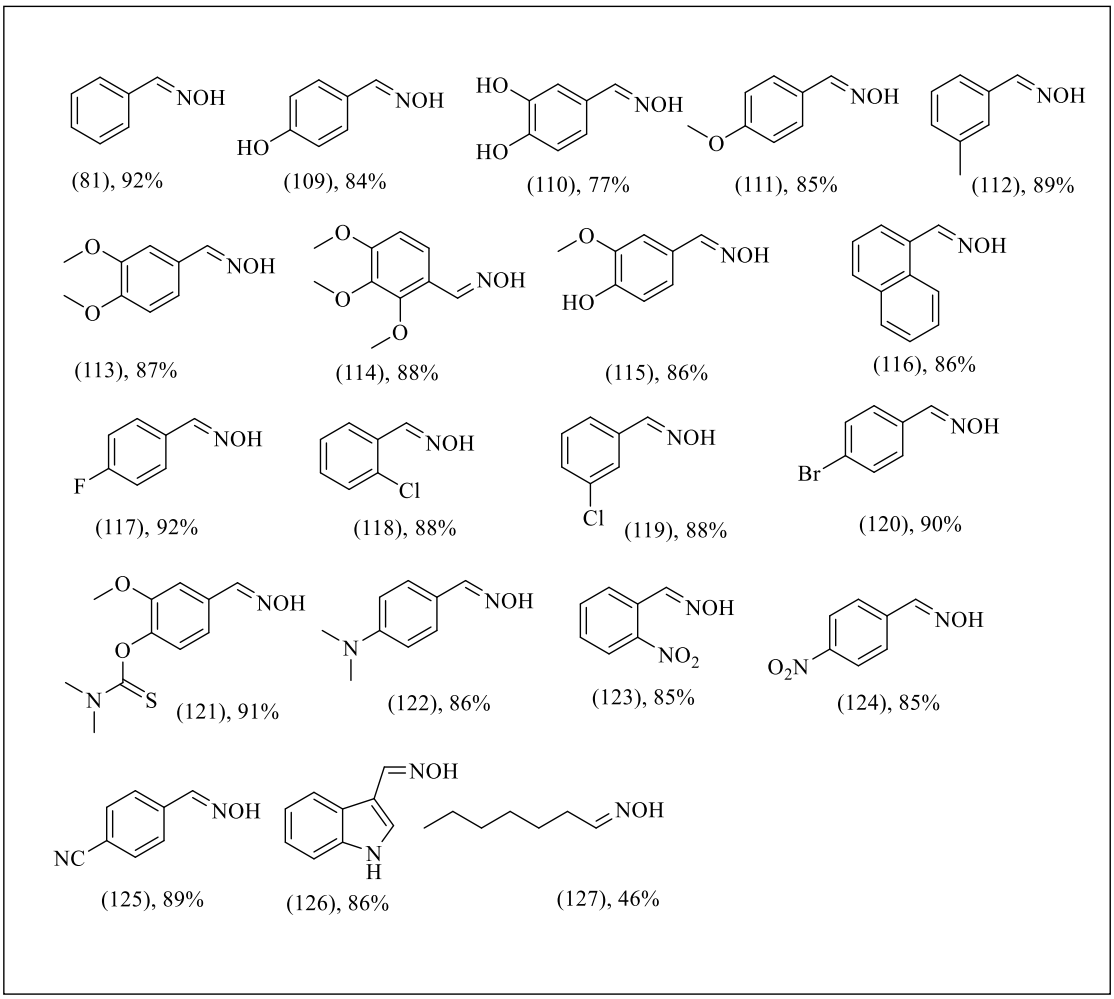

With the optimized conditions in hand, we turned our attention to the scope of the reaction. As summarized in (Table 5.6), a variety of ethyl cyano aryl acrylates were converted to corresponding oximes. The reaction could be successfully applied to a range of different substituted substrates yielding the corresponding oximes in in almost good yields. Ethyl cyano aryl acrylates with either electron-donating or electron withdrawing groups on the benzene ring smoothly generated the corresponding products, however in varying yields. Clearly, electronic effects play an important role, as electron-withdrawing substituents (Table 5.6, **(123)**) on the benzene ring favoured the transformation. Meanwhile, electron donating substituents (Table 5.6, entries **(109)–(115)**, and **(121), (122)**) hindered the transformation. This is evident from the mechanism given in (Scheme 5.14), since electron withdrawing groups will facilitate nucleophilic attack at α-position. The ethyl (E)-2-cyano-3-(4-methoxyphenyl) acrylate substrate gave the two isomeric products, i.e. E isomer

oxime and Z isomer oxime in 90:10 ratio. Both isomers were confirmed by melting points and 1H NMR. Additionally, the reaction conditions were also compatible for fluoro, chloro, and bromo substituents (Table 5.6, entries **(117)–(119)**). The yield was excellent in case of fluorine being in para position of benzene followed by bromine in the same position. With chlorine at either ortho or meta positions (Table 5.6, entries **(118)** and **(119)**), the yield was slightly lower than fluoro /bromo derivatives. This may be due, in part, to steric hindrance. Ethyl (*E*-2-cyano-3- (naphthalen-1-yl) acrylate could also be successfully converted into the corresponding oximes in good yields (Table 5.6, **(116)**).

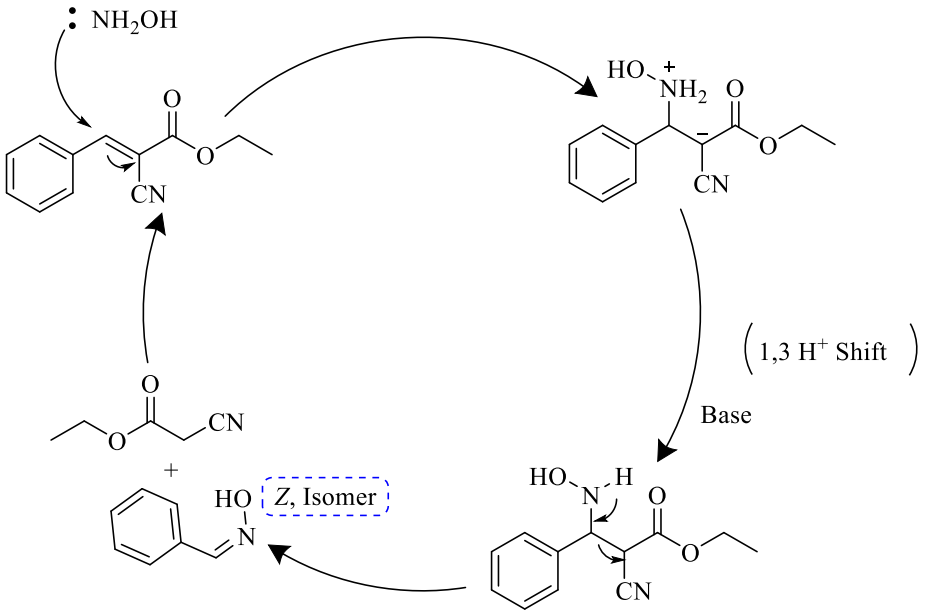

Scheme 5.14. Plausible reaction mechanism of oxime formation.

Moreover, we also conducted the reaction with heterocyclic substrates under the optimized reaction conditions (Table 5.6, **(126)**), with good yields. To our surprise, heterocyclic compounds show high reactivity to give the corresponding oximes in fairly good yields (Table 5.6, **(126)**).However , the yield in case of aliphatic oximes was quite low (See table 5.6 ; **(127)**). To demonstrate the scope and efficiency of the present method, this mild system was then extended for the synthesis of aliphatic oximes. However, we found that the heptyl substrate (Table 5.6, **(127)**) did react and gave very low conversion and amount of yield. In order to check the viability of ethyl cyanoacetate as leaving group we also replaced it with malononitrile

and dimethylmalonate group's .Using optimized reaction conditions we found that both these groups gave comparable yields of benzyl oxime (Scheme 5.12).

5.9. Conclusion:

Eighteen stereoselective aryl/alkyl oximes (*Z*-isomers) were designed and synthesized by a novel method involving an unexpected mild base catalyzed Michael type nucleophilic addition reaction followed with retro-knoevanagel reaction with aqueous hydroxylamine involving C-C bond cleavage in case of α -cyano substituted carbonyl conjugated and other similarly activated alkenes E-olefins. Substituted cyanoacrylate compounds have been prepared through Knoevenagel condensation using sodium ethoxide as an efficient catalyst under mild conditions. This method is applicable to a wide range of aldehydes, including aromatic, aliphatic, α, β-unsaturated and heterocyclic ones. The new procedure involves 1, 3 proton shift, Michael addition type reaction, followed by carbon-carbon bond cleavage resulting in elimination of ethyl cyanoacetate/ malononitrile/ dimethyl malonate. The yields of oximes were in the order heterocyclic>aryl>alkyl. Our new strategy presents one step, time and cost effective cleaner preparation of predominantly *Z* -oximes. These oximes were tested against cancer cell lines MCF-7, A431, A549, PC-3, HepG2, MDAMB-231, L-132, NCIH-520, NCIH-460 .The MTT assay and IC_{50} values indicated that (Z)- 2,3,4-trimethoxybenzaldehyde oxime **(114)** had the maximum antiproliferative activity.

5.10. Spectral Data (^{1}H and ^{13}C):

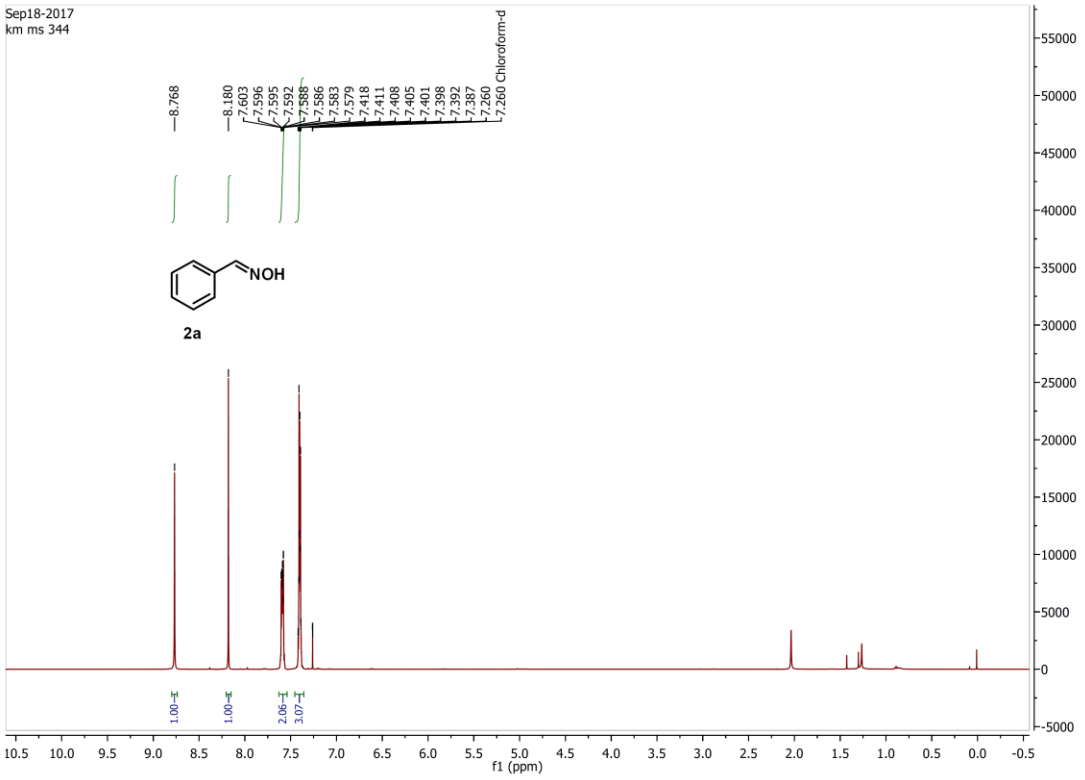

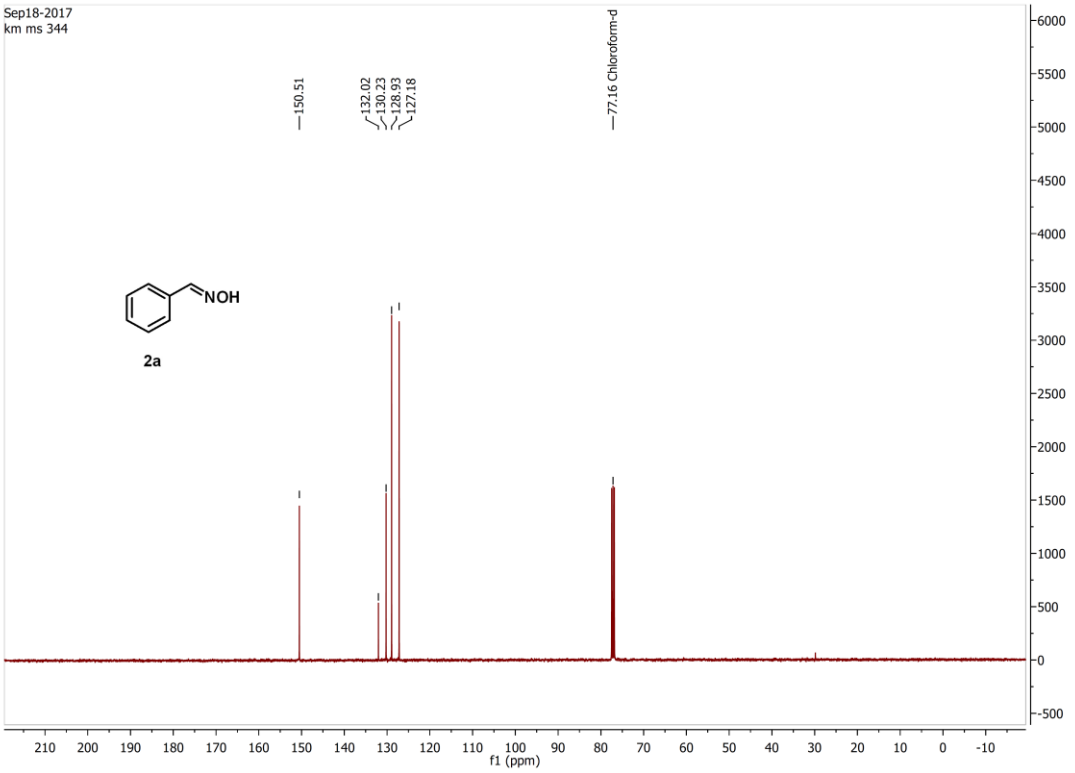

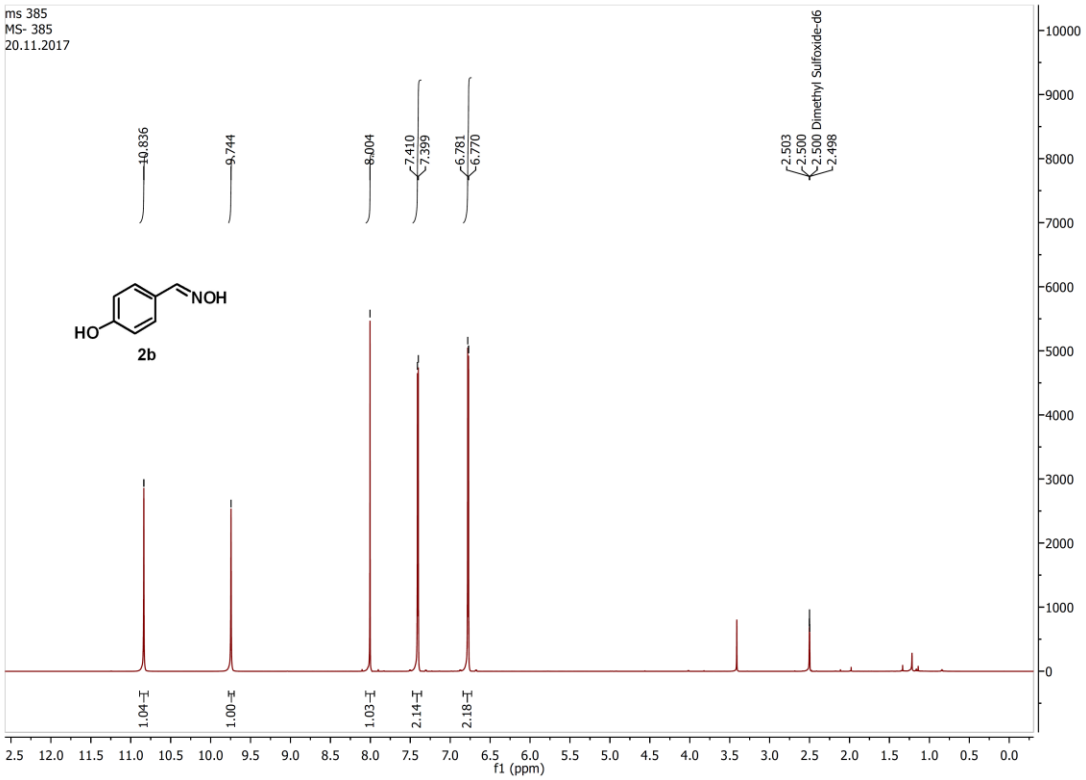
ms 385
MS- 385
20.11.2017
10.836
9.744
8.004
7.410
7.399
6.781
6.770
2.503
2.500
2.500 Dimethyl Sulfoxide-d6
2.498
NOH
HO
2b
1.04
1.00
1.03
2.14
2.18
f1 (ppm)

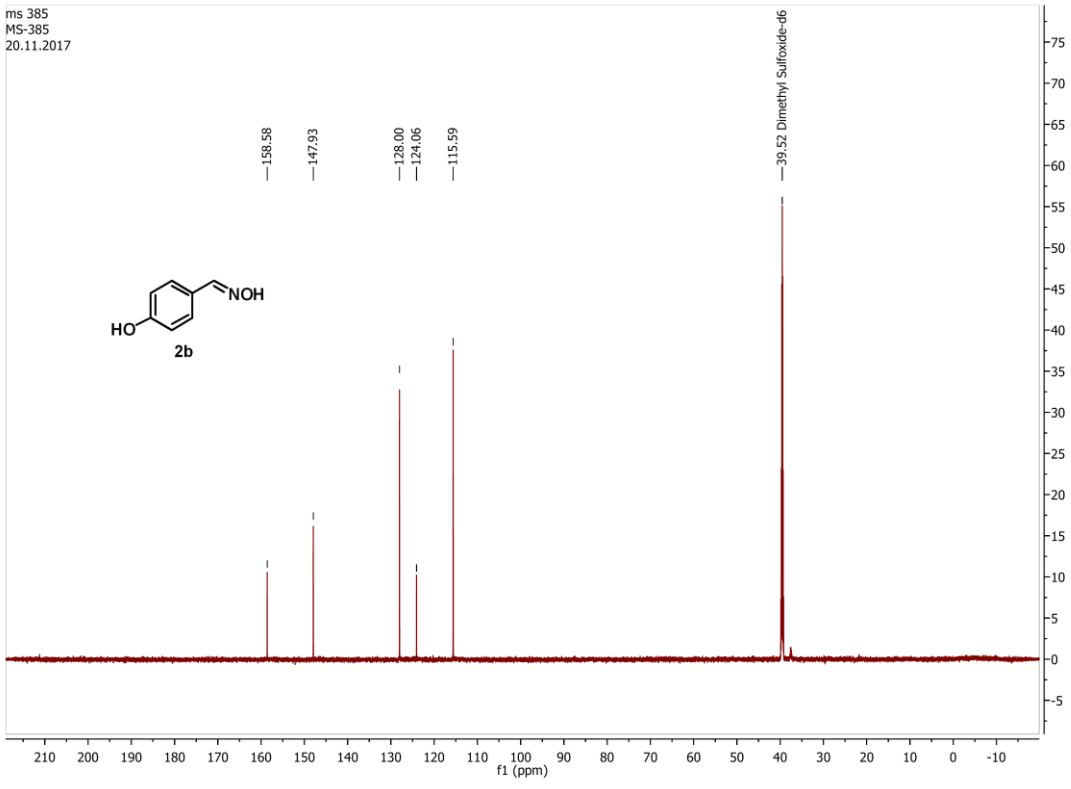
ms 385
MS-385
20.11.2017
158.58
147.93
128.00
124.06
115.59
39.52 Dimethyl Sulfoxide-d6
NOH
HO
2b
f1 (ppm)

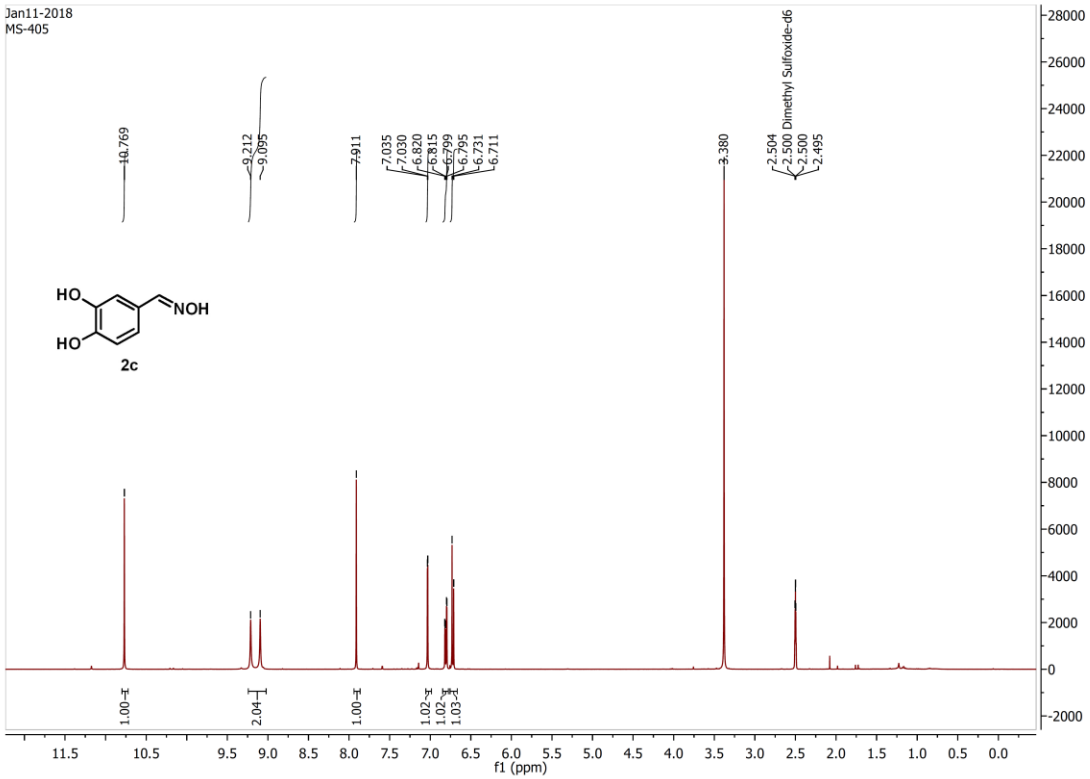
Jan11-2018
MS-405
10.769
9.212
9.095
7.911
7.035
7.030
6.820
6.815
6.799
6.795
6.731
6.711
3.380
2.504
2.500 Dimethyl Sulfoxide-d6
2.500
2.495
HO
HO
NOH
2c
1.00
2.04
1.00
1.02
1.02
1.03
f1 (ppm)

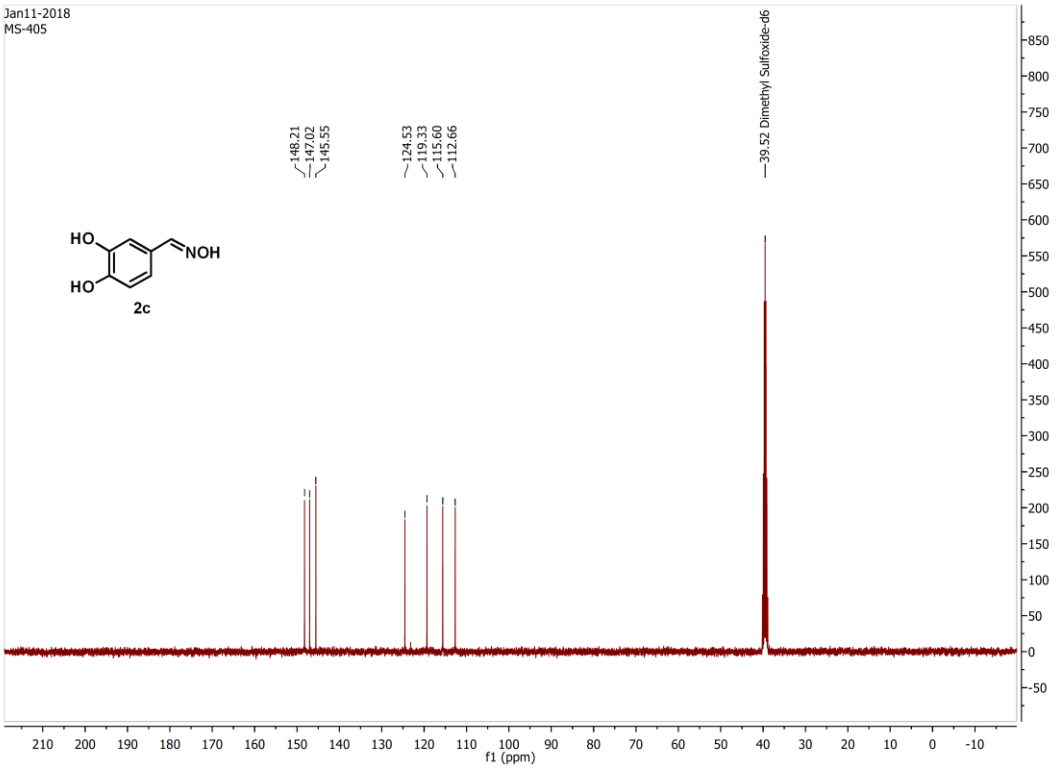
Jan11-2018
MS-405
148.21
147.02
145.55
124.53
119.33
115.60
112.66
39.52 Dimethyl Sulfoxide-d6
HO
HO
NOH
2c
f1 (ppm)

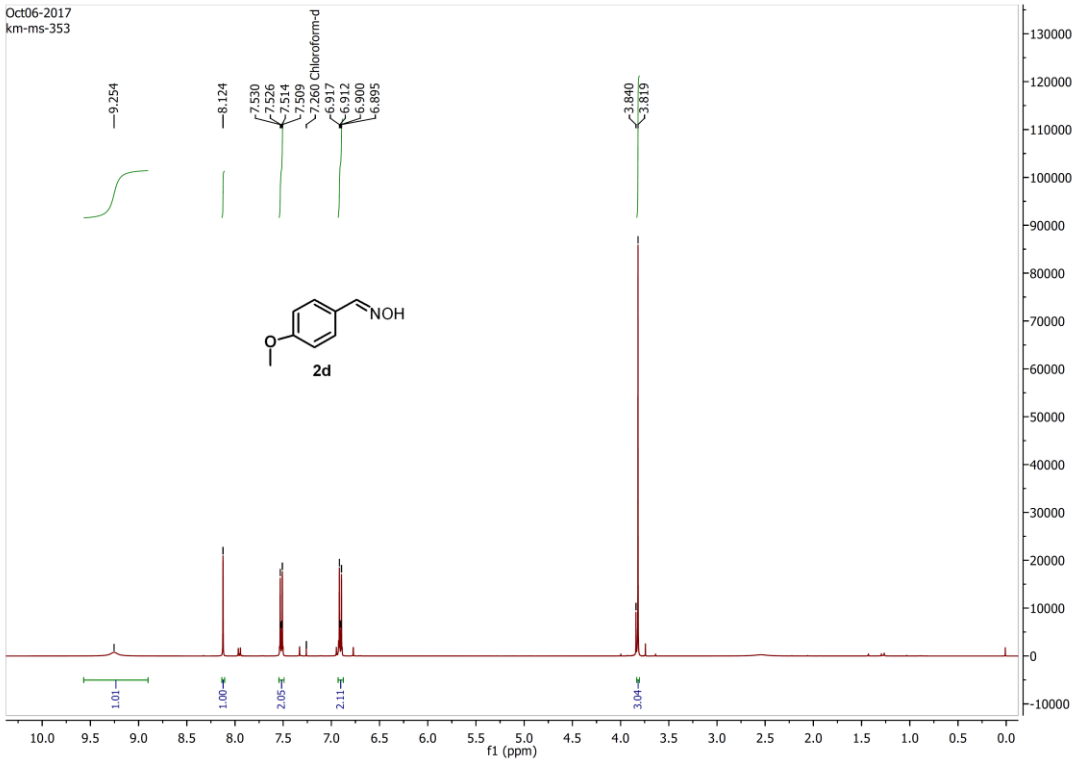
Oct06-2017
km-ms-353
9.254
8.124
7.530
7.526
7.514
7.509
7.260 Chloroform-d
6.917
6.912
6.900
6.895
3.840
3.819
NOH
O
2d
1.01
1.00
2.06
2.11
3.04
f1 (ppm)

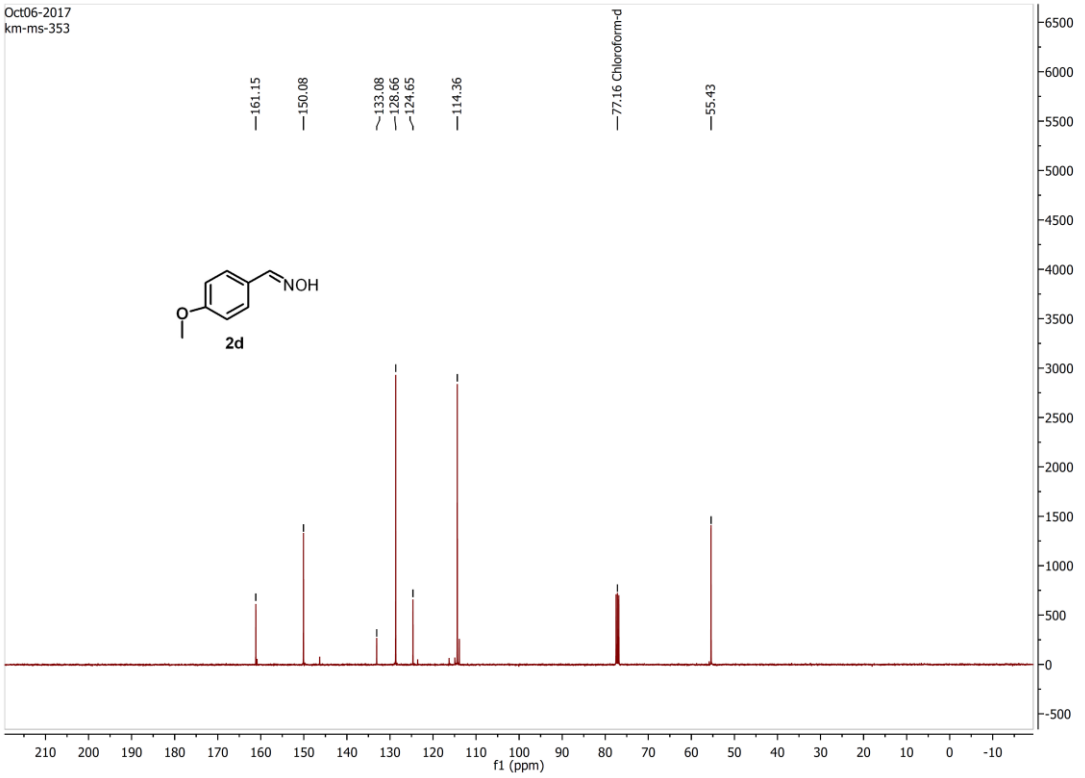
Oct06-2017
km-ms-353
161.15
150.08
133.08
128.66
124.65
114.36
77.16 Chloroform-d
55.43
NOH
O
2d
f1 (ppm)

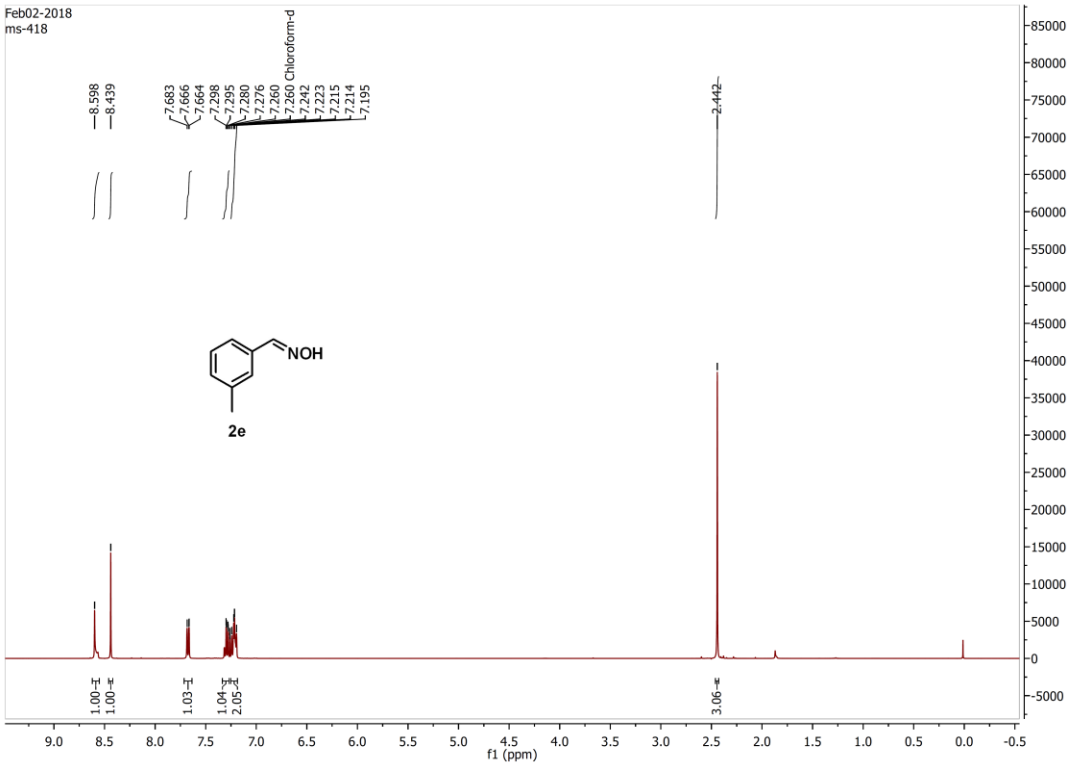
Feb02-2018
ms-418
8.598
8.439
7.683
7.666
7.664
7.298
7.295
7.280
7.276
7.260
7.260 Chloroform-d
7.242
7.223
7.215
7.214
7.195
2.442
NOH
2e
1.00
1.00
1.03
1.04
2.05
3.06
f1 (ppm)

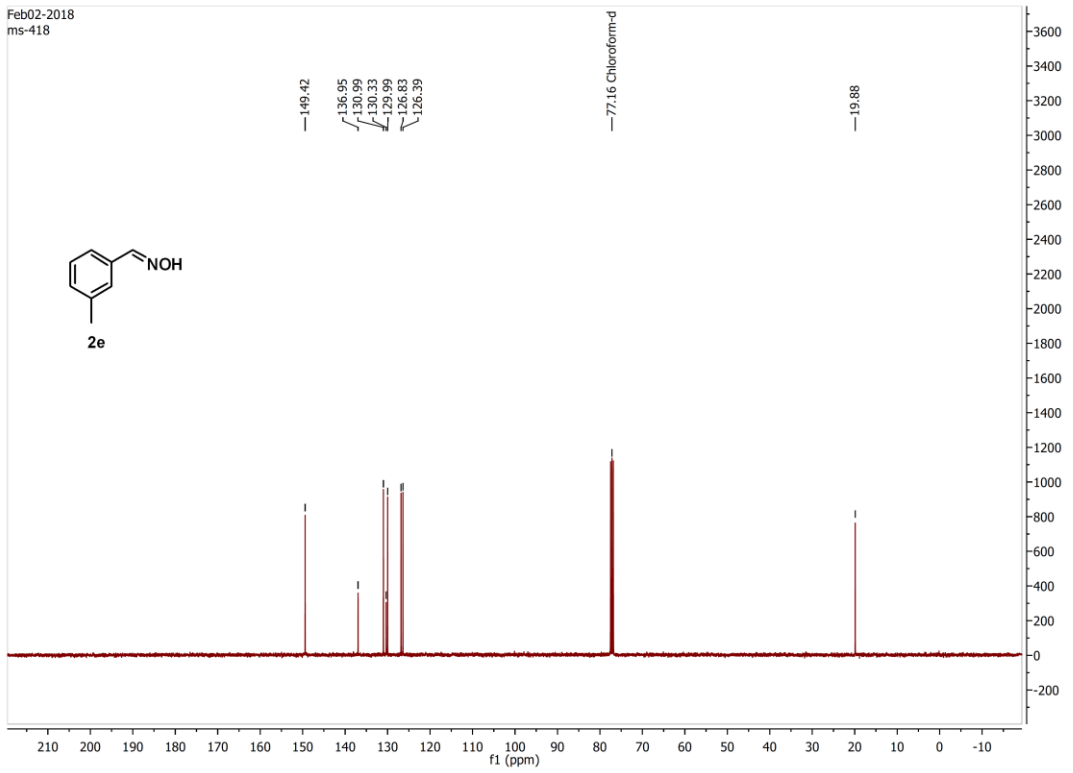
Feb02-2018
ms-418
149.42
136.95
130.99
130.33
129.99
126.83
126.39
77.16 Chloroform-d
19.88
NOH
2e
f1 (ppm)

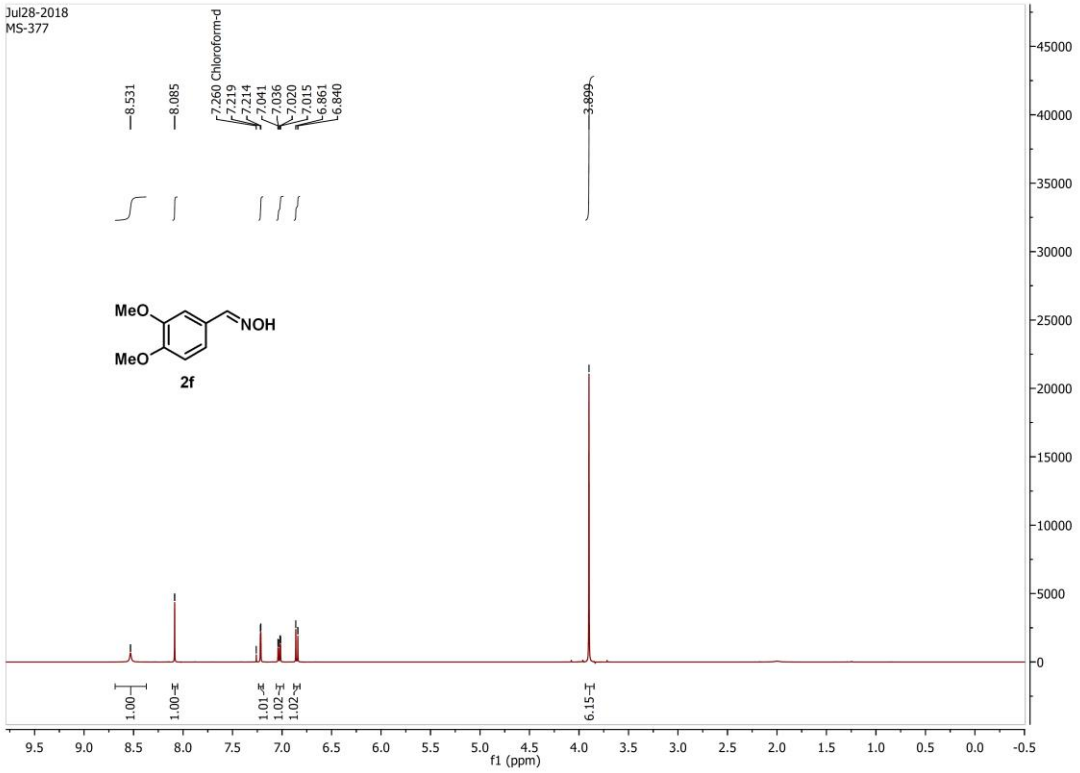
Jul28-2018
MS-377
8.531
8.085
7.260 Chloroform-d
7.219
7.214
7.041
7.036
7.020
7.015
6.861
6.840
3.899
MeO
MeO
NOH
2f
1.00
1.00
1.01
1.02
1.02
6.15
f1 (ppm)

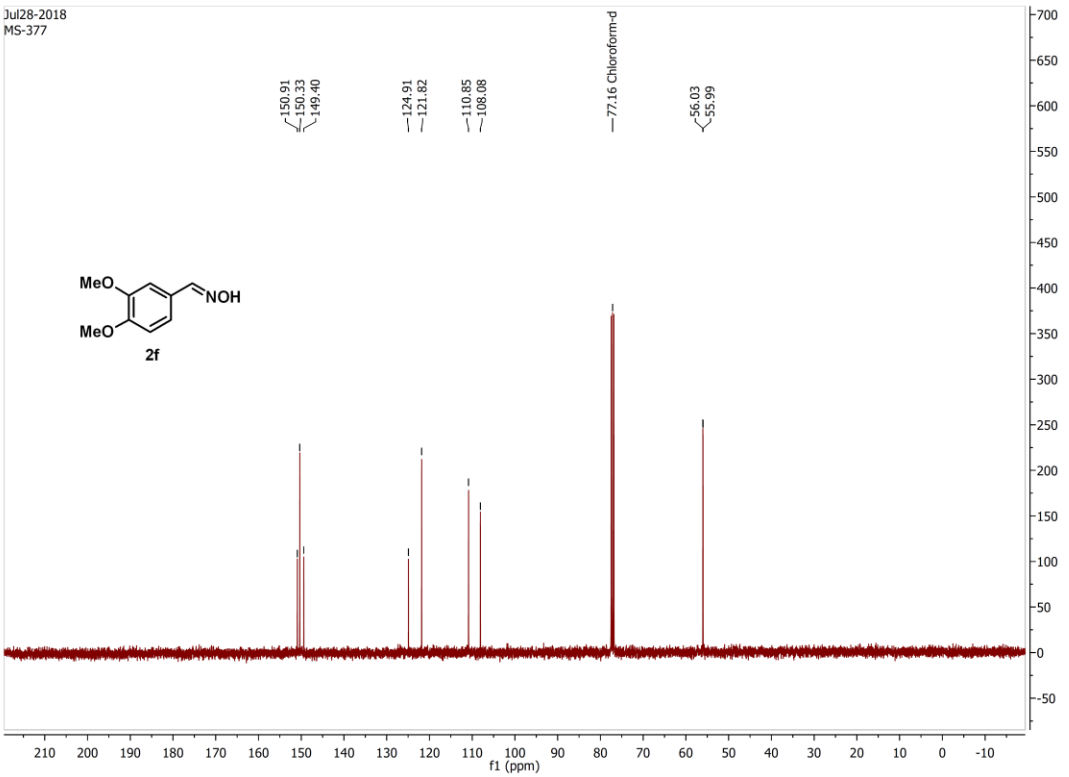
Jul28-2018
MS-377
150.91
150.33
149.40
124.91
121.82
110.85
108.08
77.16 Chloroform-d
56.03
55.99
MeO
MeO
NOH
2f
f1 (ppm)

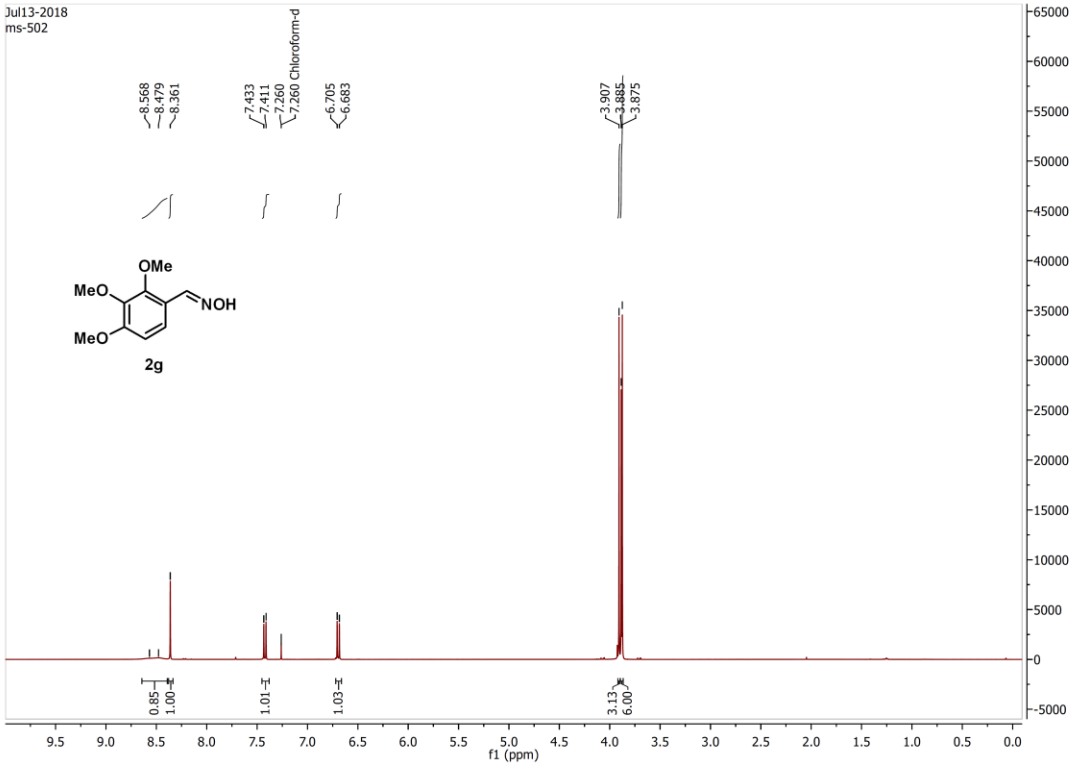
Jul13-2018
ms-502
8.568
8.479
8.361
7.433
7.411
7.260
7.260 Chloroform-d
6.705
6.683
3.907
3.885
3.875
OMe
MeO
MeO
NOH
2g
0.85
1.00
1.01
1.03
3.13
6.00
f1 (ppm)

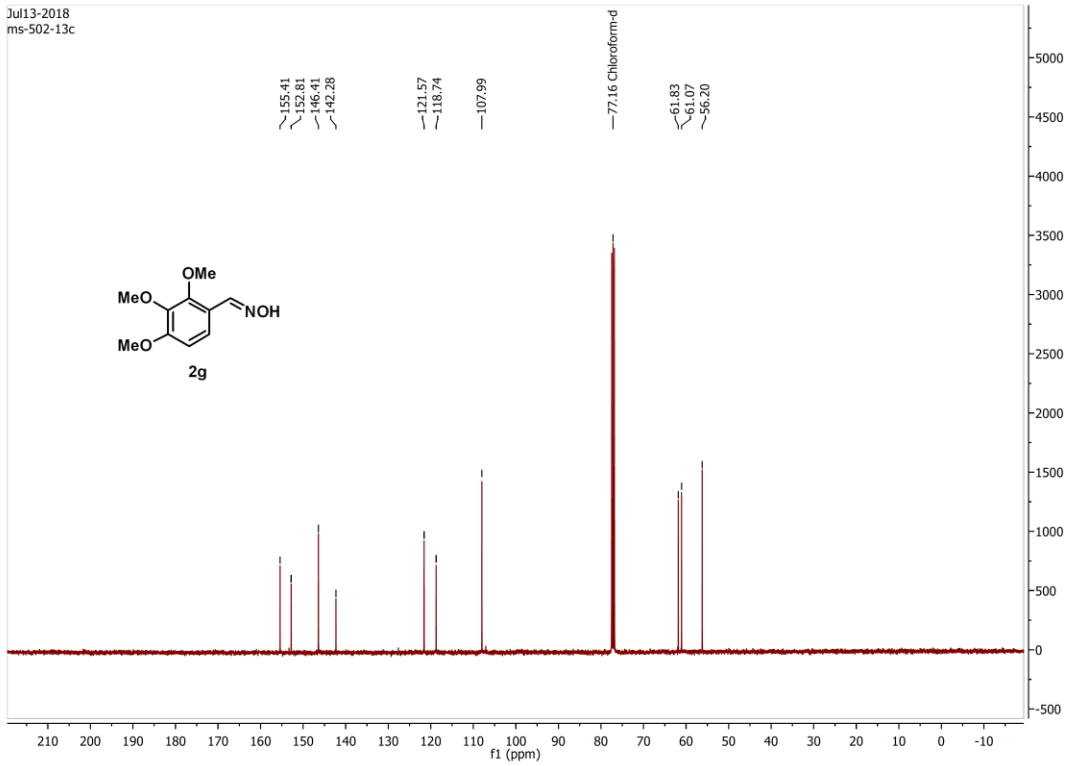
Jul13-2018
ms-502-13c
155.41
152.81
146.41
142.28
121.57
118.74
107.99
77.16 Chloroform-d
61.83
61.07
56.20
OMe
MeO
MeO
NOH
2g
f1 (ppm)

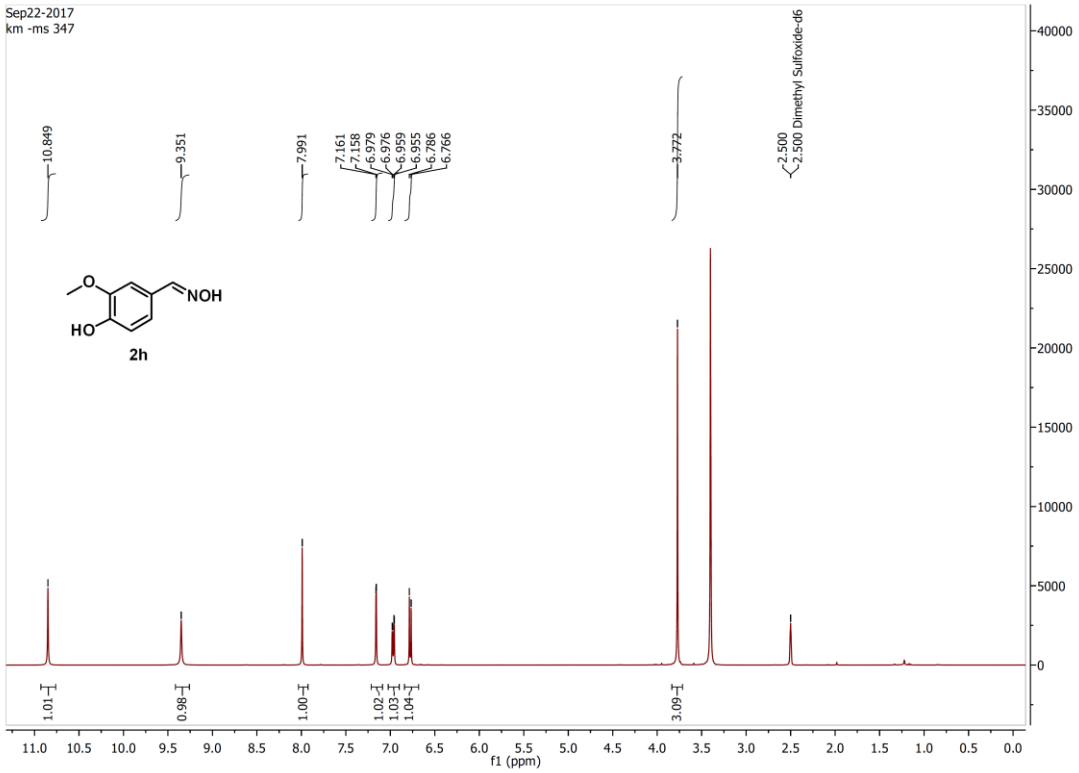
Sep22-2017
km -ms 347
10.849
9.351
7.991
7.161
7.158
6.979
6.976
6.959
6.955
6.786
6.766
3.772
2.500
2.500 Dimethyl Sulfoxide-d6
NOH
HO
O
2h
1.01
0.98
1.00
1.02
1.03
1.04
3.09
f1 (ppm)

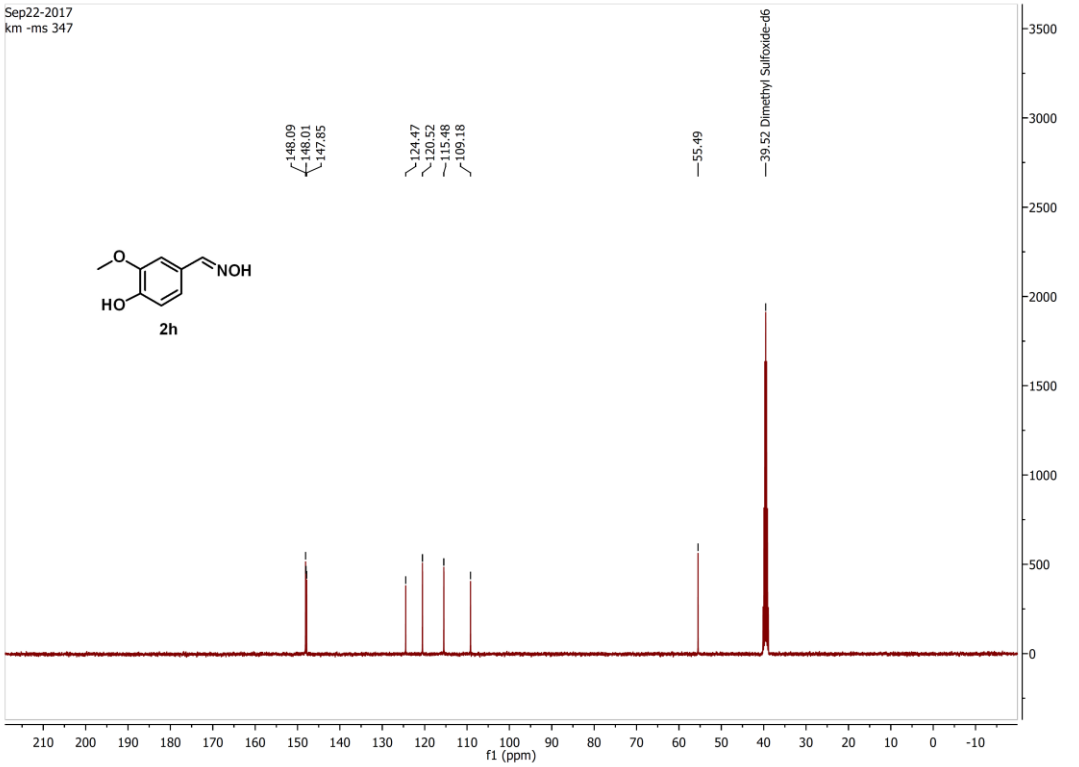
Sep22-2017
km -ms 347
148.09
148.01
147.85
124.47
120.52
115.48
109.18
55.49
39.52 Dimethyl Sulfoxide-d6
NOH
HO
O
2h
f1 (ppm)

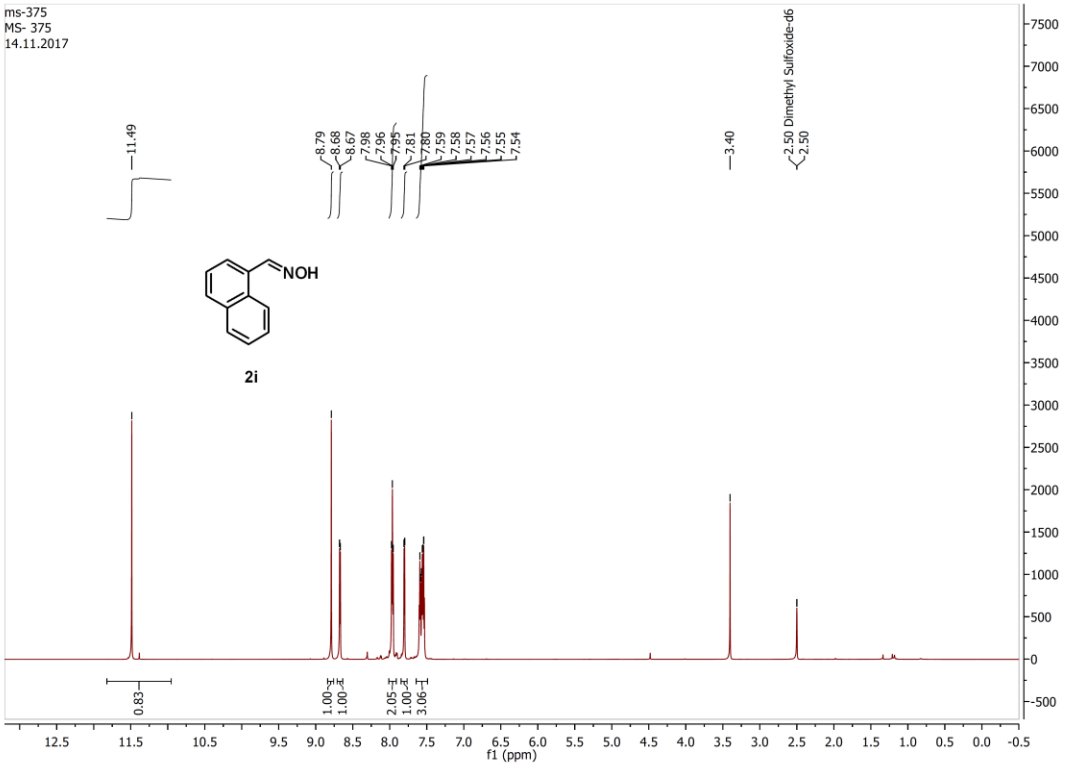
ms-375
MS- 375
14.11.2017
11.49
8.79
8.68
8.67
7.98
7.96
7.95
7.81
7.80
7.59
7.58
7.57
7.56
7.55
7.54
3.40
2.50 Dimethyl Sulfoxide-d6
2.50
NOH
2i
0.83
1.00
1.00
2.05
1.00
3.06
f1 (ppm)

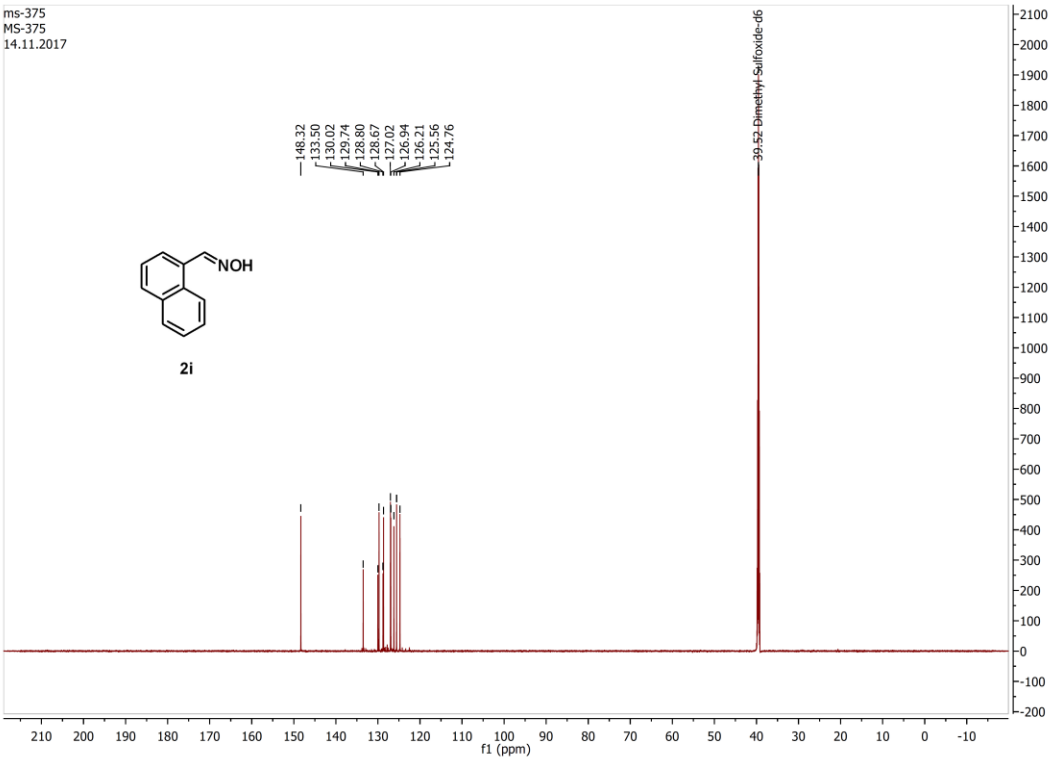
ms-375
MS-375
14.11.2017
148.32
133.50
130.02
129.74
128.80
128.67
127.02
126.94
126.21
125.56
124.76
39.52 Dimethyl Sulfoxide-d6
NOH
2i
f1 (ppm)

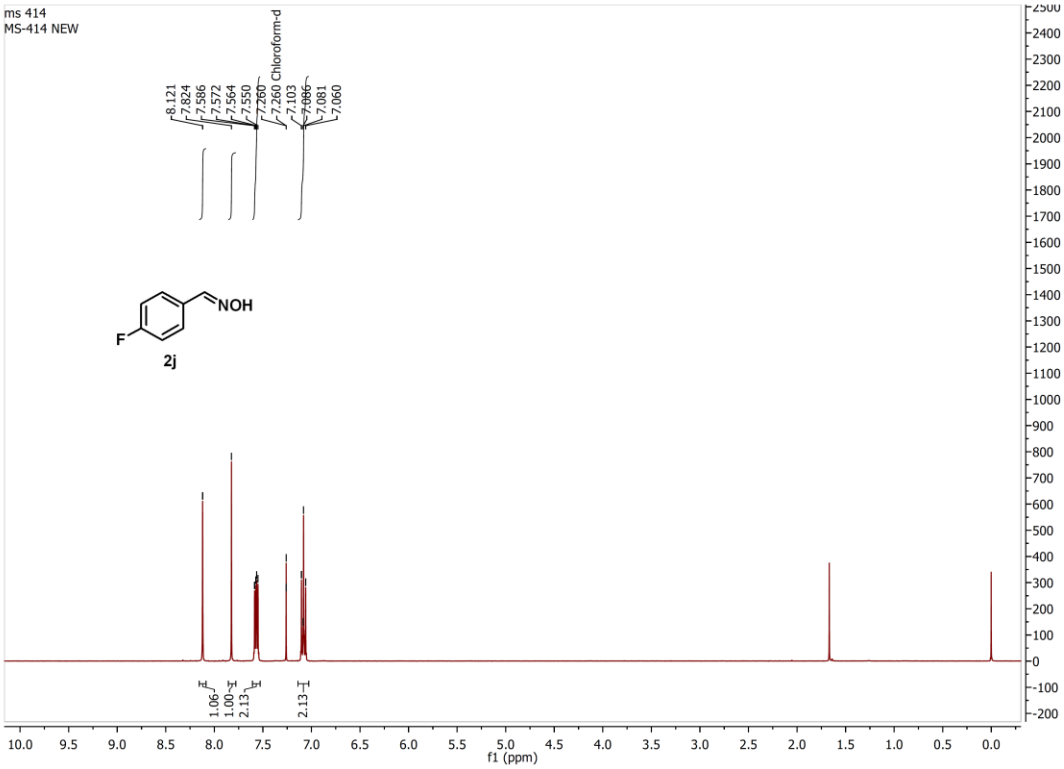
ms 414
MS-414 NEW
8.121
7.824
7.586
7.572
7.564
7.550
7.260
7.260 Chloroform-d
7.103
7.086
7.081
7.060
NOH
F
2j
1.06
1.00
2.13
2.13
f1 (ppm)

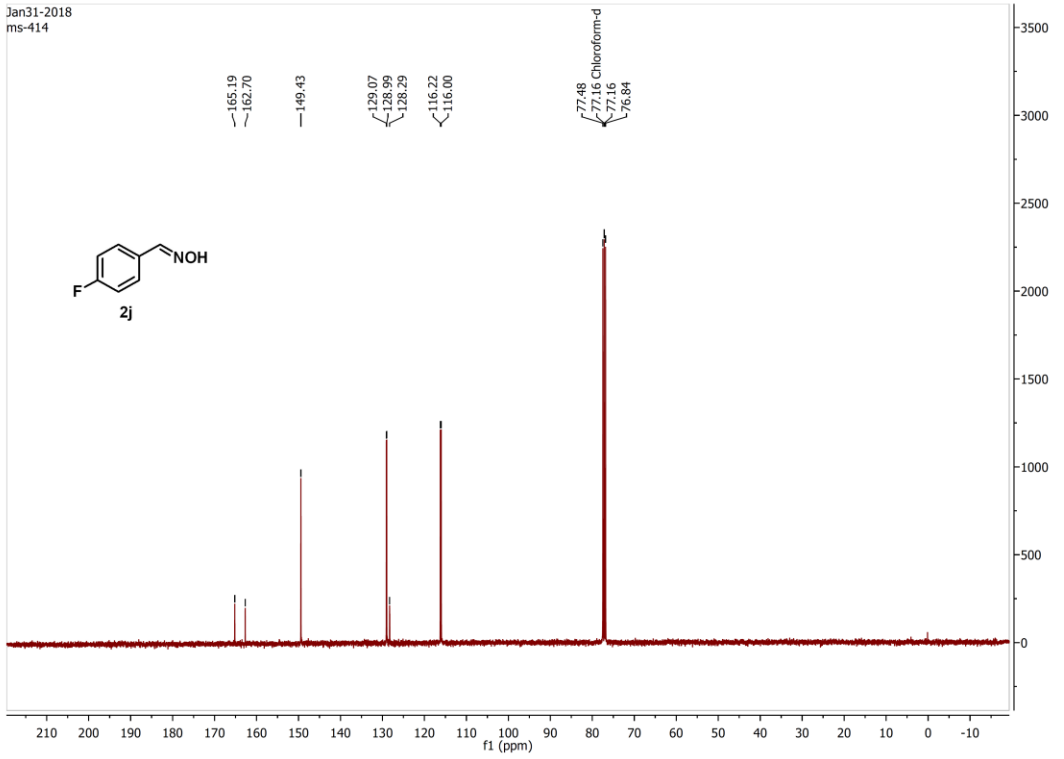
Jan31-2018
ms-414
165.19
162.70
149.43
129.07
128.99
128.29
116.22
116.00
77.48
77.16 Chloroform-d
77.16
76.84
NOH
F
2j
f1 (ppm)

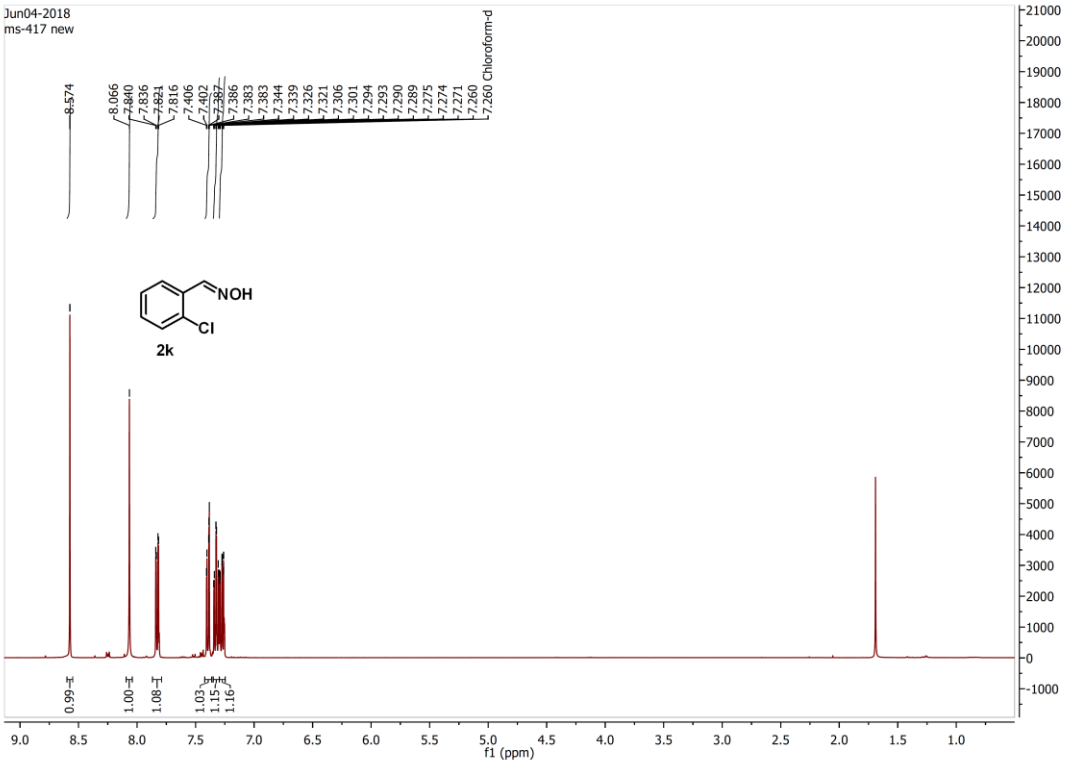
Jun04-2018
ms-417 new
8.574
8.066
7.840
7.836
7.821
7.816
7.406
7.402
7.387
7.386
7.383
7.344
7.339
7.326
7.321
7.306
7.301
7.294
7.293
7.290
7.289
7.275
7.274
7.271
7.260
7.260 Chloroform-d
NOH
Cl
2k
0.99
1.00
1.08
1.03
1.15
1.16
f1 (ppm)

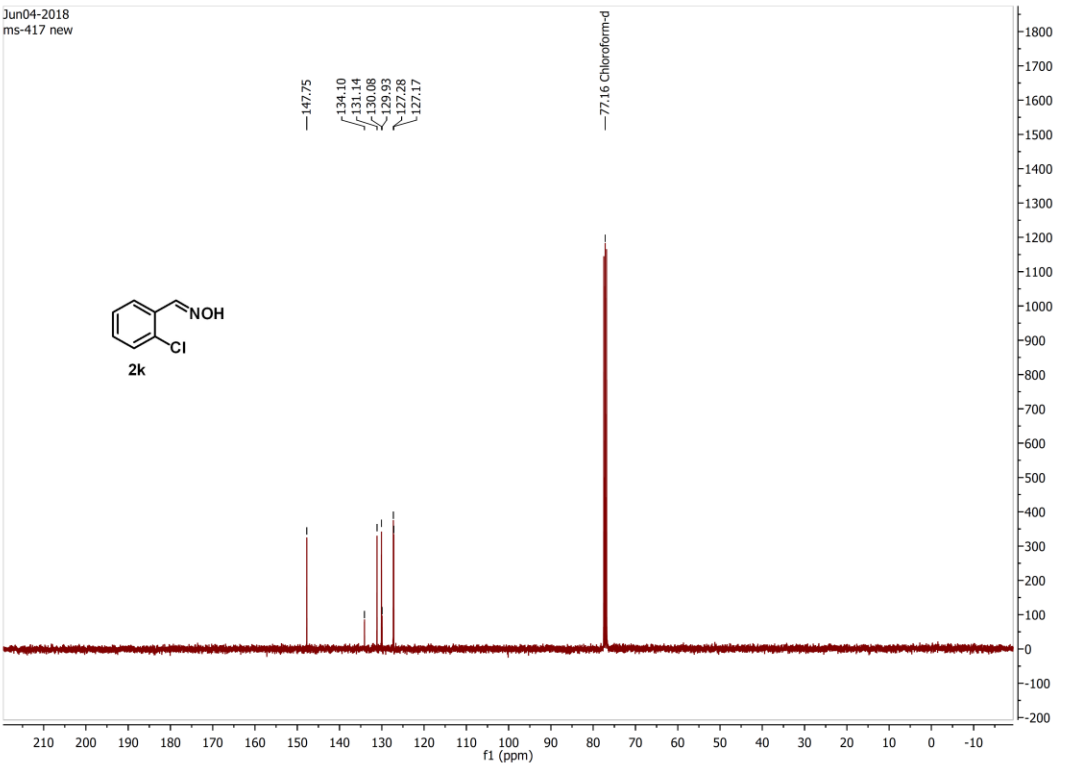
Jun04-2018
ms-417 new
147.75
134.10
131.14
130.08
129.93
127.28
127.17
77.16 Chloroform-d
NOH
Cl
2k
f1 (ppm)

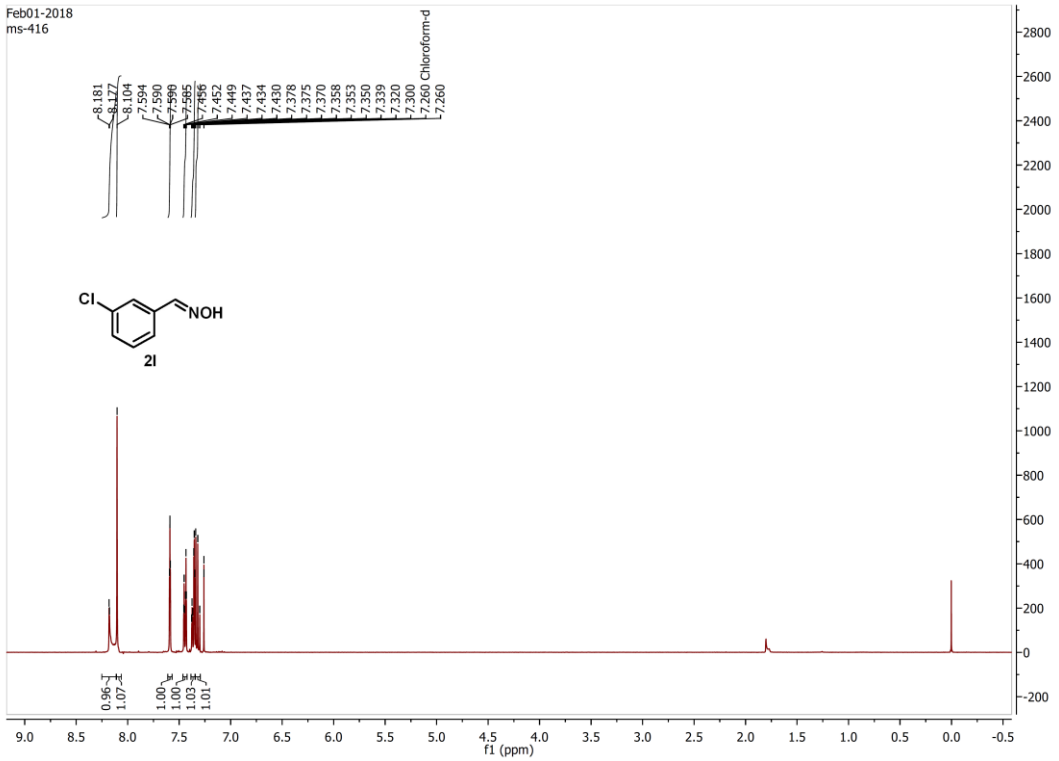
Feb01-2018
ms-416
8.181
8.177
8.104
7.594
7.590
7.590
7.585
7.456
7.452
7.449
7.437
7.434
7.430
7.378
7.375
7.370
7.358
7.353
7.350
7.339
7.320
7.300
7.260 Chloroform-d
7.260
Cl
NOH
2l
0.96
1.07
1.00
1.00
1.03
1.01
f1 (ppm)

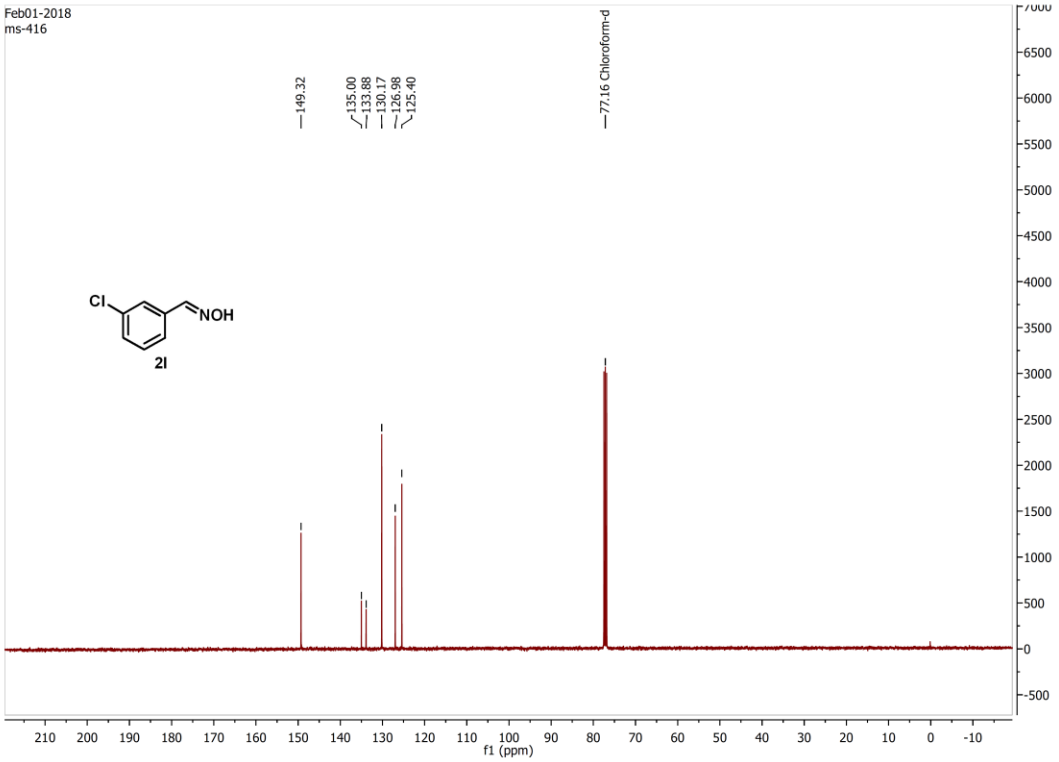
Feb01-2018
ms-416
149.32
135.00
133.88
130.17
126.98
125.40
77.16 Chloroform-d
Cl
NOH
2l
f1 (ppm)

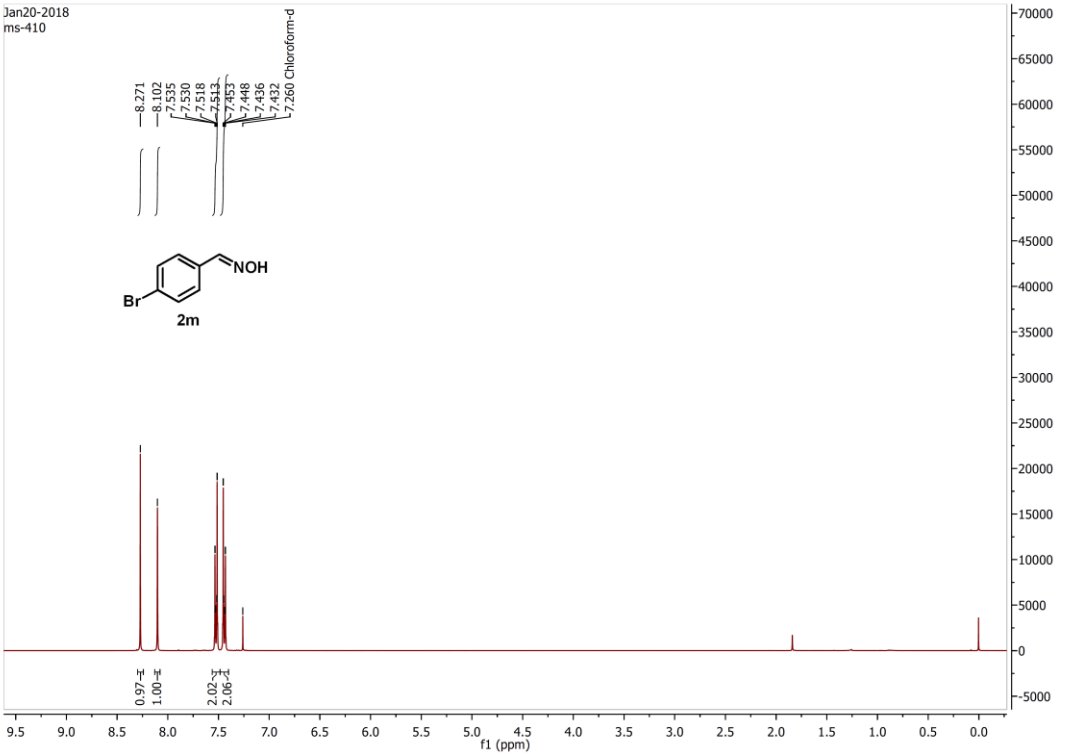
Jan20-2018
ms-410
8.271
8.102
7.535
7.530
7.518
7.513
7.453
7.448
7.436
7.432
7.260 Chloroform-d
NOH
Br
2m
0.97
1.00
2.02
2.06
f1 (ppm)

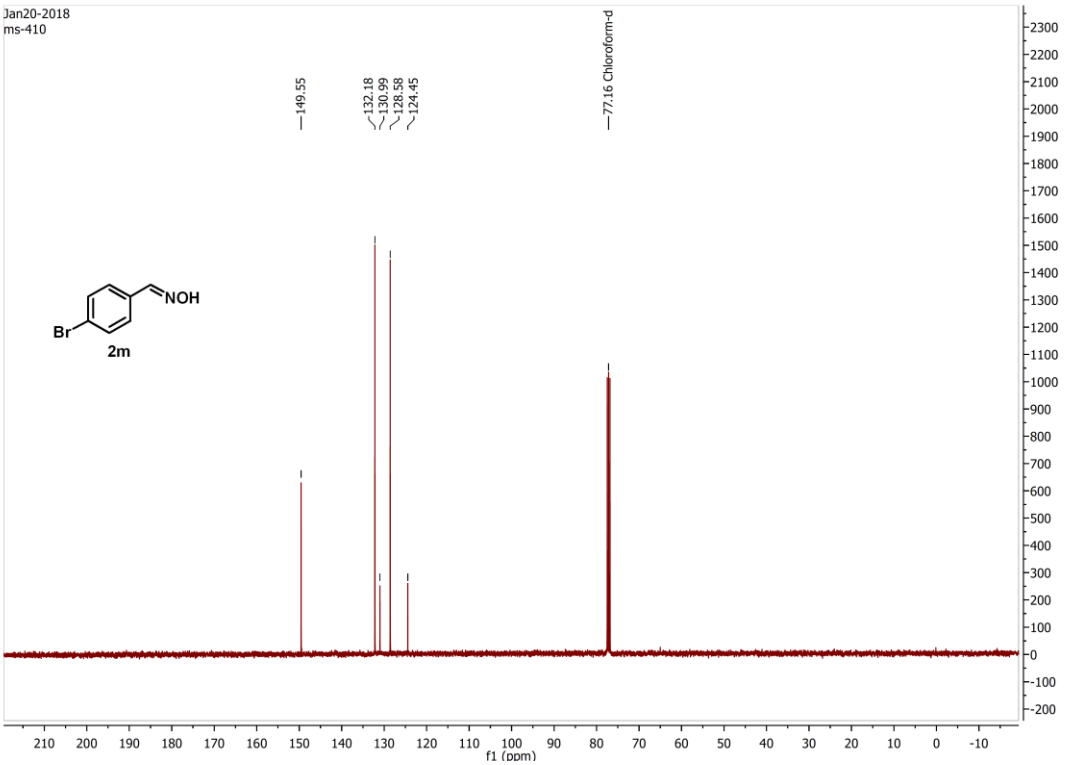
Jan20-2018
ms-410
149.55
132.18
130.99
128.58
124.45
77.16 Chloroform-d
NOH
Br
2m
f1 (ppm)

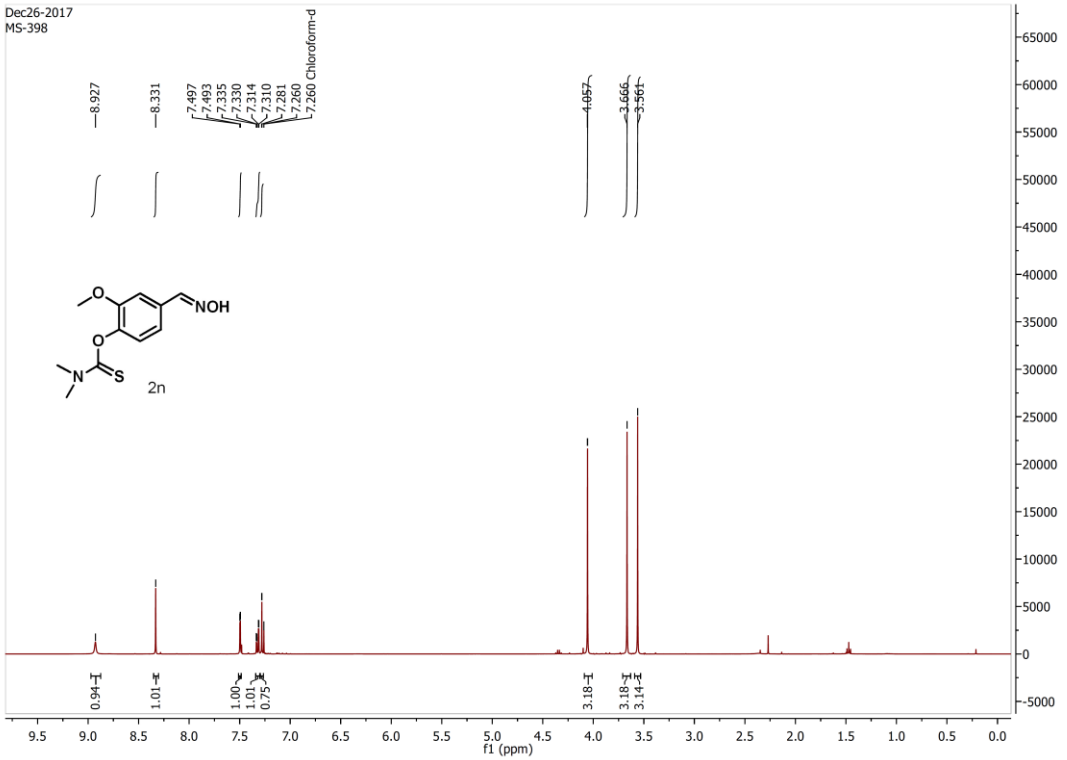
Dec26-2017
MS-398
8.927
8.331
7.497
7.493
7.335
7.330
7.314
7.310
7.281
7.260
7.260 Chloroform-d
4.057
3.666
3.561
NOH
O
O
N
S
2n
0.94
1.01
1.00
1.01
0.75
3.18
3.18
3.14
f1 (ppm)

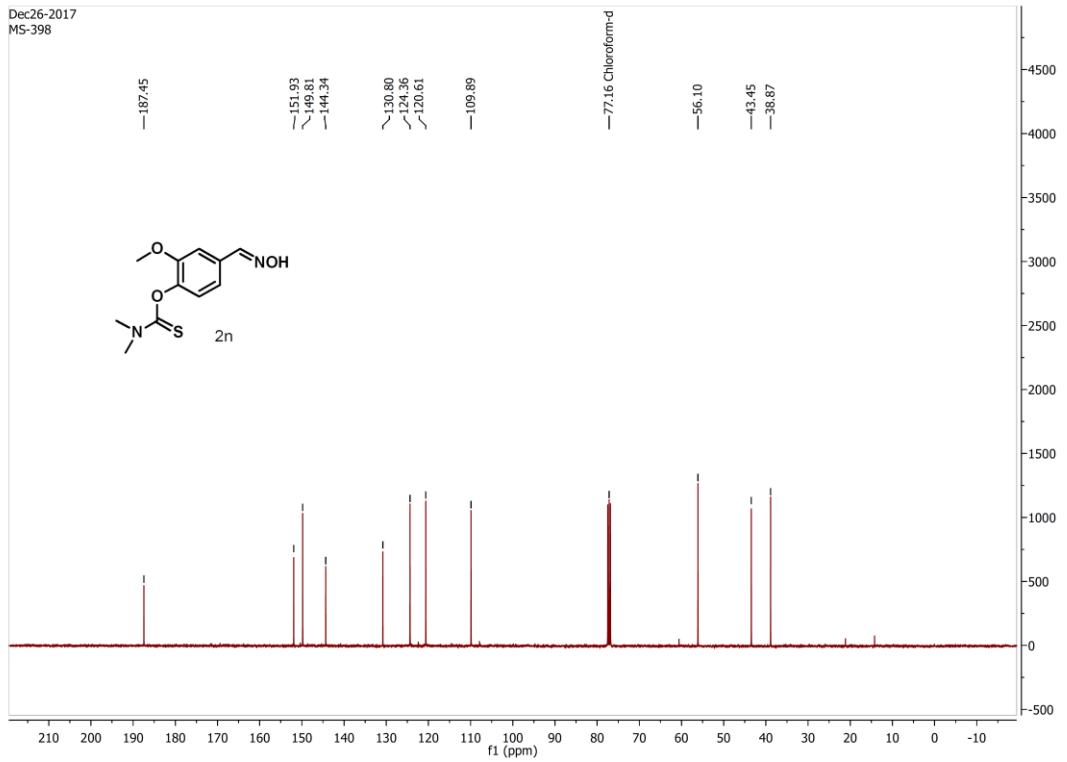
Dec26-2017
MS-398
187.45
151.93
149.81
144.34
130.80
124.36
120.61
109.89
77.16 Chloroform-d
56.10
43.45
38.87
NOH
O
O
N
S
2n
f1 (ppm)

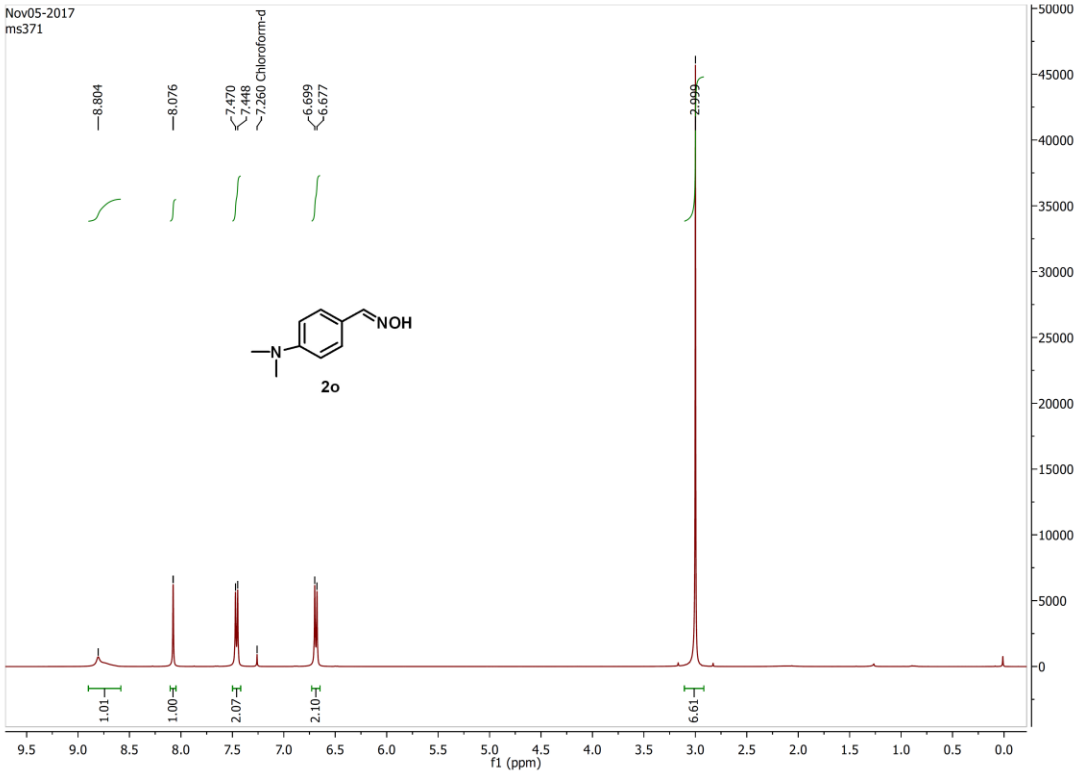
Nov05-2017
ms371
8.804
8.076
7.470
7.448
7.260 Chloroform-d
6.699
6.677
2.999
NOH
N
2o
1.01
1.00
2.07
2.10
6.61
f1 (ppm)

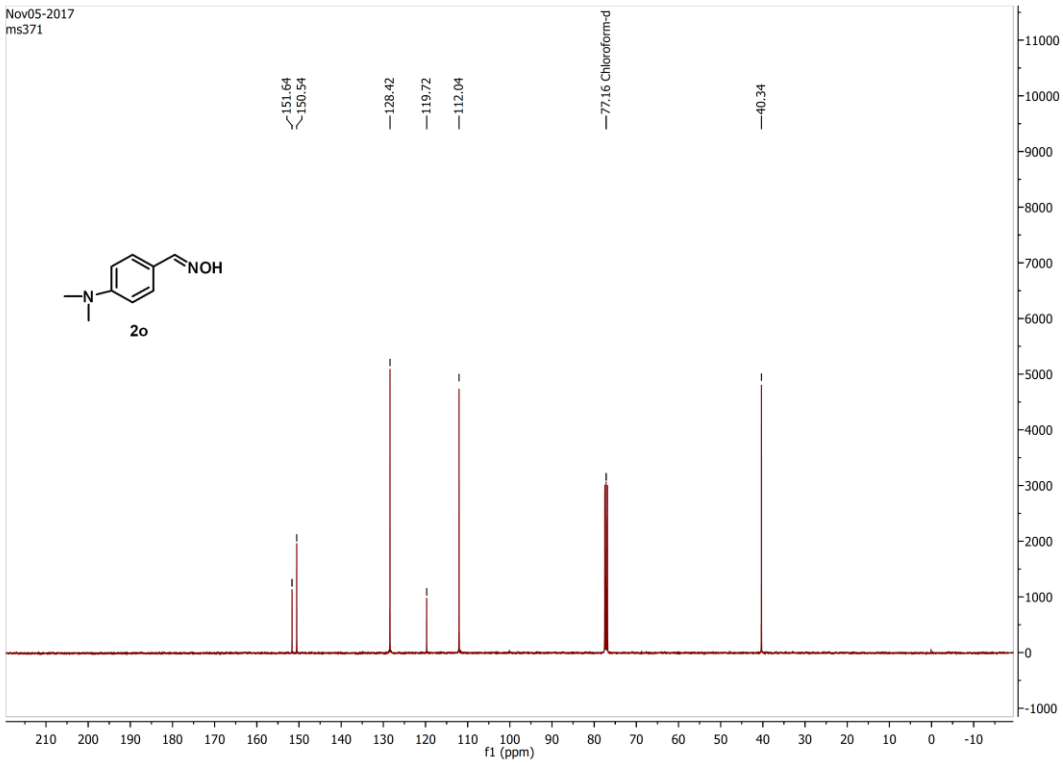
Nov05-2017
ms371
151.64
150.54
128.42
119.72
112.04
77.16 Chloroform-d
40.34
NOH
N
2o
f1 (ppm)

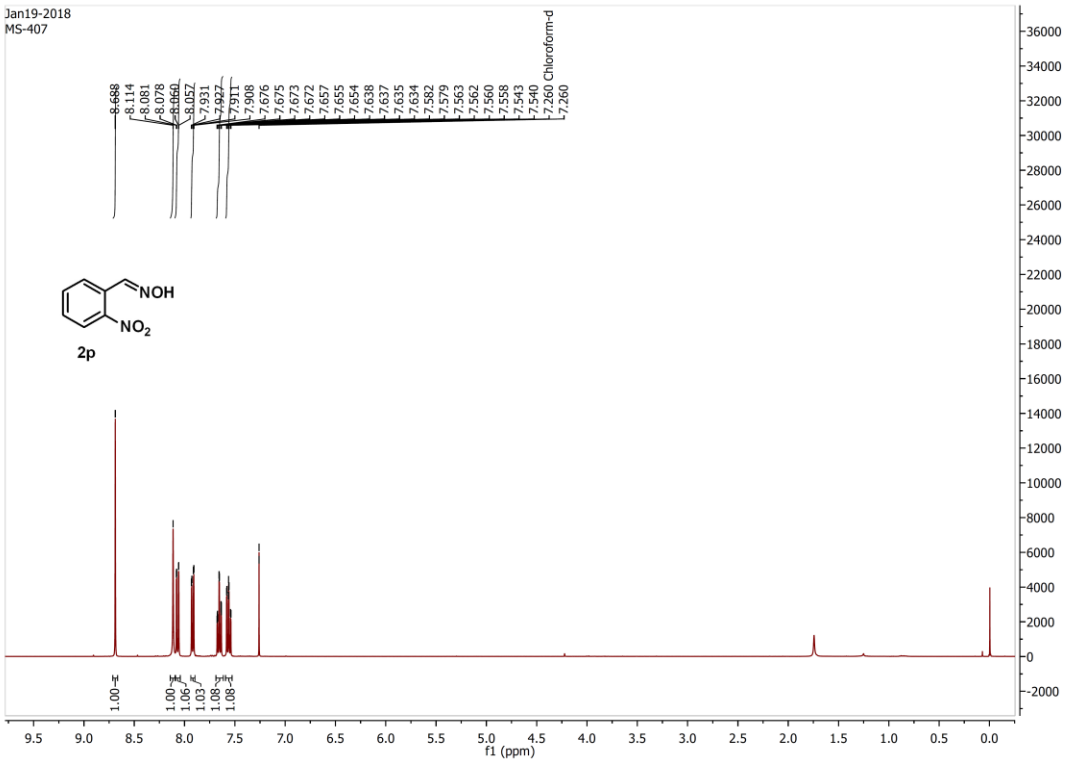
Jan19-2018
MS-407
8.688
8.114
8.081
8.078
8.060
8.057
7.931
7.927
7.911
7.908
7.676
7.675
7.673
7.672
7.657
7.655
7.654
7.638
7.637
7.635
7.634
7.582
7.579
7.563
7.562
7.560
7.558
7.543
7.540
7.260 Chloroform-d
7.260
NOH
NO2
2p
1.00
1.00
1.06
1.03
1.08
1.08
f1 (ppm)

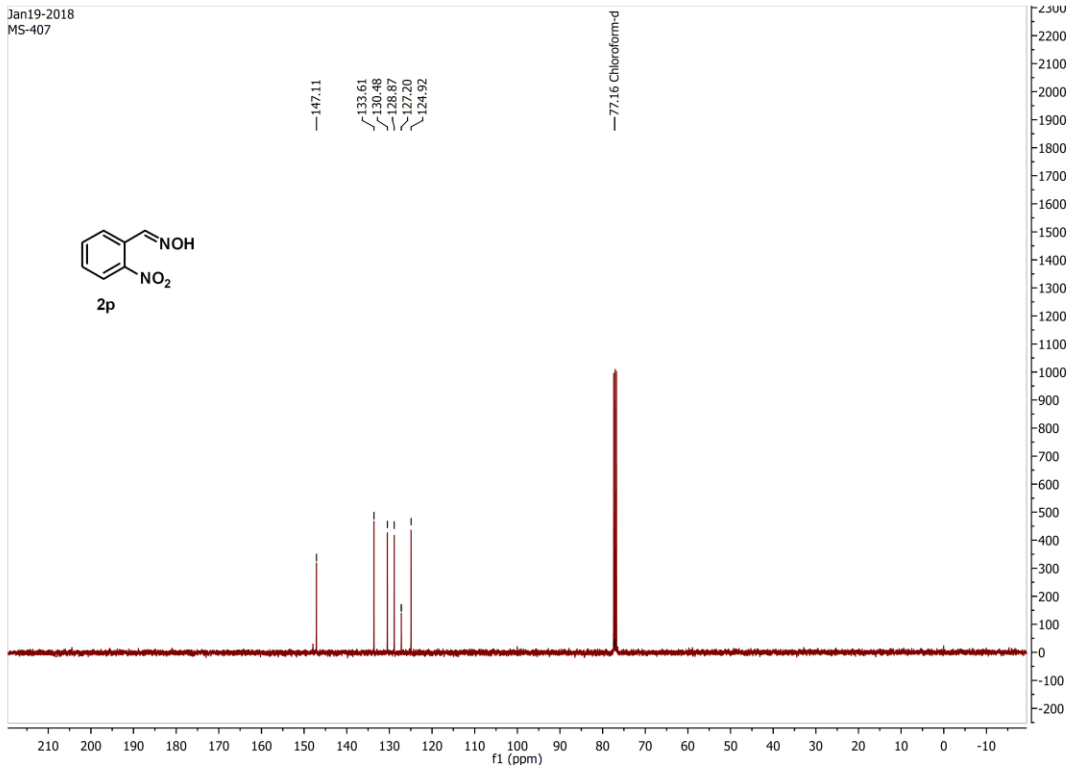
Jan19-2018
MS-407
147.11
133.61
130.48
128.87
127.20
124.92
77.16 Chloroform-d
NOH
NO2
2p
f1 (ppm)

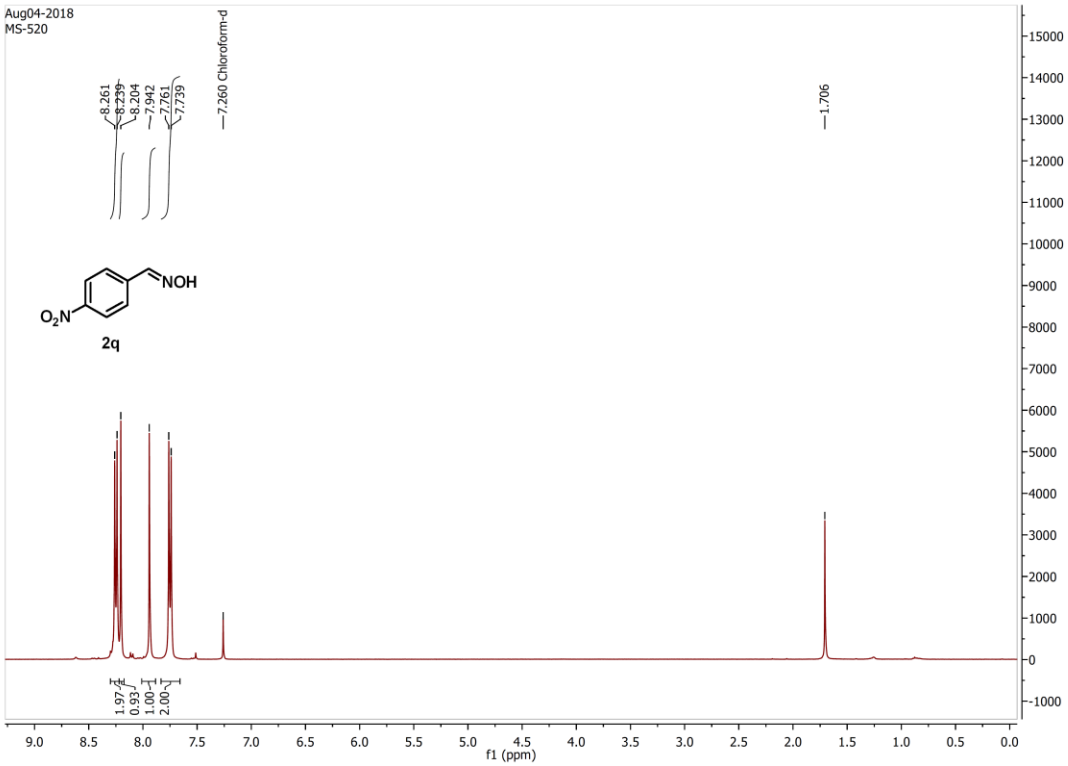
Aug04-2018
MS-520
8.261
8.239
8.204
7.942
7.761
7.739
7.260 Chloroform-d
1.706
NOH
O2N
2q
1.97
0.93
1.00
2.00
f1 (ppm)

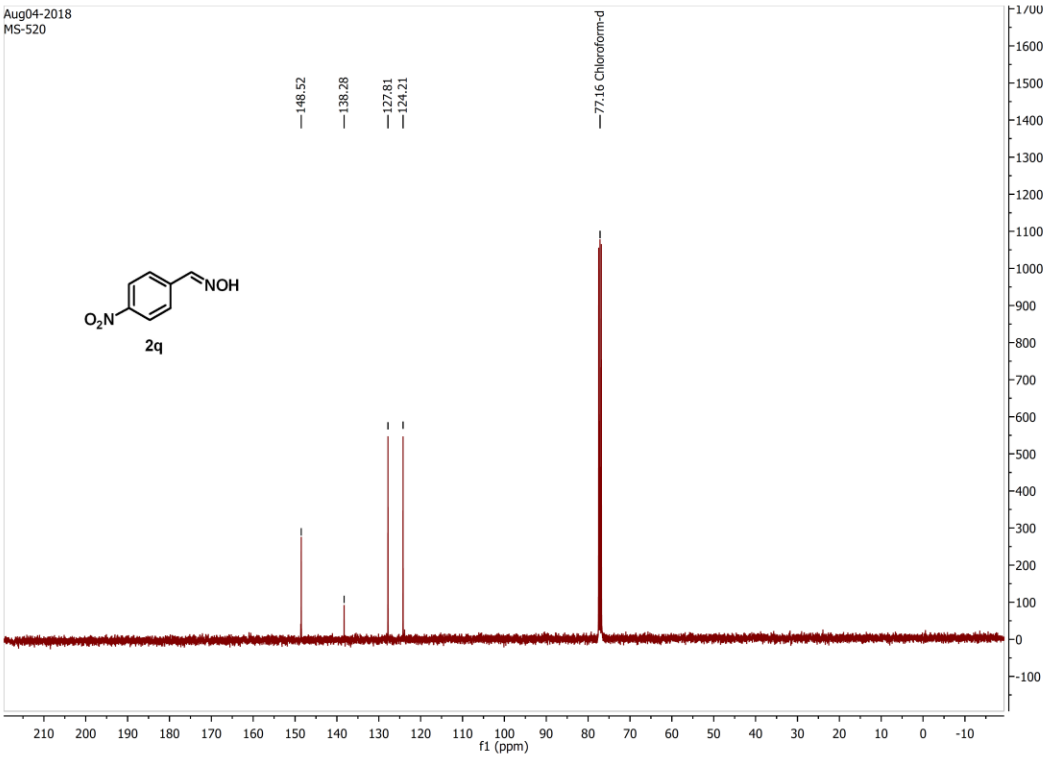
Aug04-2018
MS-520
148.52
138.28
127.81
124.21
77.16 Chloroform-d
NOH
O2N
2q
f1 (ppm)

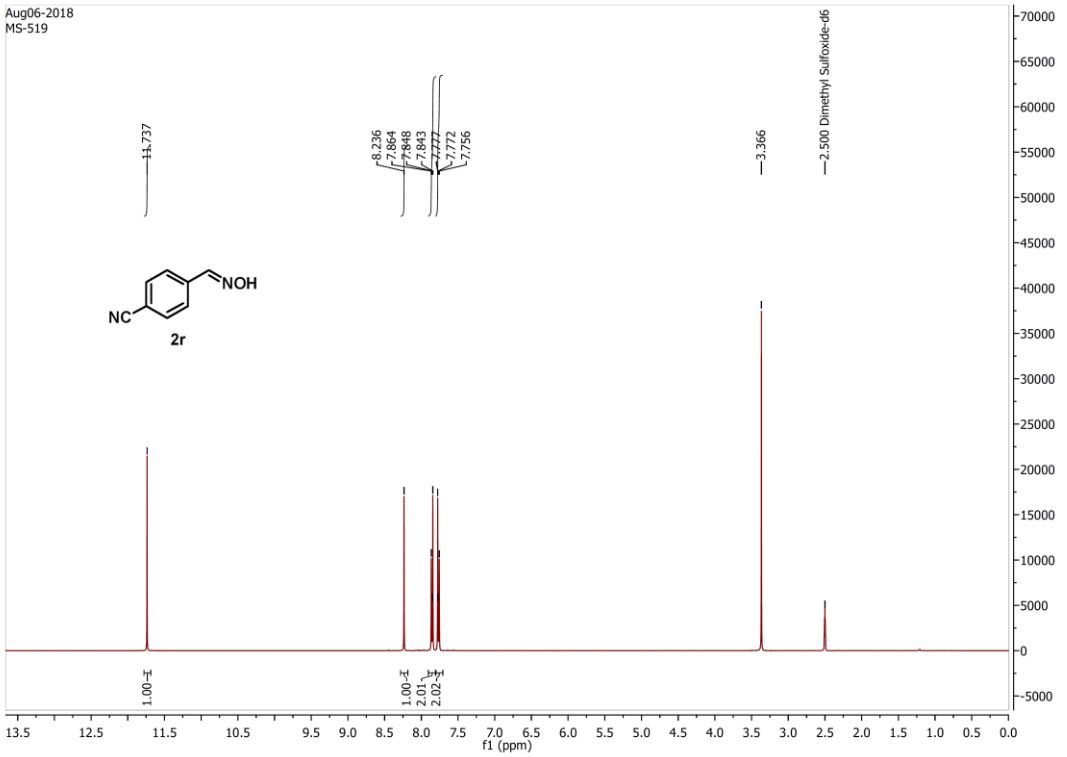
Aug06-2018
MS-519
11.737
8.236
7.864
7.848
7.843
7.777
7.772
7.756
3.366
2.500 Dimethyl Sulfoxide-d6
NOH
NC
2r
1.00
1.00
2.01
2.02
f1 (ppm)

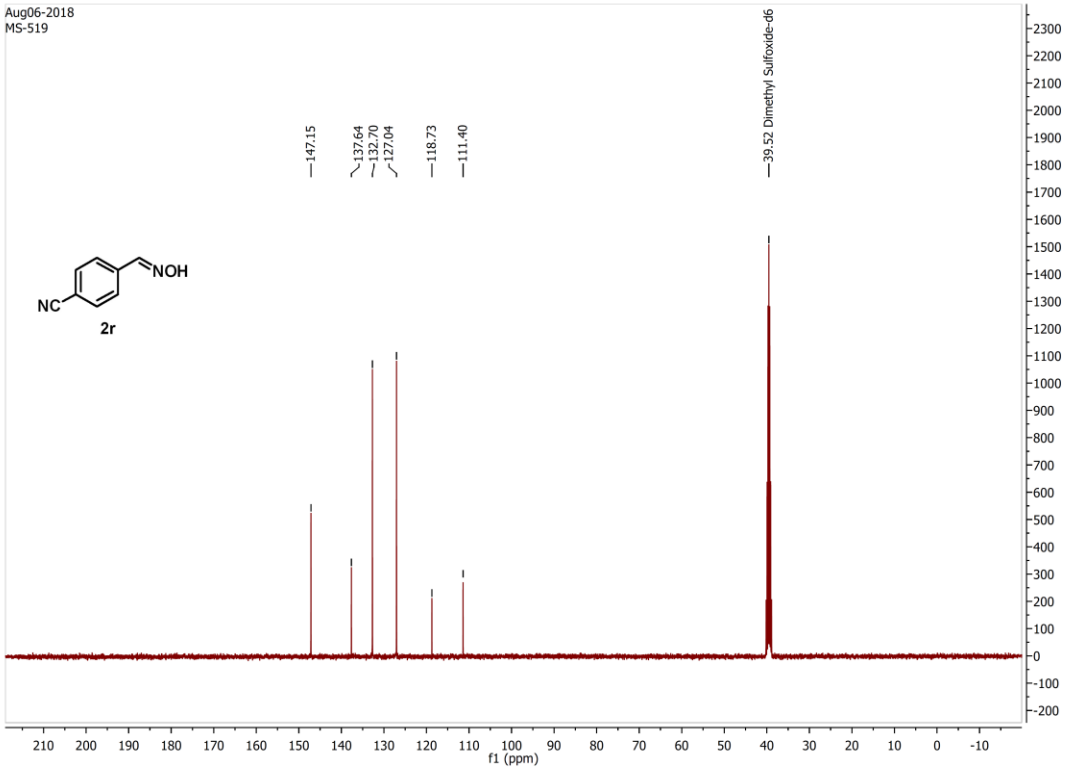
Aug06-2018
MS-519
147.15
137.64
132.70
127.04
118.73
111.40
39.52 Dimethyl Sulfoxide-d6
NOH
NC
2r
f1 (ppm)

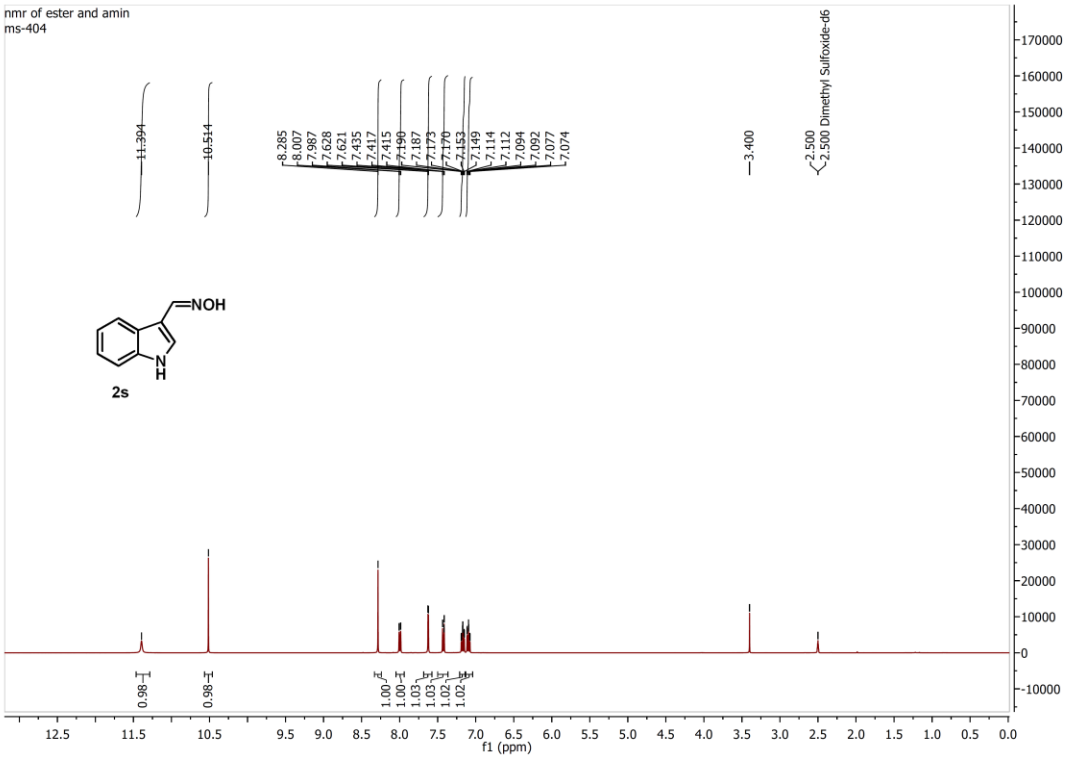
nmr of ester and amin
ms-404
11.394
10.514
8.285
8.007
7.987
7.628
7.621
7.435
7.417
7.415
7.190
7.187
7.173
7.170
7.153
7.149
7.114
7.112
7.094
7.092
7.077
7.074
3.400
2.500
2.500 Dimethyl Sulfoxide-d6
=NOH
N
H
2s
0.98
0.98
1.00
1.00
1.03
1.03
1.02
1.02
f1 (ppm)

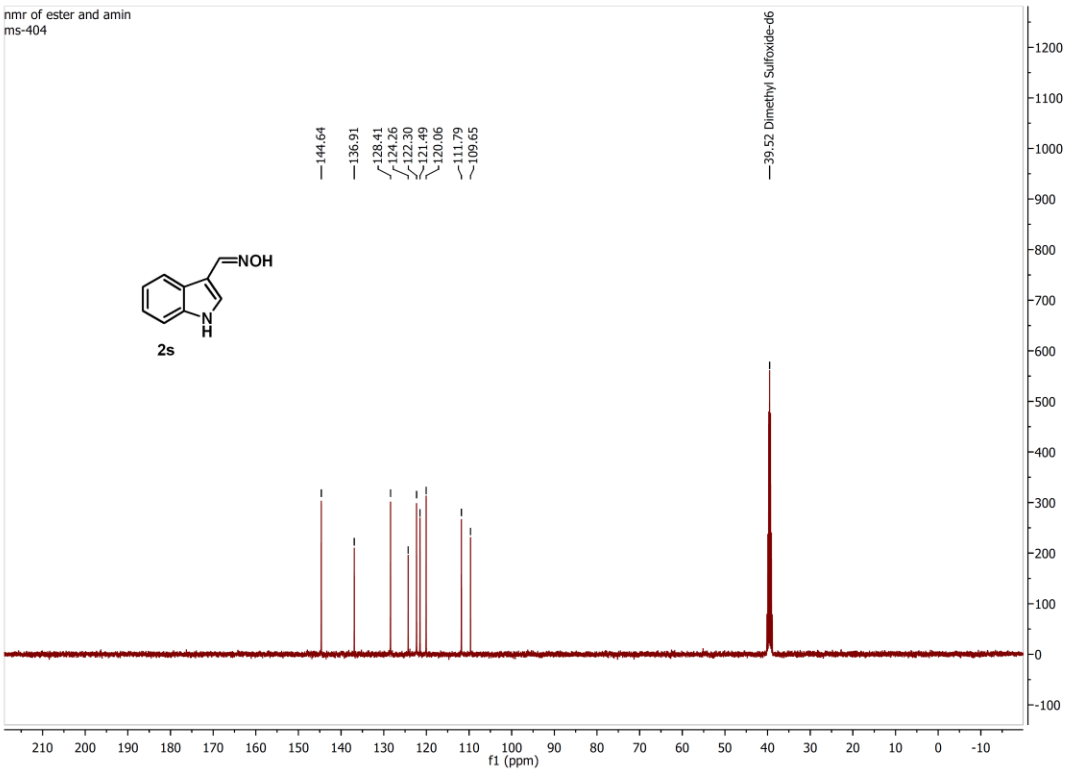
nmr of ester and amin
ms-404
144.64
136.91
128.41
124.26
122.30
121.49
120.06
111.79
109.65
39.52 Dimethyl Sulfoxide-d6
=NOH
N
H
2s
f1 (ppm)

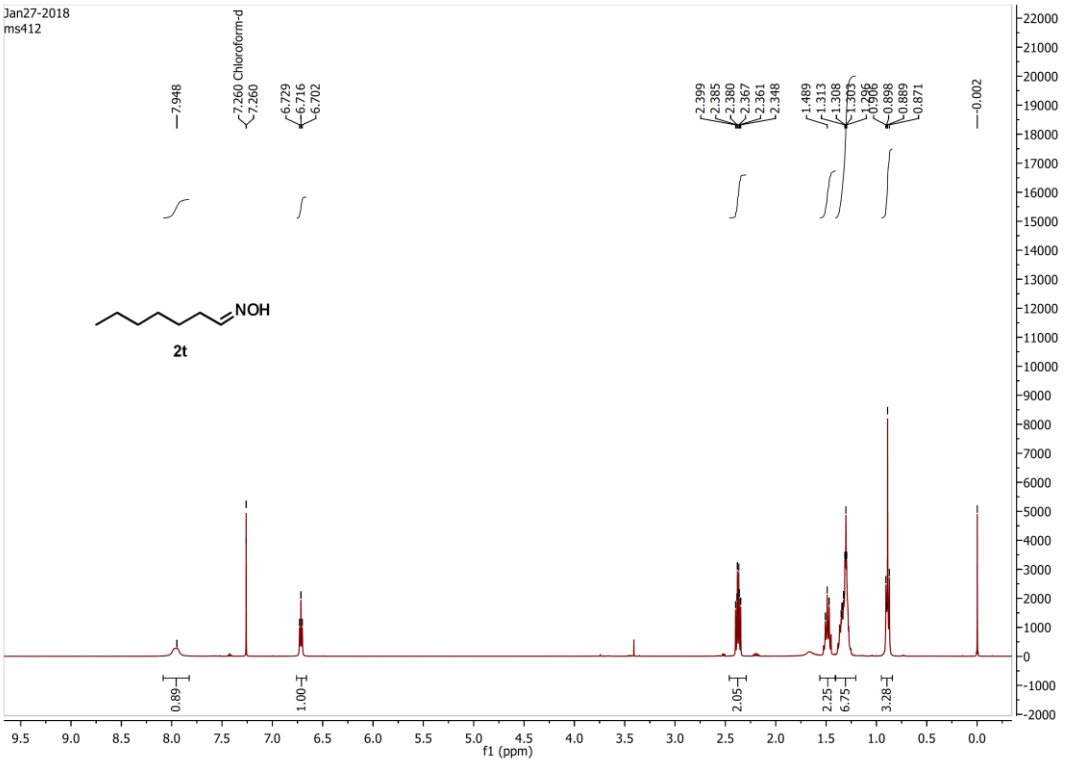
Jan27-2018
ms412
7.948
7.260 Chloroform-d
7.260
6.729
6.716
6.702
2.399
2.385
2.380
2.367
2.361
2.348
1.489
1.313
1.308
1.303
1.296
0.906
0.898
0.889
0.871
0.002
NOH
2t
0.89
1.00
2.05
2.25
6.75
3.28
f1 (ppm)

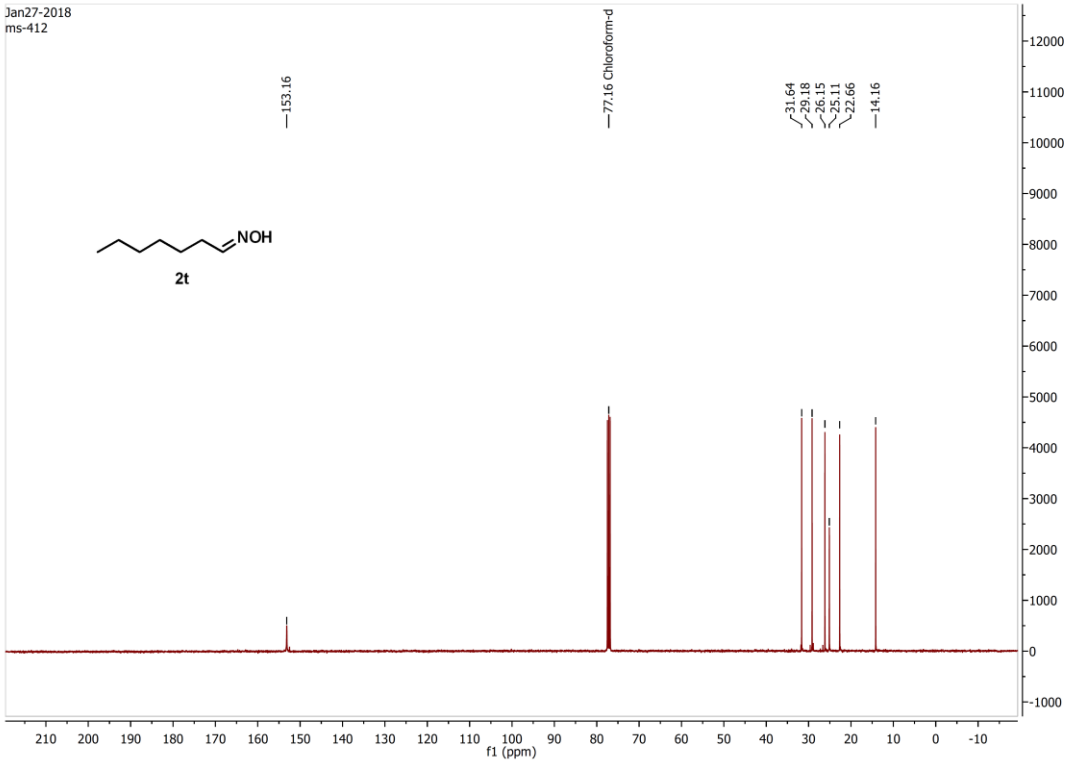
Jan27-2018
ms-412
153.16
77.16 Chloroform-d
31.64
29.18
26.15
25.11
22.66
14.16
NOH
2t
f1 (ppm)

5.11. References:

1. J. Donohue, The structure of oximes, J. Am. Chem. Soc. 78 (1956) 4172–4172.
2. V. Meyer, A. Janny, Ueber Stickstoffhaltige Acetonderivate, Ber. Dtsch. Chem. Ges. 15 (1882) 1164–1167.
3. M. Sørensen, E.H.J. Neilson, B.L. Møller, Oximes: Unrecognized Chameleons in General and Specialized Plant Metabolism, Molecular Plant 11(2018) 95–117.
4. R.L. Siegel, K.D. Miller, A. Jemal, Cancer Statistics, 2017, CA Cancer J. Clin. 67 (2017) 7–30.
5. a)R. Siegel, J. Ma, Z. Zou, A. Jemal, Cancer statistics, CA Cancer J. Clin. 64 (2014) 9–29.; b) M.R. Clemens, O.A. Gladkov, E. Gartner, V. Vladimirov, J. Crown, J. Steinberg, F. Jie, A. Keating, Phase II, Multicenter, Open-label, Randomized Study of YM155 plus Docetaxel as first-line Treatment in Patients with HER2-Negative Metastatic Breast Cancer, Breast Cancer Res. Treat. 149 (2015) 171–179.
6. The Cancer Genome Atlas Network, Comprehensive molecular portraits of human breast tumours, Nature 490 (2012) 61–70.
7. a) A. Papa, D. Caruso, S. Tomao, L. Rossi, E. Zaccarelli, F. Tomao, Triple-Negative Breast Cancer: Investigating Potential Molecular Therapeutic Target, Expert Opin. Ther. Targets 19 (2015) 55–75.; b) P. Morales, S.B. Benito, C. Andradas, M.G. Canas, J.M. Flores, P. Goya, J.F. Ruiz,C. Sanchez, N. Jagerovic, Selective, Nontoxic CB_2 Cannabinoid O-Quinone with *in vivo* Activity Against Triple-Negative Breast Cancer, J. Med. Chem. 58 (2015) 2256–2264.
8. C. Jian-Guo, F. Lei, H. Li-Liang, L. Hong-Li, Z. Ai-Min, Synthesis and Evaluation of Some Steroidal Oximes as Cytotoxic Agents: Structure/Activity Studies (I), Steroids 74 (2009) 62–72.
9. P.C. Acharya, R. Bansal, Synthesis and Antiproliferative Activity of Some Androstene Oximes and Their O-Alkylated Derivatives, Arch. Pharm. Chem. Life Sci. 347 (2014) 193–199.

10. H. Guang, M. Qing-Qing, Z. Wen, Z. Qi-Jing, D. Jin-Yun, L. Shao-Shun, Design and Synthesis of Biotinylated Dimethylation of Alkannin Oxime Derivatives, Chinese Chemical Letters 28 (2017) 453–457.
11. T. Tanaka, S. Ohashi, H. Saito, T. Wada, T. Aoyama, Y. Ichimaru, S. Miyairi, S. Kobayashi, Indirubin 3′-Oxime Inhibits Anticancer Agent-Induced YB-1 Nuclear Translocation in HepG2 Human Hepatocellular Carcinoma Cells, Biochemical and Biophysical Research Communications 496 (2018) 7–11.
12. L. Sánchez-Sánchez, M.G. Hernández-Linares, M.L. Escobar, H. López-Muñoz, E. Zenteno, M.A. Fernández-Herrera, G. Guerrero-Luna, A. Carrasco-Carballo, J. Sandoval-Ramírez, Antiproliferative, Cytotoxic, and Apoptotic Activity of Steroidal Oximes in Cervicouterine Cell Lines, Molecules, 21 (2016)1533–1550.
13. G.-F. Zha, H.-L. Qin, B.G.M. Youssif, M.W. Amjad, M.A.G. Raja, A.H. Abdelazeem, S.N.A. Bukhari, Discovery of Potential Anticancer Multi-Targeted Ligustrazine Based Cyclohexanone and Oxime Analogs Overcoming the Cancer Multidrug Resistance, European Journal of Medicinal Chemistry135 (2017) 34–48.
14. Y. Ichimaru, T. Fujii, H. Saito, M. Sano, T. Uchiyama, S. Miyairi, 5-Bromoindirubin 30-(O-oxiran-2-ylmethyl)oxime: A Long-Acting Anticancer Agent and a Suicide Inhibitor for Epoxide Hydrolase, Bioorganic & Medicinal Chemistry 25 (2017) 4665–4676
15. G. Huang, H.-R. Zhao, Q.-Q. Meng, Q.-J. Zhang, J.-Y. Dong, B.-q. Zhu, S.-S. Li, Synthesis and Biological Evaluation of Sulfur-Containing Shikonin Oxime Derivatives as Potential Antineoplastic Agents, European Journal of Medicinal Chemistry 143 (2018) 166–181.
16. V.H. Masand, N.N.E. El-Sayed, M.U. Bambole, S.A. Quazi, Multiple QSAR Models, Pharmacophore Pattern and Molecular Docking Analysis for Anticancer Activity of α,β, Unsaturated Carbonyl-Based Compounds, Oxime and Oxime Ether Analogues, Journal of Molecular Structure 1157 (2018) 89–96.
17. M.Z. Dewan, S. Ahmed, Y. Iwasaki, K. Ohba, M. Toi, N. Yamamoto. Stromal Cell-Derived Factor-1 and CXCR4 Receptor Interaction in Tumor Growth and

Metastasis of Breast Cancer. Biomedicine & Pharmacotherapy 60 (2006) 273–276.

18. H. Hirata, Y. Hinoda, N. Kikuno, K. Kawamoto, A.V. Dahiya, Y. Suehiro, Y. Tanaka, R. Dahiya, CXCL12 G801A Polymorphism is a Risk Factor for Sporadic Prostate Cancer Susceptibility, Clin. Cancer Res. 13 (2007) 5056–5062.
19. J. Miki, B. Furusato, H. Li, Y. Gu, H. Takahashi, S. Egawa, I.A. Sesterhenn, D.G. McLeod, S. Srivastava, J.S. Rhim, Identification of Putative Stem Cell mMarkers, CD133 and CXCR4, in hTERT-Immortalized Primary Nonmalignant and Malignant Tumor-Derived Human Prostate Epithelial Cell Lines and in Prostate Cancer Specimens. Cancer Research 67 (2007) 3153–3161.
20. S. Cavallaro, CXCR4/CXCL12 in Non-Small-Cell Lung Cancer Metastasis to the Brain. Int. J. Mol. Sci. 14 (2013) 1713–1727.
21. T. Gangadhar, S. Nandi, R. Salgia. The Role of Chemokine Receptor CXCR4 in Lung Cancer. Cancer Biology &Therapy 9 (2010) 409–416.
22. K. Kucukoglu, K. Kucukoglu, F. Oral, T. Aydin, C. Yamali, O. Algul, H. Sakagami, I. Gulcin, C.T. Supuran, H.I. Gul, Synthesis, Cytotoxicity and Carbonic Anhydrase Inhibitory Activities of new Pyrazolines, Journal of Enzyme Inhibition and Medicinal Chemistry 31 (2016) 20–24.
23. T. Dastan, U.M. Kocyigit, S.D. Dastan, P.C. Kilickaya, P. Taslimi, O. Cevik, M. Koparir, C. Orek, I. Gulçin, A. Cetin, Investigation of Acetylcholinesterase and Mammalian DNA Topoisomerases, Carbonic Anhydrase Inhibition Profiles, and Cytotoxic Activity of Novel bis(alpha-aminoalkyl)phosphinic acid Derivatives Against Human Breast Cancer, J Biochem Mol Toxicol. 31 (2017) 21971.
24. I. Gulcin, S. Beydemir, F. Topal, N. Gagua, A. Bakuridze, R. Bayram, A. gepdiremen, Apoptotic, Antioxidant and Antiradical Effects of Majdine and Isomajdinefrom *Vincaherbacea* Waldst. and kit, J. Enzyme Inhib. Med. Chem. 27(2012) 587–594.
25. T. Abdizadeh, M.R. Kalani, K. Abnous, Z. Tayarani-Najaran, B.Z. Khashyarmanesh, R. Abdizadeh, R. Ghodsi, F. Hadizadeh, Design, Synthesis and Biological Evaluation of Novel Coumarin Based Benzamides as Potent

Histone Deacetylase Inhibitors and Anticancer Agents, Eur. J. Med. Chem. 132 (2017) 42–62.

26. S.M. Aboutorabzadeh, F. Mosaffa, F. Hadizadeh, R. Ghodsi, Design, Synthesis, and Biological Evaluation of 6-methoxy-2-arylquinolines as Potential P-glycoprotein Inhibitors, Iran. J. Basic Med. Sci. 21 (2018) 9–18.
27. M.G. Ferlin, D. Carta, R. Bortolozzi, R. Ghodsi, A. Chimento, V. Pezzi, S. Moro, N. Hanke, R.W. Hartmann, G. Basso, G. Viola, Design, Synthesis, and Structure-Activity Relationships of Azolylmethylpyrroloquinolinesas Nonsteroidal Aromatase Inhibitors, J. Med. Chem. 56 (2013) 7536–7551.
28. R. Ghodsi, E. Azizi, A. Zarghi, Design, Synthesis and Biological Evaluation of 4-(Imidazolylmethyl)-2-(4-methylsulfonyl phenyl)-Quinoline Derivatives as Selective COX-2 Inhibitors and *in-vitro* Anti Breast Cancer Agents, Iran. J. Pharm. Res. 15 (2016) 169–177.
29. R. Ghodsia, E. Azizi, M.G. Ferlin, V. Pezzi, A. Zarghi, Design, Synthesis and Biological Evaluation of 4-(Imidazolylmethyl)-2-aryl-Quinoline Derivatives as Aromatase Inhibitors and Anti Breast Cancer Agents, Letters in Drug Design & Discovery 13 (2016) 89–97.
30. H. Sharghi, M.H. Sarvari, Selective Synthesis of *E* and *Z* Isomers of Oximes, Synlett 1 (2001) 99–101.
31. K.C. Nicolaou, C.J.N. Mathison, T. Montagnon, New Reactions of IBX: Oxidation of Nitrogenand Sulfur-Containing Substrates To Afford Useful Synthetic Intermediates, Angew. Chem. Int. Ed. 42 (2003) 4077–4082.
32. R. Badri, M.R. Shushizadeh, An Efficient Tandem Oxidative-Protection Reaction of Benzylic Alcohols to Corresponding Arylhydrazones and Oximes, Phosphorus, Sulfur, and Silicon, 182 (2007) 601–605.
33. A. Mirjafari, N. Mobarrez, R.A. O'Brien, J.H. Davis Jr, J. Noei, Microwave-Promoted one-pot Conversion of Alcohols to Oximes Using1-Methylimidazolium Nitrate, [Hmim][NO_3], as a Green Promoter and Medium, C. R. Chimie 14 (2011) 1065–1070.
34. S. Chandrappa, M. Umashankara, K. Vinaya, C.S. Ananda Kumar, K.S. Rangappa, One-pot Synthesis of Aryl oxime Analogues from Methyl Arenes using NBS and Hydroxyl amine Hydrochloride, Tetrahedron Letters 53 (2012) 2632–2635.

35. S. Wertz, A. Studer, Metal-Free 2,2,6,6-Tetramethylpiperidin-1-yloxy Radical (TEMPO) Catalyzed Aerobic Oxidation of Hydroxylamines and Alkoxyamines to Oximes and Oxime Ethers, Helvetica Chimica Acta 95 (2012) 1758–1772.
36. Q. Sha, Y. Wei, Base and Solvent Mediated Decomposition of Tosylhydrazones: Highly Selective Synthesis of N-alkyl Substituted Hydrazones, Dialkylidenehydrazines, and Oximes, Tetrahedron 69 (2013) 3829–3835.
37. J. Yu, X. Cao, M. Lu, A Novel and Efficient Catalytic System Including TEMPO/ Acetaldoxime/InCl3 for Aerobic Oxidation of Primary Amines to Oximes, Tetrahedron Letters 55 (2014) 5751–5755.
38. G. Aghapoura, Z. Abbaszadeh, Tandem and Selective Conversion of Tetrahydropyranyl and Silyl Ethers to Oximes Catalyzed with Trichloroisocyanuric Acid, Phosphorus, Sulfur, and Silicon and the Related Elements, 190 (2015) 1464–1470.
39. S. Singh, V. Dubey, D.K. Singh, K. Fatima, A. Ahmad, S. Luqman, Antiproliferative and Antimicrobial Efficacy of the Compounds Isolated from the Roots of *Oenotherabiennis L*, Journal of Pharmacy & Pharmacology 69 (2017) 1230–1243.
40. P. Maurya, S. Singh, M.M. Gupta, S. Luqman, Characterization of Bioactive Constituents from the Gum Resin of *Gardenia lucida* and its Pharmacological Potential. Biomedicine & Pharmacotherapy 85(2017) 444–456.

List of Publications, Conferences and Workshop

List of Publications:

1. **Manoj K. Shrivash**, Sonali Mishra, UpmaNarain, Jyoti Pandey, Krishna Misra "*In-silico* designing, chemical synthesis, characterization and in-vitro assessment of antibacterial properties of some analogues of curcumin" *Microbial Pathogenesis* (2018), 123, 89-97.

2. **Manoj K. Shrivash**, Sonali Mishra, Sneh Lata Panwar, Shabnam Sircaik, Jyoti Pandey and Krishna Misra." Attenuation of Pathogenicity in Candida albicans by Application of Polyphenols" *J. Microb. Biochem. Technol*, an open access journ. (2018), 10, (2): 27-39.

3. Akhilesh Kumar Shukla, Hamidullah, **Manoj Kumar Shrivash**, Vishwa Deepak Tripathi, Rituraj Konwar, Jyoti Pandey. "Identification of *N*-Hydroxycinnamamide analogues and their bio-evaluation against breast cancer cell lines" *Biomedicine & Pharmacotherapy*. (2018), 107, 475-483.

4. **Manoj K. Shrivash**, Kuruba Adeppa, Rohit Singh, Jyoti Pandey, Krishna Misra. "A Novel, Efficient and Multigram Scale Synthesis of S-Alkyl thiocarbamates via Newman Kwart Rearrangement". *Proc. Natl. Acad. Sci., India, Sect. A Phys. Sci.* (2017) 87: 189-193.

5. M. D. Pandareesh, **Manoj. K. Shrivash,** H. N. Naveen Kumar, K. Misra, M. M. Srinivas Bharath. "Curcumin Monoglucoside Shows Improved Bioavailability and Mitigates Rotenone Induced Neurotoxicity in Cell and Drosophila Models of Parkinson's Disease". *Neurochem. Res.* (2016) 41:3113–3128.

Conferences and workshop:

- Seven days' workshop on NMR/MRI from Molecule to Human Behavior sponsored by Department of Science and Technology, **June 21-27, 2015** organized by CBMR and Babasaheb Bhimrao Ambedkar University Lucknow. (Participated)

- Five days International Conference , 104th Indian Science Congress "Science and Technology for National Development", **Jan 3-7, 2017,** organized by Sri Venkateswara University, Tirupati, Andhra Pradesh.(Participated)

- One day workshop on Science of Synthesis sponsored by Thieme, **September 25, 2018,** organized by Centre of Bio-Medical Research Lucknow. (Participated)

- Three days international conference on" Chemical sciences: National and Global Prospective" **October 29-31, 2018,** orgnized by Lucknow Christian College, Lucknow.(Poster presentation)

- Three days International Conference "88th Annual session of the Academy (NASI), **December 6-8, 2018,** organized by Mahatma Gandhi GramodayaVishwavidalaya, Chitrakoot, MP. (Poster presentation)

Urkund Analysis Result

Analysed Document: Manoj thesis_Chemistry_manojshrivash@gmail.com.docx (D50863972)
Submitted: 4/20/2019 7:36:00 PM
Submitted By: shodhganga.bbau@gmail.com
Significance: 3 %

Sources included in the report:

Sunil Gaikwad.pdf (D47432835)
plagiarism check.docx (D15993377)
Final Thesis of Sinki Kolita4.pdf (D35573943)
https://www.ics.ir/Files/Content/media/13593.pdf
https://www.science.gov/topicpages/a/anticancer+therapeutic+strategies.html
https://www.ncbi.nlm.nih.gov/pmc/articles/PMC6154528/
https://www.researchgate.net/publication/306246760_Curcumin_Monoglucoside_Shows_Improved_Bioavailability_and_Mitigates_Rotenone_Induced_Neurotoxicity_in_Cell_and_Drosophila_Models_of_Parkinson's_Disease
https://www.researchgate.net/publication/5901347_Curcumin-Derived_Pyrazoles_and_Isoxazoles_Swiss_Army_Knives_or_Blunt_Tools_for_Alzheimer's_Disease
d32aae0d-1bb5-44b4-beb0-0e3897cf0101

Instances where selected sources appear:

15